

NUREG/CR-3863  
SAND84-1264  
RV

Printed March 1985

# Assessment of Class 1E Pressure Transmitter Response When Subjected to Harsh Environment Screening Tests

David T. Furgal, Charles M. Craft, Edward A. Salazar

Prepared by  
Sandia National Laboratories  
Albuquerque, New Mexico 87185 and Livermore, California 94550  
for the United States Department of Energy  
under Contract DE-AC04-76DP00789

8506140052 850430  
PDR NUREG  
CR-3863 R PDR

SF29000(8-81)  
Prepared for  
U. S. NUCLEAR REGULATORY COMMISSION

**NOTICE**

This report was prepared as an account of work sponsored by an agency of the United States Government. Neither the United States Government nor any agency thereof, or any of their employees, makes any warranty, expressed or implied, or assumes any legal liability or responsibility for any third party's use, or the results of such use, of any information, apparatus product or process disclosed in this report, or represents that its use by such third party would not infringe privately owned rights.

Available from  
GPO Sales Program  
Division of Technical Information and Document Control  
U.S. Nuclear Regulatory Commission  
Washington, D.C. 20555  
and  
National Technical Information Service  
Springfield, Virginia 22161

NUREG/CR-3863  
SAND84-1264  
RV

ASSESSMENT OF CLASS 1E PRESSURE TRANSMITTER RESPONSE  
WHEN SUBJECTED TO HARSH ENVIRONMENT SCREENING TESTS

David T. Furgal\*  
Charles M. Craft  
Edward A. Salazar

March 1985

Sandia National Laboratories  
Albuquerque, New Mexico  
Operated by  
Sandia Corporation  
for the  
U. S. Department of Energy

Prepared for  
Office of Nuclear Regulatory Research  
Division of Facility Operations  
U. S. Nuclear Regulatory Commission  
Washington, DC 20555  
Under Interagency Agreement 40-550-75  
NRC FIN No. A1327

---

\*Ktech Corporation

## ABSTRACT

An experimental investigation into the performance of Class 1E electronic pressure transmitters exposed to environments within and beyond the design basis has been conducted. Emphasis was placed on determining the instruments' failure and degradation modes in separate and simultaneous environmental exposures. Five unaged ITT Barton Model 763 pressure transmitters were tested; each transmitter was exposed to a unique environment. The environments were (1) simulated Loss of Coolant Accident (LOCA) steam/chemical spray conditions alone, (2) temperature alone, (3) radiation alone, (4) simultaneous radiation and LOCA temperature (no steam) conditions, and (5) simultaneous radiation and simulated LOCA steam/chemical spray conditions.

The response of the transmitters showed that temperature was the primary environmental stress affecting the tested transmitters' performance. Initial large errors that decrease with time-at-temperature were observed. We believe the source of these errors to be a common mode design weakness in the transmitter's calibration potentiometers. This weakness results from a dependency of material dielectric properties on temperature. The modification recommended by the manufacturer, although palliative in nature, did reduce this temperature-induced effect after the first few minutes of accident exposure. A potential second common failure mode which activates slowly with time-at-temperature was also identified. We believe the operation of this failure mechanism is catalyzed by the presence of a lubricant used in the production of some potentiometers. The design of this transmitter proved to be exceptionally hard to radiation effects and there appeared to be no significant synergistic effects between radiation and temperature. The observed responses of the transmitters offer support for the position of IEEE 381-1977 which recommends that electronic modules aged to varying degrees of advanced life should be tested.

## CONTENTS

	<u>Page</u>
Executive Summary.....	1
1.0 INTRODUCTION.....	6
1.1 General.....	6
1.2 Overview of Tests Performed.....	6
2.0 TEST SPECIMENS.....	8
2.1 Specifications.....	8
3.0 TEST ENVIRONMENT EXPOSURES.....	11
3.1 LOCA and Chemical Spray.....	11
3.2 Temperature Only.....	11
3.3 Radiation Only.....	11
3.4 Radiation and Temperature.....	12
3.5 Radiation, LOCA, and Chemical Spray.....	12
3.6 Special LOCA Transient Exposure.....	12
4.0 TEST FACILITIES.....	14
4.1 Test Apparatus.....	14
4.2 Test Configuration.....	14
4.3 Data Acquisition.....	19
5.0 DATA PRESENTATION.....	20
5.1 Organization of Figures in Appendices.....	20
5.2 Constant Pressure Data.....	20
5.3 Functional Test Data.....	21
6.0 TEST OBSERVATIONS.....	22
6.1 Radiation Tolerance.....	22
6.1.1 Discussion of Observations.....	22
6.1.2 Comparison of Observations.....	24
6.2 Temperature Effects.....	25
6.2.1 Performance Observations.....	27
6.3 Functional Test Data.....	28
6.3.1 Temperature Relationships.....	28
6.3.2 Transmitter Correlation Stability.....	29
6.3.3 Calibration Correlation.....	29
6.3.4 Temperature Stability of Functional Tests..	33
6.3.5 Comment on Error Calculation Method.....	33
7.0 EVALUATION OF THERMAL INSTABILITY.....	34
7.1 Potentiometer Design and Materials.....	34
7.2 Hypothesis on the Failure Mechanism.....	37
7.3 Test Methodology Implications.....	38
8.0 EVALUATION OF POTENTIOMETER MODIFICATION KIT.....	39
8.1 Initial Screening Test.....	39
8.2 Special LOCA Transient Exposure.....	39
8.3 Evaluation of Test Results.....	42

CONTENTS  
(continued)

	<u>Page</u>
9.0 POTENTIOMETER FAILURE.....	44
9.1 Failure Analysis.....	44
9.2 Analysis of Non-Failed Potentiometers.....	50
10.0 POST-TEST OBSERVATIONS.....	57
10.1 Moisture Intrusion.....	57
10.2 Print Circuit Board Conformal Coating.....	57
10.3 Water in Cable Conduit.....	57
10.4 Cable Insulation.....	64
10.5 T4 Steam Isolation.....	64
10.6 Cover Mounting Bolts.....	64
11.0 CONCLUSIONS.....	66
References.....	67
Appendix A-Transmitter Response at 600 psig Nominal Pressure.....	69
Appendix B-Transmitter Response During Functional Tests.....	99

LIST OF FIGURES

<u>Figure</u>		<u>Page</u>
2-1	Barton Model 763 Transmitter.....	10
3-1	Transmitter T4 in Stainless Steel Enclosure.....	13
4-1	Transmitter T1 Test Configuration.....	15
4-2	Transmitters T3, T4, and T5 Test Configuration.....	16
4-3	Transmitter T2 Test Configuration.....	17
4-4	Test Configuration Schematic.....	18
4-5	Pressure Station.....	19
7-1	Disassembled Potentiometer From Transmitter T1.....	35
8-1	Potentiometer Modification Kit.....	40
9-1	Scanning Electron Micrograph (SEM) of C-Ring (20x)..	45
9-2	Elemental Analysis of C-Ring.....	45
9-3	SEM of Flat Washer (20x).....	46
9-4	Elemental Analysis of Flat Washer.....	46
9-5	SEM of the Break Occurring in the Active Circuit Portion of the Potentiometer Resistive Element (40x).....	47
9-6	SEM of the Wire Cross Section Resulting From the Test-Induced Break Occurring in the Active Portion of the Potentiometer Resistive Element (2000x).....	48
9-7	Elemental Analysis of the Test-Induced Break Wire End Shown in Figure 9-6.....	48
9-8	SEM of the Wire Cross Section Resulting From the Ductile Fracture of an Intact Portion of the Potentiometer Resistive Element (2000x).....	49
9-9	Elemental Analysis of the Ductile Fracture Break Wire End Shown in Figure 9-8.....	49
9-10	SEM of Foreign Material Found Near Wire Break Shown in Figure 9-5 (150x).....	51
9-11	Enlarged View of Partially Corroded Winding Shown in Figure 9-10 (500x).....	51

LIST OF FIGURES  
(continued)

<u>Figure</u>		<u>Page</u>
9-12	Elemental Analysis of Area E as Indicated in Figure 9-11.....	52
9-13	SEM of a Second Break Area Showing Separation of Two Adjacent Windings (200x).....	52
9-14	SEM End View of One of the Broken Wires Shown in Figure 9-13 (1500x).....	53
9-15	Elemental Analysis of One Portion of the Break Area Shown in Figure 9-13.....	53
9-16	SEM of a Purposely Broken Segment of the Potentiometer Resistive Element.....	54
9-17	Elemental Analysis of Deposit Found Under the Wire Break Shown in Figure 9-16.....	54
9-18	Typical Elemental Analysis of Non-Failed Potentiometers.....	55
10-1	Transmitter T1 Cover Showing Moisture Intrusion.....	58
10-2	Transmitter T4 Cover Showing Moisture Intrusion.....	59
10-3	Post-Test View of Transmitters T2, T3, and T5 .....	60
10-4	Transmitter T4 Showing Cracks in Circuit Board Conformal Coating.....	61
10-5	Transmitter T5 Showing Cracks in Circuit Board Conformal Coating.....	62
10-6	Transmitter T3 Showing Darkening of PC Board Material.....	63

LIST OF TABLES

<u>Table</u>		<u>Page</u>
2-1	Model 763 Gauge Pressure Electronic Transmitter Specifications.....	8
6-1	Radiation-Exposed Transmitter Errors at 100 Mrd Intervals.....	22
6-2	LOCA Temperature-Exposed Transmitter Error Observations at Selected Intervals.....	26
6-3	Correlation of Information for the Ten Functional Tests.....	29
6-4	Transmitter T3 Zero and Span Error Shifts During Irradiation.....	30
6-5	Errors Observed During Functional Test Measurements for 0, 200, and 1000 psig Readings.....	32
8-1	Screening Test Errors for Transmitter T2 Before and After Modification.....	39
8-2	Pre- and Post-Modification Performance of Transmitters T1, T2, and T5 at 173°-175°C.....	41

#### ACKNOWLEDGMENTS

The contributions of several individuals made this project a success. The guidance and test systems preparation provided by Tim Gilmore as well as his attention to minute details are thoughtfully appreciated. The following are acknowledged for their significant contribution: Frank Wyant for software and computer support in acquiring test data; Pat Drozda, Jerry Seitz and Mike Luker for their assembly of the data acquisition systems; John Lewin, Craig Ginn, Bob Padilla, Jack Benson and Don Hente for their assistance in test setup; Mark Jacobus for his engineering support; Dave Huskisson for assistance in SEM and EDXA analysis; Ann Shiver for data reduction and graphics support; and Della Vigil for painstaking manuscript preparation.

## EXECUTIVE SUMMARY

Research conducted at Sandia National Laboratories within the Component Assessment Program (CAP) evaluated the failure and degradation modes of unaged electronic equipment exposed to environments within and beyond the design basis. Current qualification test requirements as they relate to the operation of electronic instrumentation in containment were also evaluated.

Transmitters were chosen for testing because they are a basic component in Class 1E instrumentation circuits, provide critical reactor and plant state information, and may provide vital information for accident management. To implement the program, one typically-used model of nuclear power plant pressure transmitter was chosen for testing. Emphasis was placed on determining the instrument's fragility (i.e., failure and degradation modes) in separate and simultaneous environmental exposures. Specific objectives were (1) to determine and isolate the effects of individual and simultaneous environmental stresses, (2) to address severe accident questions by testing beyond the normal design basis environmental envelope, (3) to investigate the current qualification test methodology as it pertains to electronic components, and (4) to identify and analyze any weak-link circuit components for the mechanisms contributing to their degradation. In addition, this test effort was able to independently evaluate the merits of a modification recommended by the vendor to improve the temperature stability of the transmitter model tested.

Our test matrix exposed five ITT Barton Model 763, 0-1000 psig, 4-20 mA pressure transmitters to five separate environments. One transmitter was exposed to each environment. The five environments were (1) simulated Loss of Coolant Accident (LOCA) steam/chemical spray conditions alone (transmitter T1), (2) temperature alone (transmitter T2), (3) radiation alone (transmitter T3), (4) simultaneous radiation and LOCA temperature (no steam) conditions (transmitter T4), and (5) simultaneous radiation and simulated LOCA steam/chemical spray conditions (transmitter T5). Unaged equipment was tested to establish a baseline performance and to avoid introducing failures which might result from an accelerated aging process.

Subsequent to the main test, a special test was conducted to evaluate a modification recommended by Barton to improve the transmitters' temperature stability. This temperature sensitivity has been reported by Barton in a series of 10 CFR 21 disclosures [1,2,3]. In this special test, four of the already-tested transmitters were modified as recommended by Barton and then exposed to the first high temperature peak of the IEEE 323-1974, Appendix A [4] simulated LOCA profile. Subsequent to the testing, the span and zero calibration potentiometers were disassembled and evaluated to determine the root cause of the temperature instability.

The test configuration connected each transmitter in series with two 500-ohm resistors and a dc power supply which was set to 40 V. The current in the transmitter instrumentation loop was monitored via the voltage drop across one of the resistors. The reference pressure gauges located in an ambient temperature, nonradiation environment were used to monitor the applied pressure. During most of the test sequence, 600 psig nitrogen was applied to the transmitters as the pressure stimulus. To obtain data on transmitter response over the entire calibrated range of the electronics, ten functional tests were conducted during the first 172 hours of the exposure. These functional tests exercised the transmitters over their 0 to 1000 psig range in 200 psi increments.

Test results showed that the Model 763 transmitter design has excellent radiation resistance. The radiation exposure produced a small gradual degradation in transmitter output. This degradation was observed for the transmitter exposed to radiation alone and for the transmitter exposed to the radiation and LOCA steam environment. The radiation effects were manifested as a negative shift in transmitter calibration. The shift averaged -0.7 percent of full scale per 100 Mrd of exposure for transmitter T3. Measurements made after 200 Mrd exposure compared favorably with the published specification of  $\pm 10$  percent of full scale [5].

Temperature was the primary environmental stress affecting transmitter performance. The four transmitters exposed to a thermal environment all experienced temperature-related and time-at-temperature-related effects. The temperature effects appeared as distinct shifts in transmitter output at exposure temperature transitions above 122°C (252°F), and as decreases in these shifts as the time-at-temperature increased. The direction of these shifts generally followed the direction of the temperature change. During the first 30 minutes of LOCA simulation exposure, maximum errors ranging from -9.0 percent to +26.8 percent of full-scale reading were recorded. At temperatures of 122°C (252°F) and below, transmitter error remained relatively constant except for long-term drift.

The functional tests evaluated whether or not the behavior observed at a constant pressure of 600 psig was consistent over the entire operating range of the transmitter, and whether any nonlinearities in transmitter response existed. For transmitter T3, the radiation exposure alone produced little change in its response over the calibrated range. Temperature, however, produced positive shifts in both the zero and span of the instruments. As time-at-temperature increased, the magnitude of the zero and span shifts decreased, though at different rates and there was an observed nonlinearity in the span as it decreased.

One and possibly two common mode failures were identified during the test. Both appeared to be thermally activated and

both were related to the zero and span potentiometers. The first was a thermal instability problem which has already been reported by Barton [1,2,3]. The magnitude of the instabilities observed in our tests were, however, greater than those reported by Barton. The second potential common mode failure was the corrosion-induced opening of the span potentiometer which caused the transmitter to exhibit short circuit-like conditions.

Our analyses confirmed Barton's finding that the primary cause of the thermal instability problem was leakage current from the zero and span potentiometers to the transmitter housing [2]. We hypothesize that the basic cause of the leakage currents is a materials-related problem. Internally, the potentiometer's shaft is molded into a nylon rotor assembly. This rotor assembly provides both the mechanical support for the slider and the electrical isolation between the shaft and the wiper. The shaft itself is in intimate mechanical and electrical contact with the potentiometer case. Thus, the only electrical isolation between the circuit elements and the potentiometer case (and hence the transmitter housing) is the nylon rotor assembly.

Since nylon has a hydrogen-bonded molecular structure, it has a strong affinity to absorb moisture. We believe that as temperature was increased, the mobility of hydrogen ions formed from absorbed moisture increased, causing the dielectric qualities of the nylon to degrade; consequently, the conducting path between the electronics and the potentiometer case was enhanced. As time-at-temperature increased, some of the absorbed moisture was outgassed, partially restoring the dielectric qualities of the nylon. Also, as the temperature was lowered, ion mobility was decreased, tending to further restore the dielectric qualities of the nylon. Because moisture had been driven off, these qualities may even have been restored to values better than the original values. Thus, after the thermal transients, the amount of leakage current that occurred at reduced or ambient temperatures was possibly less than prior to the transient. This improvement in the nylon dielectric properties as a result of thermal cycling may account for the observed negative shift in output. At the lower temperatures, the moisture tends to be reabsorbed by the nylon. Therefore, over time the dielectric qualities of the nylon tended to return to their original values, restoring the original calibration of the transmitter. We did not investigate this nylon's moisture absorption/desorption characteristics and therefore cannot comment on the relative rates of desorption and absorption. However, we believe that the reabsorption process was slow compared to the initial desorption at elevated temperatures. This reabsorption process may have accounted for the slow drift back toward calibration observed in the long, low temperature portions of our test.

This hypothesis is consistent with the shifts in transmitter output observed at environmental profile temperature

transition points, and with the observed time-at-temperature behavior. Thus, we infer that the root cause of the leakage currents is a deterioration of the dielectric qualities of the nylon rotor material caused by elevated temperature and absorbed moisture. To be more definitive would require more testing of the potentiometers. However, an initial step toward eliminating this failure mechanism would be to use a nonhydrogen-bonded dielectric material in the potentiometer rotor assembly.

To enhance the temperature stability of the transmitter design, Barton has recommended the installation of new potentiometer mounting brackets and fiberglass washers to electrically isolate the potentiometers from the transmitter housing [3]. As such, this corrective action does not address what we believe is the basic mechanism causing the leakage current, but does isolate the leakage path by the addition of dielectric material. Tests of the isolation washer modification showed a significant long-term improvement in transmitter temperature sensitivity. Test results also showed that three of the four modified transmitters tested exhibited large positive error pulses during the first 40 seconds of exposure. While a definite long-term improvement in performance can be attributed to the installation of the isolation washers, this short-term anomaly prevents us from drawing a firm conclusion about the isolation washer effectiveness.

The second potential common mode failure mechanism is corrosion of the potentiometer's resistive element. Approximately 550 hours into the initial test, output from the transmitter exposed to the LOCA steam only environment exhibited short circuit conditions. Upon examination, we found that the resistive element in the span potentiometer had opened, thus breaking the circuit. Scanning electron micrographs of the failure point show distinct characteristics of corrosion. The timing of the failure is also consistent with the operation of a corrosion mechanism activated by high temperatures. Analysis of the corrosion point and the underlying mandrel wire showed the presence of chlorine and sulphur, both elements that tend to initiate and enhance corrosion processes. We traced the origin of these elements to lubricants applied during the manufacture of the potentiometers. Further evaluation of this problem is necessary to confirm its generic implications.

The observed thermal behavior of the transmitters coupled with the hypothesized mechanism causing this behavior, raises a question about whether accelerated thermal aging to an intended end-of-life condition produces the most vulnerable operational state for this transmitter. Since the magnitude of the error decreased with the time-at-temperature, we believe the thermal aging exposure of a qualification sequence may mask or diminish the errors observed during a subsequent LOCA exposure. Thus, thermal aging may not place this model of transmitter in its most vulnerable state prior to the LOCA exposure. This possibility is recognized by IEEE Standard 381-1977 [6] which

states in Section 5.8.1 that "in some instances, aging may actually improve equipment capability to perform." Even though we did not investigate the response of aged equipment, our testing appears to have discovered an example where such an effect may occur. We therefore agree with the recommendation of IEEE 381-1977 [6] that an understanding of equipment failure modes is essential to the qualification process. Obtaining this understanding may dictate that "more than one piece of equipment or component thereof may have to be tested such that samples are aged to different degrees of advanced life and then analyzed/ tested to establish limiting cases" [6]. It is also important that the instruments' performance be recorded at each temperature level and across its entire range of operation.

## 1.0 INTRODUCTION

### 1.1 General

Research has been conducted at Sandia National Laboratories (SNL) within the Component Assessment Program to evaluate the failure and degradation modes of unaged electronic instruments exposed to environments within and beyond the design basis. Current qualification test requirements as they relate to electronic instruments in containment were also evaluated. This report summarizes an experimental evaluation of pressure transmitter performance in harsh environments.

The specific objectives of this work were (1) to determine and isolate the effects of individual and simultaneous environmental stresses, (2) address severe accident questions by testing beyond normal design basis environments envelopes, (3) to investigate current qualification test methodology for instrumentation incorporating electronic circuitry, and (4) to identify and analyze weak-link circuit components to ascertain the mechanisms causing their degradation. In addition, this test effort was able to provide an independent source of information for evaluating the merits of an equipment modification recommended by the vendor for improving transmitter temperature characteristics.

### 1.2 Overview of Tests Performed

To achieve these research objectives, pressure transmitters were chosen as test specimens. Pressure transmitters are a basic component in Class 1E instrumentation circuits, provide critical reactor and plant state information, and may provide vital information for accident management. Our test matrix exposed five ITT Barton Model 763, 0-1000 psig, 4-20 mA, pressure transmitters to five separate environments. One transmitter was exposed to each environment. They are referred to herein as transmitters T1 through T5. The environments were (1) simulated Loss of Coolant Accident (LOCA) steam/chemical spray conditions alone (transmitter T1), (2) temperature alone (transmitter T2), (3) radiation alone (transmitter T3), (4) simultaneous radiation and LOCA temperature (no steam) conditions (transmitter T4), and (5) simultaneous radiation and simulated LOCA steam/chemical spray conditions (transmitter T5). The lengths of exposure ranged from 24 to 58 days.

LOCA simulation exposure generally followed the temperature profile recommended in IEEE 323-1974 Appendix A [4]. However, saturated steam conditions were maintained throughout the exposure and hence the pressure profile did not follow IEEE 323 Appendix A recommendations.

During the majority of the test sequence, a process pressure stimulus of 600 psig nitrogen was applied. In the first 172 hours of exposure, ten functional tests were conducted. Pressures at 200 psi increments over the range of 0 to 1000 psig were applied to observe environment-induced effects on transmitter calibration.

Subsequent to the main test exposures, a special test was conducted to evaluate a modification recommended by Barton to improve the transmitters' temperature stability. This temperature sensitivity has been reported by Barton in a series of 10 CFR 21 disclosures [1,2,3]. Data from this test allowed direct comparison of transmitter behavior during the initial LOCA transient before and after modification.

## 2.0 TEST SPECIMENS

The specific instruments used in these tests were ITT Barton Model 763, 0-1000 psig, 4-20 mA, pressure transmitters. The instruments tested have serial numbers 1479, 1480, 1481, 1483, and 1484 and were manufactured in August 1982.

### 2.1 Specifications

Technical specifications for the Barton Model 763 gauge pressure transmitter are given in Table 2-1 [5]. Figure 2-1 is a photo of the transmitter.

---

Table 2-1

Model 763 Gauge Pressure  
Electronic Transmitter Specifications

Input.....	0-1000 psig
Output.....	4-20 mA dc
Reference Accuracy.....	$\pm 0.5\%$ of maximum span including the effects of conformance (nonlinearity), deadband, hysteresis, and repeatability. Calibration is by the end point method with calibrated zero and full-scale held to $\pm 0.05\%$ of true calibrated values.
Sensitivity.....	$\pm 0.01\%$ of maximum span
Power Requirements.....	15 Vdc plus 2 Vdc per 100 ohm load to 50 Vdc maximum (4-20 mA).
Load Range.....	4-20 mA dc. Total loop resistance: 50 ohms per Vdc above 15 Vdc (1750 ohms max.)
Load Effects.....	Less than $\pm 0.05\%$ of maximum span per 100 ohm change (4-20 mA dc)
Zero Suppression.....	Factory adjustable up to 100%. Field adjustable up to 30% with potentiometer
Power Supply Effects...	Less than $\pm 0.025\%$ of maximum span per 1 Vdc change (4-20 mA dc)

Table 2-1 (continued)

Model 763 Gauge Pressure  
Electronic Transmitter Specifications

Temperature Effects....	$\pm 1.0\%$ of maximum span per 100°F change from +40°F to +150°F
	$\pm 1.5\%$ of maximum span per 100°F change from +150°F to +320°F
Radiation Effects	
Gamma.....	$\pm 10\%$ at $2 \times 10^8$ Rads total integrated dose
Beta.....	Pressure boundaries tested to $9 \times 10^8$ Rads total integrated dose
Seismic Effects	
Input.....	Random bi-axial inputs from 2 Hz to 33 Hz
Level.....	9.0G for OBE at 5% critical damping-- 12.5G for SSE at 5% critical damping
	Less than $\pm 5\%$ error during the event for ranges of 500 to 5000 psig
	Less than $\pm 10\%$ error during the event for ranges of 100 to 500 psig
Safety Function	
Performance.....	5.0% error during the first five minutes of the DBE Simulation, $\pm 10.0\%$ error thereafter to the conclusion of the DBE test as performed per ITT Barton Document No. 9999.3093.2 (100 days)
Time Response.....	Less than 180 ms for 10% to 90% step function
Maximum Safe Working Pressure.....	150% of maximum span without damage
Process Connection.....	1/2 inch NPT (female)
Weight.....	15 lbs
Electrical Interface...	96", 18 AWG, 2-wire pigtail, color coded

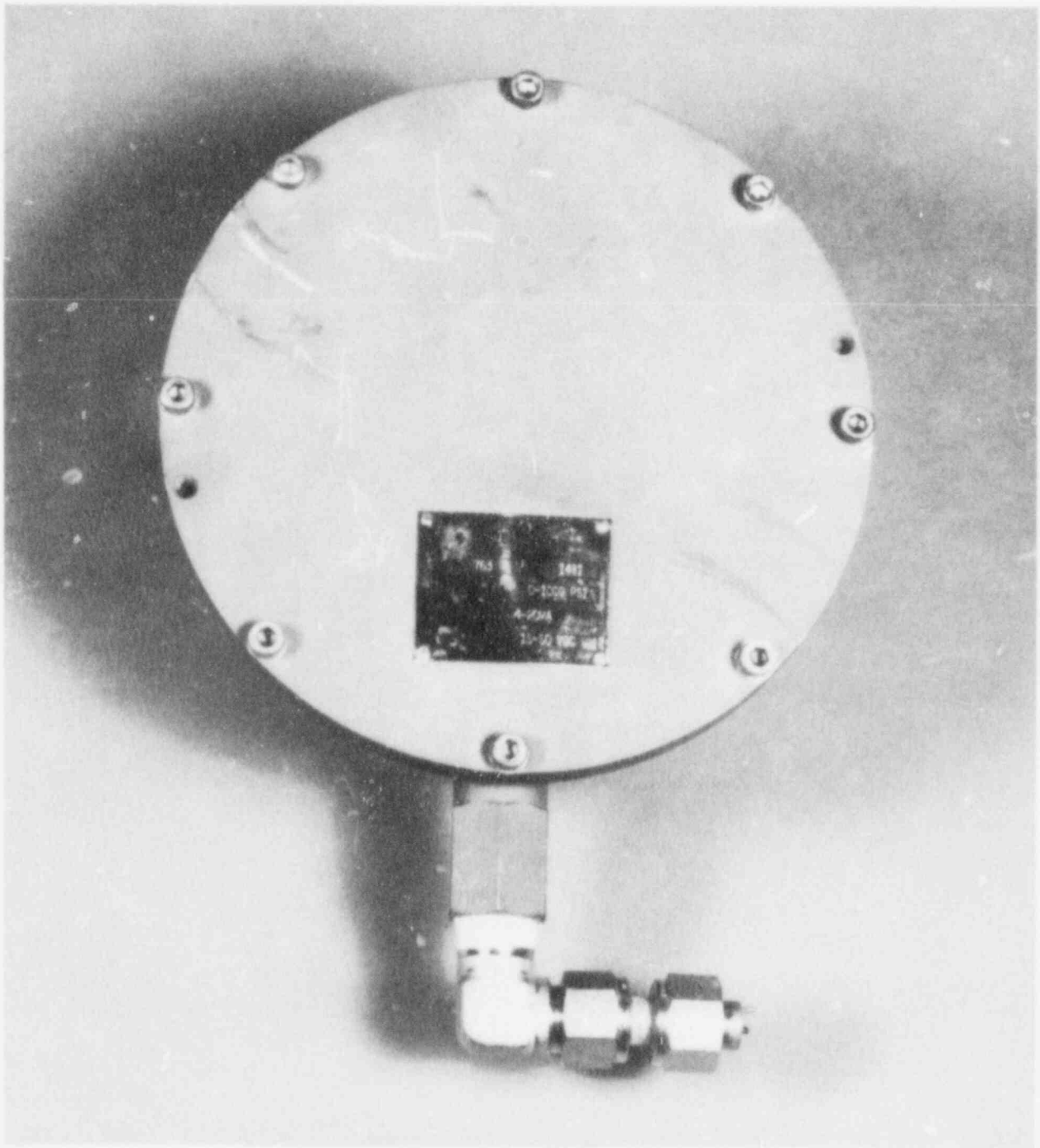


Figure 2-1 Barton Model 763 Transmitter

### 3.0 TEST ENVIRONMENT EXPOSURES

In order to establish a baseline performance and to avoid introducing failures which might result from an accelerated aging process, the transmitters were tested in the "as received" condition. Neither thermal nor radiation aging was performed prior to the testing. Two steam chambers were used; one was located inside the radiation cell and one was located outside the radiation cell. Both were connected in parallel to the steam supply system and hence, except for exposure duration, both experienced the same environmental profile. A brief description of each test environment follows.

#### 3.1 LOCA and Chemical Spray

Transmitter T1 (Serial Number (S/N) 1480) was exposed to a Design Basis Event (DBE) Loss of Coolant Accident (LOCA) steam environment for 575 hours (24 days) without radiation. The temperature profile of the exposure generally followed the recommendations of IEEE 323-1974 Appendix A [4]. Plots of the actual temperature histories are shown in Appendix A, Figures A-1, A-3, and A-5. A comparison of the temperature profile with those indicated in the ITT Barton qualification document [7] shows that our temperature profiles were less severe than those achieved by Barton in their tests. Saturated steam conditions prevailed throughout the exposure, and therefore the achieved pressure profile was more severe than IEEE 323-1974 Appendix A recommendations. The saturated steam conditions enhanced the heat transfer rates to the transmitters over those experienced by the vendor in their qualification tests [8]. A borated chemical spray solution having the formulation described in IEEE 323-1974 Appendix A [4] was applied during the first 24 hours of LOCA simulation exposure.

#### 3.2 Temperature Only

Transmitter T2 (S/N 1481) was mounted in an air circulating oven and was exposed to a dry, thermal environment. During the experiment, the oven temperature was varied over a range of 105°C to 180°C (221°F to 356°F) to observe temperature effects. The temperature profile was chosen somewhat arbitrarily and did not follow the temperature profile of the LOCA exposure sequence.

#### 3.3 Radiation Only

Transmitter T3 (S/N 1479) was exposed to Cobalt-60 radiation at a dose rate of 413 kilorads per hour (air) at temperatures of 18 to 35°C (64 to 95°F) for 1294 hours (58 days). This exposure resulted in a total integrated dose (TID) of approximately 527 megarads. The transmitter was rotated periodically to achieve uniform exposure.

### 3.4 Radiation and Temperature

Transmitter T4 (S/N 1484) was exposed simultaneously to a Cobalt-60 radiation and a DBE LOCA temperature environment. To achieve the radiation and temperature (no steam) environment, the transmitter was sealed inside a stainless steel enclosure (see Figure 3-1) that was in turn placed inside the steam chamber located in the radiation cell. Radiation exposure was approximately 482 megarads (air) TID at 603 kilorads per hour. For the chamber inside the radiation cell, the LOCA exposure lasted 33 days.

During post-test inspection, we found that the seal between the transmitter and the stainless steel enclosure shown in Figure 3-1 had failed, allowing water to enter the enclosure. Therefore, the intended objective--to isolate the transmitter from the steam environment--was not maintained throughout the entire test sequence (see Section 10.5).

### 3.5 Radiation, LOCA, and Chemical Spray

Transmitter T5 (S/N 1483) was exposed simultaneously to a Cobalt-60 radiation, DBE LOCA steam and chemical spray environment. This transmitter was installed in the steam chamber located inside the radiation cell along with transmitter T4. Hence the radiation exposure and LOCA profile for T5 was identical to those for T4; however since T5 was not protected by the stainless steel enclosure, it was exposed to the steam and chemical spray. Except for irradiation and duration of exposure (33 days versus 24 days), transmitters T5 and T1 experienced the same environmental exposure.

### 3.6 Special LOCA Transient Exposure

To evaluate the modification recommended by ITT Barton for improving transmitter temperature stability, four transmitters were modified. These were transmitters T1, T2, T3, and T5. The modification kits were supplied by Barton. After modification, the transmitters were resealed using new O-rings and were exposed to the initial LOCA transient and held at a temperature of 175°C (347°F) for approximately one hour. The exposure temperature was then decreased to ambient during a 1.6-hour period.



Figure 3-1 Transmitter T4 in Stainless Steel Enclosure

## 4.0 TEST FACILITIES

### 4.1 Test Apparatus

Testing was performed at the Sandia National Laboratories High Intensity Adjustable Cobalt Array (HIACA) facility [9]. The configuration of the transmitters in the steam chambers is shown in Figures 4-1 and 4-2. Steam entered the chambers from ports in the top of the chamber head (approximately 60 cm from the transmitters). The steam inlet ports contained baffles to preclude direct steam impingement.

Dry thermal testing was accomplished using a Hotpack Model 817B air circulating oven (see Figure 4-3) having temperature control accuracy of  $\pm 2$  percent. The temperature set points were manually adjusted to the desired temperature.

Exposure environment and transmitter temperatures were monitored using Type K thermocouples having 0.75 percent accuracy and a time constant of approximately 3.5 seconds. The temperature at each transmitter location was separately monitored. Vessel pressures were monitored using dual high-range (0-200 psig) and low-range (0-30 psig) electronic pressure transducers with 5.0 percent measurement accuracy.

### 4.2 Test Configuration

The test configuration of each transmitter is shown schematically in Figure 4-4. The pressure transmitters were connected in series to two 500-ohm (nominal) resistors and a 40 volt dc power supply. The current in the instrumentation loop was monitored by measuring the voltage drop across one of the 500-ohm resistors. The voltage appearing across the second resistor was connected to the input of an ac-coupled EG&G PAR Model 103 adjustable gain amplifier to obtain circuit noise data. The amplifier outputs from all five transmitter circuits were recorded using a Honeywell 101 Wideband II FM recorder. Noise data in the dc to 25 kHz frequency spectrum was simultaneously viewed on a Hewlett Packard Model 3532 fast Fourier transform spectrum analyzer. Analysis of the noise data is not included in this report.

The test pressure applied to the sensing element of each transmitter was controlled by a pressure station. That pressure station, shown in Figure 4-5, consisted of a valving network which connected a pressure header to each transmitter's pressure port. A main pressure regulator allowed adjustment of header pressure between 0 and 1000 psig. The valving at the pressure station allowed each transmitter to be independently pressurized, vented, and isolated from the pressure header.

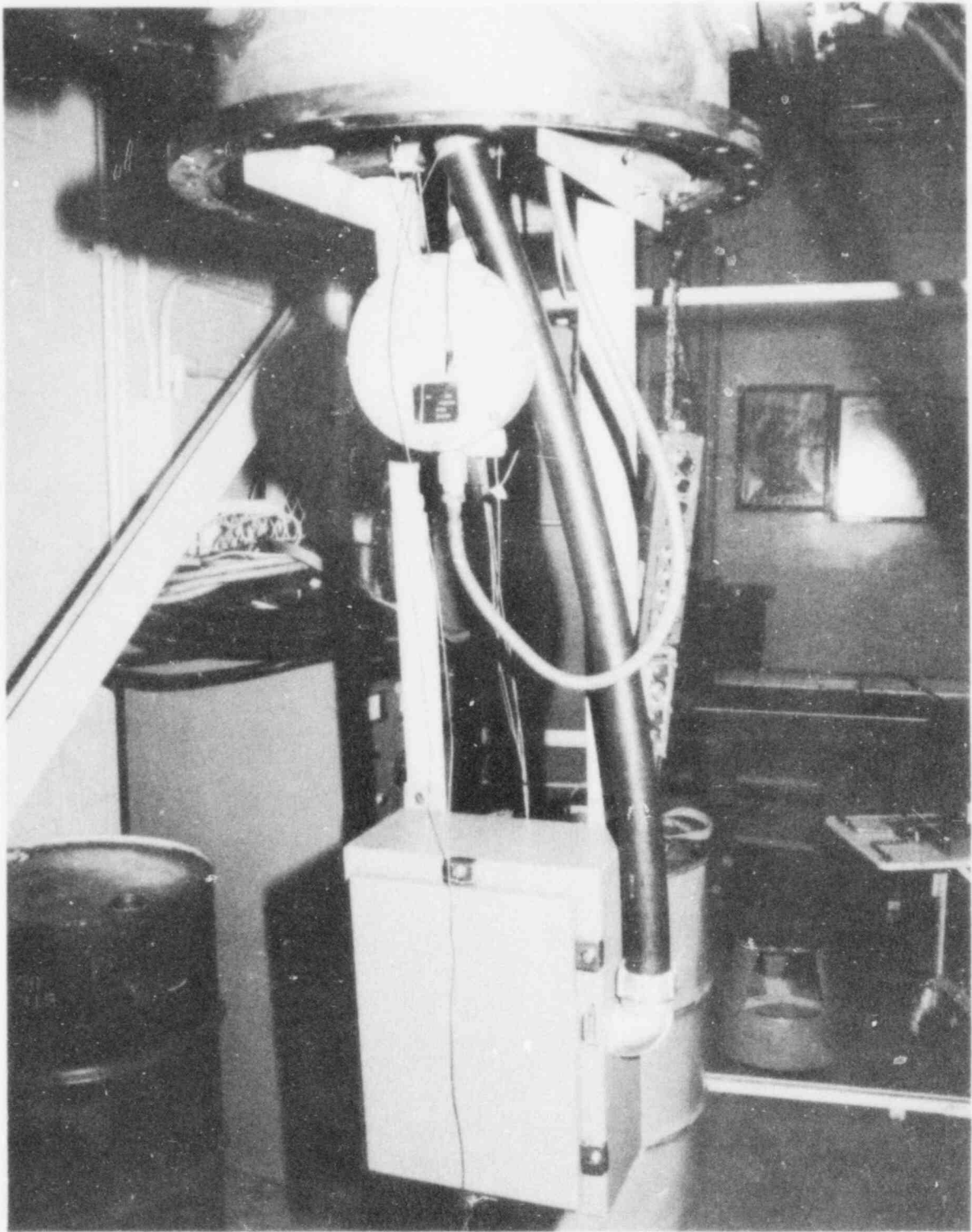


Figure 4-1 Transmitter T1 Test Configuration

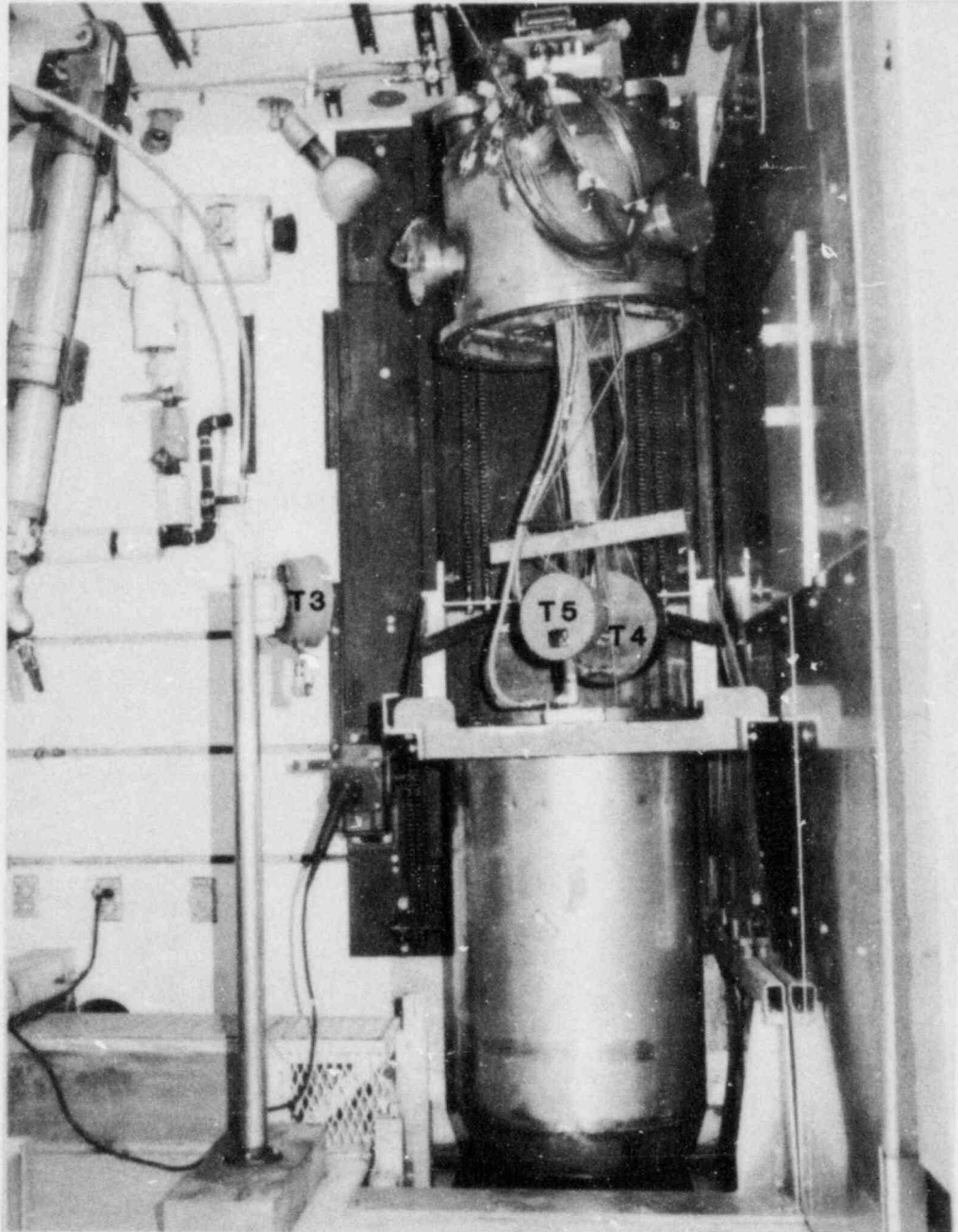


Figure 4-2 Transmitters T3, T4, and T5 Test Configuration

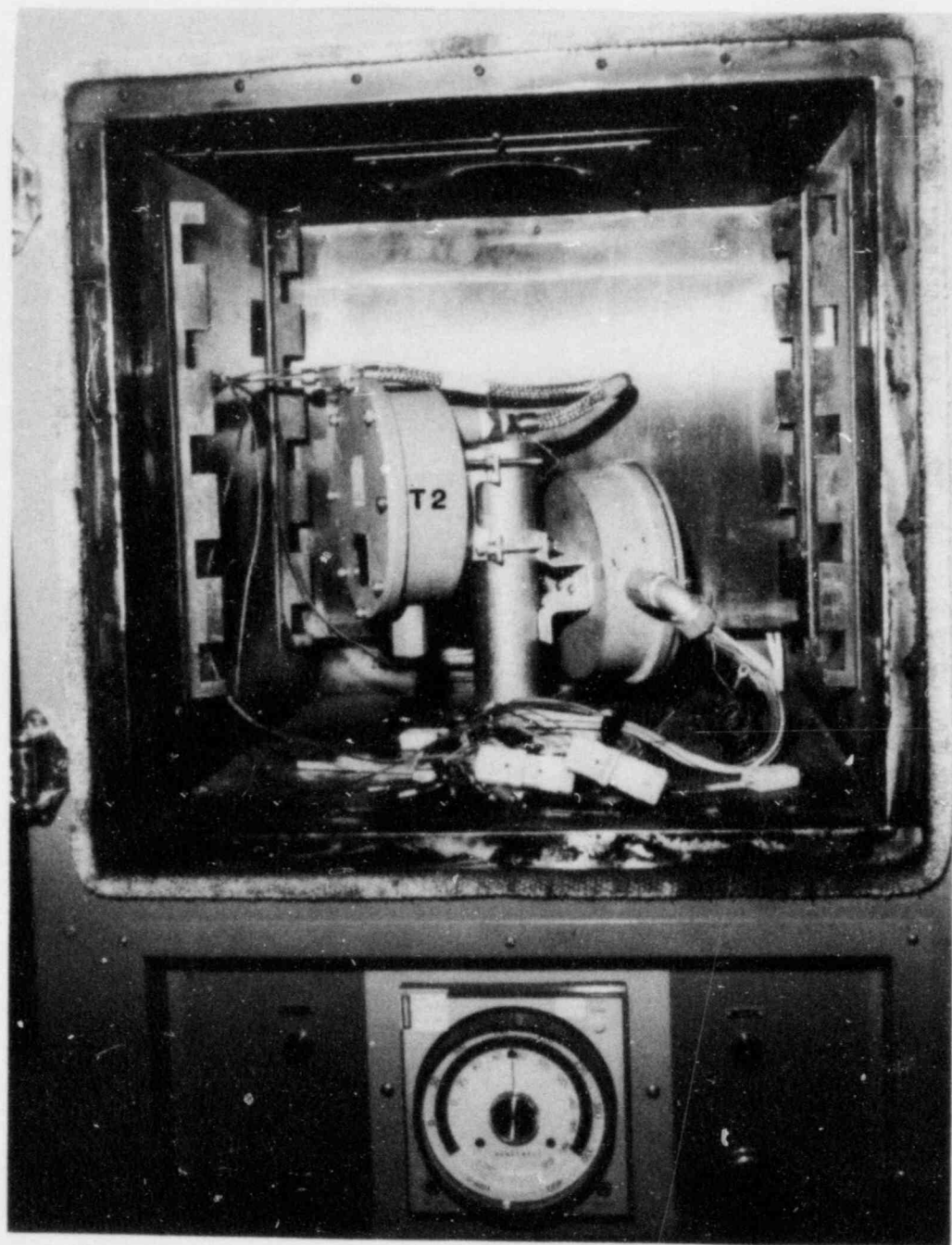


Figure 4-3 Transmitter T2 Test Configuration. The second transmitter shown was modified to allow thermocouples to be inserted and was used only to monitor temperatures of electronic components inside the transmitter. It served no other purpose in this test.

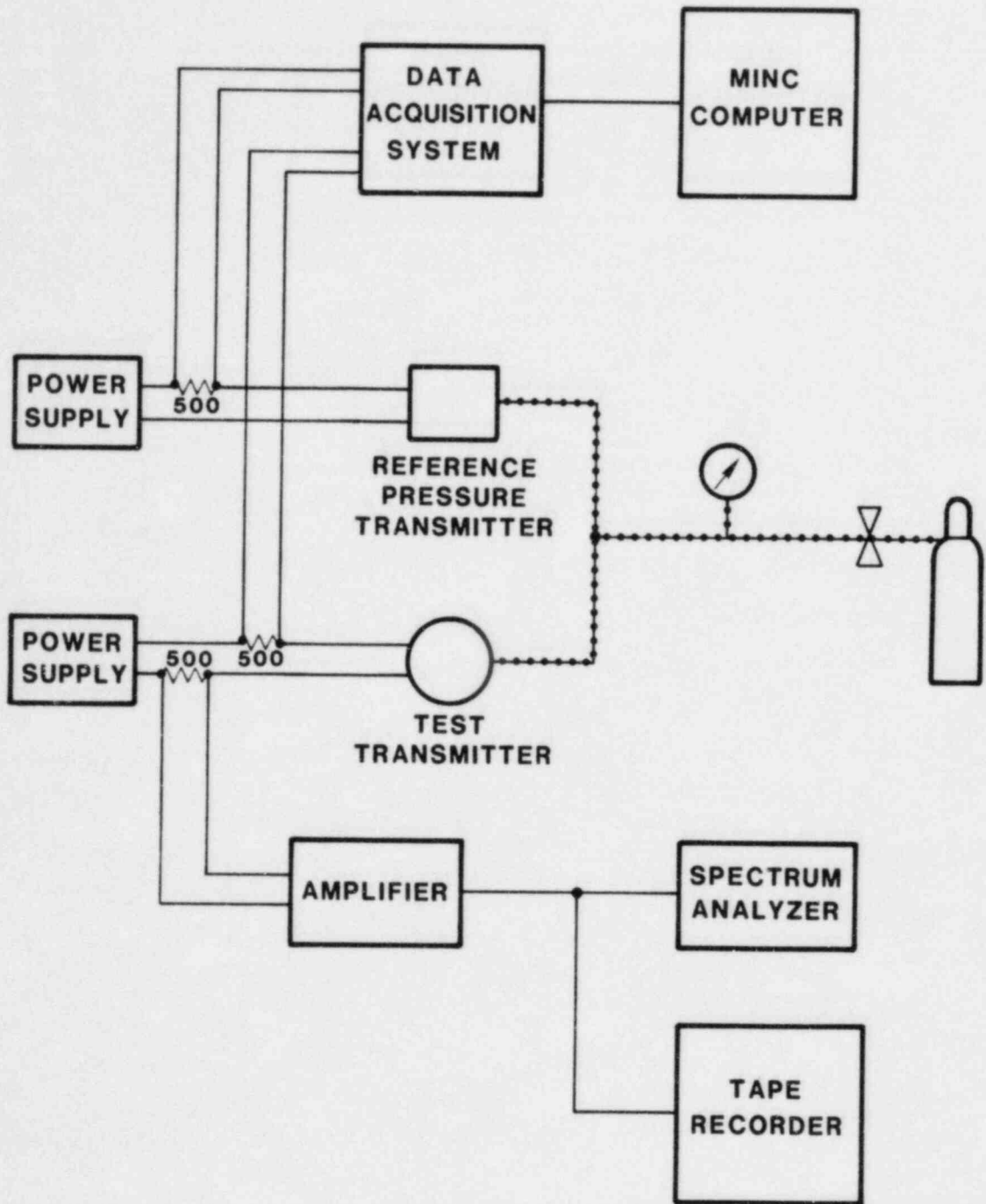


Figure 4-4 Test Configuration Schematic

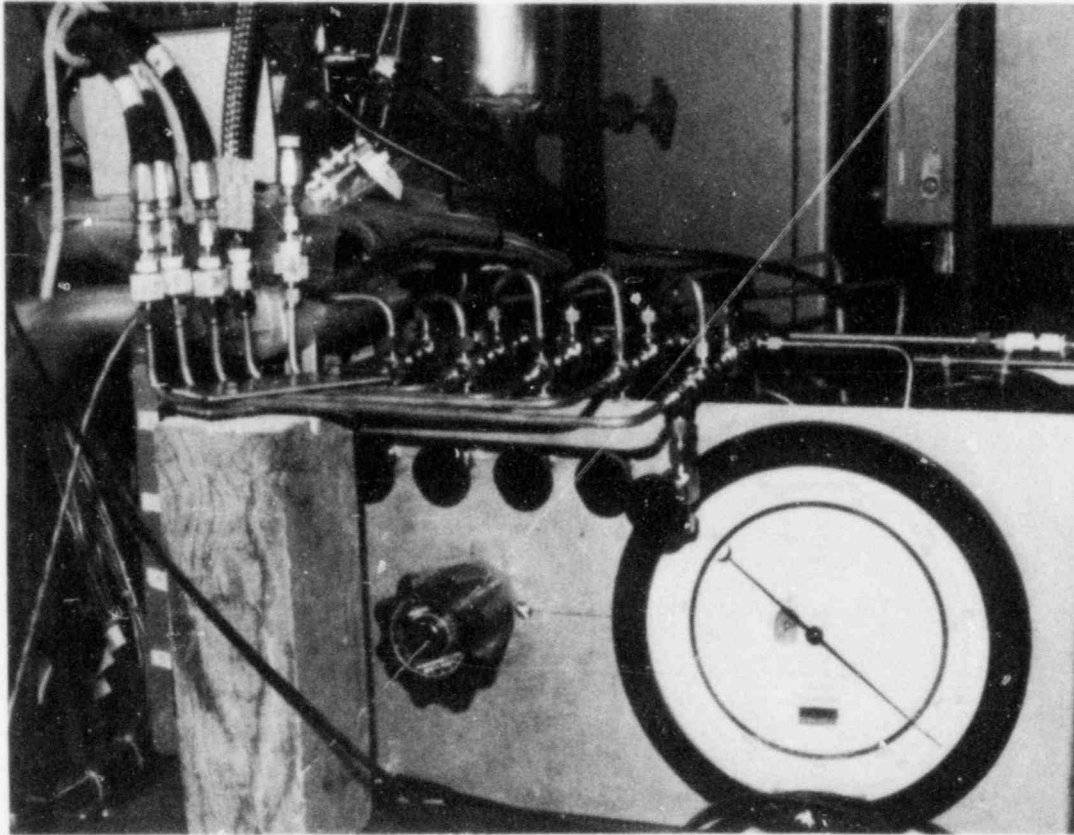


Figure 4-5 Pressure Station

Reference pressure was monitored by two separate means. Header pressure was indicated by a 0-1000 psig Heise pressure gauge model CMM having a calibrated accuracy of  $\pm 1$  percent of full scale. The pressure applied to each transmitter was measured using a Wallace and Tiernan Model 66-300, 0-1000 psig digital pressure gauge. The digital pressure gauge has a calibrated accuracy of  $\pm 0.1$  percent of full-scale reading.

The Wallace and Tiernan digital pressure gauge electrical outputs are 4-20 mA dc. Their instrumentation loop, shown in Figure 4-4, consisted of a 40 volt dc power supply and a 500-ohm resistor in series with the pressure instrument. The voltage appearing across the 500-ohm resistor was monitored by the data logger similar to test specimen signals. This allowed for simultaneous logging of reference and test specimen pressures.

#### 4.3 Data Acquisition

Electrical, temperature, and pressure data were recorded using Autodata A901 and A Ten/10 data loggers. The data was transmitted to a Digital Equipment Corporation MINC computer where it was stored on hard disk files. Specific analog information was recorded using Hewlett Packard Model 7132A chart recorders.

## 5.0 DATA PRESENTATION

### 5.1 Organization of Figures in Appendices

Due to the need to present the data in many different formats, a large number of plots is contained in the appendices to this report. They are organized into five sections, one section for each of the five transmitters tested. The primary figure number is used to indicate the format of the data presentation. To uniquely identify data for each transmitter, a prefix is added to this figure number. For example, Figure A-2 shows the error profile throughout the experiment for the transmitters. Figure T1-A-2 shows the error profile for transmitter T1. Similarly, T4-A-2 shows the error profile for transmitter T4.

Thus, references to plots can be either specific (i.e., T1-B-1) referring only to one figure or multiple referring to a series of plots of the same format for all transmitters (i.e., B-3 or B-12). For consistency with industry specification practices, error data is presented in this report as a percent of full-scale unless otherwise noted.

### 5.2 Constant Pressure Data

The constant pressure data contains information characterizing the behavior of each transmitter while pressurized at 600 psig (nominal). This data is presented in Appendix A in the following formats:

- 1) Temperature History - provides a graphical history of the applied temperature during the test. Data is plotted for the first 26 and first 100 hours of exposure (Figures A-5 and A-3) and for the entire exposure interval (Figures A-1). Similarly, data is plotted for the special LOCA transient exposure conducted after the main test (Figures A-9).
- 2) Error vs Temperature - indicates error as a function of temperature. Two plots are presented. One plot (Figures A-7) shows the data for the entire exposure interval. The second plot (Figures A-8) shows data for the special LOCA test conducted after the main test.
- 3) Error History - four plots show error as a function of time for the periods of 26, 100, and 1300 hours (Figures A-6, A-4, and A-2) as well as the special LOCA transient test conducted after the main test (Figure A-10).

### 5.3 Functional Test Data

During the test, ten functional tests were conducted. Readings were taken upscale and downscale at 0, 200, 400, 600, 800, and 1000 psig levels. This data is presented in Appendix B in the following formats:

- 1) Error vs Temperature - indicates error as a function of temperature. Figures B-1 shows the scatter in readings from nominal for all functional tests.
- 2) Data Scatter (Actual vs Reference) - shows the variability in transmitter readings at each of the measurement points. This is shown in Figures B-2.
- 3) Calibration Correlation - indicates the correlation between the actual and reference readings for each of the ten functional tests. Upscale and downscale readings are plotted. These are shown in Figures B-3 through B-12. For reference purposes, a dotted line on each figure indicates desired correlation.
- 4) Error vs Pressure - shows error as a function of applied pressure during each of the ten functional tests. Upscale and downscale readings are plotted. These are shown in Figures B-13 through B-22.
- 5) Temperature History - provides a graphical history of the temperatures applied during each of the functional tests. This plot (Figures B-23), when evaluated with the error versus temperature (B-1) allows for concurrent analysis of the error with respect to temperature at the time of reading.
- 6) Error History - shows error at each of the six pressure measurement points (0, 200, 400, 600, 800, and 1000 psig). Upscale and downscale readings are plotted. The error histories are shown in Figures B-24 through B-29.

## 6.0 TEST OBSERVATIONS

### 6.1 Radiation Tolerance

Transmitters T3, T4, and T5 were exposed to radiation. Transmitter T3 was exposed to radiation alone. Transmitter T4 was exposed to the radiation and LOCA temperature environment. Transmitter T5 was exposed to the radiation and the LOCA steam/chemical spray environment. All three transmitters exhibited excellent radiation tolerance. Table 6-1 contains a tabulation of the calibration error observed prior to exposure and at 100 Mrd exposure increments, to 400 Mrd exposure. Readings at 200 Mrd compare favorably with the ITT Barton specification of a  $\pm 10$  percent at 200 Mrd exposure (see Table 2-1).

---

Table 6-1

Radiation-Exposed Transmitter Errors at 100 Mrd Intervals  
(Percent of Full Scale)

<u>Exposure</u>	<u>Transmitter</u>		
	<u>T3</u>	<u>T4</u>	<u>T5</u>
Initial	+0.01%	-0.06%	-0.002%
100 Mrd	-0.4%	-2.0%	-2.7%
200 Mrd	-1.2%	-2.9%	-3.4%
300 Mrd	-1.9%	-3.4%	-5.1%
400 Mrd	-2.8%	-5.0%	NA

---

Total exposure dose/dose rate (air): T3 - 527 Mrd @ 413 krd/hr  
T4, T5 - 482 Mrd @ 603 krd/hr

---

#### 6.1.1 Discussion of Observations

##### Radiation Environment Alone

Figure T3-A-2 shows the performance of T3 which operated over a temperature range of 18° to 35°C (64°F to 95°F) during its exposure. Transmitter error decreased from an initial value of +0.01 percent to -1.5 percent in the first 50 hours (20 Mrd) of exposure, recovering to +0.12 percent at approximately 300 hours (115 Mrd). As the exposure continued to approximately 1300 hours (527 Mrd), the error gradually decreased to -4.9 percent. Closer examination of the figure shows that T3 began exhibiting an increased rate of degradation after approximately 870 hours (350 Mrd). Between that time and the end of the test (177 Mrd of

exposure), the transmitter produced a -2.8 percent change in error compared with a -2.1 percent change during the prior 350 Mrd of exposure. The change in calibration depicted by the slope of the curve between 300 and 1300 hours is -1.2 percent/100 Mrd.

Investigation of transmitter response during radiation exposure transitions produced additional information. During irradiation, transmitter T3 was rotated periodically so that the electronics would receive uniform exposure. Rotation allowed the front or either side of the transmitter to face the radiation source. We analyzed the change in transmitter output at each rotation and found that the transmitter was essentially position insensitive. The maximum short-term change in output after rotation was less than  $\pm 0.5$  percent. Initial short-term change in performance when one side of the transmitter or the other faced the source was less than 0.3 percent. This initial change mitigated and in the long term essentially no difference in performance was observed when either side faced the source. Comparing transmitter performance during side and front irradiation, we found a 0.1 percent increase in error when the transmitter faced the radiation source.

We evaluated transmitter T3 response to the raising and lowering of the radiation source. By "lowering the source" we mean discontinuing irradiation. During the early hours of exposure (~30 Mrd), lowering the source produced less than -0.2 percent change in transmitter output. At approximately 300 hours (~100 Mrd), the transmitter showed about a -1.2 percent change in output when the source was lowered; while at approximately 800 hours exposure (~300 Mrd), a 0.9 percent sensitivity was observed. Error increased negatively when the source was lowered. The error returned to prior values when irradiation resumed.

#### Radiation and Temperature Environment

The performance of T4 shown in Figure T4-A-2 indicates a markedly different profile than that for T3. However, the general slope of the error plot continues negatively throughout the entire exposure. Linearizing the slope of the curve between 30 and 700 hours (17-415 Mrd), the change in calibration is -1.1 percent/100 Mrd. The large positive and negative errors shown during the first 17 hours of exposure are related to temperature effects associated with LOCA exposure (see Section 6.2).

In Figure T4-A-2, the perturbations shown at approximately 310 hours are attributed to: (1) a temporary excursion from 105°C (221°F) to 38°C (100°F) caused by a steam system anomaly and (2) a temporary suspension of radiation exposure. Also, at approximately 360 hours, a temporary steam system temperature excursion from 105°C (221°F) to 83°C (181°F) produced another perturbation in the error profile. The change in error profile

beyond 650 hours is attributed to leakage current between the transmitter's external wires and from the wires to ground. The shape of this portion of the error plot is similar to the characteristic leakage current profile reported earlier [10]. Post-test analysis of T4 showed that the transmitter wiring was brittle and cracked and that water had entered the transmitter's isolating enclosure (see Sections 10.3 and 10.4).

The performance of transmitter T5 shown in Figure T5-A-2 is similar to that shown for T4. The general slope of the error plot is negative as exposure dose is increased. For the first 300 hours (180 Mrd), the change in calibration follows a slope of -2.4 percent/100Mrd. Between 300 hours and 500 hours (300 Mrd), the slope is -1.3 percent/100 Mrd. As for transmitter T4, the large errors during the early hours of the test are related to temperature effects.

The perturbations at approximately 310 and 360 hours are caused by the same temperature- and radiation-related events described for transmitter T4. The erratic error profile after 430 hours is attributed to leakage current between conductors and ground. A chart recorder trace of T5 output showed the presence of a significant amount of noise (characteristic of moisture-related leakage current) [10]. Post-test analysis of T5 showed that the transmitter wiring was brittle and cracked and that water was contained in the transmitter's wiring conduit (see Sections 10.3 and 10.4).

Transmitter T4's response when raising and lowering the radiation source was also evaluated. The error increased (became more negative) when the source was lowered. The error returned to prior values when irradiation resumed. For transmitter T4 the change in error profile ranged between -0.2 and -0.6 percent when the source was lowered. Sufficient data was not available to evaluate T5 response.

#### 6.1.2 Comparison of Observations

The most significant difference between the performance of T3 exposed to radiation alone and T4 and T5 exposed to radiation and LOCA environments are the large shifts in output of transmitters T4 and T5 during the early hours of LOCA exposure. We attribute these shifts to temperature effects. Comparing transmitter errors at 200 Mrd exposure, we find that transmitters T4 and T5, exposed to radiation and LOCA environments, exhibited at least twice the error of transmitter T3, exposed to radiation alone. Again, we believe this difference is due mainly to the effects of the elevated thermal exposure at the beginning of the test.

Observing the effects produced by raising and lowering the radiation source, we find that the changes in output for T3, T4,

and T5 are similar and that the output changes less than 1.5 percent. Finer analysis of data for T4 and T5 concurrently exposed to a thermal environment could not be made. On some occasions, temperature changes were occurring at the same time the radiation source was lowered. With respect to radiation, we conclude that this transmitter design is relatively hard to the effects of Cobalt 60 radiation.

## 6.2 Temperature Effects

Transmitters T1, T2, T4, and T5 were exposed to thermal environments. Transmitter T2 received its temperature exposure in an oven, while Transmitters T1, T4, and T5 received their LOCA profile exposure in steam chambers. Transmitters T4 and T5 were also exposed to radiation.

Transmitters T1, T4, and T5 exhibited similar responses during the initial 100 hours of exposure (see Figures A-4). The transmitters all showed temperature-related and time-at-temperature-related effects. These effects appeared as distinct calibration shifts at exposure temperature transitions. As the temperature was increased or decreased stepwise during the LOCA test sequence, concurrent increases or decreases in error were generally observed.

Changes in transmitter output became noticeable above 122°C (252°F). Temperature increases above 122°C generally produced positive increases in error. While maintaining a constant temperature at the 173°C or 160°C (343°F or 320°F) levels, error decreased exponentially with time. At 140°C (284°F), the error reversed direction and became negative. As the temperature was further decreased to 122°C (252°F), the error shifted even further negatively. At the temperature transition from 122°C (252°F) to 105°C (221°F), a corresponding permanent shift in calibration was not observed, though a small variation in the output is apparent. Transmitter response at each temperature plateau of the LOCA profile is compared in Table 6-2.

To verify that the observed errors were related only to temperature and not to the combination of the temperature and steam environment, oven temperature was varied over a range of 105-180°C (221-356°F). Over this temperature range, the response of transmitter T2 was in agreement with the responses of T1, T4, and T5.

When the error profiles for T1, T3, T4, and T5 are compared after 22 hours elapsed time, (i.e., when the environmental temperatures are 122°C (352°F) or below) the effects of radiation become noticeable. Referring to Figures A-2, between approximately 22 hours and approximately 330 hours, transmitters T1 and T3 exhibited a positive slope in their error curves (back towards zero error), whereas for the same time period, transmitters T4

Table 6-2

LOCA Temperature-Exposed Transmitter Error  
Observations at Selected Intervals  
(Percent of Full Scale)

	Temp °C (°F)	T1	T4	T5	Error* Specification T1/T4 & T5
Maximum Error 1st LOCA Peak	173 (343)	+21.1%	-9.0%	+26.8%	+4.0%/+4.0%
End 1st LOCA Peak	173 (343)	+10.7%	+5.7%	+12.4%	+4.0%/+4.1%
Maximum Error 2nd LOCA Peak	173 (343)	+10.3%	+5.5%	+12.0%	+4.0%/+4.2%
End 2nd LOCA Peak	173 (343)	+8.3%	+4.4%	+8.8%	+4.0%/4.3%
Beginning 1st Plateau	160 (320)	+3.6%	+2.3%	+4.3%	+3.7%/+4.1%
End 1st Plateau	160 (320)	+3.0%	+1.2%	+3.2%	+3.7%/+4.2%
Beginning 2nd Plateau	140 (381)	-0.7%	-7.0%	-0.2%	+3.1%/+3.6%
End 2nd Plateau	140 (381)	-0.4%	-7.1%	+0.1%	+3.1%/+3.5%
Beginning 3rd Plateau	122 (252)	-1.8%	-1.3%	-1.0%	+2.6%/+3.3%
End 3rd Plateau	122 (252)	-0.9%	-1.7%	-1.4%	+2.6%/+5.4%
Beginning 4th Plateau	105 (221)	-1.4%	-1.8%	-1.8%	+2.2%/+5.0%
At 500 Hrs Elapsed Time	105 (221)	+ 1.0%	-3.4%	-4.9%	+ 2.2%/+12.2%

\* Maximum allowable temperature error from specifications in Table 2-1. T4 and T5 specification includes allowance for radiation effects proportional to exposure dose based on 10 percent maximum error at 200 Mrd exposure.

and T5 exhibited negative slopes in their error curves (increasing negative error). In fact, the error curves for transmitters T1 and T3 are almost identical between hours 22 and 330. Noting that the two transmitters in single environments (T1 and T3) behaved alike and that the two transmitters in combined environments (T4 and T5) behaved alike, we can conclude that a small synergistic effect may have been occurring. However, the magnitudes of the errors at these times were within specification, and the data beyond 330 hours cannot be consistently interpreted to support the conclusion that a temperature-radiation synergism existed. Thus, we must opt for a less definite position and say that no significant synergisms were observed. Further investigation into this point would be warranted if synergistic effects become important.

#### 6.2.1 Performance Observations

To illustrate typical transmitter temperature effects during LOCA simulation exposure, the performance of transmitter T1, maintained at 600 psig (nominal), will be described using Figures T1-A-5 and T1-A-6.

Application of the initial LOCA transient rapidly increased transmitter temperature from ambient to 173°C (343°F). This rapid increase in temperature caused a negative shift in calibration in the first 30 seconds of exposure from an initial value of -0.02 percent to -4.0 percent. The output then shifted positively very dramatically as the transmitter temperature stabilized. After approximately 30 minutes, the error indicated was +21.1 percent. During the next 2.5 hours while maintaining a temperature of 173°C (343°F), the error decreased exponentially to a value of +10.7 percent.

During the cooldown between initial exposure peaks, the error profile followed the temperature profile. At the bottom of the cooldown between peaks, at a temperature of 101°C (214°F), a -2.9 percent error was observed. When the temperature was again rapidly increased to 173°C (343°F), the transmitter produced an initial error of -4.1 percent followed by a rise to +10.3 percent in 45 minutes. During the remaining 3.5 hours of the second 173°C (343°F) plateau, the error decreased exponentially to +8.3 percent. The transition to 160°C from 173°C was not smooth and temperatures dipped to 136°C. The corresponding dip in transmitter output is apparent. At 160°C (320°F), the error decreased from +3.6 percent to +3.0 percent in 3.3 hours.

The transition from 160°C to 140°C caused the transmitter error to decrease to -0.7 percent. While maintaining 140°C (284°F), the error decreased from -0.7 percent to -0.4 percent in approximately 5 hours. Note that the error trend changed direction and was now approaching zero from the negative side.

At 122°C (252°F), the error initially shifted to -1.8 percent, but then began to decrease to -0.9 percent during a 72-hour period. The temperature transition from 122°C (252°F) to 105°C (221°F) produced very little permanent change in output error. Initial error at 105°C was -1.4 percent. During the next 400 hours, the error slowly increased to +1.0 percent.

The response of transmitter T5 was very similar to that of transmitter T1. This indicates that the effects attributable to the added radiation exposure were minimal when compared to temperature effects. Transmitter T4 also produced similar performance with the exception of the first 30 minutes of exposure. During that period, transmitter T4 produced a large negative error which reversed with a positive change of approximately 16 percent. After this point, transmitter T4 behaved like transmitters T1 and T5. We believe that this initial negative shift may be due to the reduced rate of heat transfer to transmitter T4 due to it being enclosed in the stainless steel can.

### 6.3 Functional Test Data

The discussions in Sections 6.1 and 6.2 concentrated on transmitter response while maintaining a 600 psig (nominal) applied pressure. To better understand environment-induced effects on transmitter performance over its entire operating range, transmitter calibration was verified at 10 points during the first 172 hours of the LOCA test sequence. Functional test measurements were made by applying test pressures at 200 psi increments from 0 to 1000 psig. (Note that functional test 0 recorded pressures at 100 psi increments). To determine if there was a direction sensitivity or hysteresis, measurements were taken upscale from 0 to 1000 psig then downscale from 1000 to 0 psig. Transmitter functional test error data was plotted with respect to time, temperature and reference pressure to develop calibration correlation and error relationship profiles. Table 6-3 identifies each functional test and indicates the figure numbers, elapsed time, and test temperature during each functional test.

#### 6.3.1 Temperature Relationships

Data for each transmitter are plotted as a function of temperature in Figures B-1. As shown, the magnitude and range of the errors increase as the temperature increases. The errors are especially pronounced at 173°C (343°F). This relationship is in agreement with the results presented in Section 6.2.

Table 6-3

Correlation of Information for the  
Ten Functional Tests

Functional Test Number*	Figure**	Elapsed Time (hr)	Test Temperature °C (nominal)		
			T1, T4 & T5	T2	T3
0	B-3,13	-0.7	21	21	21
1	B-4,14	1.5	173	150	35
2	B-5,15	7	173	150	35
3	B-6,16	13	160	150	33
4	B-7,17	23	122	150	31
5	B-8,18	29	122	173	31
6	B-9,19	95	105	150	31
7	B-10,20	121	105	146	30
8	B-11,21	167	105	21	31
9	B-12,22	172	105	180	30

\*Also referred to herein as Cal Number, e.g., Cal 0, Cal 1, etc.  
\*\*Indicates Appendix B Figure Number

### 6.3.2 Transmitter Correlation Stability

The data was replotted with respect to reference pressure. Functional test data in Figures B-2 indicate the distribution of errors at each pressure throughout the sequence of functional tests and indicate the amount of pressure sensitivity. Observing these figures, we note that the correlation curves do shift from test to test. The shifts are more pronounced for transmitters T1, T2, T4, and T5, subjected to 105-173°C (221-343°F), than that for T3, exposed at 18-35°C (64-95°F).

### 6.3.3 Calibration Correlation

The variations in output for each functional test as a function of applied pressure are presented in Figures B-3 through B-22. Figures B-3 through B-12 present the data as test instrument readings, while Figures B-13 through B-22 present the data as error in percent of full scale. These figures can be interpreted in terms of zero and span errors. Either presentation format contains the necessary information; however, the error as a percent of full scale presentation more clearly illustrates the changes in error across the calibrated range of the instruments.

Zero and span are the two adjustments made to calibrate the transmitter. These adjustments are made via two potentiometers in the transmitter. The zero potentiometer sets the transmitter's output to 4 mA with zero pressure applied. The span potentiometer adjusts the slope of the transmitter's correlation curve between applied pressure and transmitter output. Span is adjusted to produce full output (20 mA) when the maximum calibrated pressure is applied (1000 psig). In the context of the following discussion, zero errors refer to errors when zero psi is applied and span errors refer to the deviations in slope of the correlation curve from an original value. The original pretest correlation curve is shown with a dotted line in the Figures B-3 through B-12.

#### Radiation Exposure

Figures T3-B-3 through T3-B-12 for transmitter T3 show slight negative shifts in the correlation curve as time and hence accumulated dose increased. The magnitude of these shifts for the first and last functional tests are shown in Table 6-4. Figures T3-B-13 through T3-B-22 show that these shifts in output are composed of both small zero and span shifts. The character of these shifts is not the same as those observed when high temperature was part of the exposure environment, indicating that radiation exposure and temperature exposure affected different circuit components.

Table 6-4

Transmitter T3 Zero and Span Error Shifts During Irradiation  
(Percent of Full Scale)

	<u>0 psi</u>	<u>1000 psi</u>
Pre-Exposure Functional Test (Cal 0)	-0.1	-0.1
Last Functional Test (Cal 9) (~70 Mrd exposure)	-0.6	-1.1

#### Temperature Exposure

The strong effect of temperature is evident when the plots for transmitters T1, T2, T4, and T5 are reviewed. At elevated temperatures, shifts in both zero and span occurred. The magnitudes of these shifts are more pronounced at 173°C (343°F), but are also apparent at the other temperatures. Figures B-13

through B-22 show the zero and span shifts most clearly. Because of changes in slope of the correlation curve, the error across the calibrated range was not constant. During Cal 1, for example, the error in transmitter T1 at 0 psig was approximately 8 percent of full scale, while at 1000 psig, it was approximately 20 percent of full scale. As temperature decreases, we observe that both zero and span errors decrease. The shifts in these errors reflect the general trends with temperature described for the 600 psig data in Section 6.2. A nonlinearity in the decrease of the correlation curve slope is evident at 200 psig (especially for transmitter T4) where a bend in the correlation curve appears. This bend is an indication of a nonlinear offset in the transmitter measurement system. A summary of the errors observed at 0, 200, and 1000 psig during the ten functional tests is given in Table 6.5.

A hysteresis is apparent in instrument output at the higher temperatures. This effect is especially apparent for transmitters T1, T2, and T5. This effect may be a manifestation of the time-at-temperature decrease in errors since approximately five minutes elapsed between upscale and downscale measurement at a given pressure. Since the measurements were started at the low pressures, the most delay occurred at the low pressures.

The functional test data also illustrates the dependence of transmitter error on recent temperature exposure history. Consider Figures T2-B-13 (Cal 0) and T2-B-18 (Cal 5) which respectively show the error at 21°C (70°F) and 173°C (343°F) early in the test and Figures T2-B-21 (Cal 8) and T2-B-22 (Cal 9) which respectively show the error at 21°C (70°F) and 180°C (356°F) later in the test. Comparing the first pair of figures, we find that early in the test, there was a +2.7 percent increase in error at 0 psig and a +9.0 percent increase in error at 1000 psig. Comparing the second pair of figures, we find that later in the test there was a +2.8 percent increase in error at 0 psig and +3.4 percent increase in error at 1000 psig. Since the primary difference is at 1000 psi, the temperature exposure history has clearly decreased the span error that occurs over approximately equivalent temperature transitions. This behavior further illustrates the time-at-temperature behavior discussed in Section 6.2.

Table 6-5

Errors Observed During Functional Test Measurements  
for 0, 200, and 1000 psig Readings  
(Percent of Full Scale)

	T4 & T5 Exposure Dose (Mrd)	Temp °C (°F)	Error* Specification T1/T4 & T5	T1	T4	T5
Cal 0						
0 psi		21 (70)	$\pm 0.3/\pm 0.3$	-0.1	-0.0	-0.2
200 psi	0			-0.0	-0.1	-0.2
1000 psi				-0.0	-0.1	-0.2
Cal 1						
0 psi		173 (343)	$\pm 4.0/\pm 4.1$	+6.6	+1.2	+6.9
200 psi	0.9			+9.4	-15.0	+10.9
1000 psi				+19.0	+5.7	+23.6
Cal 2						
0 psi		173 (343)	$\pm 4.0/\pm 4.2$	+5.0	+4.4	+4.4
200 psi	3.0			+6.6	+2.1	+6.0
1000 psi				+13.1	+9.0	+15.5
Cal 3						
0 psi		160 (320)	$\pm 3.7/\pm 4.0$	+2.8	+3.2	+2.3
200 psi	6.6			+2.7	+0.2	+1.8
1000 psi				+4.1	+4.2	+6.8
Cal 4						
0 psi		122 (242)	$\pm 2.6/\pm 3.2$	+0.9	+1.3	+0.2
200 psi	12.3			-1.3	-1.3	-1.4
1000 psi				-2.2	-0.9	-1.0
Cal 5						
0 psi		122 (242)	$\pm 2.6/\pm 3.2$	+1.0	+1.1	+0.2
200 psi	16.2			-1.1	-1.1	-1.0
1000 psi				-1.6	-0.4	-0.3
Cal 6						
0 psi		105 (221)	$\pm 2.2/\pm 3.5$	+0.9	+0.7	-0.2
200 psi	56.3			-0.6	-1.5	-1.7
1000 psi				-1.4	-1.5	-1.5
Cal 7						
0 psi		105 (221)	$\pm 2.2/\pm 3.5$	+0.8	+0.7	-0.1
200 psi	71.5			-0.7	-1.5	-2.2
1000 psi				-1.3	-1.5	-1.7
Cal 8						
0 psi		105 (221)	$\pm 2.2/\pm 7.2$	+0.7	+0.7	-0.2
200 psi	99.3			-0.6	-1.7	-3.0
1000 psi				-1.2	-2.0	-2.5
Cal 9						
0 psi		105 (221)	$\pm 2.2/\pm 7.4$	+0.9	+0.7	-0.1
200 psi	103			-0.4	-1.6	-3.0
1000 psi				-1.0	-2.0	-2.5

\*Error specification for T4 and T5 includes allowances for radiation effects proportional to exposure dose based on 10 percent maximum error at 200 Mrd exposure.

#### 6.3.4 Temperature Stability of Functional Tests

Figures B-23 shows the temperature at each of the ten functional test points. The line connecting these temperatures merely connects the points; it has no meaning with respect to temperature profile between the points. Figures B-24 through B-29 show the stability of the transmitters at each of the six reference pressure levels. Clearly, the variations at each pressure correlate to changes in the temperature. Also apparent is the increasing magnitude of error as pressure increases.

#### 6.3.5 Comment on Error Calculation Method

The method used for calculating error percentage has a dramatic effect on the shape of the functional test error curves. The data and curves presented in this report show error as a percent of full-scale (F.S.) readings. This is the same basis used by transmitter manufacturers for specifying transmitter performance. Specifying error by this method allows a constant amount of actual error over the instruments calibrated range (i.e., 0-1000 psig for the transmitters we tested). However, if the error percentage is calculated as a percent of the applied reference pressure, a significantly different picture is presented. Using this method, the actual error is proportionately less as pressure is lowered.

The two methods allow the same actual error only at the full-scale readings. For example, a 10 percent F.S. error specification for a 0-1000 psig device allows an actual 100 psi error over the entire range of 0-1000 psig. However, using the "percent of reference" method, a 10 percent error equates to 100 psi error only at 1000 psig. At 100 psig, the allowable error would only be 10 psi. If the data in Figures B-24 through B-29 had been presented as a percent of reference pressure, the error percentages at 200, 400, 600, and 800 psi would be factors of 5.0, 2.5, 1.7, and 1.3 times greater than shown. In this format, we would see that error decreases as pressure is increased.

## 7.0 EVALUATION OF THERMAL INSTABILITY

Based on information made available through 10 CFR 21 disclosures [1,2,3] and through analysis of the data obtained in this test series, thermally-induced leakage current between the potentiometers and the transmitter housing are the primary cause of anomalies that we observed. This section gives our analysis of the mechanism causing the leakage currents. Section 8.0 gives our evaluation of the modification kit provided by Barton to alleviate this problem.

### 7.1 Potentiometer Design and Materials

With respect to the thermally-induced leakage currents, the important design feature of the potentiometer is the rotor assembly. The shaft which is in intimate electrical and mechanical contact with the potentiometer case is molded into the rotor assembly. The rotor assembly provides the mechanical support for the slider and other conductors that are part of the electrical circuit. Thus, the rotor provides the electrical isolation between the circuit and the shaft. Figure 7-1 shows a disassembled potentiometer. The major piece parts are indicated in the figure. The potentiometer manufacturer was contacted to obtain detailed information about the potentiometer piece part material compositions. The following information was obtained [11]:

<u>Item</u>	<u>Materials</u>
Front Lid & Shaft.....	Stainless Steel with Nickel Plated Bushings
Body.....	Phenolic-Fiberite FM400S
Rotor.....	Nylon 6/10-Short Fiberglass Filled
Slider and.....	Nylon 6/6-25 percent Glass Spheres
Rear Lid	-15 % Short Fiberglass Filled
Terminals.....	Brass
Resistive Element	
100K.....	Moleculoy (Molecule Wire Corp.) 75% Ni, 20% Ca, 3% Al, 2% Co
2K.....	Evenohm (Amax Speciality Metals Corp.) 54% Fe, 29% Ni, 17% Co, less than 1% Mn
Mandrel.....	20 AWG heavy insulated Dupont polyimide
Resistive Element.....	BASD 36238-EP (Ball Bros.)
Lubricant	
Shaft Lubricant.....	Royco 27A Aircraft & Inst. Grease

---

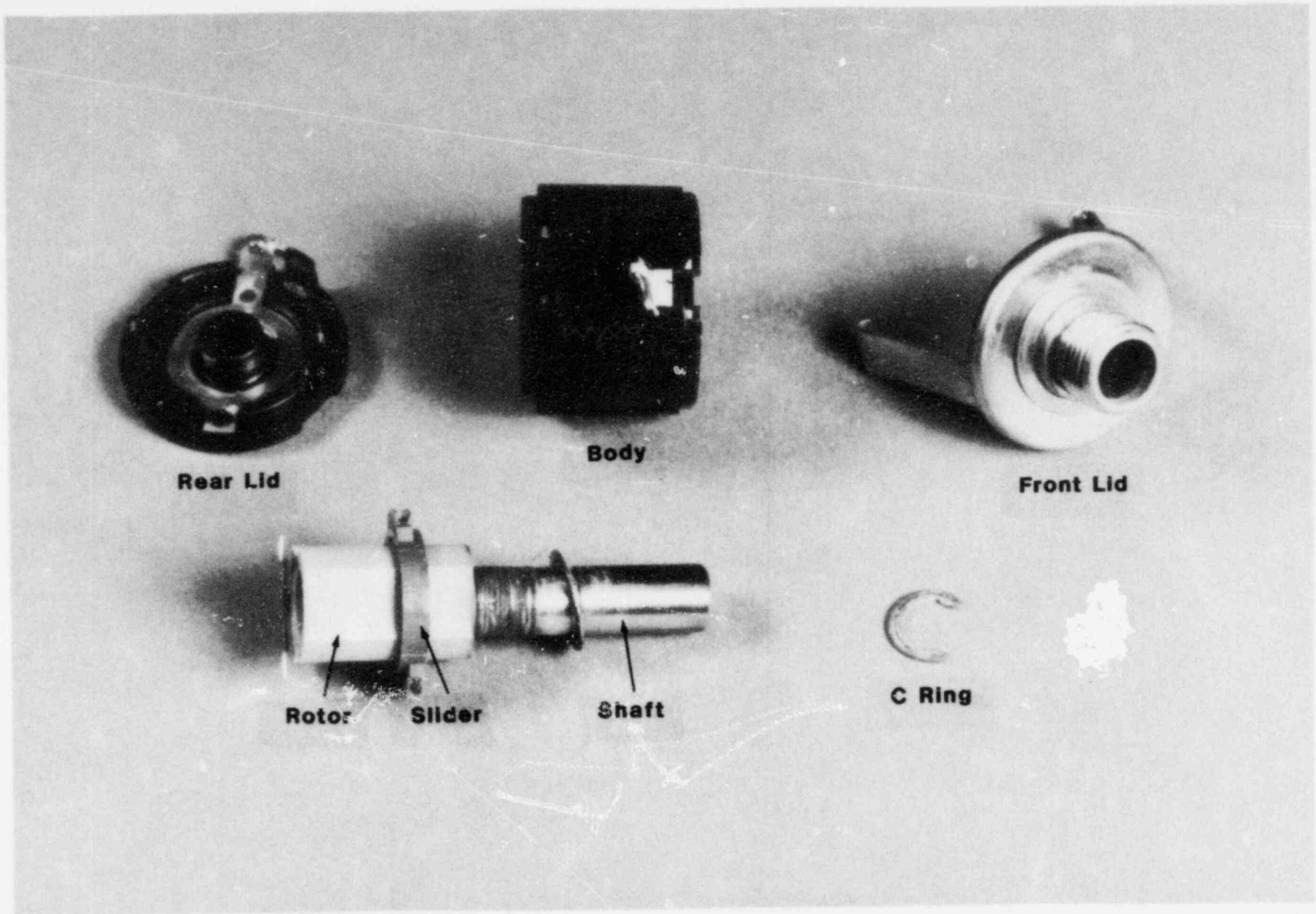


Figure 7-1 Disassembled Potentiometer From Transmitter T1

Comments on two of these materials are pertinent. First, nylon is not the best material for use in dielectric applications above 150°C (300°F) [12]. Since nylon has a hydrogen-bonded molecular structure, it has a strong affinity to absorb moisture. Some of this absorbed moisture ionizes and at elevated temperatures, these hydrogen ions become more mobile. Consequently, the dielectric properties of the nylon decrease and more conduction can occur. However, at elevated temperatures, a competing process also occurs. Absorbed moisture is outgassed from the nylon causing a reduction in the ion concentration and an improvement in nylon dielectric properties. The desorption of moisture is relatively rapid, but slow in comparison to the increase in ion mobility. Thus when submitted to a rapid temperature rise, the dielectric properties of nylon initially decrease and then, if the elevated temperature is maintained, begin to improve. When the nylon is returned to lower temperatures, the reduced ion mobility plus the now lower ion concentration combine to give improved dielectric properties over those that existed before the exposure to elevated temperature. Since the moisture content of the nylon is the result of an equilibrium process, the desorption of moisture is not permanent and at lower temperatures a reabsorption of desorbed moisture occurs. This process is slow in comparison to the elevated temperature desorption process, but eventually tends to restore equilibrium amounts of absorbed moisture and hence the initial equilibrium values of dielectric properties. Thus the dielectric properties of nylon are dependent upon temperature and temperature history [12].

Second, the potentiometer lubricants may also undergo changes in their dielectric properties at elevated temperatures [12]. Particularly, lubricant materials which contain zinc compounds may become more conductive. To determine if the lubricants contain zinc compounds, the lubricant manufacturers were contacted. They provided the following information:

The Ball Brothers BASD 36238-EP lubricant was developed for space applications with benign thermal environments [13]. The lubricant's major constituents are zinc, sulphur, carbon, and hydrogen. The oxidation inhibitor in the formulation is not appropriate for use at service temperatures above 150°C (302°F) service temperatures.

The Royco 27A MIL-G-23827A lubricant is a lithium stearate-thickened ester with load carrying additives [14]. Its constituents are sulphur, phosphorous, nitrogen, oxygen, carbons, hydrocarbon components, amines, and a corrosion inhibitor whose major constituents are sulphur and calcium. The formulation has traces of sodium, tin, and chlorine. It has a 125°C (257°F) service temperature. Exposure to 173°C (343°F) causes it to flow and to volatilize, leaving a dry residue when cooled.

## 7.2 Hypothesis on the Failure Mechanism

Considering the temperature behavior of nylon dielectric properties and the critical role that the nylon rotor assembly plays in providing electrical isolation between the circuit and the potentiometer case, we infer that the primary cause of the thermally-induced leakage currents is the change in dielectric properties of the nylon as a function of temperature. We have previously noted that initially large positive shifts in transmitter output occurred at temperatures above 122°C and that the magnitude of these shifts decreased with time at temperature. We have also noted that as exposure temperature decreased, negative shifts in transmitter output occurred and at the lower temperature plateaus (140°C (284°F) or below), the output was less than the original output of the transmitter (i.e., negative error). These changes in output have also been characterized as zero and span shifts with span error having the most dominant effect.

A rather simplistic explanation of the span potentiometer function in the circuit will illustrate how this observed behavior is consistent with the temperature behavior of the nylon. A key element of the transmitter's circuit is the operational amplifier which controls the correlation between sensed pressure and current output. The span potentiometer is the adjustable element in the feedback loop of this operational amplifier and therefore controls the slope (span) of the transmitter's correlation curve. When the dielectric properties of the nylon decrease, the leakage current from the circuit to the potentiometer case (and hence the transmitter housing and ground) increases. The result is a decrease in the feedback signal. In response, the operational amplifier increases its gain, which increases transmitter output. We observed this increased output as the large shifts as temperature increased. As time-at-temperature increases, the nylon's dielectric properties improve, decreasing the leakage current to ground and increasing the feedback signal to the operational amplifier. The result is decreased gain from the operational amplifier which decreases transmitter output as observed. As lower temperatures are reached later in the exposure profile, the nylon's dielectric properties improve over original values and hence less than original leakage current to ground exists. The result is more than original feedback signal and hence the operational amplifier decreases its gain, reducing transmitter output. We observed this reduced output as negative error later in the test. The reabsorption of moisture at lower temperatures and the slow return towards original values of dielectric properties accounts for the slow drift back towards original output levels.

A similar explanation could be made for the zero potentiometer which adjusts the bridge circuit supplying input to the operational amplifier. It would be similar to the span potentiometer explanation described above. Since changes in the input

to a high gain device do not affect output as dramatically as changes to the gain of the device itself, the effect of leakage currents in the zero potentiometer is not as pronounced as the effect of the span potentiometer.

We reemphasize that the above discussion is a hypothesis and that to confirm or deny it will require more testing of the potentiometers. However, the explanation is consistent with known behavior of nylons and the observed results in this test. We also suggest that an initial step in eliminating the cause of the leakage currents would be to use a nonhydrogen-bonded material in the potentiometer rotor assembly.

### 7.3 Testing Methodology Implications

The observed thermal behavior coupled with the hypothesized mechanism causing this behavior, raises a question about whether accelerated aging to an intended end-of-life condition produces the most vulnerable operational state for this transmitter. Since the magnitude of the error decreased with the time at temperature, the thermal aging exposure of a qualification sequence may mask or diminish the errors observed during a subsequent LOCA exposure. Thus, thermal aging may not place this transmitter in its most vulnerable state prior to the LOCA exposure. This possibility is recognized by IEEE Standard 381-1977 [6] which states in Section 5.8.1 that "in some instances, aging may actually improve equipment capability to perform." Even though we did not investigate the response of aged equipment, our testing appears to have discovered an example where such an effect may occur. We therefore believe our data supports the recommendation of IEEE 381-1977 that an understanding of equipment failure modes is essential to the qualification process. Obtaining this understanding may dictate that "more than one piece of equipment or component thereof may have to be tested such that samples are aged to different degrees of advanced life and then analyzed/tested to establish limiting cases" [6].

## 8.0 EVALUATION OF POTENTIOMETER MODIFICATION KIT

To enhance the thermal stability of this transmitter design, ITT Barton has recommended the installation of new potentiometer mounting brackets and fiberglass washers to electrically isolate the potentiometers from the transmitter housing [3]. The modification kit is shown in Figure 8-1. The fiberglass washers are made with an epoxy binder and hence do not have the same dielectric property sensitivity to thermal exposure [12]. To evaluate the effectiveness of the modification kits, four transmitters were modified and subjected to special tests. The transmitters were recalibrated after the modification kits were installed.

### 8.1 Initial Screening Test

The modification kit was initially installed in transmitter T2 exposed to the thermal only environment in the oven. The oven temperature was increased in steps to 110°C, 130°C, 150°C, and 170°C (230°F, 266°F, 302°F, and 338°F). Measurements were made at these temperatures at two different times 13 days apart. This data is compared in Table 8-1 with data taken at the beginning of the test and 7 days into the test.

---

Table 8-1

Screening Test Errors for Transmitter T2  
Before and After Modification  
(Percent of Full Scale)

Temp °C (°F)	Before Modification		After Modification	
	Day 0*	Day 7*	Day 20*	Day 33*
22 (72)	-0.10	-1.46	+0.10	-0.30
110 (230)	-0.60	-0.50	+0.88	+0.72
130 (266)	-0.40	-0.40	+0.56	+0.34
150 (302)	+2.10	-0.02	+0.21	-0.22
170 (338)	+6.40	+1.23	-0.45	-0.65

\*Total elapsed time from beginning of test

---

The data indicates that a significant improvement resulted at 170°C (nominal) when the potentiometer modification kit was installed.

### 8.2 Special LOCA Transient Exposure

Subsequent to completion of the LOCA test series, the special LOCA test described in Section 3.6 was conducted. In

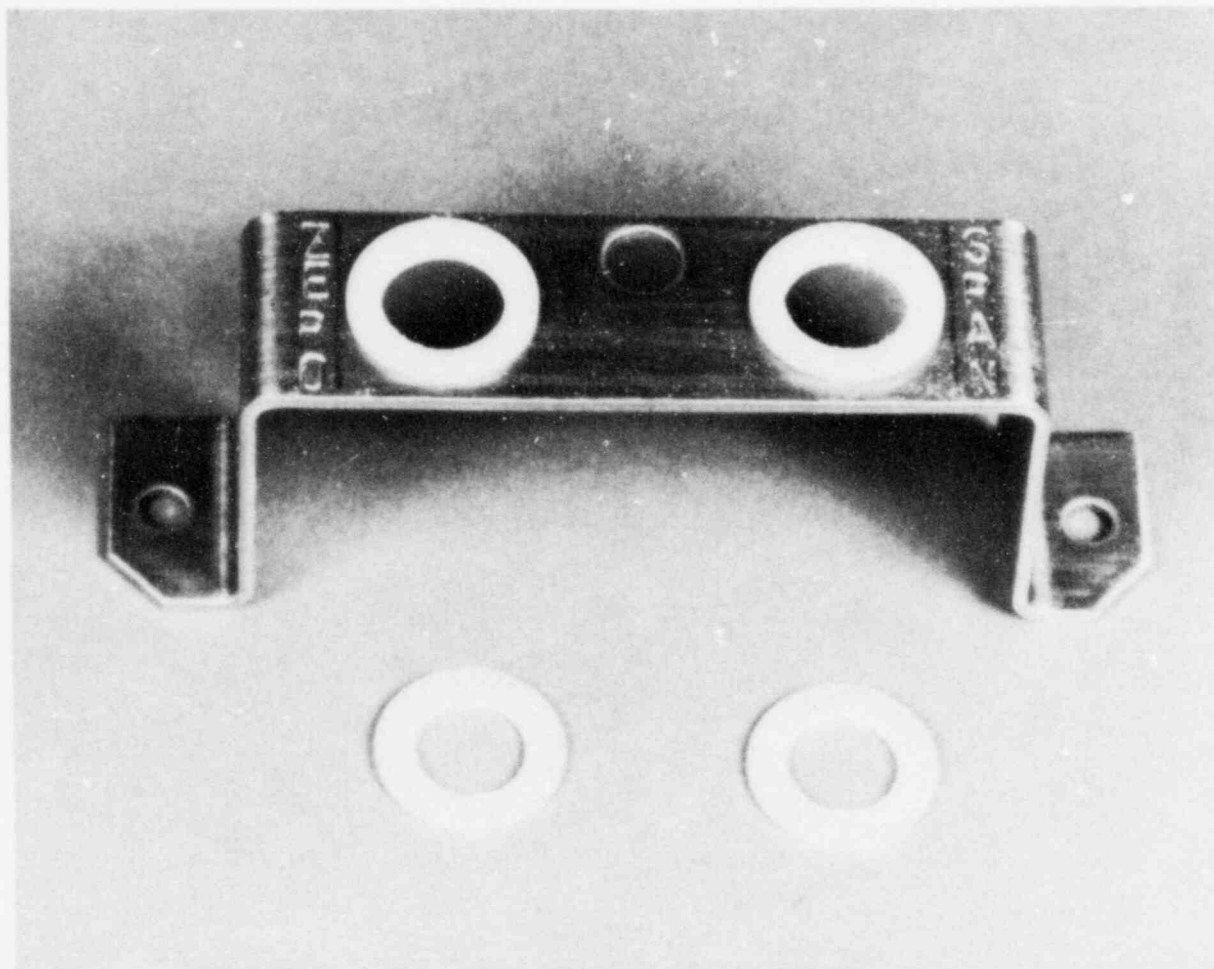


Figure 8-1 Potentiometer Modification Kit

addition to the already modified transmitter T2, transmitters T1, T3, and T5 were also modified. In addition, the failed potentiometer in transmitter T1 was replaced with one supplied by the manufacturer (see Section 9.0). All four transmitters were subjected to the initial transient of the LOCA exposure sequence. Exposure temperatures reached 175°C (347°F).

The four transmitters were modified and resealed using new O-rings and silicone lubricant obtained from ITT Barton. Modification was accomplished per ITT Barton field modification instructions [15].

The temperature profile achieved during the special test is shown in Figures A-9. Figures A-11 are an expanded version of the first portion of these plots. The responses of transmitters T1, T2, T3, and T5 are shown in Figures A-10 and A-12. Though sharing some of the same characteristics, the responses of the four transmitters were all different. Transmitters T1 and T2

operated throughout the test sequence. Transmitter T3 ceased providing meaningful data 1.7 minutes into the test. Transmitter T5 developed an anomaly 3.3 minutes into the test and we discount its response after this point. The response of each transmitter during this special test sequence is described below. The maximum stable errors observed for transmitters T1, T2, and T5 before and after modification are compared in Table 8-2. Data for transmitter T3 is not included in Table 7-2 for two reasons: (1) during the special test, insufficient stable data was obtained for this transmitter to make meaningful comparisons, and (2) transmitter T3 was tested at ambient temperatures during the main test and high temperature data does not exist to make comparisons.

Table 8-2

Pre- and Post-Modification Performance  
of Transmitters T1, T2, and T5\* at 173-175°C  
(Percent of Full Scale)

	<u>T1</u>	<u>T2</u>	<u>T5</u>
Pre-modification	+21.1	+6.4	+26.8
Post-modification	<u>+0.9</u>	<u>-2.0</u>	<u>+7.8</u>

Error specification:  $\pm 4.0\%$  at 173°C

\* Transmitter T3 performance could not be compared due to insufficient stable test data.

The response of transmitter T1 was in agreement with data obtained in the initial screening test of transmitter T2. As shown in Figure T1-A-12 (an expanded version of the initial part of Figure T1-A-10) at the beginning of the test, the initial error value was -0.6 percent. At 40 seconds elapsed time, the transmitter showed a -4.0 percent error followed by a rise to +0.9 percent error at 4.5 minutes elapsed time. As the exposure temperature was decreased, the error slowly decreased. At room temperature, the error indicated was -0.9 percent.

As shown in Figure T2-A-12, before the special test, transmitter T2 experienced a slight ramp from almost zero error to about +0.6 percent error. Ten seconds into the test sequence, a +16.5 percent error spike was observed. The error then decreased to -1.7 percent 40 seconds into the sequence, reaching -1.3 percent at 3.5 minutes elapsed time. The error settled at -1.9 percent after 5 minutes elapsed time and remained there during the entire 175°C (347°F) exposure. It returned to -0.7 percent as the transmitter reached room temperature.

Transmitter T3 had an initial error of +0.5 percent (see Figure T3-A-12). Twenty seconds into the test sequence, it produced a positive error spike of +19.4 percent. The error dropped sharply to a value of -0.9 percent at 1.5 minutes elapsed time. Ten seconds later, T3 showed overrange readings. The overrange condition was maintained throughout the balance of the sequence. During post-test disassembly, we noticed exposed conductors at the base of the transmitter's conduit fitting due to cracked wire insulation. We believe the extremely high total integrated dose received by transmitter T3 in the main test was the primary cause of insulation failure. Further comments on this failure are given in Section 10.0.

Figure T5-A-12 shows that transmitter T5 began the test with an initial error of +1.8 percent. Twenty seconds into the test sequence, the output shifted positively to +14.9 percent. A rapid decrease to +3.5 percent error was observed at 60 seconds into the sequence, followed by a rise to +7.8 percent error at 3.3 minutes elapsed time. This error level was followed by a sharp fall to -58.7 percent error which abated when the temperature was returned to ambient. The error at ambient temperature was +6.4 percent.

During post-test disassembly, we noted that the wire crimp connections between the transmitter wiring and the data acquisition cable were loose. This may have been the cause for transmitter T5's large negative error excursion.

Transmitter T4 was not tested because insulation on the lead wires had crumbled off near the transmitter housing, making reliable connection difficult. The cracked wire insulation was apparently due to embrittlement of the insulation material by radiation and thermal exposure combined with mechanical stress imparted to the wire when the transmitter was removed from the LOCA exposure test vessel.

### 8.3 Evaluation of Test Results

With the diversity in test data, it is difficult to draw a firm conclusion as to the effectiveness of the potentiometer modification kit. The data shown in Table 8-2 does indicate that the addition of the modification kit caused a significant improvement in long-term, stable error values observed at elevated temperatures. However, the error pulses produced by transmitters T2, T3, and T5 within the first 40 seconds of exposure shadow our ability to draw a definite conclusion regarding the effectiveness of the modification kit. We cannot satisfactorily explain what caused the error pulses.

It is clear that the modification is only palliative in nature; even if our hypothesized mechanism causing the leakage currents is wrong, the modification, by introducing a dielectric between the potentiometer case and the transmitter housing, does

not address the cause of the leakage currents. However, not eliminating the root cause of the leakage currents does not mean the modification is not beneficial. To the contrary, our data indicate a reasonable improvement in the long-term stability of the transmitter when exposed to elevated temperature environments. We do believe, though, that further testing is necessary to provide conclusive evidence about the precise contribution of the modification kit in reducing error and to determine the cause of the error pulses.

## 9.0 POTENTIOMETER FAILURE

At approximately 552 hours (23 days) elapsed time with the exposure temperature at 105°C (221°F), readings for transmitter T1 indicated an "overrange" condition.\* This condition was preceded by a rapid rise in transmitter error (see Figure T1-A-2). Subsequent measurements indicated an extremely large shift in calibration. For example, an applied pressure of 20 psig produced a transmitter output indication of 1515 psig. This result indicated that the gain of the transmitter's operational amplifier had increased dramatically. At this point, we discontinued testing transmitter T1. The steam chamber was allowed to cool and the transmitter removed and inspected.

We found that the winding of the span potentiometer which controls the gain of the operational amplifier had failed open, causing amplifier gain to rise.\* We replaced the span potentiometer with an equivalent potentiometer obtained from Sandia stock. The transmitter was recalibrated and operated at room temperature throughout the balance of the main test without further incident. When this transmitter was modified for the special test, the Sandia stock potentiometer was replaced with an "original equipment" potentiometer supplied by Barton.

### 9.1 Failure Analysis

The failed potentiometer was disassembled and inspected. The most observable macroscopic features were: (1) the buildup of a whitish powder on the C-ring and (2) appearance of a dark residue on the shaft, the front of the rotor assembly, the flat washer, and mounting lid. Residue samples were analyzed by laser raman microprobe technique and scanning electron microscopy. Figures 9-1 and 9-2 show a scanning electron micrograph (SEM) at 20x magnification of the C-ring and its energy dispersive X-ray analysis (EDXA) spectrum, respectively. Figures 9-3 and 9-4 show an SEM of the flat washer at 20x magnification and its EDXA spectrum, respectively. Of note is the appearance of chlorine, sulphur and potassium on the C-ring.

---

\*The observed "overrange" condition refers to the high voltage across one of the external loop resistors. This condition implies excessive loop current, and is entirely consistent with the opening of the span potentiometer which removes the feedback to the operational amplifier. Without feedback, the gain of the amplifier increases almost without limit, increasing the current output of the transmitter. The limit to the process is the voltage drop across the external loop resistance. We measured 29 volts across the 1000-ohm external loop resistance, leaving only 11 volts to drop across the transmitter which is below the 15 volt minimum operating specification.



Figure 9-1 Scanning Electron Micrograph (SEM) of C-Ring (20x)

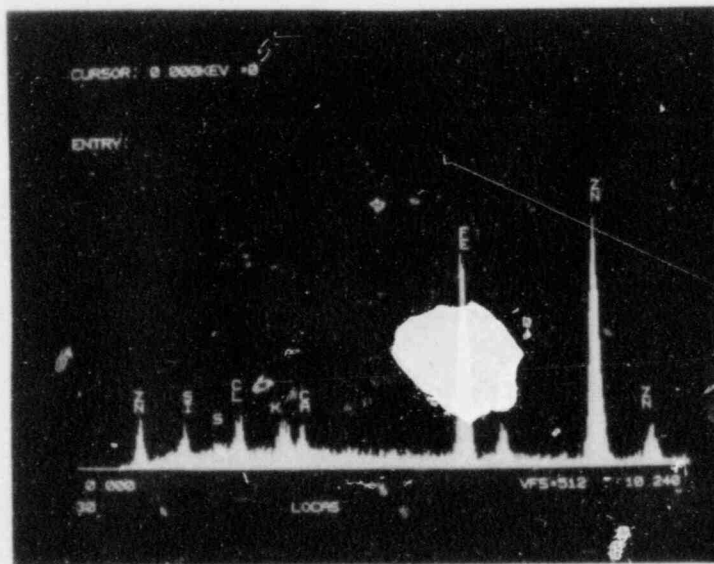


Figure 9-2 Elemental Analysis of C-Ring



Figure 9-3 SEM of Flat Washer (20x)

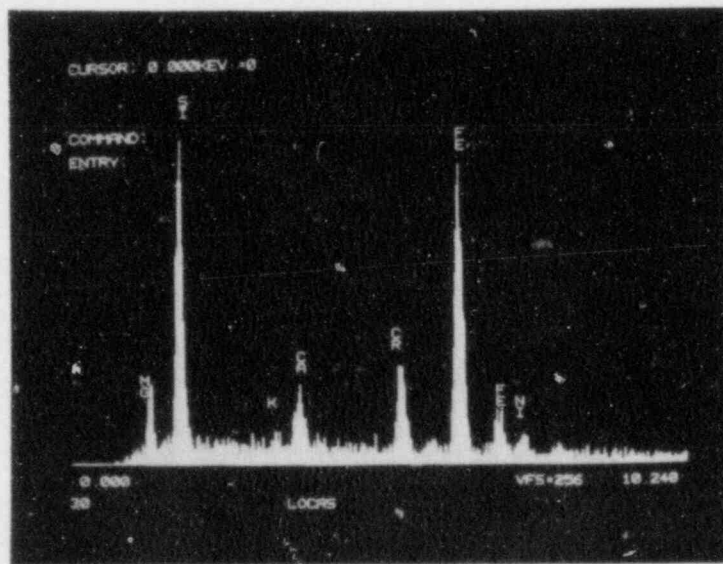


Figure 9-4 Elemental Analysis of Flat Washer

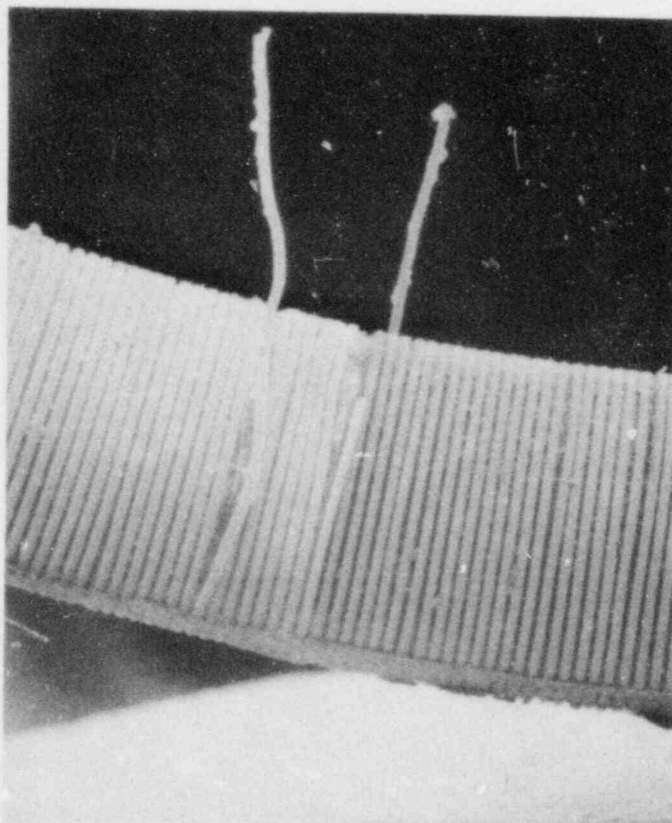


Figure 9-5 SEM of the Break Occurring in the Active Circuit  
Portion of the Potentiometer Resistive Element  
(40x)

We also found that the wire forming the potentiometer's resistive element had three breaks in it. One of these breaks had occurred in the portion of the winding that was part of the circuit, and two of the breaks had occurred beyond the set point of the slider and hence had no effect on the transmitter's operation. Figure 9-5 is a SEM at 40x magnification of the break occurring in the active portion of the resistive wire. The protrusion of the resistive element wire from the mandrel wire was not the result of the breaking process, but rather was caused by the analysis procedure. Figure 9-6 shows a SEM end view of this break at 2000x magnification. An EDXA elemental analysis spectrum of this break is shown in Figure 9-7. For comparison purposes, a good section of the resistive element wire was manually stressed to the ductile fracture point. The 2000x magnification SEM end view of this break is shown in Figure 9-8 and the corresponding elemental analysis is shown in Figure 9-9. Comparing Figures 9-6 and 9-8, we see that the character of these two breaks is different. As expected, the elemental analyses show



Figure 9-6 SEM of the Wire Cross Section From the Test-Induced Break Occurring in the Active Portion of the Potentiometer Resistive Element (2000x)

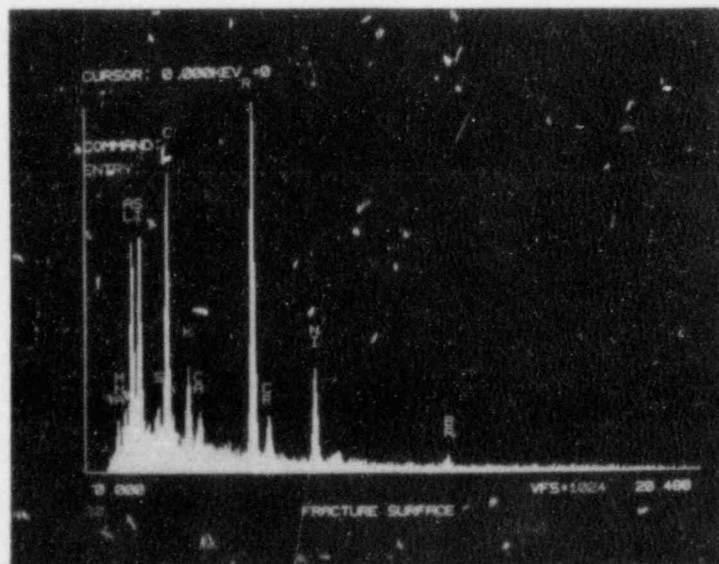


Figure 9-7 Elemental Analysis of the Test-Induced Break Wire End Shown in Figure 9-6

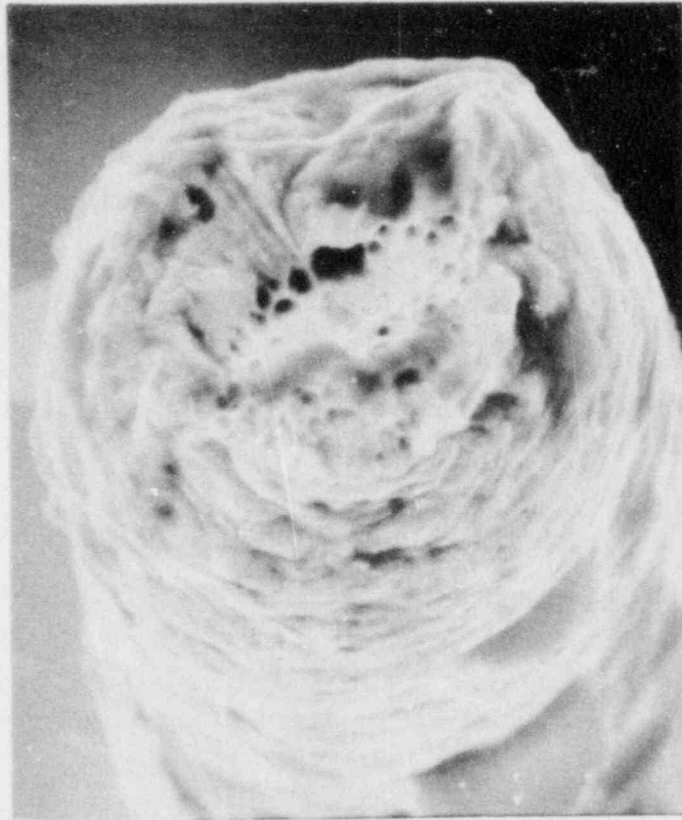


Figure 9-8 SEM of the Wire Cross Section Resulting From the Ductile Fracture of an Intact Portion of the Potentiometer Resistive Element (2000x)

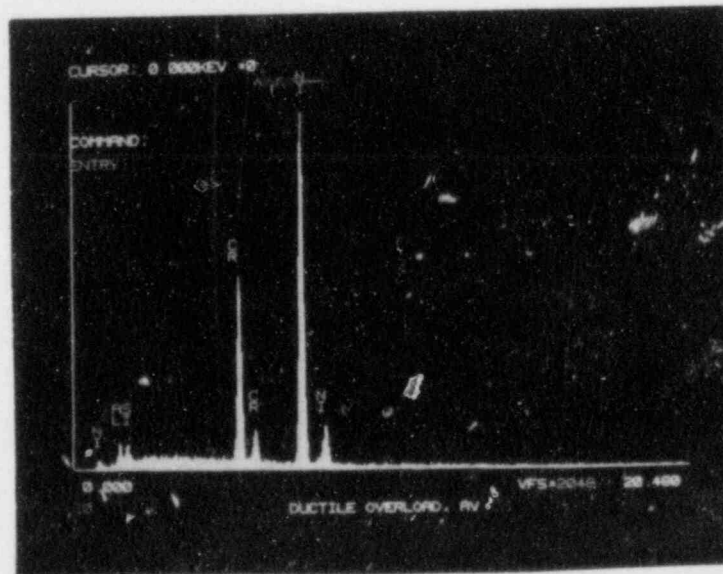


Figure 9-9 Elemental Analysis of Ductile Fracture Break Wire End Shown in Figure 9-8

the major constituents of the wire which was 75 percent nickel, 20 percent chromium, 3 percent aluminum, and 2 percent cobalt [17]. In addition, the spectrum for the test-induced break shown in Figure 9-7 indicates the presence of chlorine, sulphur, and potassium.

In an area close to this test-induced break, a large deposit of material was found. Figure 9-10 shows the micrograph of this region at 150x magnification. Slightly above and to the left of the picture center, one turn of the resistive element contains a hole which almost completely separates the wire. Figure 9-11 is a 500x magnification of this area and clearly shows the hole in the resistive wire. EDXA spectra of the material in and around this hole, one of which is shown in Figure 9-12, again showed the presence of chlorine, sulphur, and potassium. Figure 9-13 is a 200x magnification micrograph of one of the other breaks in the resistive element wire. This SEM shows two adjacent windings separated and similar deposits of material. An end view of one of these wires is shown in Figure 9-14. It shares many of the same characteristic as the break shown in Figure 9-6. Figure 9-15 is an EDXA spectrum of one portion of this second break area which again shows the presence of chlorine. Figures 9-16 and 9-17 show a micrograph of a purposely broken segment of the wire and the EDXA spectrum of the deposit found under that segment of wire. Chlorine, sulphur, potassium, and sodium were found in this deposit.

The timing of the potentiometer failure, plus the difference between the character of the breaks occurring during the experiment and ductile fracture break, plus the presence of chlorine and sulphur all point to corrosion as the mechanism causing the resistive element wire to separate during the test. We hypothesize that the chlorine and sulphur combined with moisture to produce hydrochloric and sulphuric acids which attacked the wire. The elevated temperatures initiated and/or accelerated these processes. The moisture could have come from several sources. Some may have been trapped within the transmitter housing during the initial assembly process, some may have come from moisture in the nylon rotor, and some may have diffused into the transmitter housing before and during the experiment [16]. We believe that the source of the chlorine and sulphur is the lubricants applied to the potentiometers during manufacture. Section 7.0 gives the composition of these lubricants.

## 9.2 Analysis of Non-Failed Potentiometers

Since corrosion was hypothesized to be the mechanism causing one potentiometer to fail open, we suspected corrosion processes may have been underway in other potentiometers. We therefore analyzed five additional potentiometers for signs of this mechanism. These potentiometers were removed from transmitters T1, T3,



Figure 9-10 SEM of Foreign Material Found Near Wire Break Shown in Figure 9-5 (150x). Partially corroded winding is indicated by arrow.

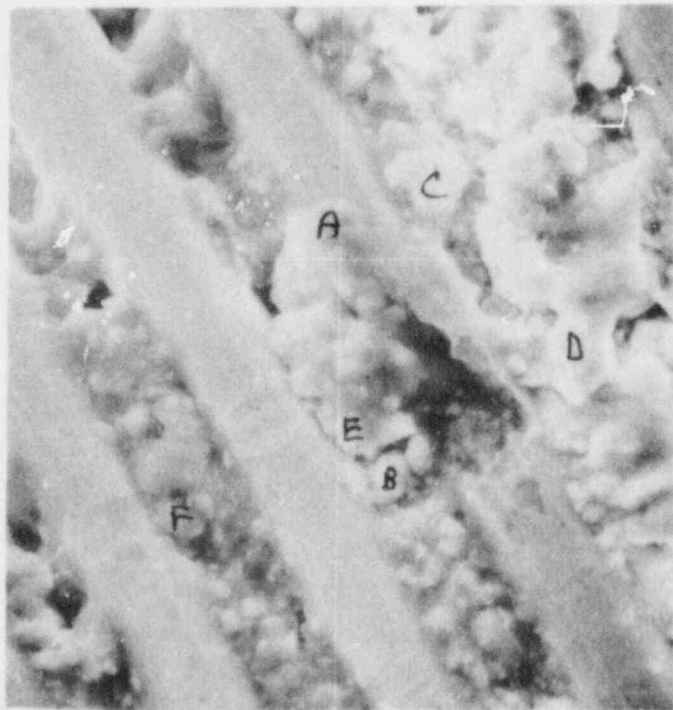


Figure 9-11 Enlarged View of Partially Corroded Winding Shown in Figure 9-10 (500x)

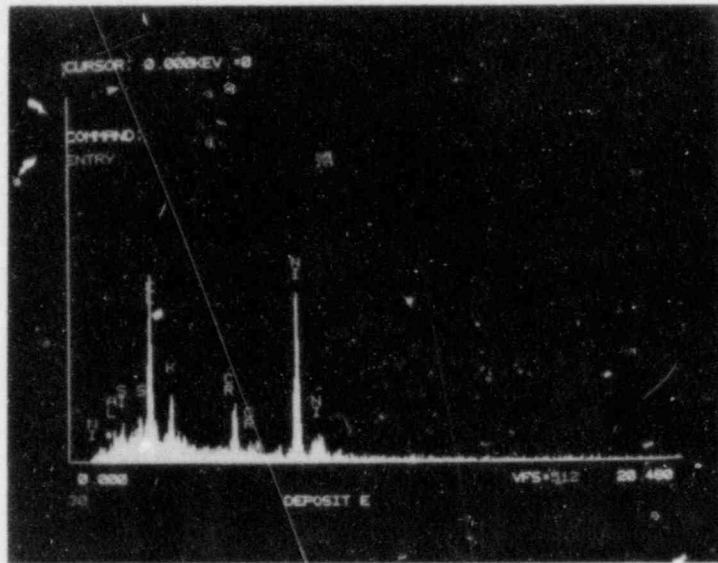


Figure 9-12 Elemental Analysis of Area E as Indicated in Figure 9-11

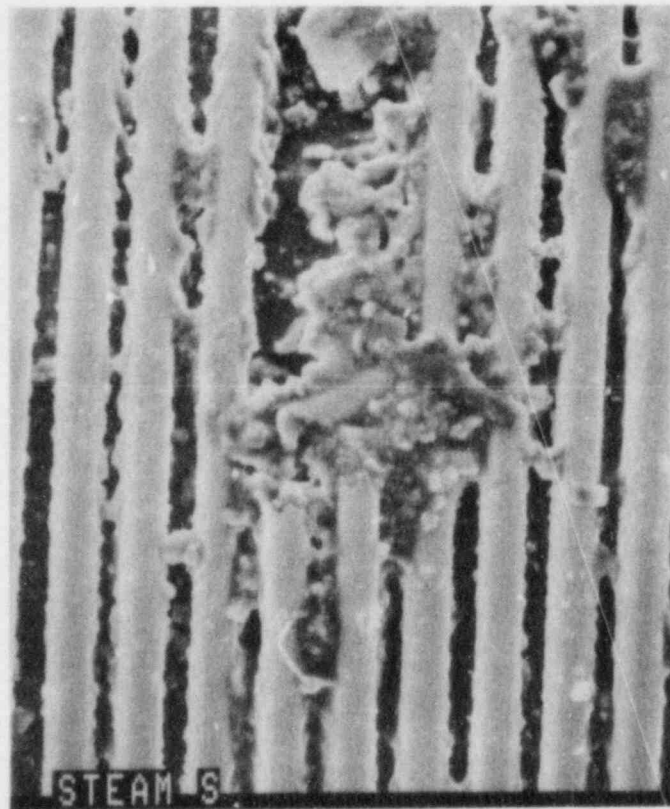


Figure 9-13 SEM of a Second Break Area Showing Separation of Two Adjacent Windings (200x)



Figure 9-14 SEM End View of One of the Broken Wires Shown in Figure 9-13 (1500x)

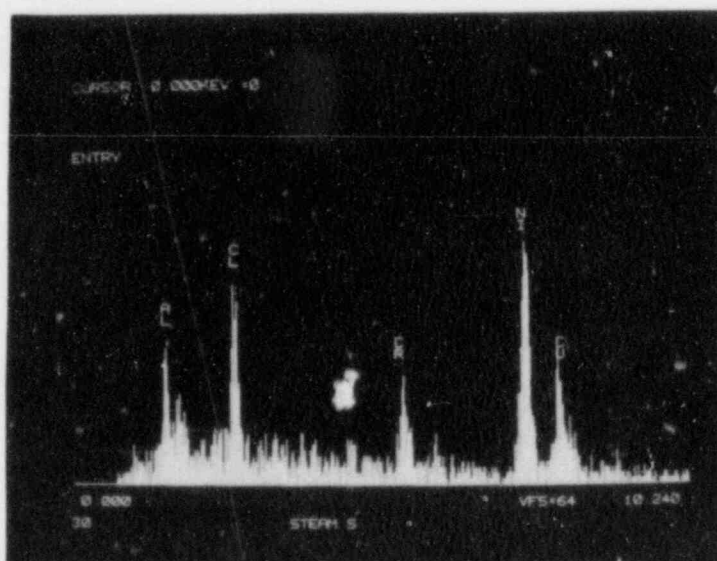


Figure 9-15 Elemental Analysis of One Portion of the Break Area Shown in Figure 9-13

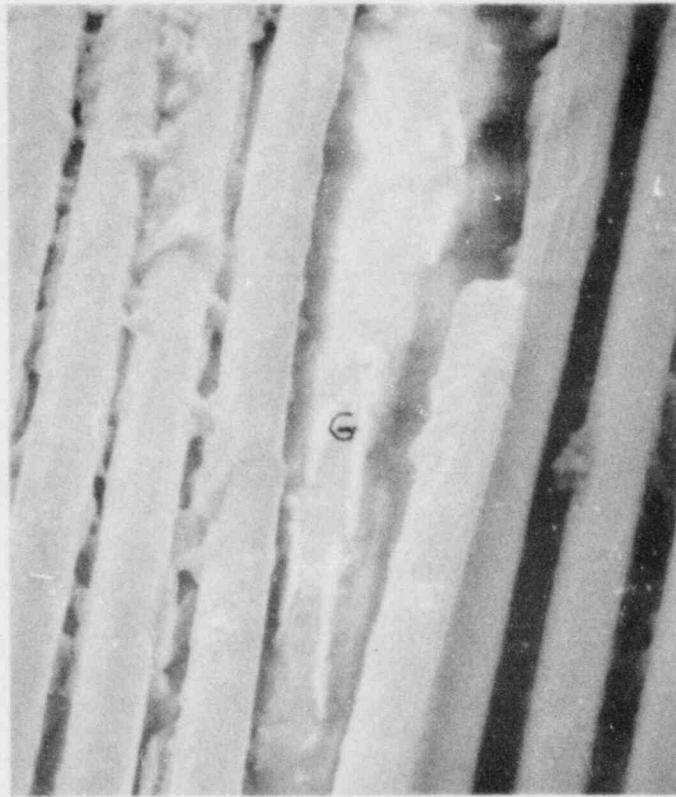


Figure 9-16 SEM of a Purposely Broken Segment of the Potentiometer Resistive Element

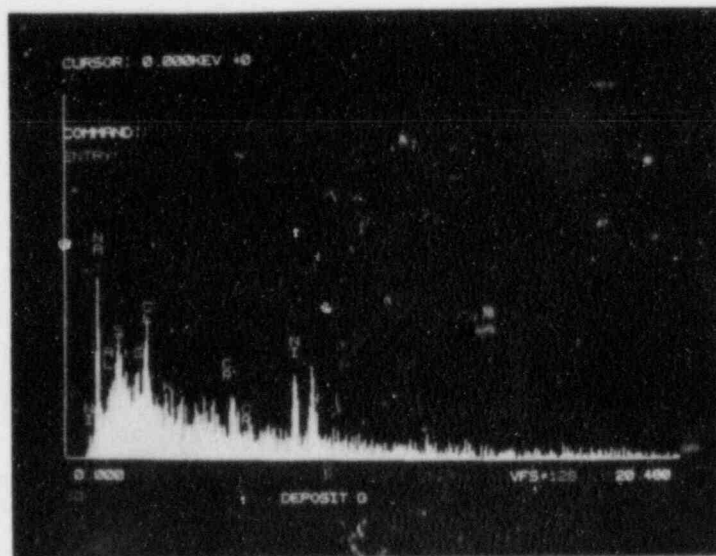


Figure 9-17 Elemental Analysis of Deposit Found Under the Wire Break Shown in Figure 9-16

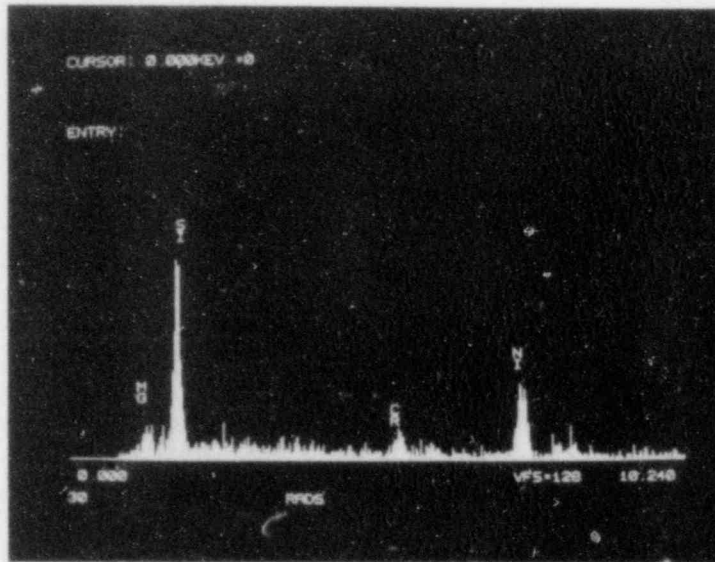


Figure 9-18 Typical Elemental Analysis of Non-Failed  
Potentiometers

and T5. The span and zero adjustment potentiometers from transmitters T3 and T5 were analyzed along with the zero adjustment potentiometer from transmitter T1. Scanning electron microscope analysis of these potentiometers showed no signs of corrosion; neither were concentrations of chlorine, sulphur or potassium found. EDXA analyses of these potentiometer windings (Figure 9-18) showed only high concentrations of silicon and small concentrations of manganese.

We did not expect the potentiometers from transmitter T3 to show many (if any) signs of corrosion because they had not been subjected to the high temperature, steam environment for any significant period of time. However, we did expect to find signs of the lubricant in this transmitter. We did expect to find signs of corrosion in the zero potentiometer from transmitters T1 and the zero and span potentiometers from transmitter T5, because these transmitters had experienced exposure to the high temperature, steam environments. The high concentrations of Si, along with the lack of evidence of the other lubricants was puzzling. We therefore contacted the potentiometer manufacturer [17] and learned that the lubricant type was changed in late 1982 to mid-1983 from the Ball Bros. lubricant given in Section 7.0 to a General Electric silicon-based product, GE F50.

The transmitters that we tested were manufactured in the summer of 1982 which would imply that they all should contain potentiometers that had been lubricated with the Ball Bros. lubricant. Our analysis data, however, indicated that only one of the potentiometers analyzed contained these lubricants and that the others had been lubricated with the GE product. We therefore recontacted the potentiometer manufacturer and discovered that the permanent change to GE F50 lubricant was made in late-1982 to mid-1983, but that GE F50 had been used sporadically in the production of the potentiometers for quite some time [18]. It was therefore not surprising to find some potentiometers containing the GE F50 lubricant, while others contained the Ball Bros. lubricant. The potentiometer manufacturer had considered the lubricants interchangeable and had therefore not controlled which production lots contained which lubricant. It was therefore impossible to trace what transmitters might contain potentiometers lubricated with the Ball Bros. lubricant. However, it is fair to say that some fraction of the transmitters contain potentiometers lubricated with Ball Bros. lubricant and may therefore be susceptible to this corrosion failure mechanism. We also suspect that the earlier the manufacture date of the transmitters, the more likely they are to contain potentiometers with this lubricant.

## 10.0 POST-TEST OBSERVATIONS

After the LOCA test sequence was completed, the transmitter cover plates were removed for post-test observation. Our observations are described below.

### 10.1 Moistur Intrusion

Examining the covers of transmitter T1, T4, and T5, we observed evidence of a small amount of moisture intrusion into the electronics enclosure. This appeared as a discoloration of the passivation on the inside of the transmitter cover as shown in Figures 10-1, 10-2, and 10-3. This is contrasted to the cover in the center of Figure 10-3 from transmitter T3 which was exposed only to the radiation environment and shows no discoloration.

The Barton qualification test report [7] did not indicate any observation of moisture intrusion into the transmitter's electronics enclosure. A possible explanation for this different behavior is the exposure environment. During our tests, saturated steam at pressures up to 112 psig were applied. The Barton qualification report shows that superheated or saturated steam at 80 psig or less was applied during LOCA testing. Therefore, moisture intrusion would not have been as likely in the Barton tests.

### 10.2 Print Circuit Board Conformal Coating

As shown in Figures 10-4 and 10-5, we observed that the printed circuit (PC) board silicone conformal coating for transmitters T4 and T5 had become brittle and cracked. We also noted an acrid odor when opening the cover of the transmitter housing. Some silastic compounds like those coating the printed circuit board use acetic acid (hence the smell) as a constituent in the curing process [19]. We noted that the PC board in transmitter T3, exposed to radiation alone (Figure 10-6), turned dark brown and that the conformal coating was darkened and brittle. However, it had not cracked. We therefore believe that the combination of thermal and radiation environments led to the cracking of the coating observed in transmitters T4 and T5. The Barton qualification test report [7] indicated that they had observed similar cracking of the PC board conformal coating subsequent to their LOCA exposure of aged instruments. We do not believe that the cracks in the coating adversely affected transmitter operation.

### 10.3 Water in Cable Conduit

Inside the steam chambers, wires to the transmitters were isolated from steam exposure by routing them inside a conduit of flexible high pressure metal hose (see Figure 3-1). This precaution was taken to minimize the effects of the LOCA steam environment on the cables which, in turn, minimized the effects of cable deterioration on test results [20-22].

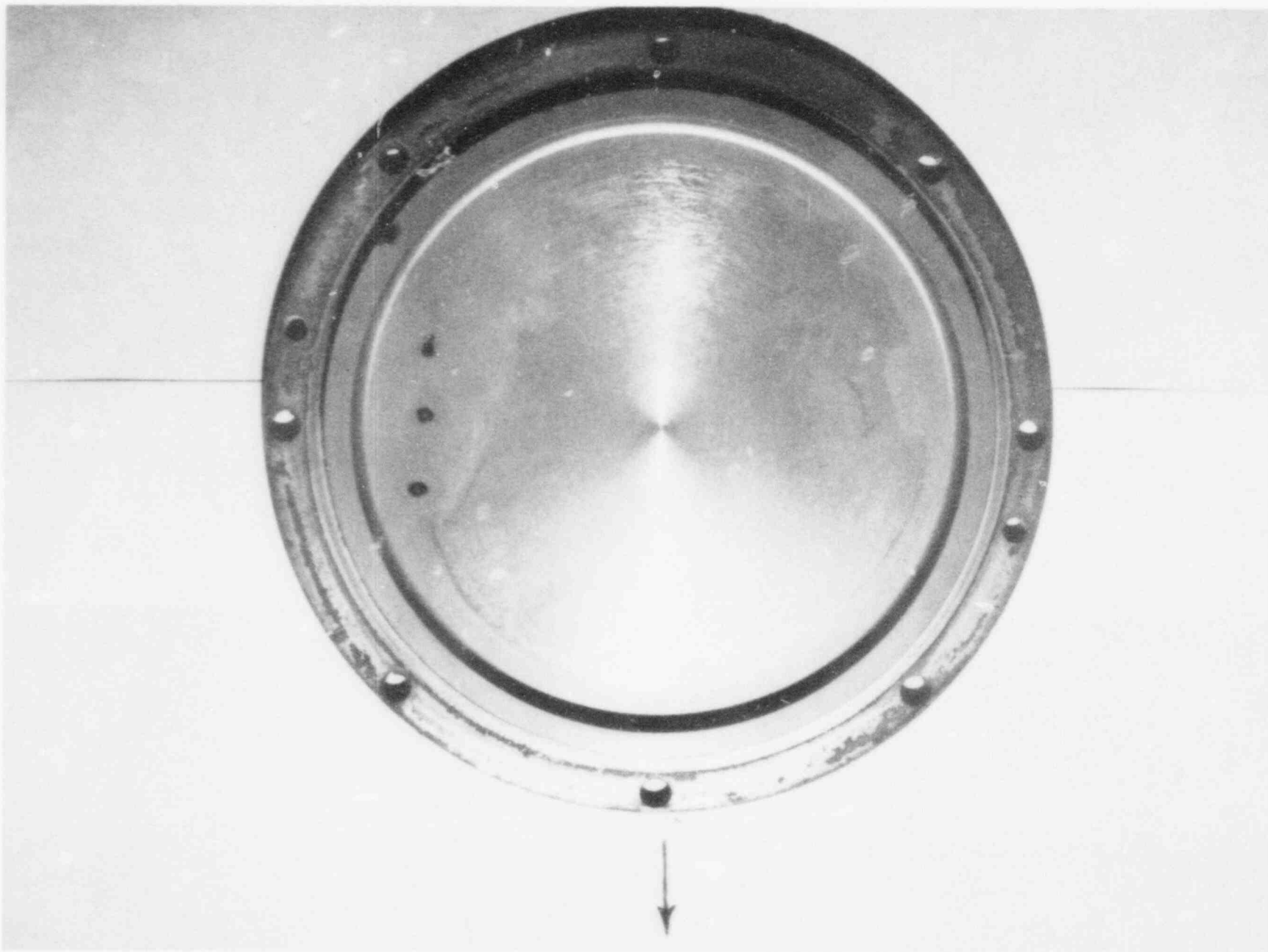


Figure 10-1 Transmitter T1 Cover Showing Moisture Intrusion

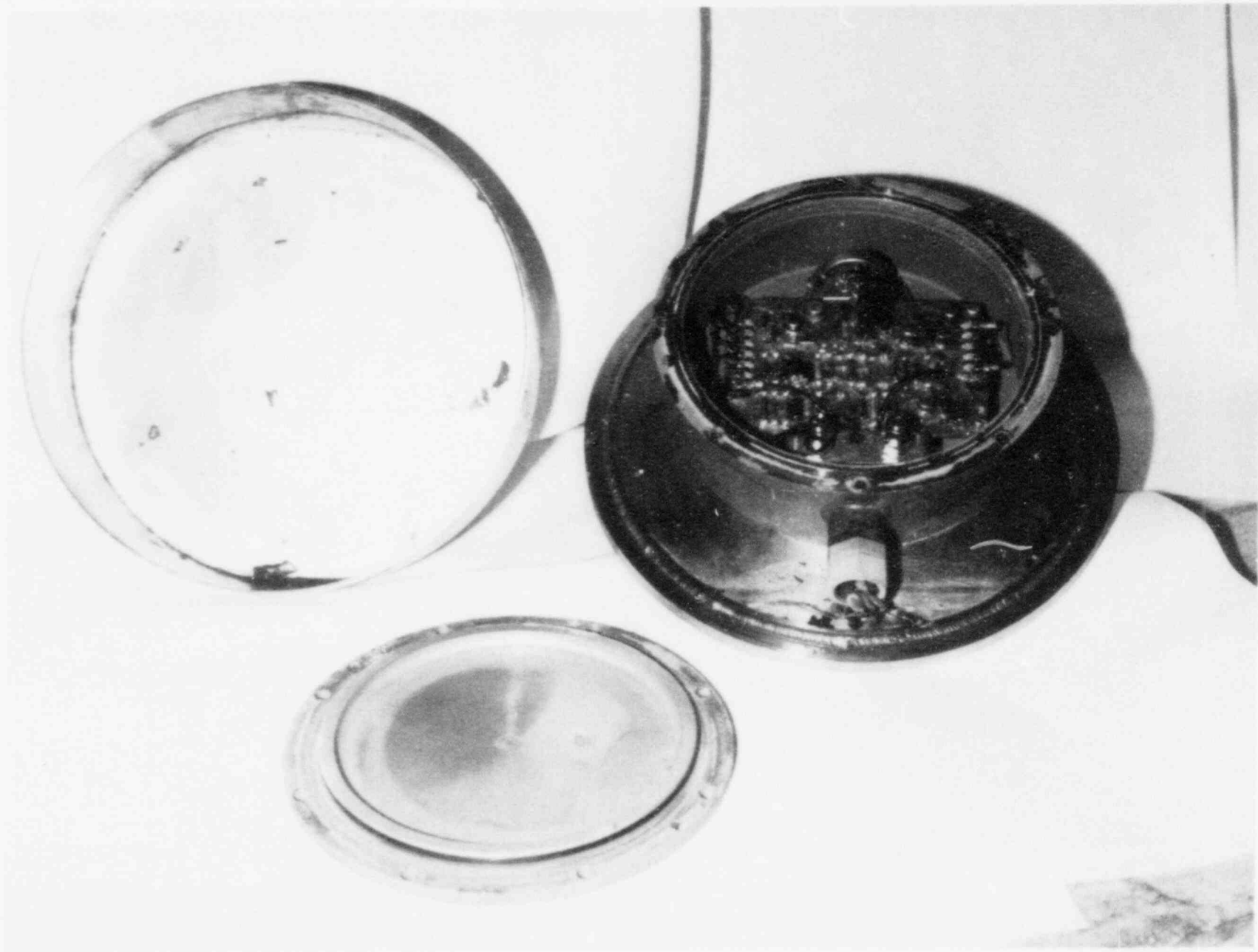


Figure 10-2 Transmitter T4 Cover Showing Moisture Intrusion

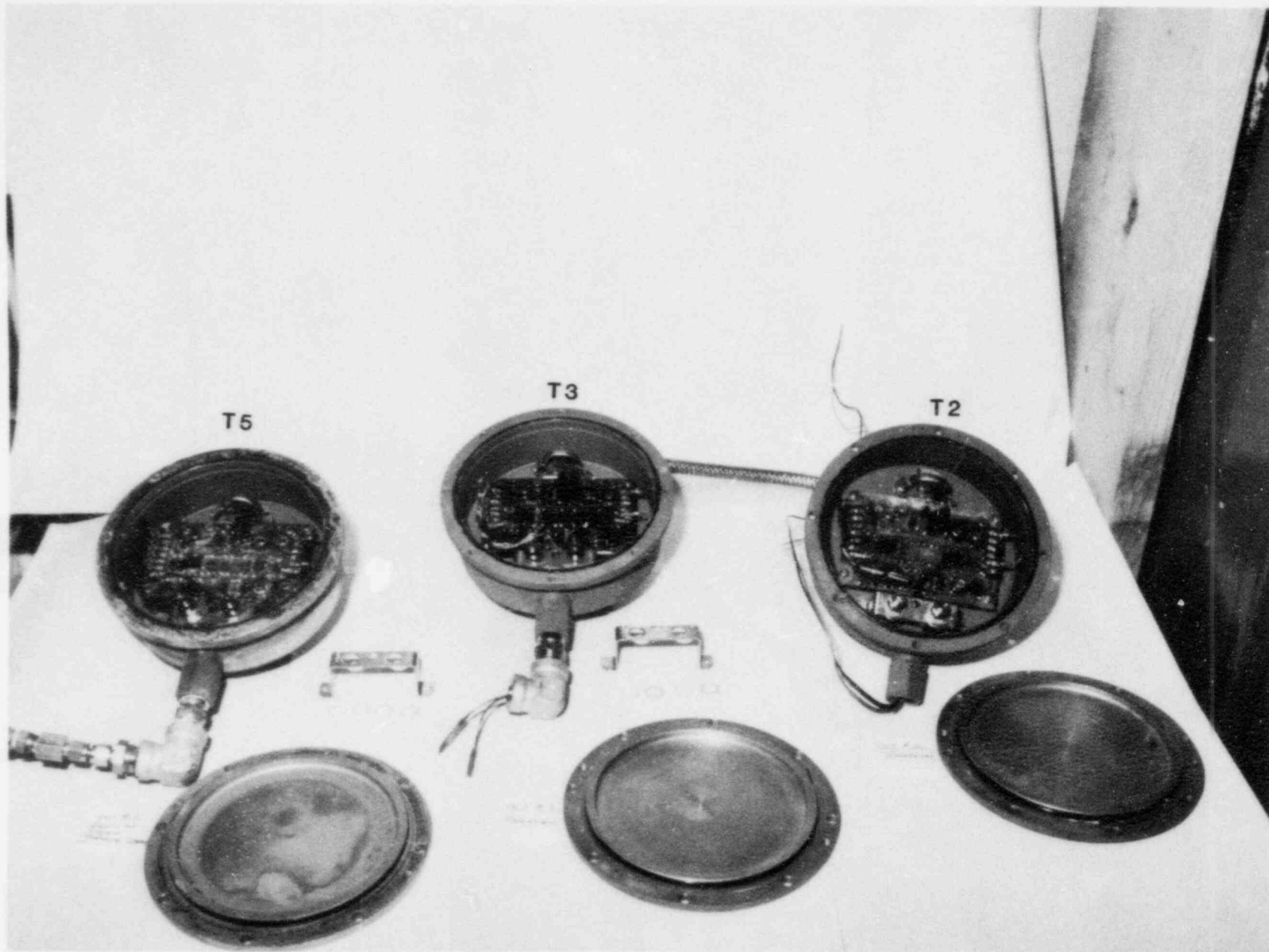


Figure 10-3 Post-Test View of Transmitters T2, T3, and T5

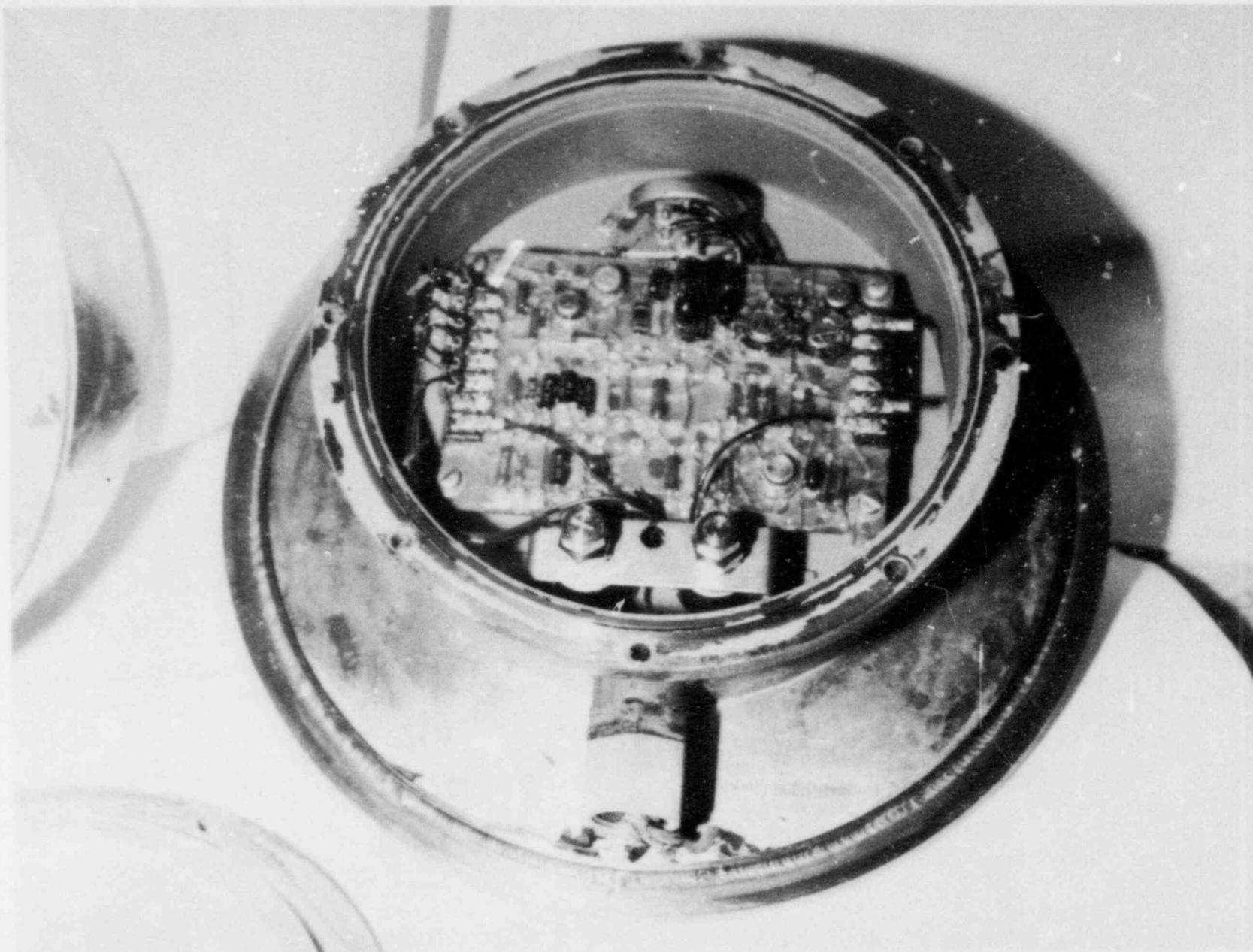


Figure 10-4 Transmitter T4 Showing Cracks in Circuit Board  
Conformal Coating

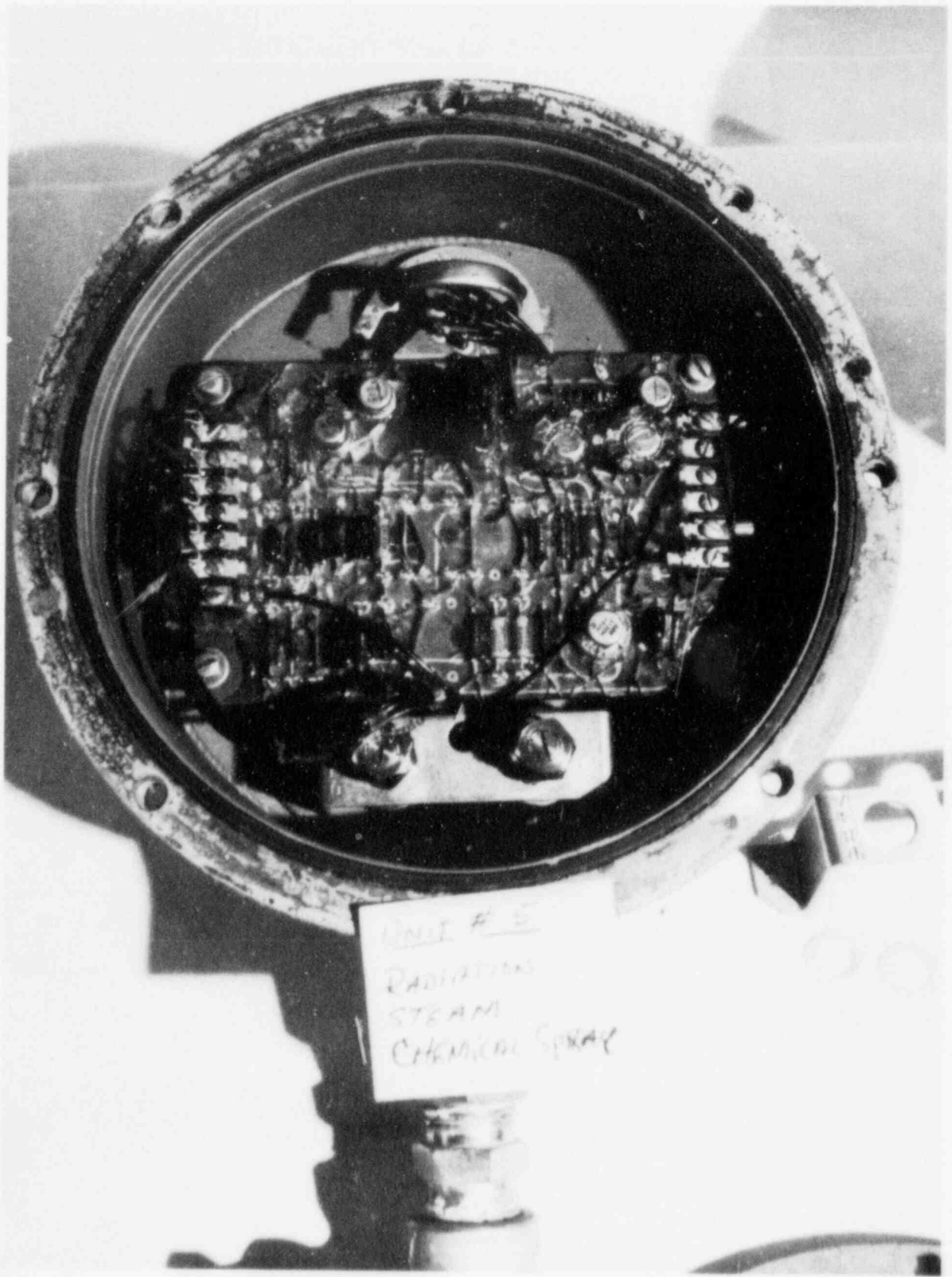


Figure 10-5 Transmitter T5 Showing Cracks in Circuit Board  
Conformal Coating

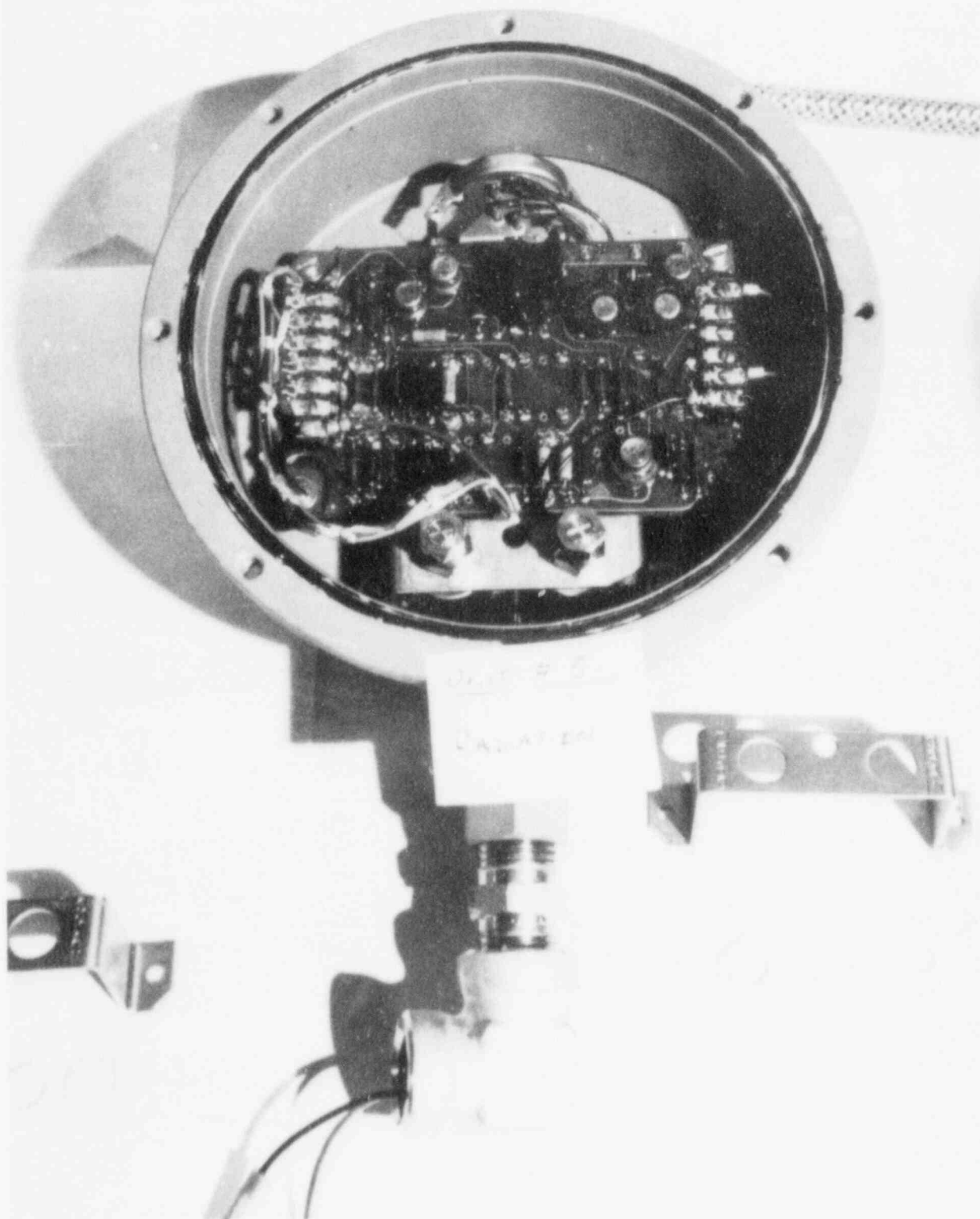


Figure 10-6 Transmitter T3 Showing Darkening of PC Board Material

During post-test disassembly, significant amounts of water (not measured) were observed coming out of conduits for transmitters T4 and T5. We suspect that conduit connections were not perfectly sealed, allowing moisture to be forced into the conduit.

#### 10.4 Cable Insulation

Inspection of the transmitter pigtail wiring external to the housing showed that the insulation was brittle and cracked in several places. We also noticed that there were places where the bare conductor was exposed. The insulation on wiring inside the transmitter was stiff but still intact. Cable insulation was discolored in transmitter T3 and was black in transmitters T4 and T5.

These effects on polymer materials, exposed to radiation and/or thermal environments, are not unexpected. We reiterate that our tests exposed the transmitters to radiation environments well beyond the design basis. Though we cannot pinpoint when the insulation material degraded beyond acceptable limits, we can speculate based on the observed behavior of two transmitters. Transmitter T4 began showing erratic output at 650 hours, while transmitter T5 began showing erratic output after 430 hours (see Figures T4-A-2 and T5-A-2). The radiation exposures of transmitters T4 and T5 at these times were 370 Mrd and 240 Mrd, respectively. Considering that water was found in the metal conduit intended to isolate the cables from the steam exposure, this erratic behavior could be the result of moisture penetrating cracked insulation and causing low conductor-to-conductor insulation resistance. If our speculation about the cause of the erratic behavior is correct, then the total doses received at the onset of the erratic behaviors were beyond the design basis. We can therefore speculate that the useful life was beyond that required for the design basis.

#### 10.5 T4 Steam Isolation

Upon inspection of T4 subsequent to the test, we observed that the can enclosing the transmitter contained a substantial amount of water (not measured). Therefore, the intended objective of subjecting T4 only to the thermal and not the moisture environment was not accomplished. We suspect that during one of the initial LOCA pressure ramps, the sealant between the enclosure and transmitter fittings failed, allowing the moisture to enter and collect in the enclosure.

#### 10.6 Cover Mounting Bolts

During removal of the transmitter front cover plates, we noted that the cover bolts could be removed rather effortlessly. Most bolts could be removed without the aid of an allen wrench

and our efforts to measure the necessary loosening torque were fruitless since all bolts turned without registering on the torque wrench. Prior to test initiation, cover bolt torque was checked to assure the 3 inch-pound specification [23] recommended by Barton. This looseness we attribute to the effects of compressive set in the O-ring material used to seal the cover and housing interface.

## 11.0 CONCLUSIONS

This research has provided both specific equipment performance and general qualification methodology insights. By testing in individual and combined environments, we were able to isolate environmental effects on equipment performance. The primary environmental stress affecting the Barton Model 763 transmitter was temperature. We confirmed the ITT Barton finding that leakage current originating in the zero and span potentiometers was the major contributor to the transmitters' thermal instability. We also observed that the time-at-temperature significantly reduced the magnitude of the output shifts. Analyses of the potentiometer piece parts indicated that the root cause of the temperature instability was a thermally-activated decrease in the dielectric qualities of the nylon insulating material used in the construction of the potentiometers. The recommended modification, which electrically isolates the potentiometers from the transmitter housing, does improve the long-term performance of the transmitters; however, this modification is only palliative in nature. We also experienced a second, thermally-activated, failure mechanism which caused a potentiometer to open. This failure mechanism caused the transmitter to exhibit short circuit conditions. We believe that corrosion was the mechanism causing the potentiometer winding to fail and that lubricants applied during manufacture were the primary contributor to the corrosive environment. If our analysis is correct, we may have identified a second potential common failure mode.

The effects of radiation on this transmitter design are secondary to thermal effects. In fact, the transmitter electronics proved to be exceptionally hard to the effects of gamma radiation. Simultaneous exposure to radiation and thermal environments did not produce significant synergistic effects relative to the operation of the transmitter electronics. There was, however, a noticeable embrittlement of the polymer materials used in the transmitter construction such as the wire insulation and circuit board conformal coating.

This test reinforced the testing methodology implications of IEEE 381-1977 [6]. In particular, we believe that, even though we did not test aged equipment, the transmitter's time-at-temperature behavior indicated that a thermal aging exposure may mask or diminish the errors observed during subsequent LOCA exposure. Thus, this transmitter design may actually be an example where "... aging may actually improve equipment capability to perform" [6]. We therefore agree with the recommendation of IEEE 381-1977 [6] that an understanding of equipment failure modes is essential to the qualification process. Obtaining this understanding may dictate that "more than one piece of equipment or component thereof may have to be tested such that samples are aged to different degrees of advanced life and then analyzed/ tested to establish the limiting cases" [6]. It is also important to record the instruments' performance at each temperature level and across its entire range of operation.

## REFERENCES

1. 10 CFR 21 Notification: Telex to R. C. DeYoung, Office of Inspection and Enforcement, USNRC, from T. J. Shideler, Barton Instrument Co., October 29, 1982.
2. 10 CFR 21 Notification: Telex to R. C. DeYoung, Office of Inspection and Enforcement, USNRC, from T. J. Shideler, Barton Instrument Co., November 19, 1982.
3. 10 CFR 21 Notification: Telex to R. C. DeYoung, Office of Inspection and Enforcement, USNRC, from T. J. Shideler, Barton Instrument Co., May 18, 1983.
4. IEEE Standard 323-1974, "IEEE Standard for Qualifying Class 1E Equipment for Nuclear Power Generating Stations," Institute of Electrical and Electronic Engineers, New York, 1974.
5. Technical Manual Model 763 Gage Pressure Electronic Transmitter, Manual 82C1, ITT Barton Instruments, City of Industry, CA.
6. IEEE Standard 381-1977, "IEEE Standard Criteria for Type Tests of Class 1E Modules Used in Nuclear Power Generating Stations," Institute of Electrical and Electronic Engineers, New York, 1977.
7. Qualification Test Report - Barton Model 763 Gage Pressure Electronic Transmitter, Report R3-763-6, ITT Barton Instruments, City of Industry, CA.
8. Private communication with W. McCulloch, Sandia National Laboratories, August 16, 1984.
9. Buckalew, W. H. and F. V. Thome, "Radiation Capabilities of the Sandia High Intensity Adjustable Cobalt Array," SAND81-2655, NUREG/CR-1682, Sandia National Laboratories, March 1982.
10. Craft, C. M., "Screening Tests of Terminal Block Performance in a Simulated LOCA Environment," SAND83-1617, NUREG/CR-3418, Sandia National Laboratories, August 1984.
11. Phone Conversation with B. Provines, Spectrol Corporation, February 1, 1984.
12. Private Communication with L. Harrah and J. Sayer, Sandia National Laboratories, February 3, 1984.
13. Phone Conversation with G. Alborne, Ball Brothers, Inc., March 16, 1984.

REFERENCES  
(continued)

14. Phone Conversation with M. Marron, Royal Labs, March 19, 1984.
15. Engineering Instructions for Field Modification of Potentiometer Assembly for ITT Barton Models 763, 764, and 765 Electronic Transmitters, Document 0764-1240B, ITT Barton Instruments, City of Industry, CA, April 1983.
16. Keenan, M. R., "Moisture Permeation into Nuclear Reactor Pressure Transmitters," SAND83-2165, Sandia National Laboratories, March 1984.
17. Phone Conversation with W. Galvan, Spectrol Corporation, March 19, 1984.
18. Private Communication with W. Galvan, Spectrol Corporation, November 7, 1984.
19. Private Communication with L. Harrah, Sandia National Laboratories, February 3, 1984.
20. Bustard, L. D., "The Effect of LOCA Simulation Procedures on Cross-Linked Polyolefin Cable's Performance," SAND83-2406, NUREG/CR-3588, Sandia National Laboratories, April 1984.
21. Bustard, L. D., "The Effect of LOCA Simulation Procedures on Ethylene Propylene Rubber's Mechanical and Electrical Properties," SAND83-1258, NUREG/CR-3538, Sandia National Laboratories, October 1983.
22. Minor, E. E. and D. T. Furgal, "Equipment Qualification Research Test of Electric Cable with Factory Splices and Insulation Rework Report Nos. 1 and 2," SAND81-2027, NUREG/CR-2932, Sandia National Laboratories, September 1982.
23. Phone Conversation between E. Salazar, Sandia National Laboratories, and E. Romo, ITT Barton, October 25, 1983.

APPENDIX A

TRANSMITTER RESPONSE AT  
600 PSIG NOMINAL PRESSURE

This appendix contains a series of plots depicting the response of five transmitters while maintaining 600 psig (nominal) pressure input. The plots show the relationship of transmitter data to temperature and time for an initial test sequence and a retest sequence. The five sets of plots have similar figure numbers but are distinguished from each other by a prefix identifier (i.e., T1-A-3 and T2-A-3 are plots of the initial test sequence temperature profiles for transmitters T1 and T2, respectively). A listing of the figures in this appendix is contained below:

- A-1 Initial Test Sequence Temperature Profile
- A-2 Initial Test Sequence Error Profile
- A-3 First 100 Hours Test Sequence Temperature Profile
- A-4 First 100 Hours Error Profile
- A-5 First 26 Hours Test Sequence Temperature Profile
- A-6 First 26 Hours Error Profile
- A-7 Initial Test Sequence Data Scatter-Error vs  
Temperature
- A-8 Special Test Sequence Temperature Profile
- A-9 Special Test Sequence Error Profile
- A-10 Special Test Sequence Initial 3 Hour Error Profile
- A-11 Special Test Sequence Data Scatter Error vs  
Temperature

The error data plotted herein is shown in percent of full-scale reading. The error can be converted to error in psi by multiplying the ordinate by 10 (i.e., 6.0 percent FS error equals 60 psi error). The error data can be evaluated as a percent of applied pressure basis by dividing the ordinate by 0.6 (i.e., 6.0 percent FS error equals 10.0 percent error at applied pressure).

For convenience, the test environment applied to each transmitter are repeated below:

- T1 LOCA Steam and Chemical Spray
- T2 Dry Temperature Exposure (oven)
- T3 Steady State Radiation Exposure at Ambient Temperature
- T4 LOCA Temperature Profile and Steady State Radiation
- T5 LOCA Steam Profile, Chemical Spray, and Steady State  
Radiation

Figure T1-A-1

Transmitter T1 Test Sequence Temp. Profile

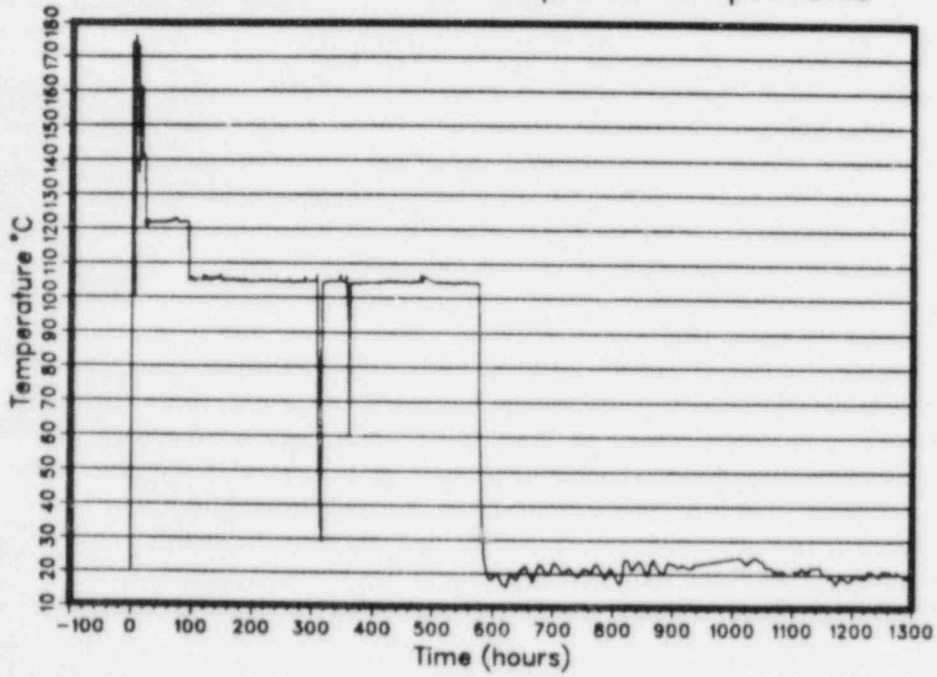


Figure T1-A-2

Transmitter T1 Test Sequence Error Profile

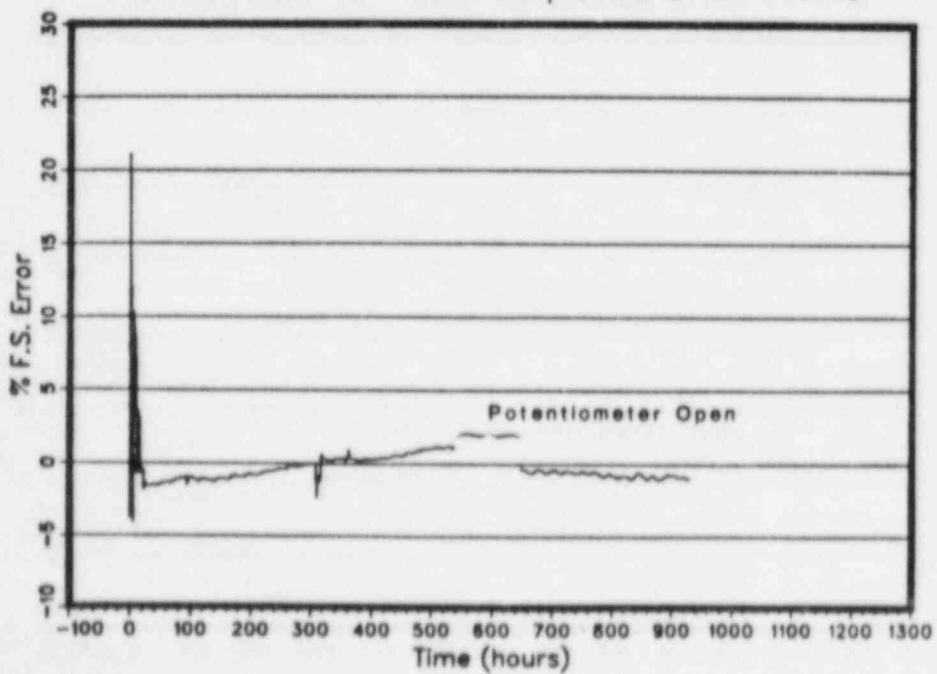


Figure T1-A-3

Trans. T1 First 100 hrs Temp. Profile

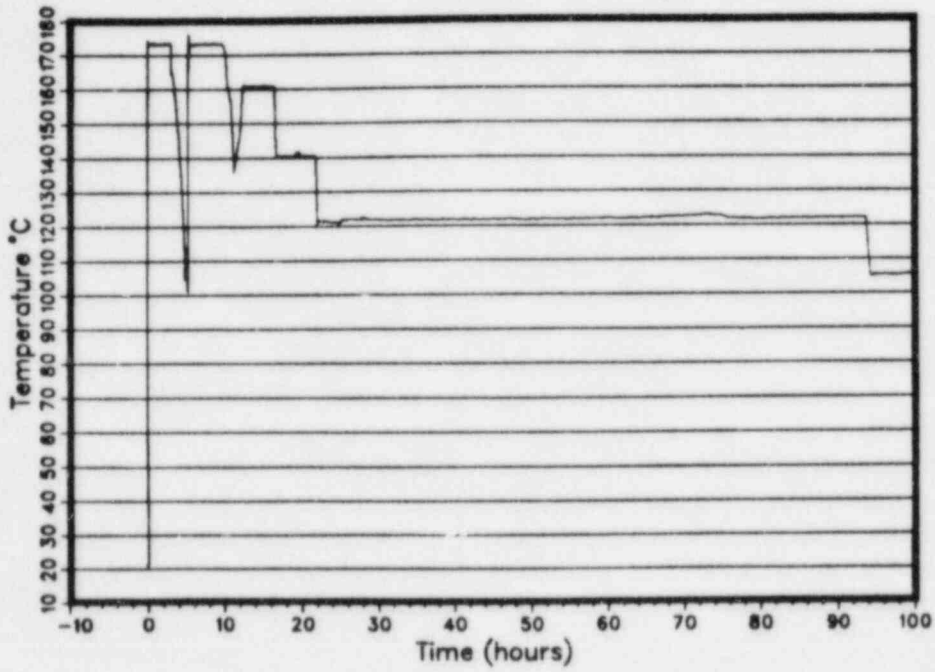


Figure T1-A-4

Trans. T1 First 100 hrs Error Profile

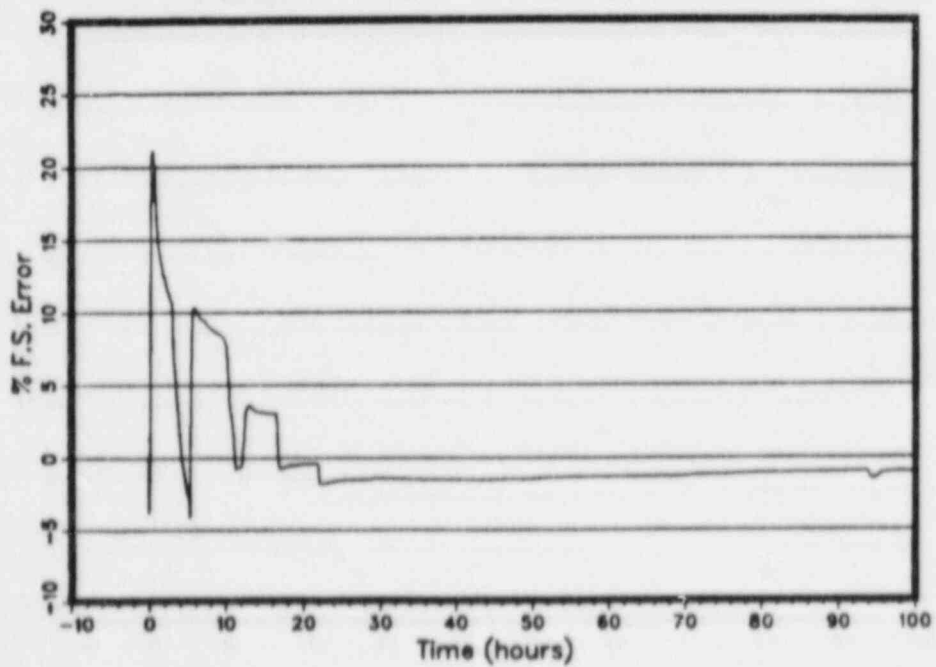


Figure T1-A-5

Trans. T1 First 26 hrs. Temp. Profile

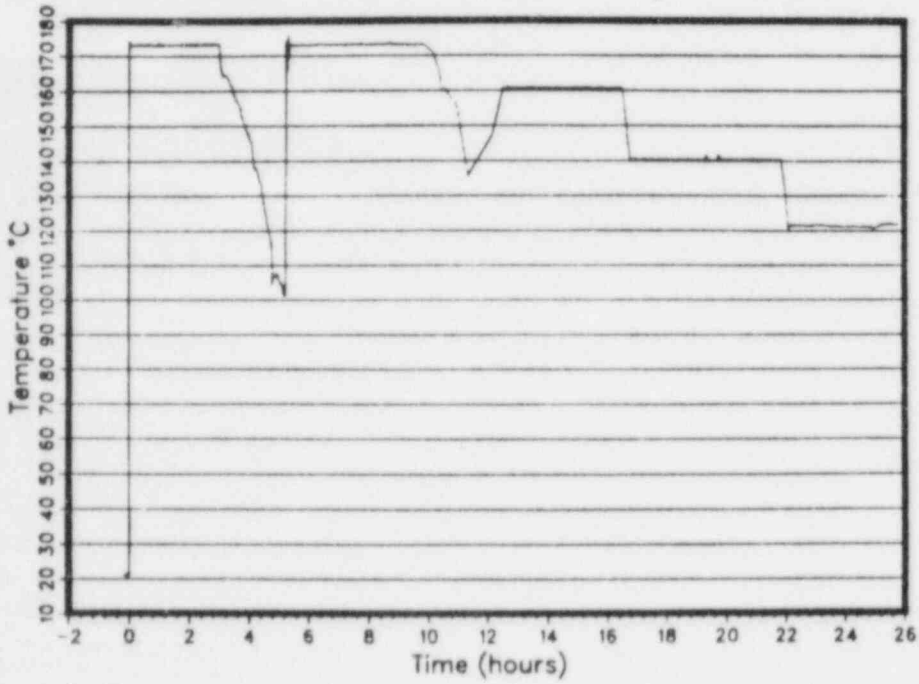


Figure T1-A-6

Trans. T1 First 26 hrs. Error Profile

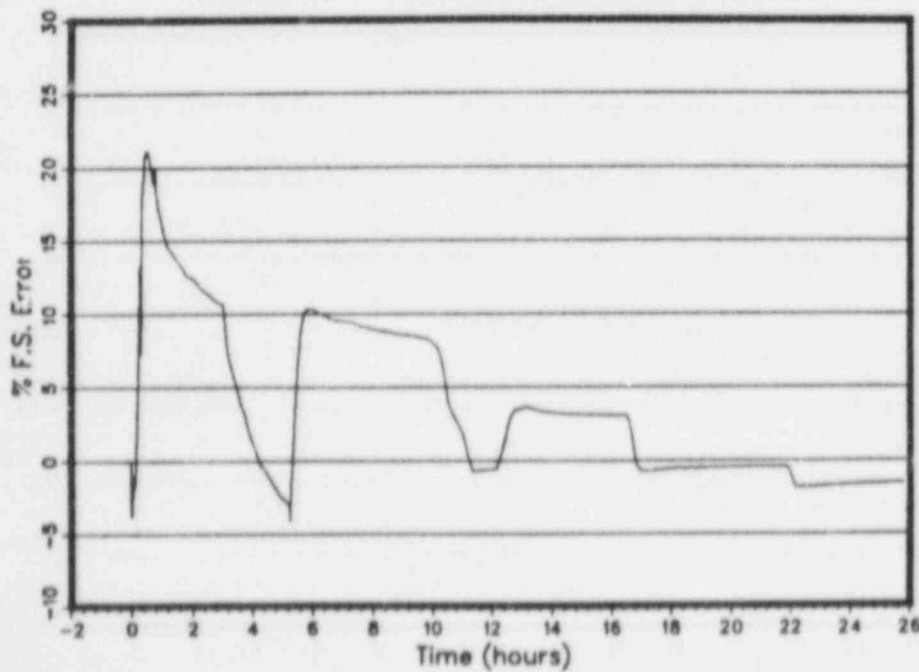


Figure T1-A-7

Transmitter T1 Test Sequence Data Scatter

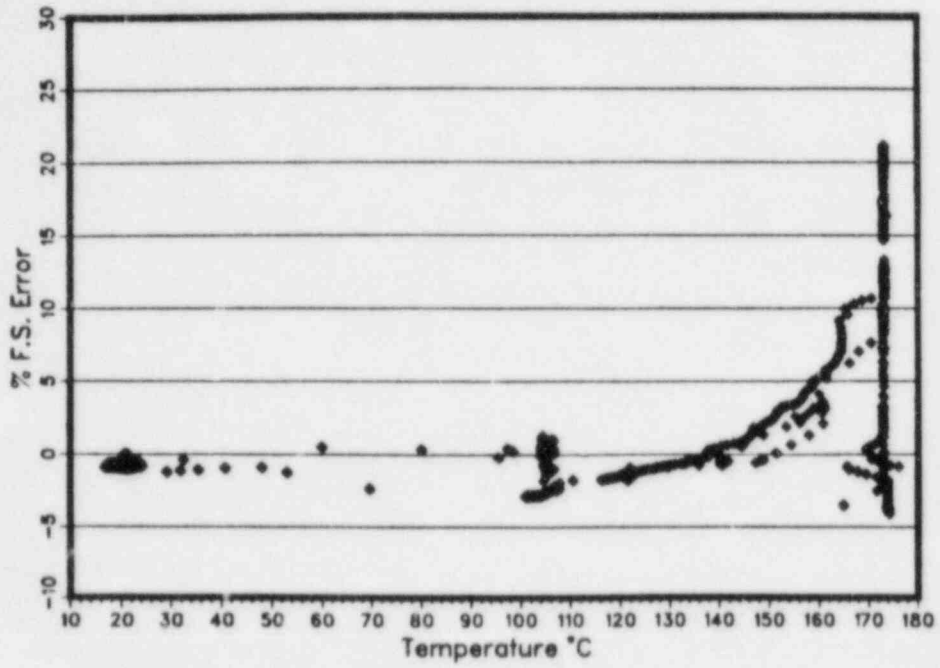


Figure T1-A-8

Trans. T1 Special Test Sequence Data Scatter

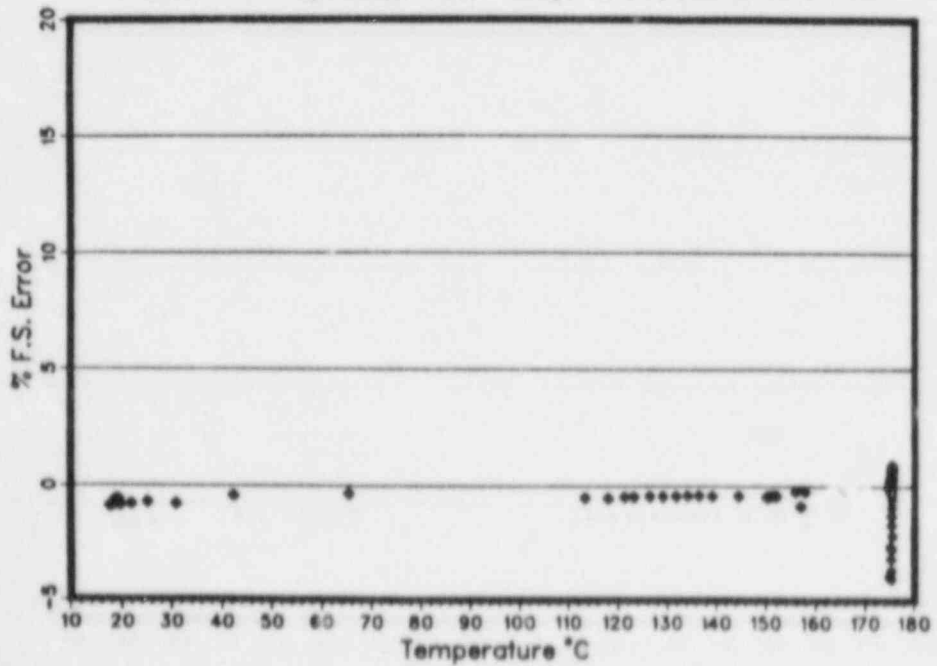


Figure T1-A-9

Trans. T1 Special Test Sequence Temp. Profile

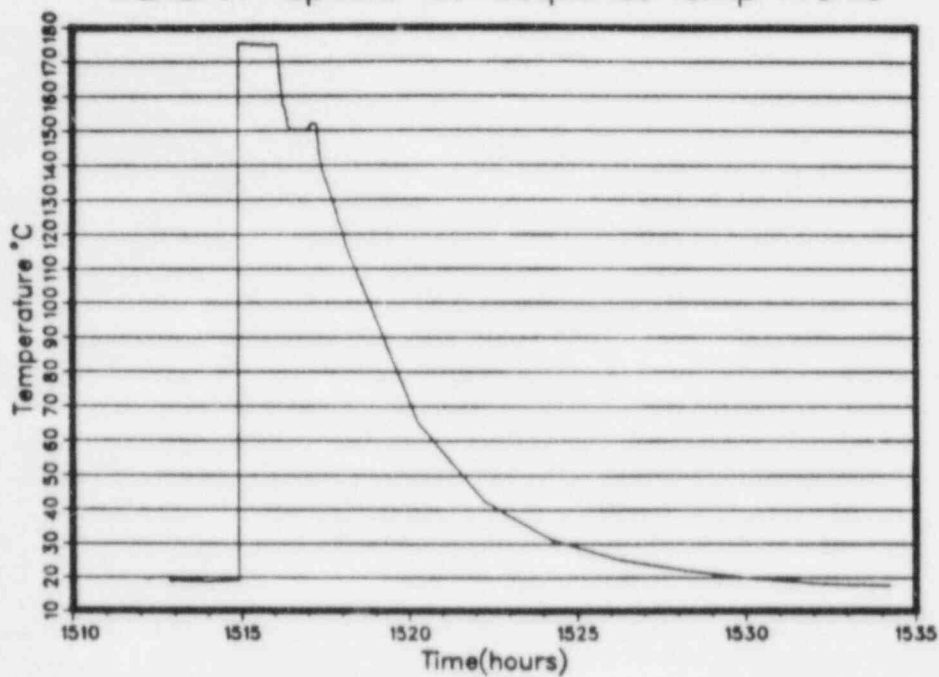


Figure T1-A-10

Trans. T1 Special Test Sequence Error Profile

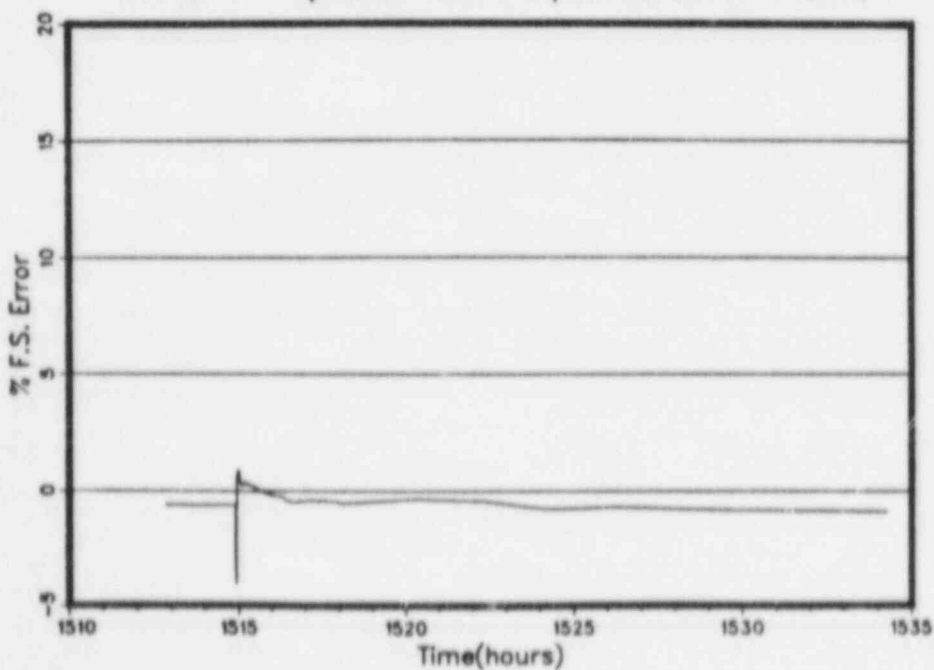


Figure T1-A-11

Trans. T1 Special Test 3 Hour Temp. Profile

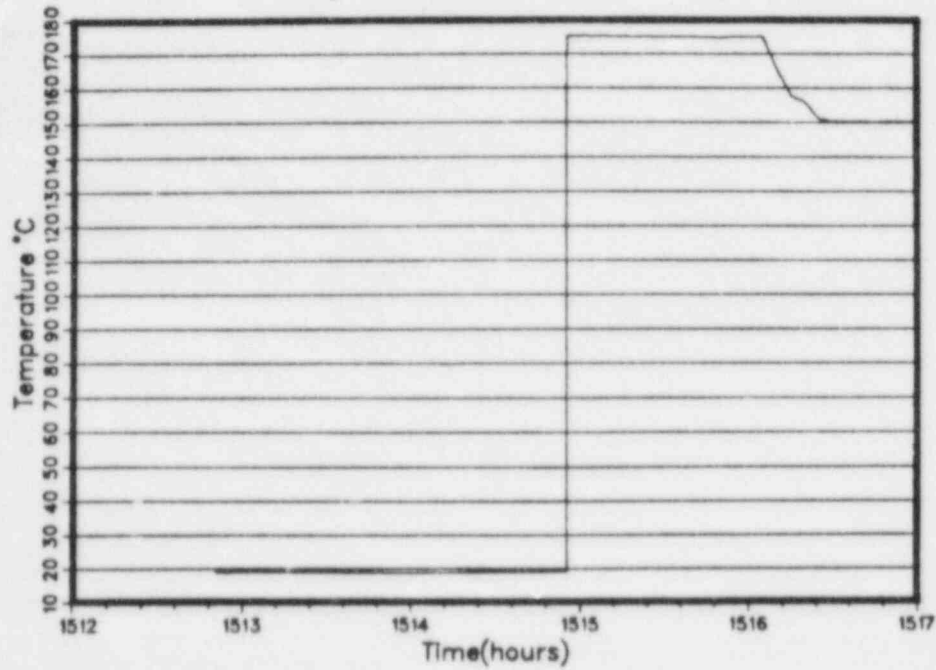


Figure T1-A-12

Trans. T1 Special Test 3 Hour Error Profile

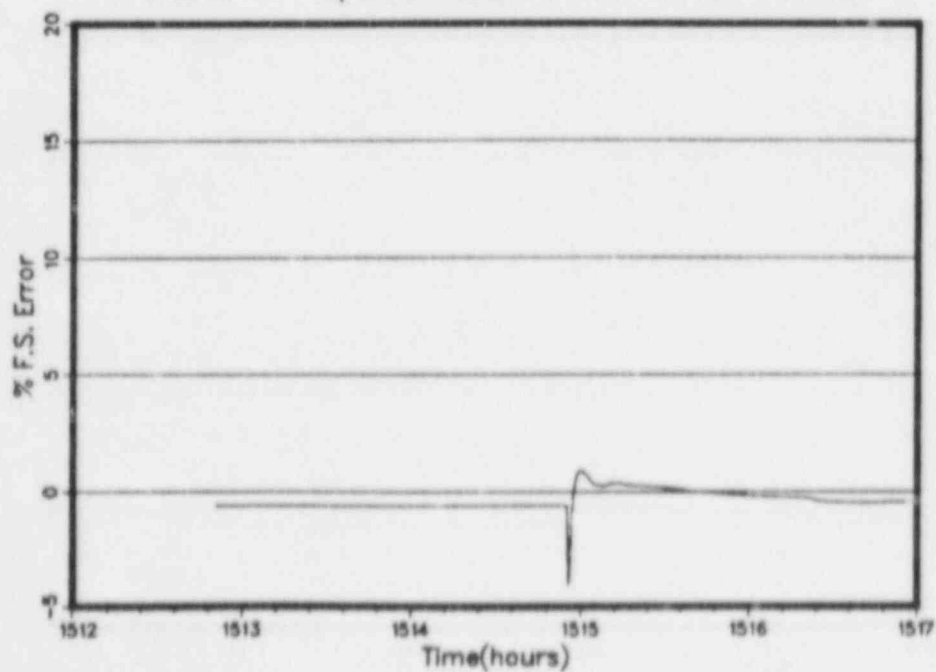


Figure T2-A-1

Transmitter T2 Test Sequence Temp. Profile

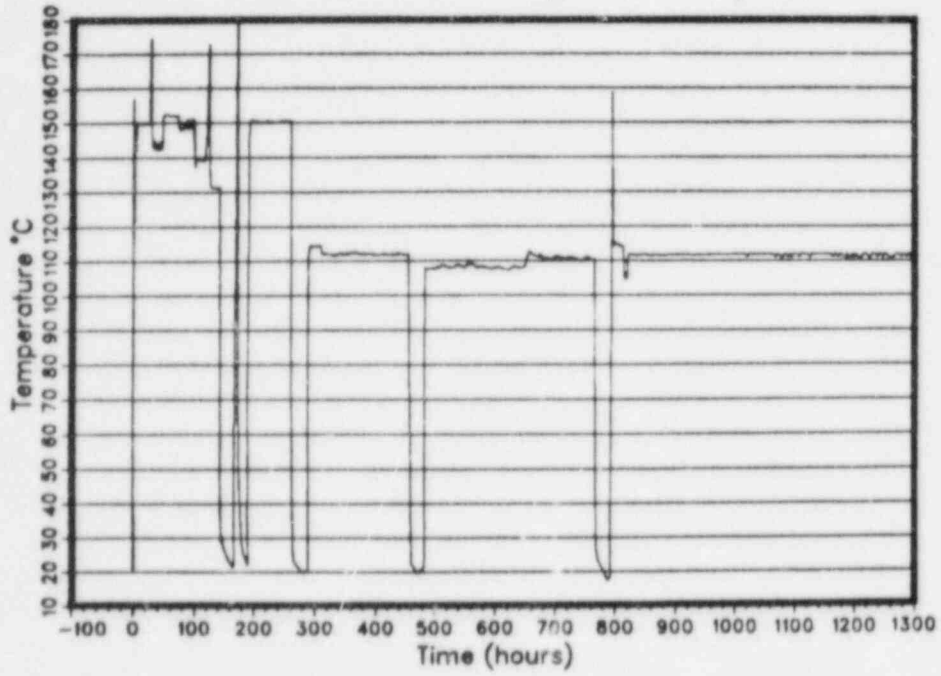


Figure T2-A-2

Transmitter T2 Test Sequence Error Profile

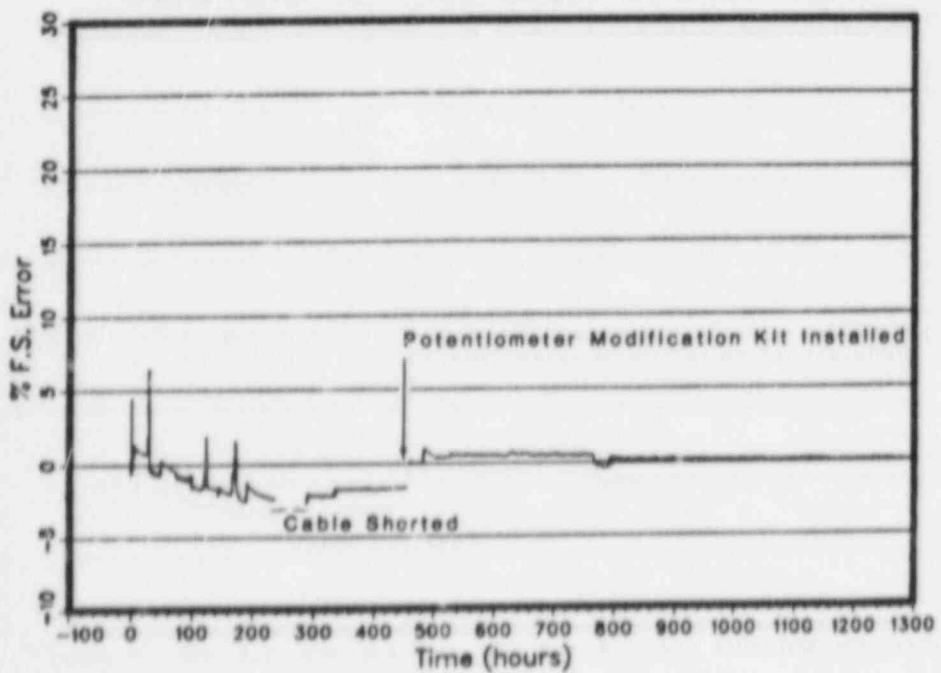


Figure T2-A-3

Trans. T2 First 100 hrs Temp. Profile

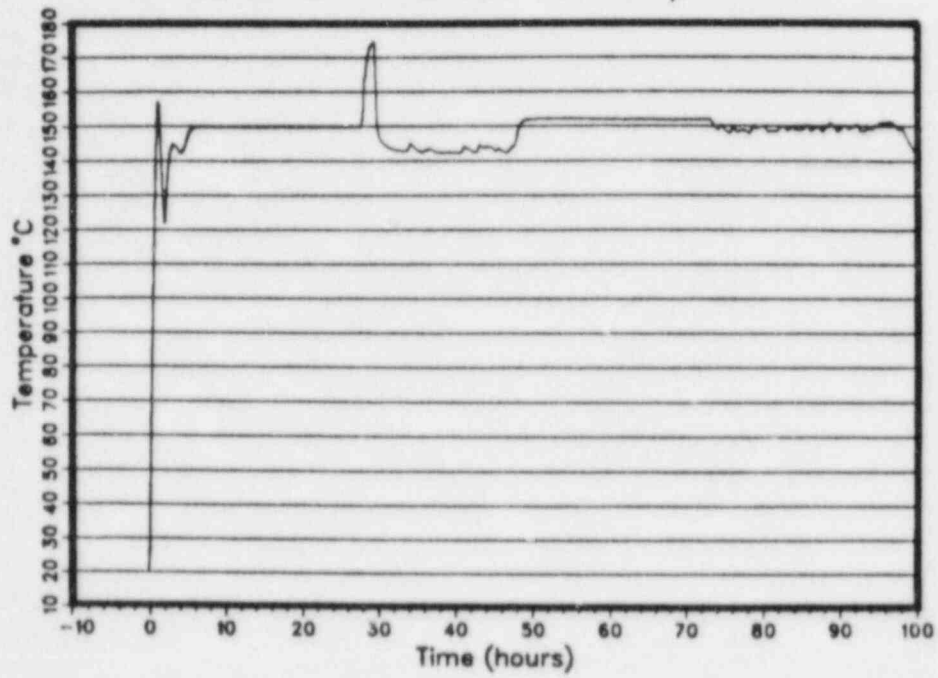


Figure T2-A-4

Trans. T2 First 100 hrs Error Profile

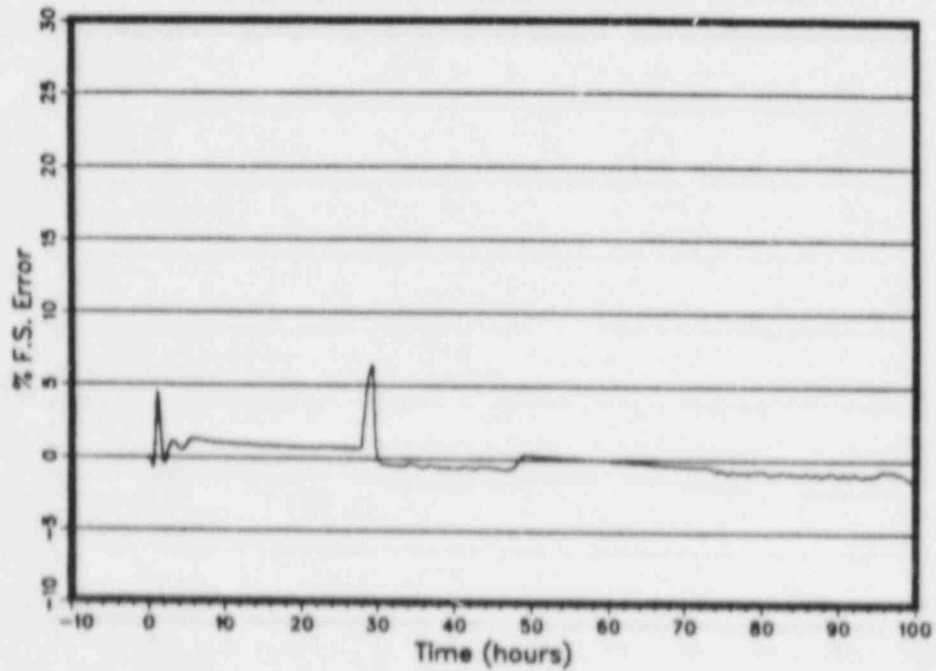


Figure T2-A-5

Trans. T2 First 26 hrs. Temp. Profile

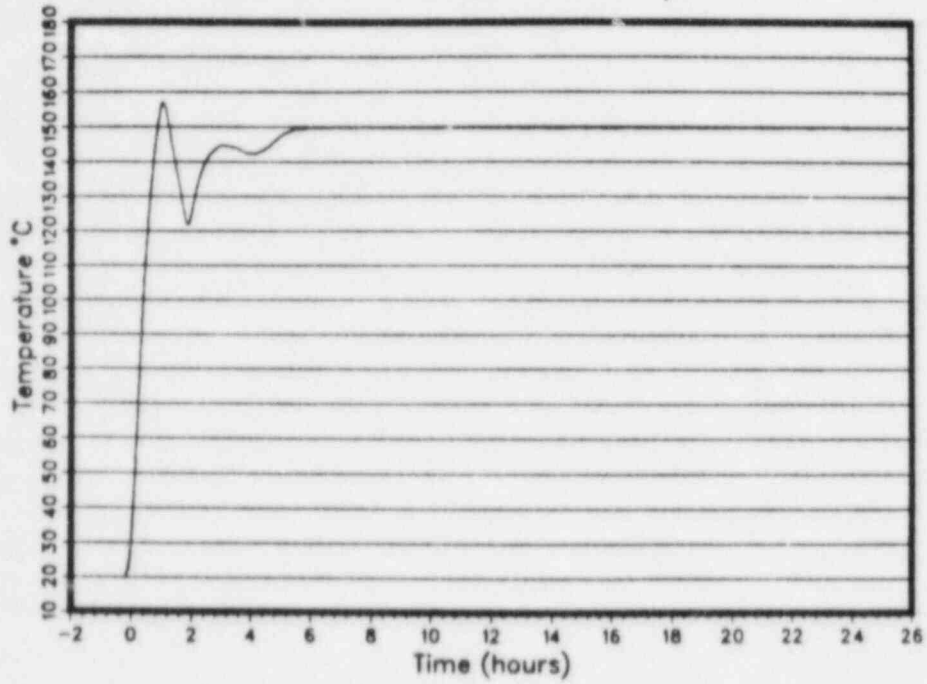


Figure T2-A-6

Trans. T2 First 26 hrs. Error Profile

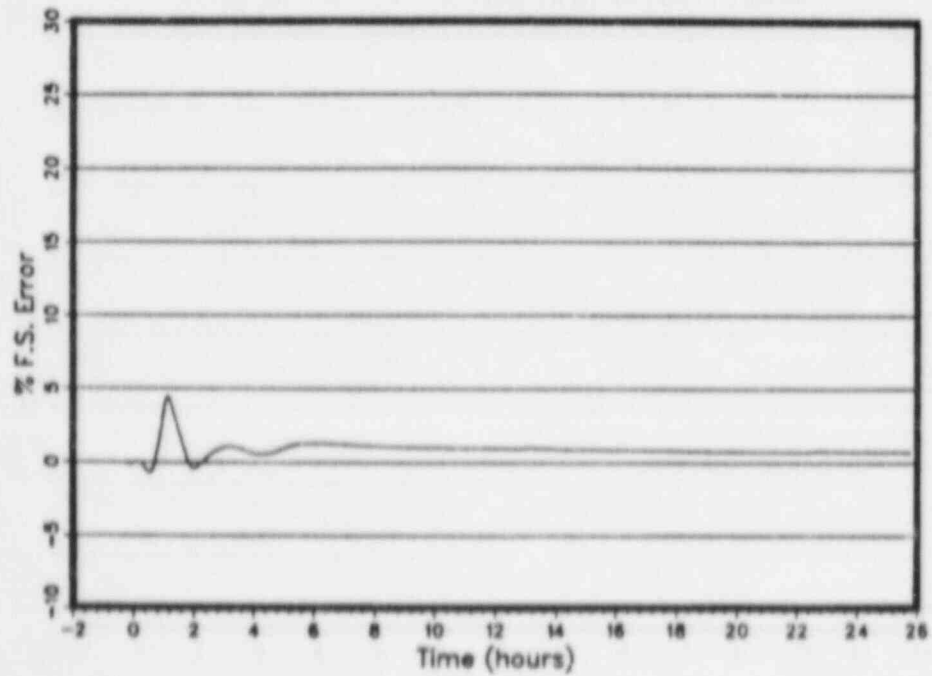


Figure T2-A-7

Transmitter T2 Test Sequence Data Scatter

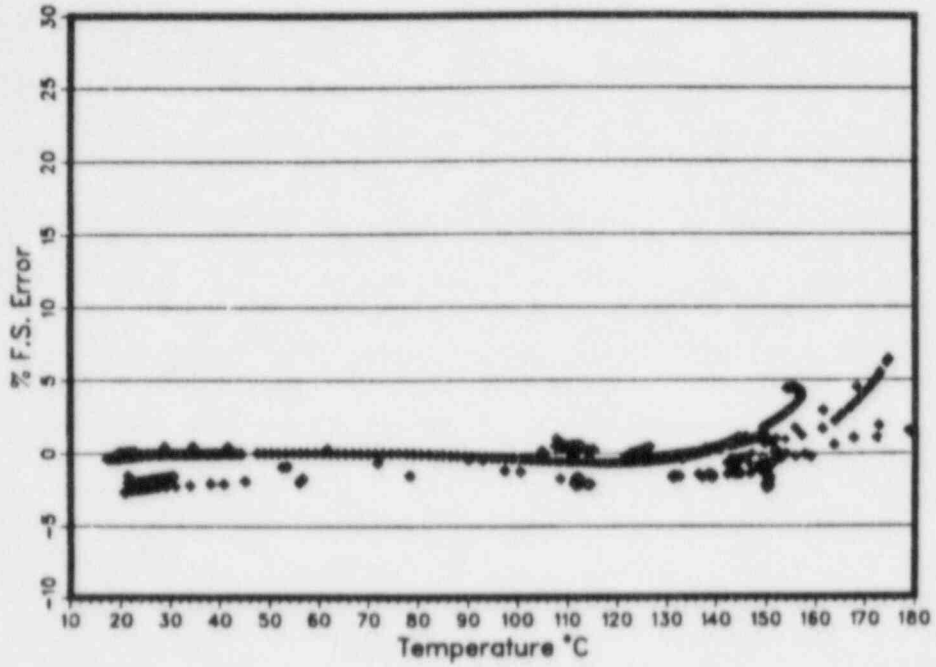


Figure T2-A-8

Trans. T2 Special Test Sequence Data Scatter

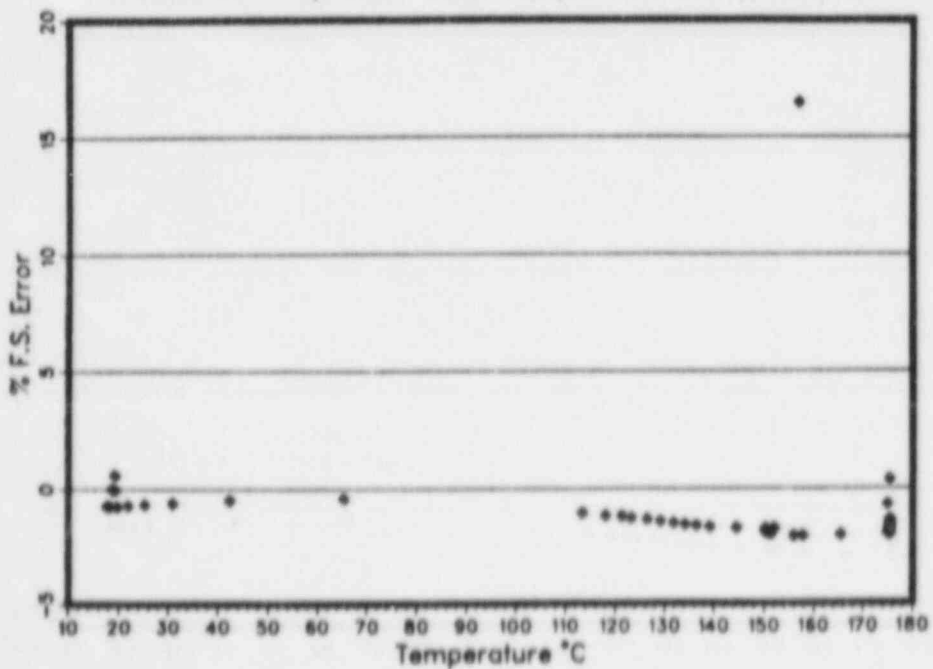


Figure T2-A-9

Trans. T2 Special Test Sequence Temp. Profile

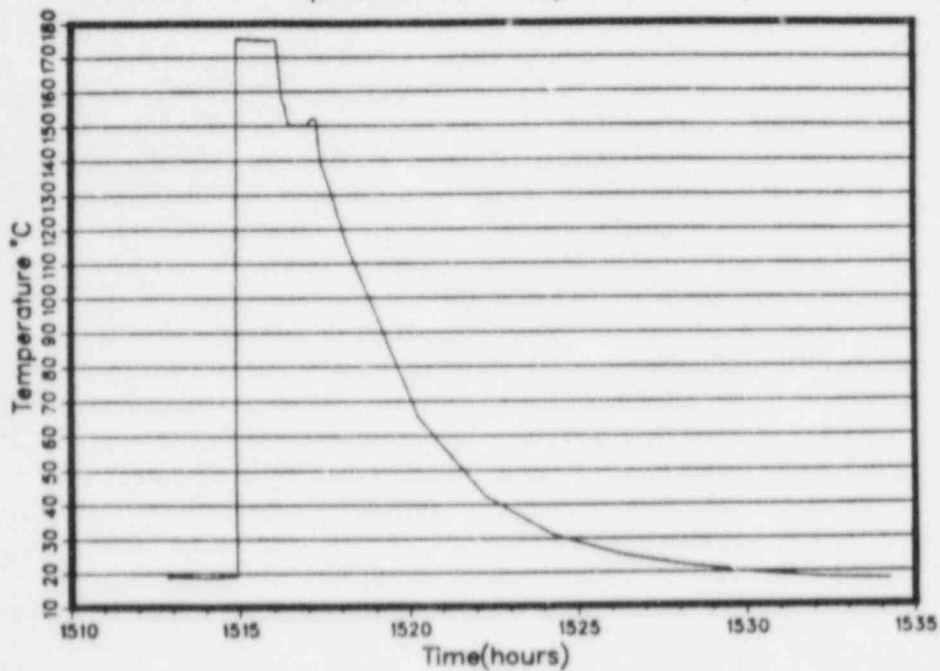


Figure T2-A-10

Trans. T2 Special Test Sequence Error Profile

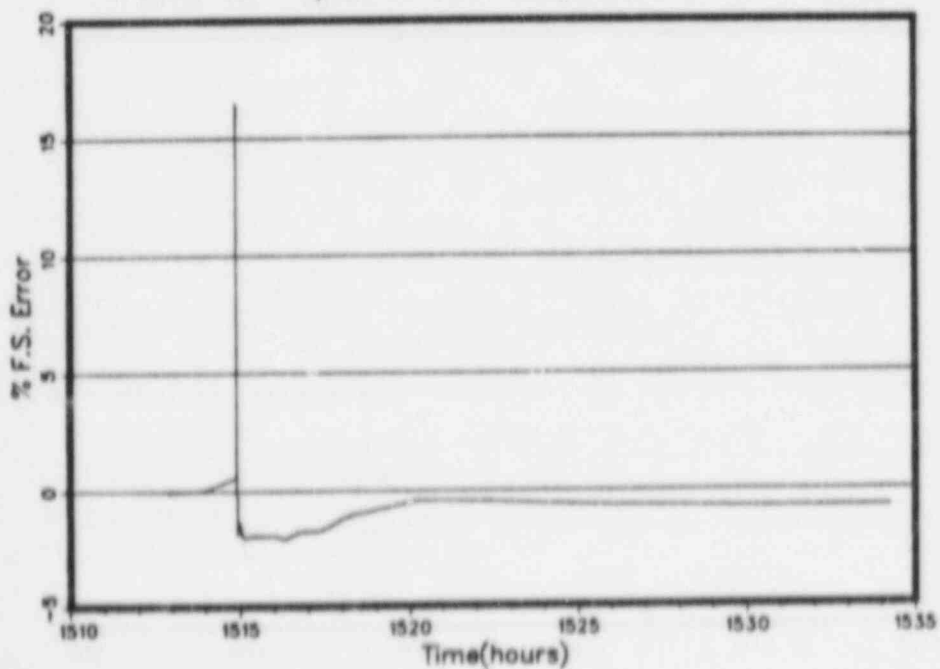


Figure T2-A-11

Trans. T2 Special Test 3 Hour Temp. Profile

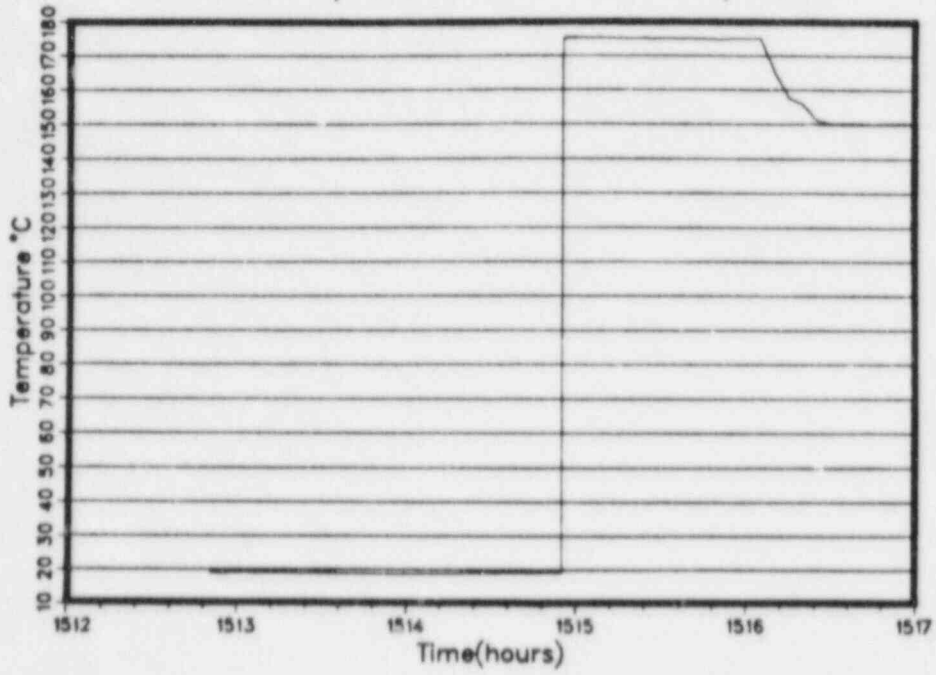


Figure T2-A-12

Trans. T2 Special Test 3 Hour Error Profile

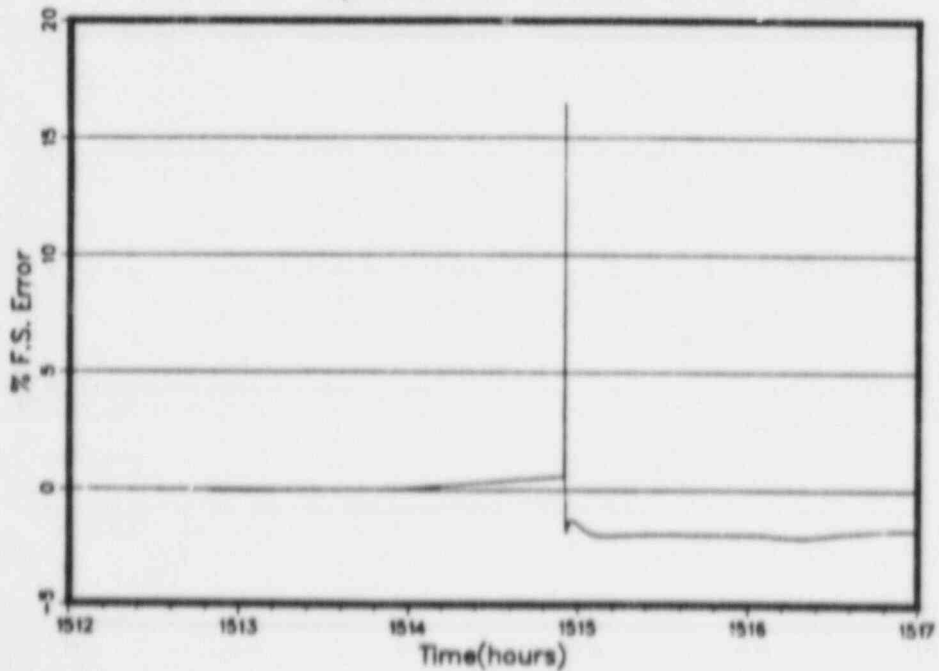


Figure T3-A-1

Transmitter T3 Test Sequence Temp. Profile

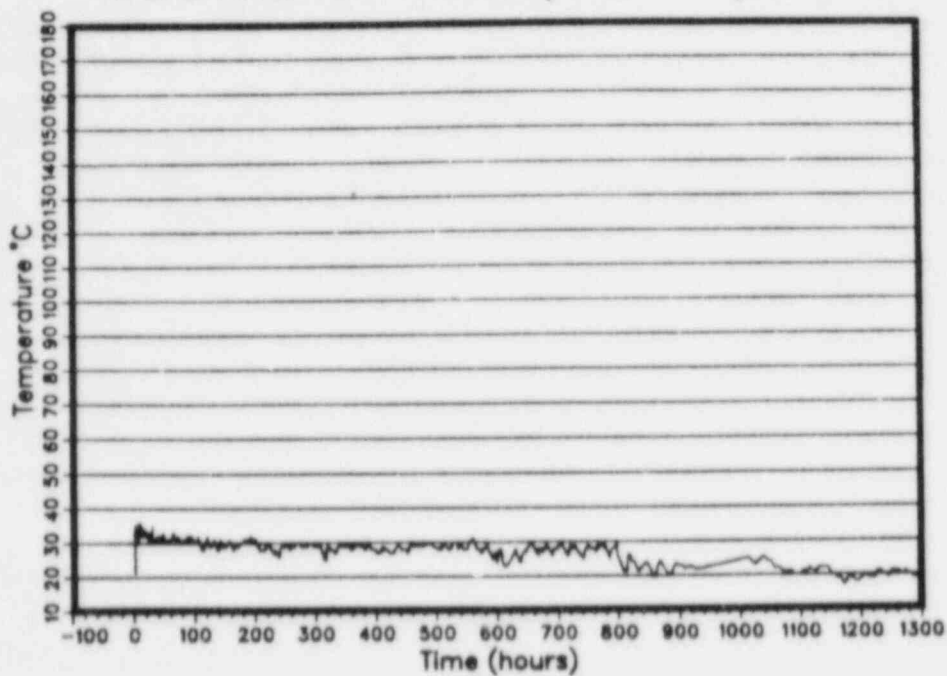


Figure T3-A-2

Transmitter T3 Test Sequence Error Profile

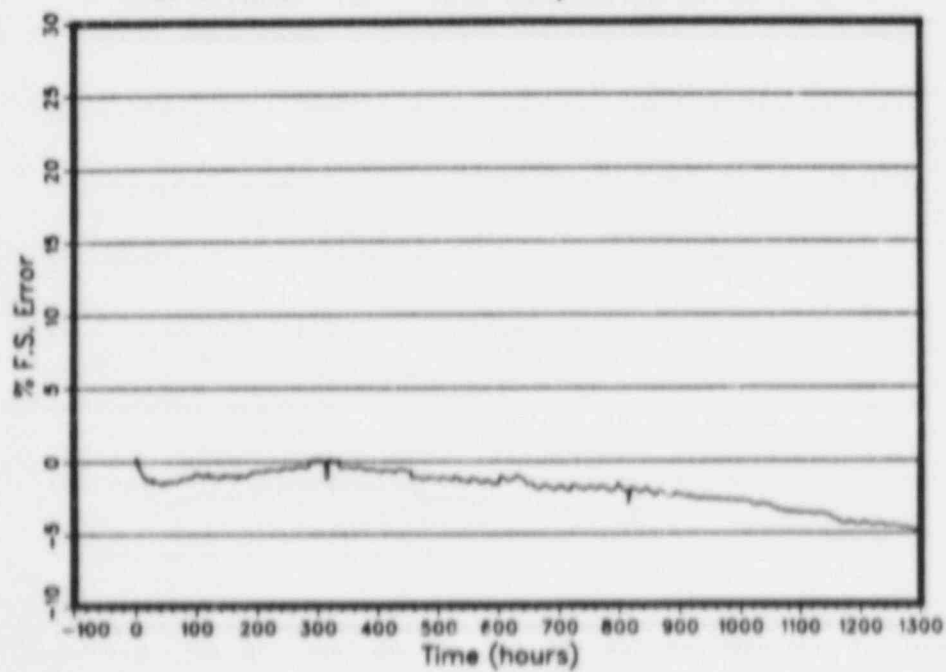


Figure T3-A-3

Trans. T3 First 100 hrs Temp. Profile

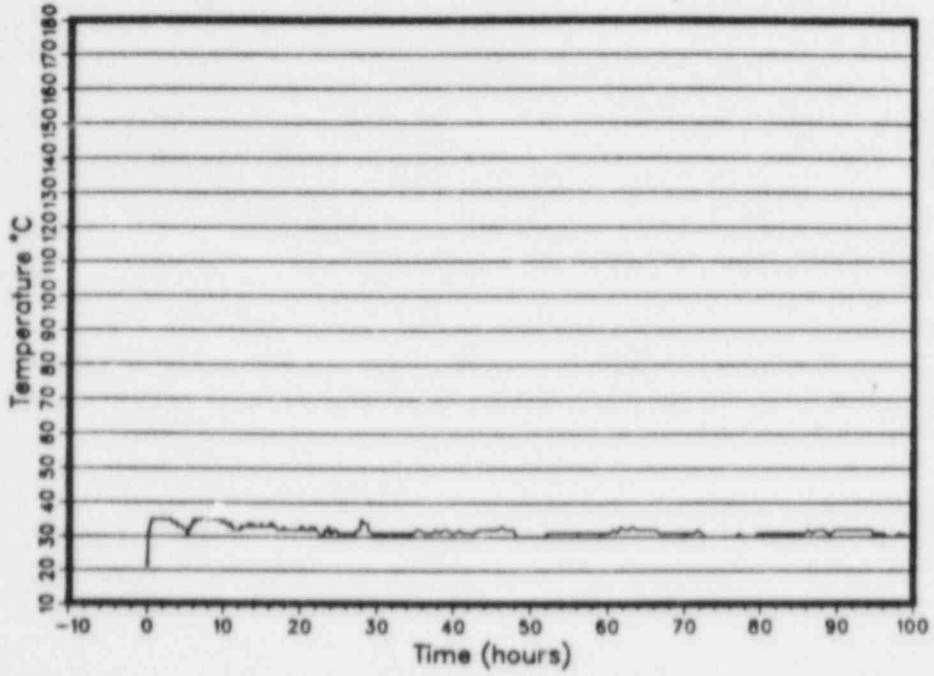


Figure T3-A-4

Trans. T3 First 100 hrs Error Profile

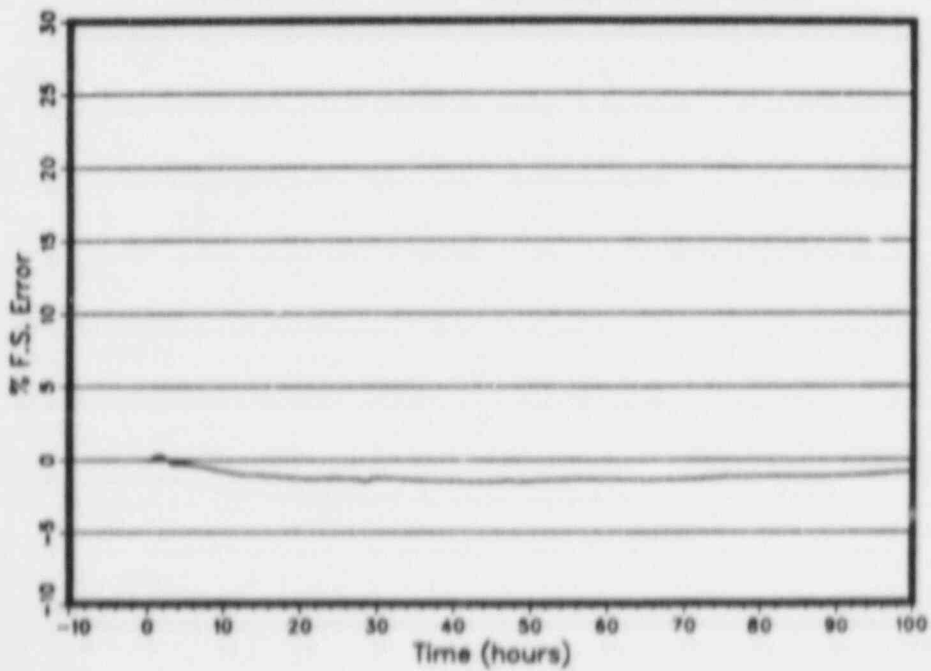


Figure T3-A-5

Trans. T3 First 26 hrs. Temp. Profile

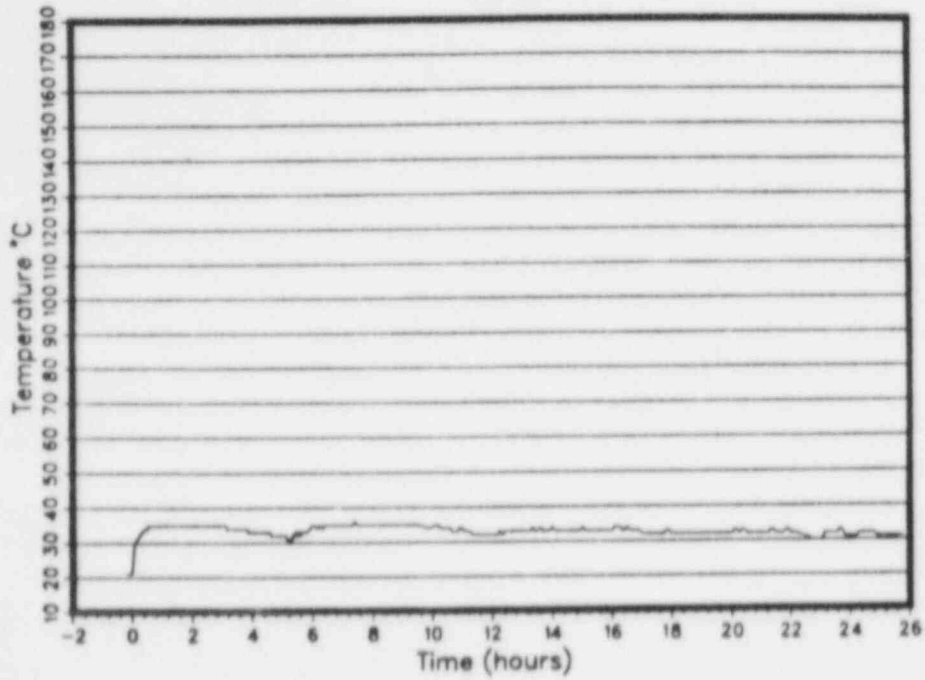


Figure T3-A-6

Trans. T3 First 26 hrs. Error Profile

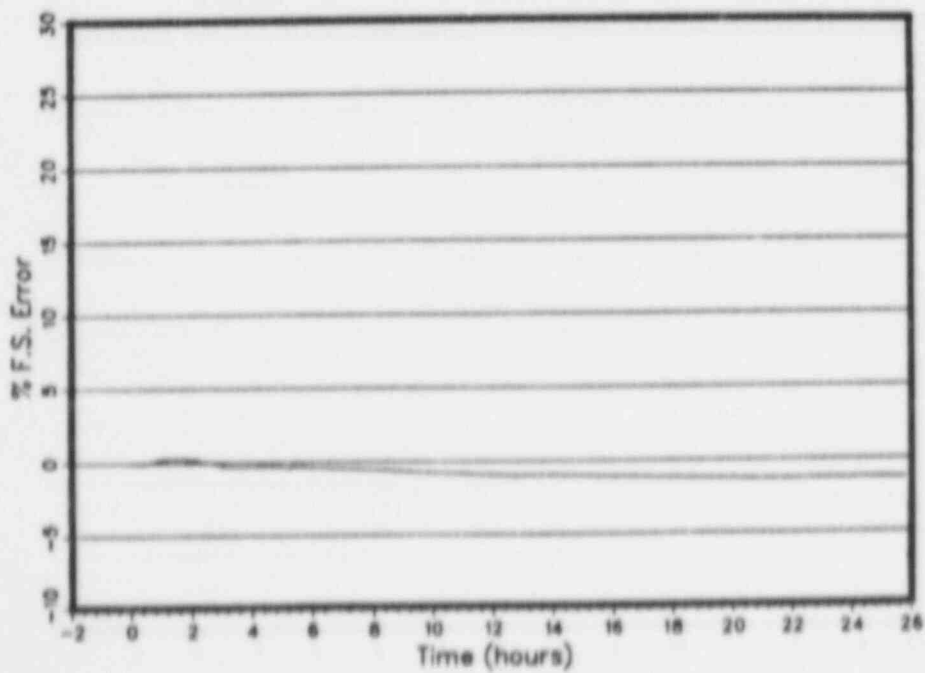


Figure T3-A-7

Transmitter T3 Test Sequence Data Scatter

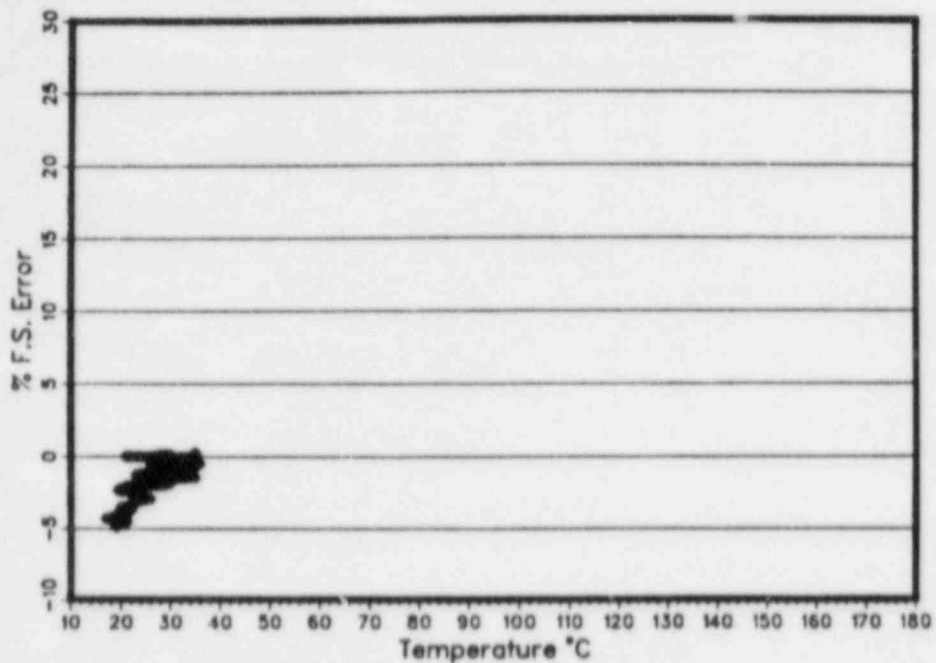


Figure T3-A-8

Trans. T3 Special Test Sequence Data Scatter

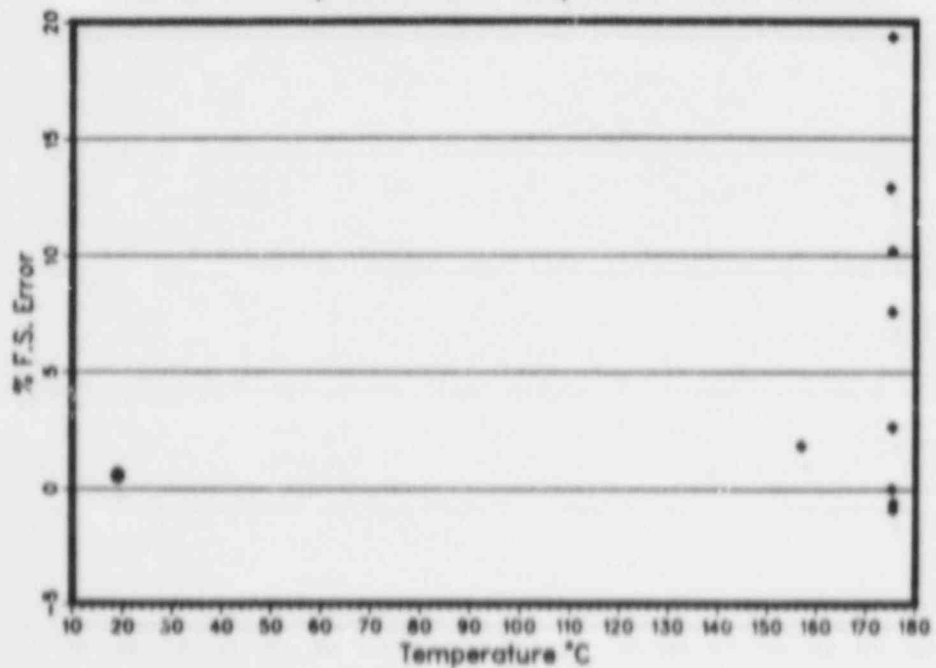


Figure T3-A-9

Trans. T3 Special Test Sequence Temp. Profile

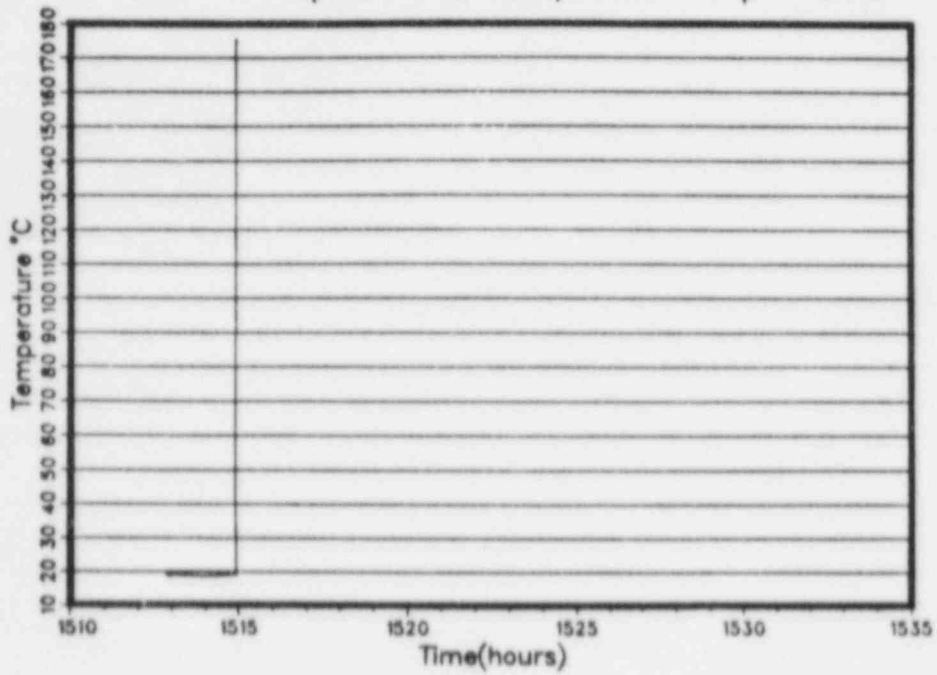


Figure T3-A-10

Trans. T3 Special Test Sequence Error Profile

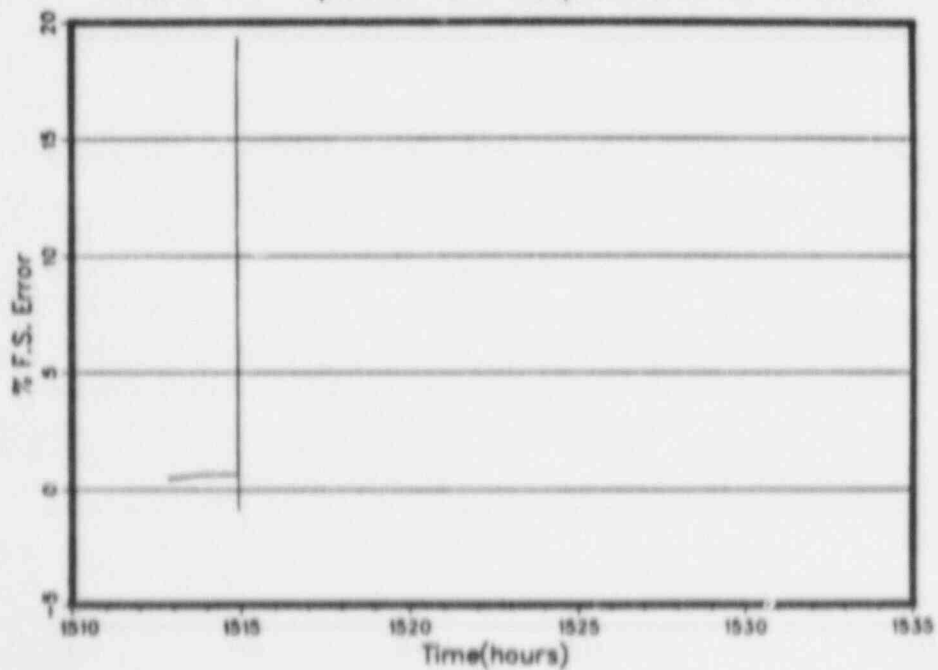


Figure T3-A-11

Trans. T3 Special Test 3 Hour Temp. Profile

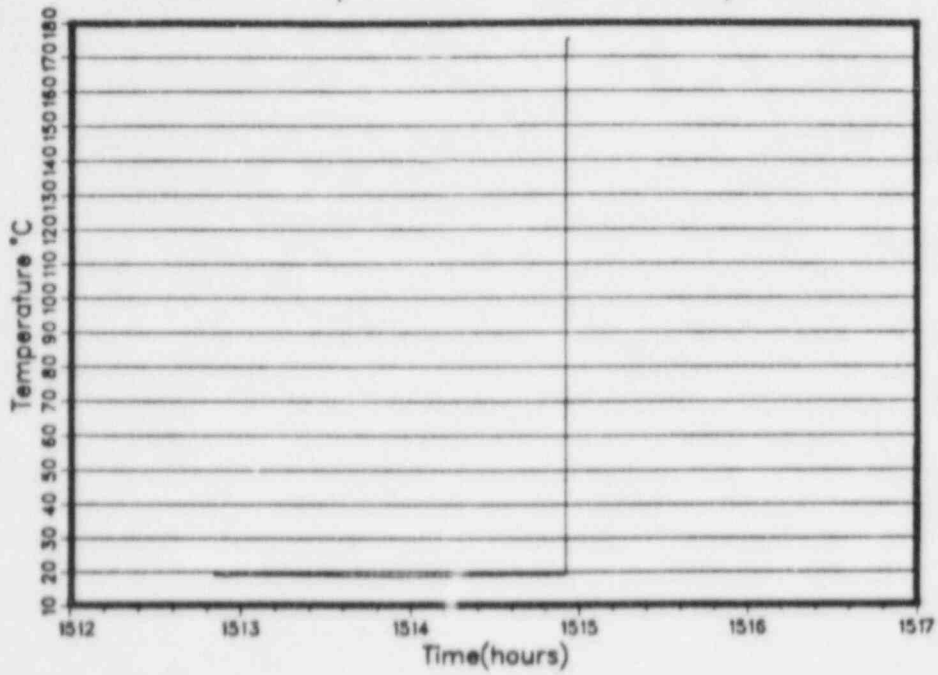


Figure T3-A-12

Trans. T3 Special Test 3 Hour Error Profile

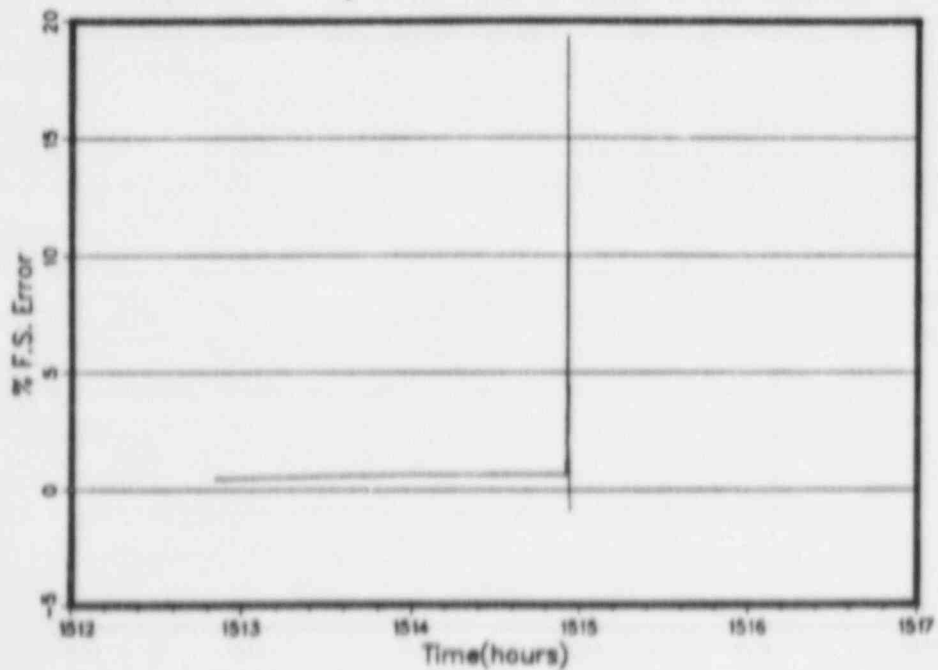


Figure T4-A-1

Transmitter T4 Test Sequence Temp. Profile

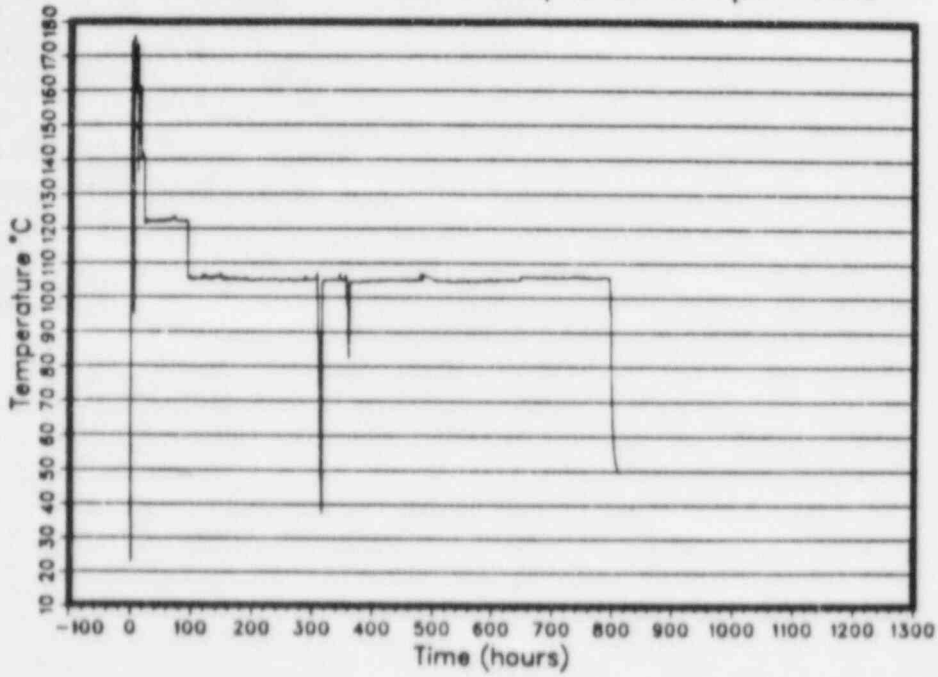


Figure T4-A-2

Transmitter T4 Test Sequence Error Profile

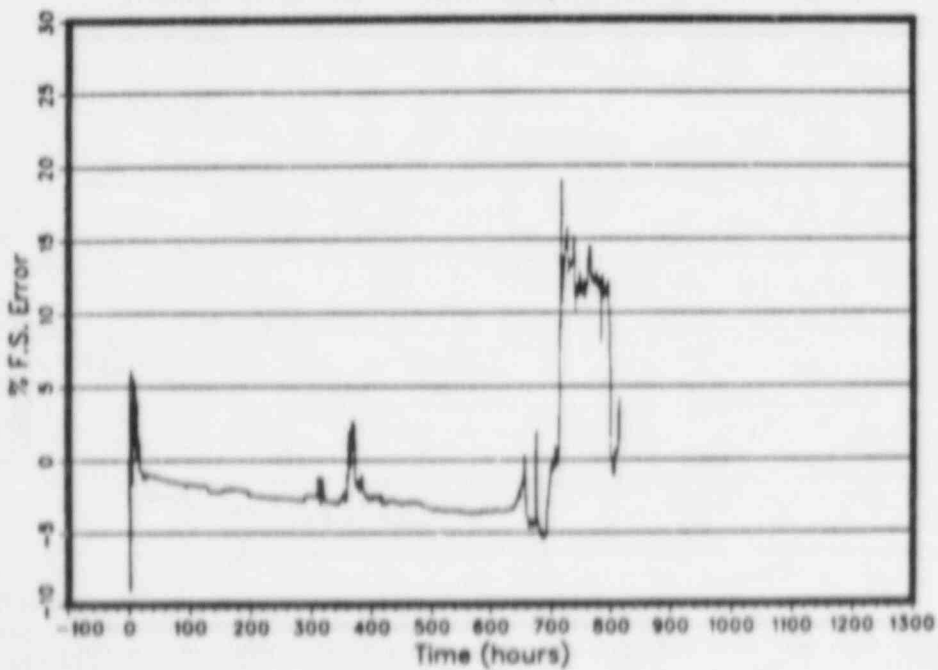


Figure T4-A-3

Trans. T4 First 100 hrs Temp. Profile

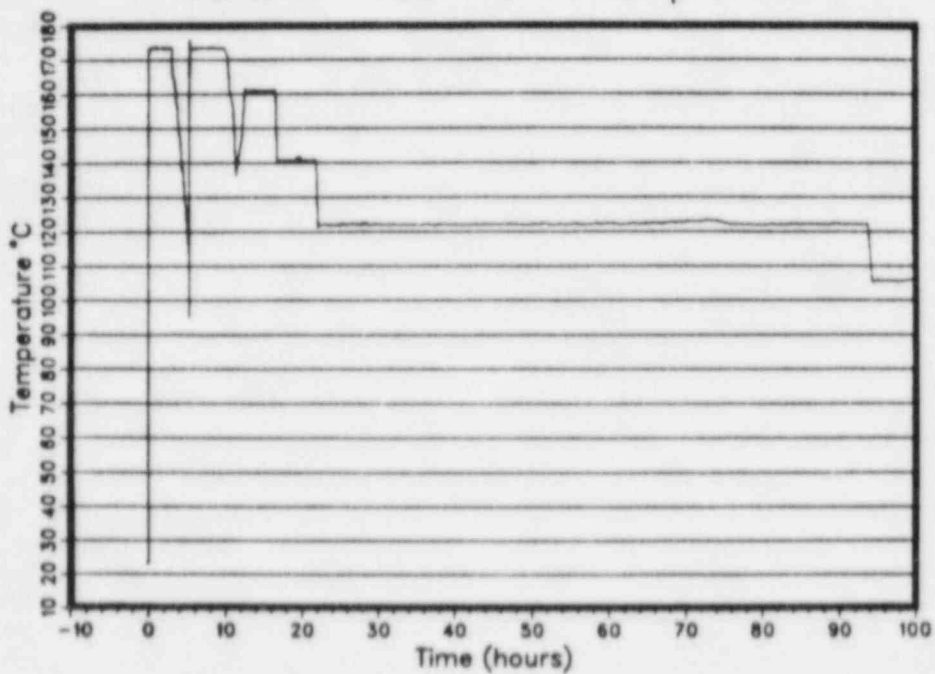


Figure T4-A-4

Trans. T4 First 100 hrs Error Profile

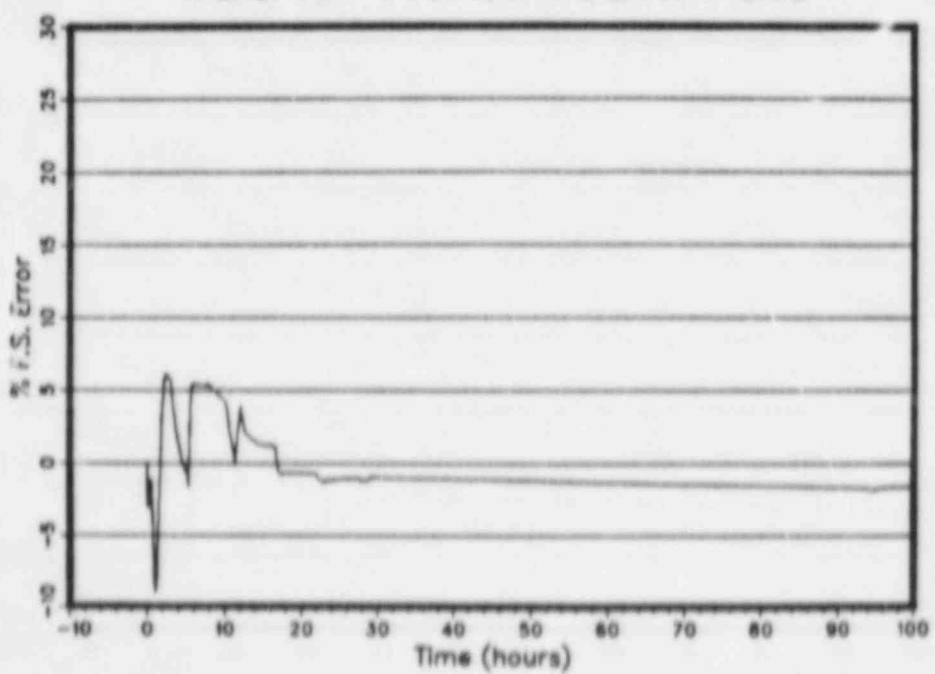


Figure T4-A-5

Trans. T4 First 26 hrs. Temp. Profile

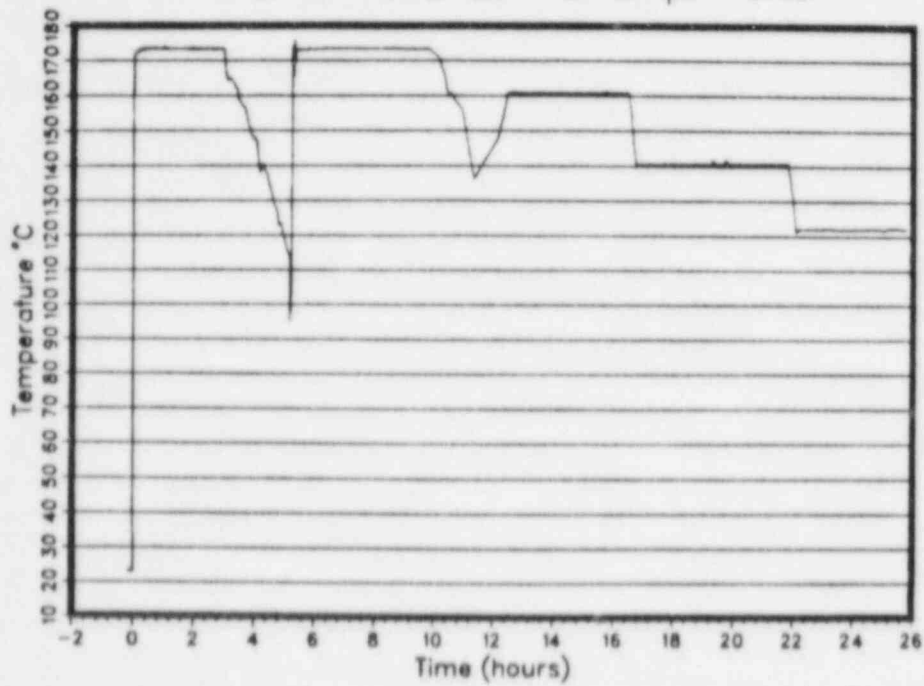


Figure T4-A-6

Trans. T4 First 26 hrs. Error Profile

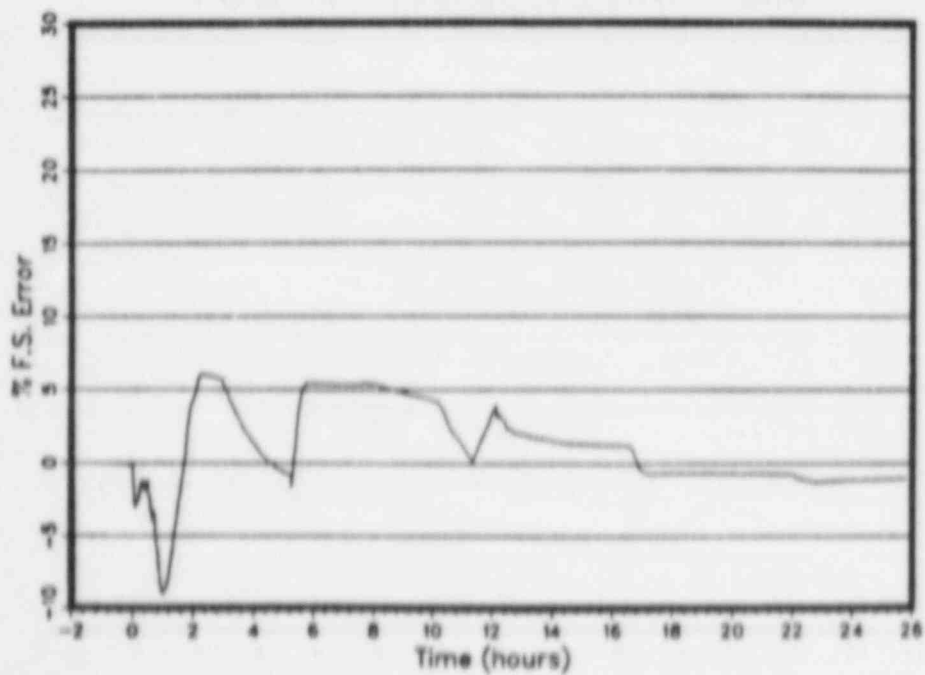


Figure T4-A-7

Transmitter T4 Test Sequence Data Scatter

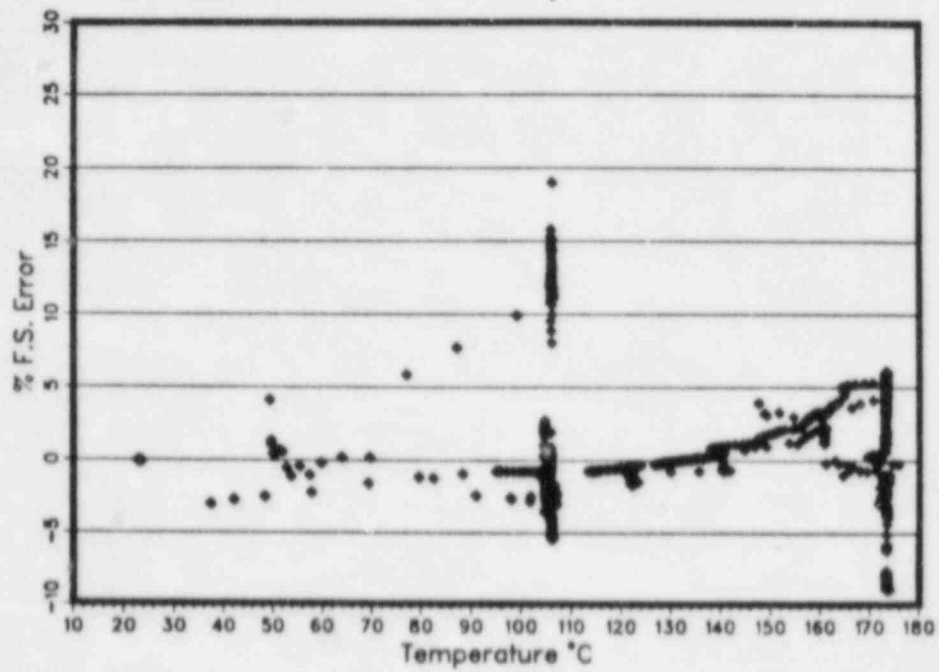


Figure T5-A-1

Transmitter T5 Test Sequence Temp. Profile

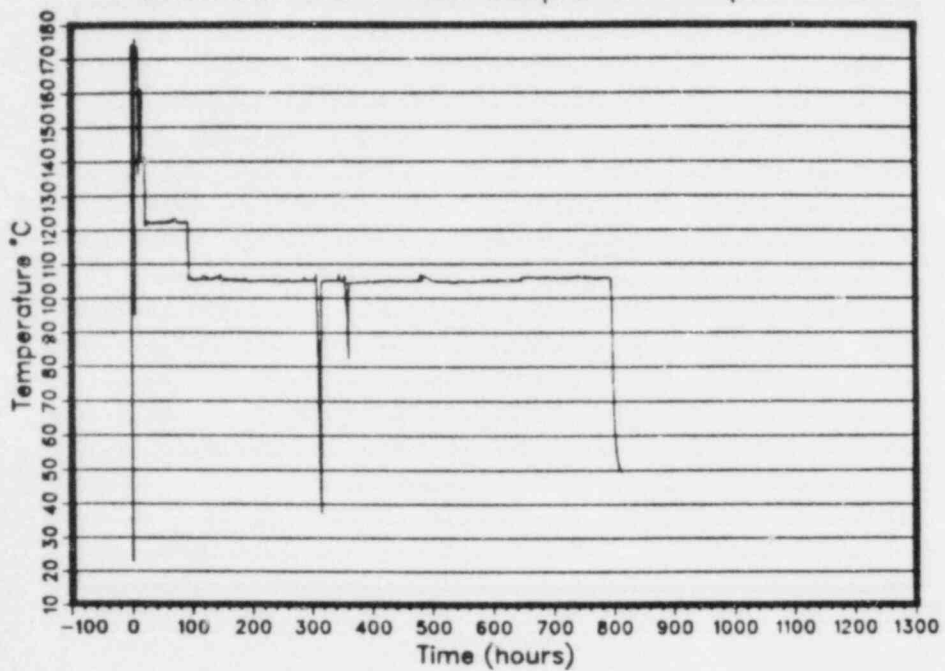


Figure T5-A-2

Transmitter T5 Test Sequence Error Profile

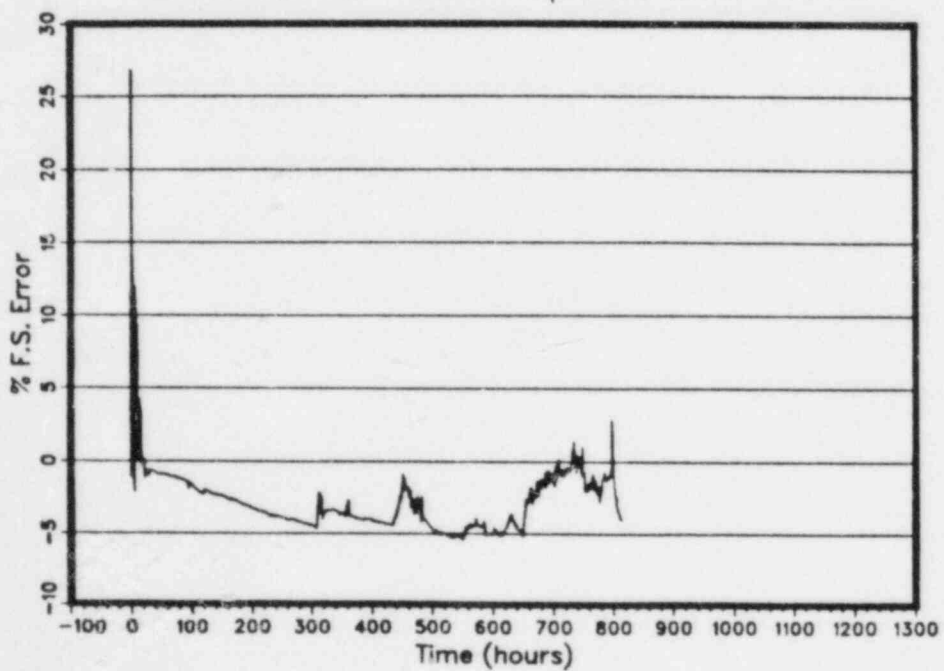


Figure T5-A-3

Trans. T5 First 100 hrs Temp. Profile

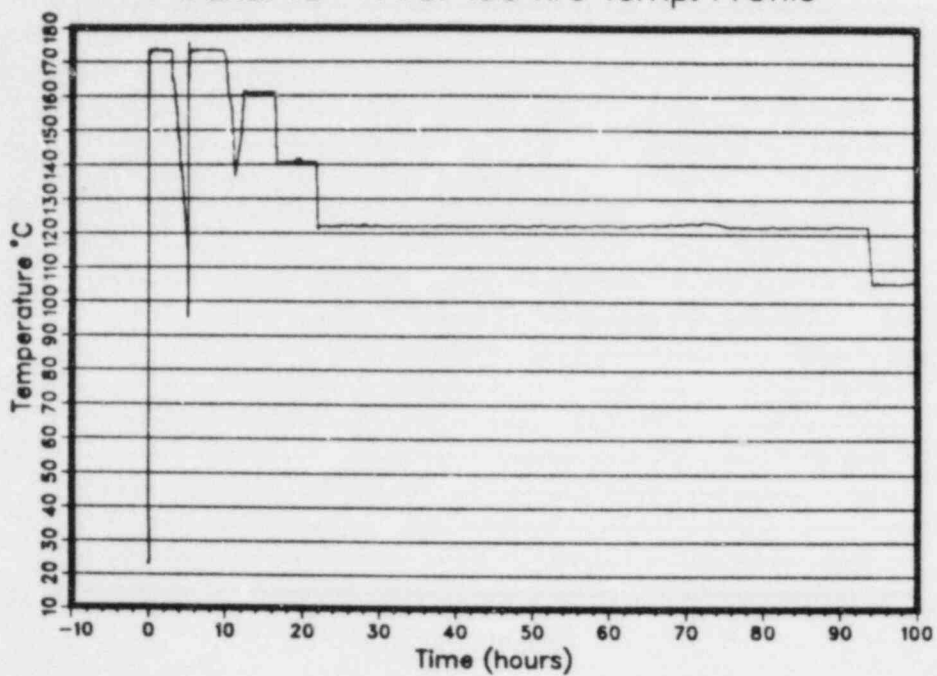


Figure T5-A-4

Trans. T5 First 100 hrs Error Profile

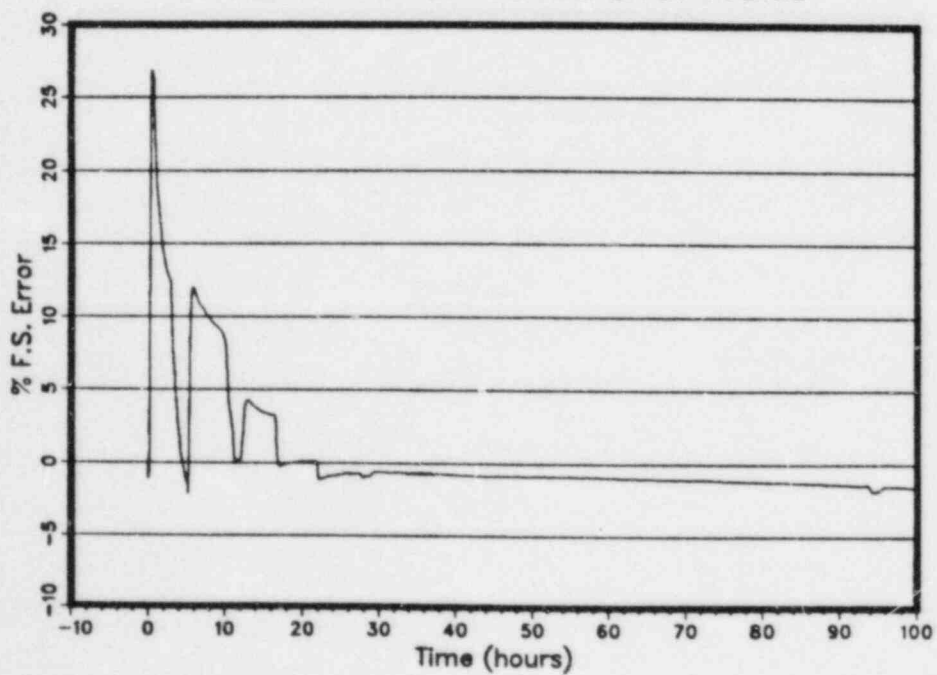


Figure T5-A-5

Trans. T5 First 26 hrs. Temp. Profile

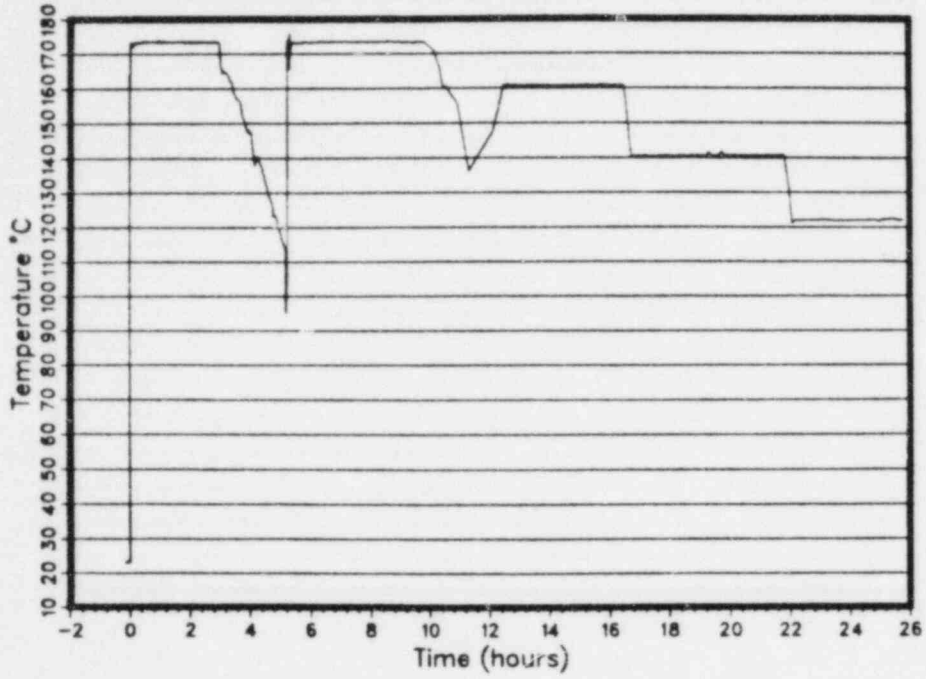


Figure T5-A-6

Trans. T5 First 26 hrs. Error Profile

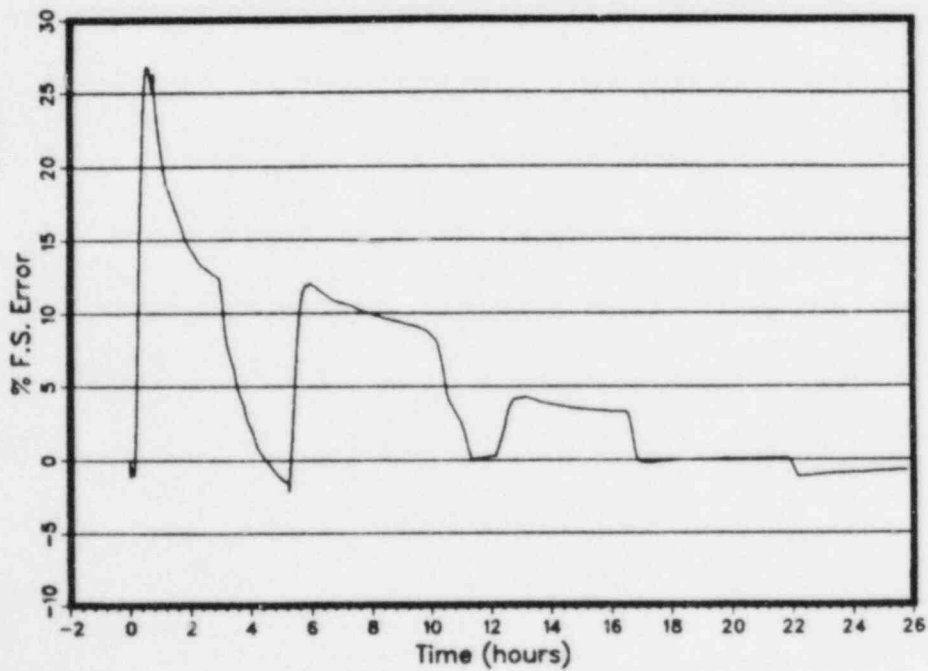


Figure T5-A-7

Transmitter T5 Test Sequence Data Scatter

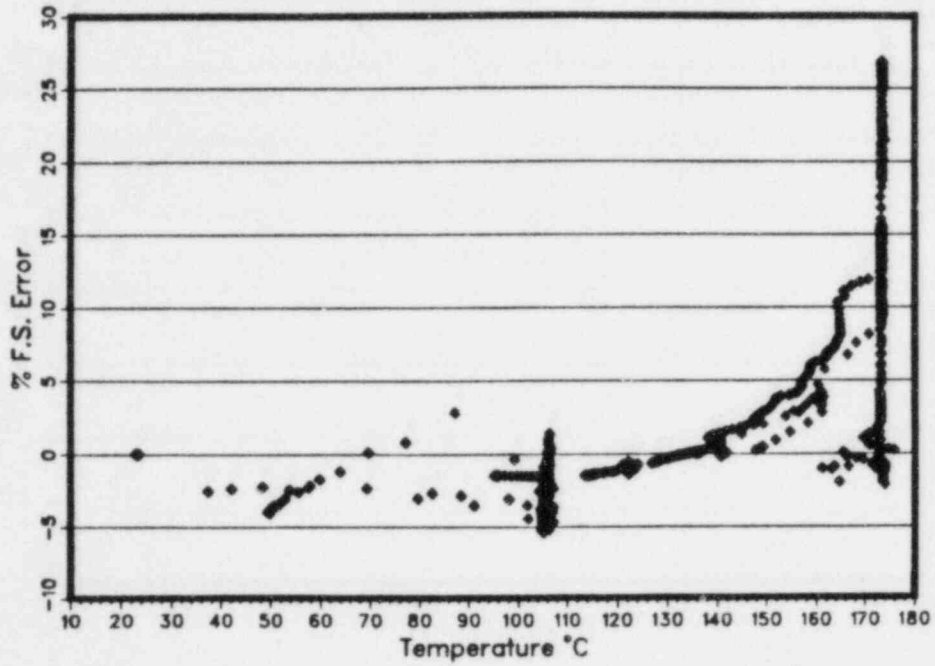


Figure T5-A-8

Trans. T5 Special Test Sequence Data Scatter

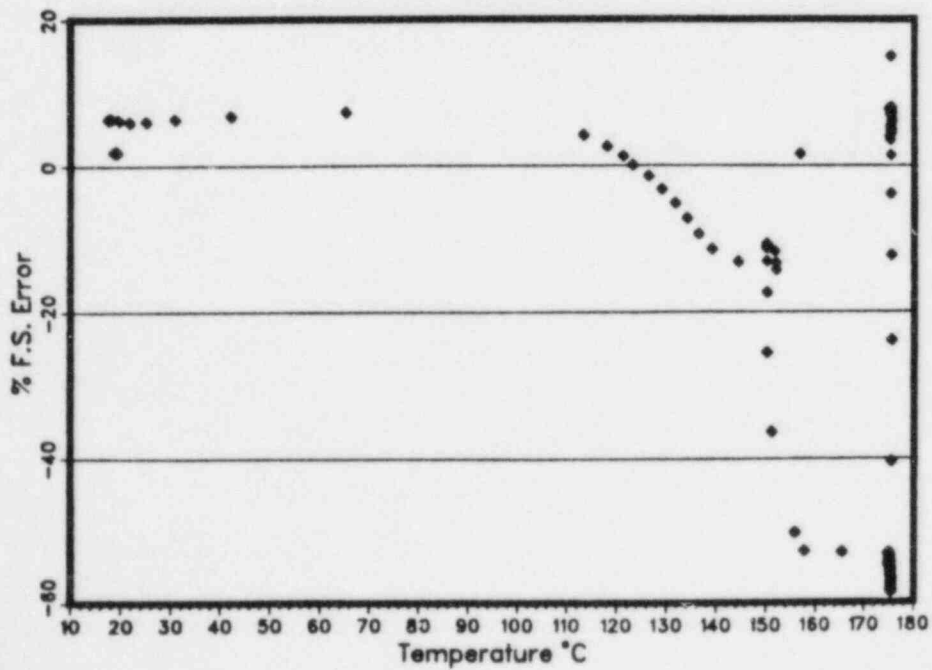


Figure T5-A-9

Trans. T5 Special Test Sequence Temp. Profile

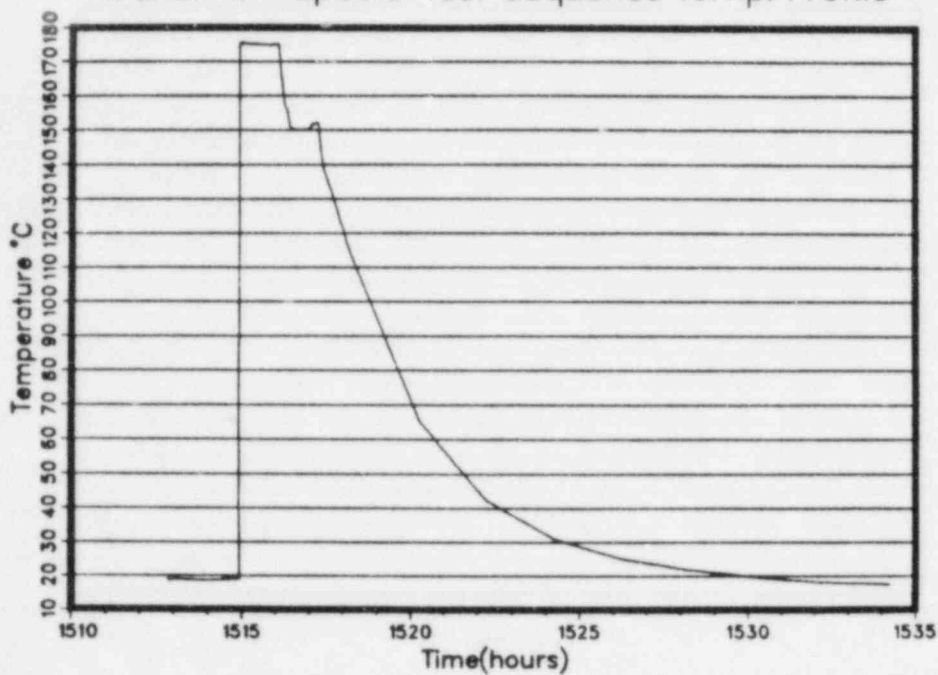


Figure T5-A-10

Trans. T5 Special Test Sequence Error Profile

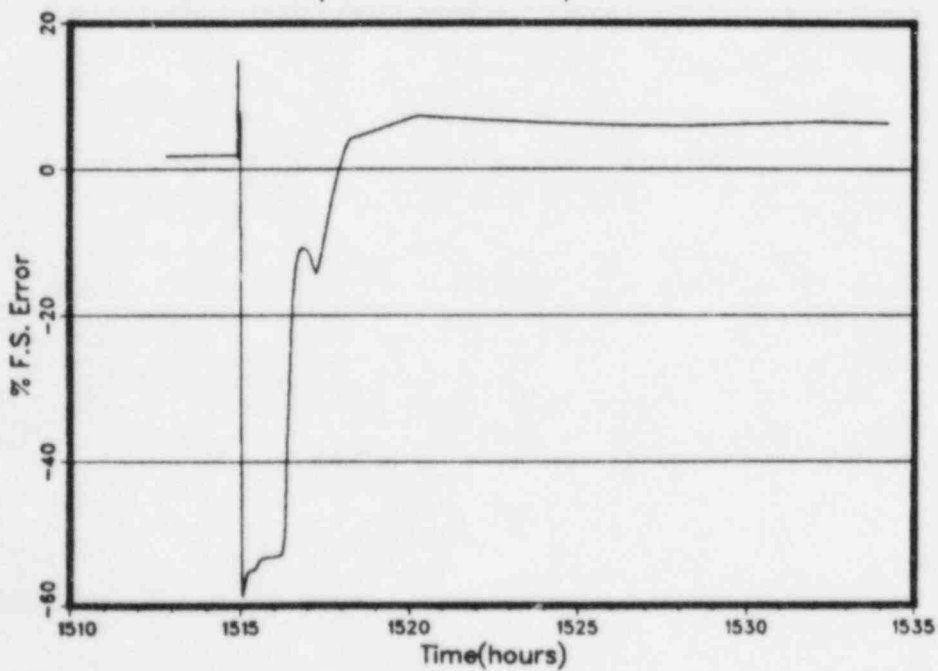


Figure T5-A-11

Trans. T5 Special Test 3 Hour Temp. Profile

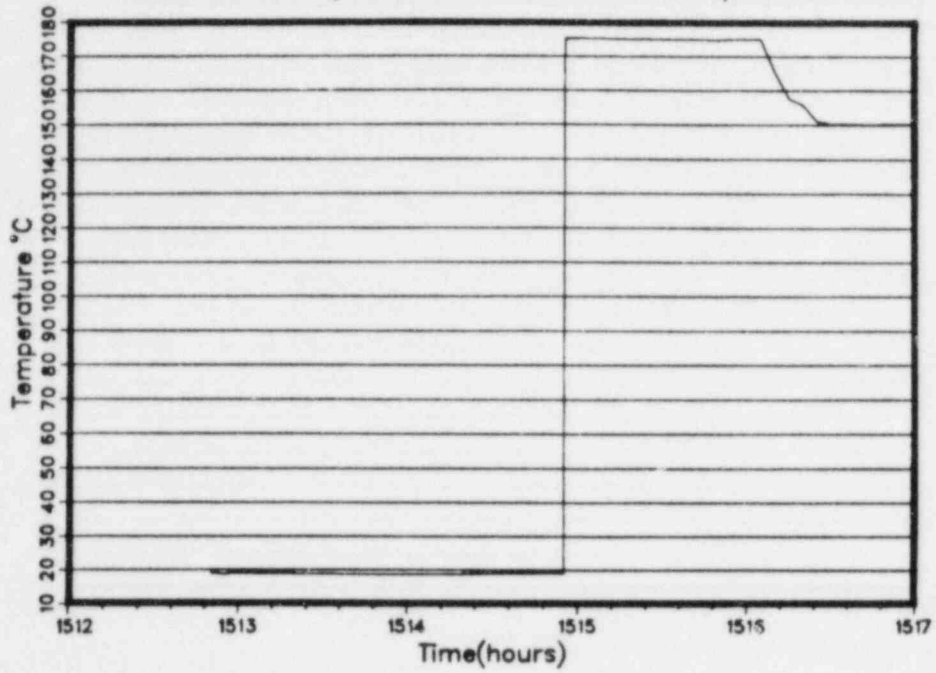
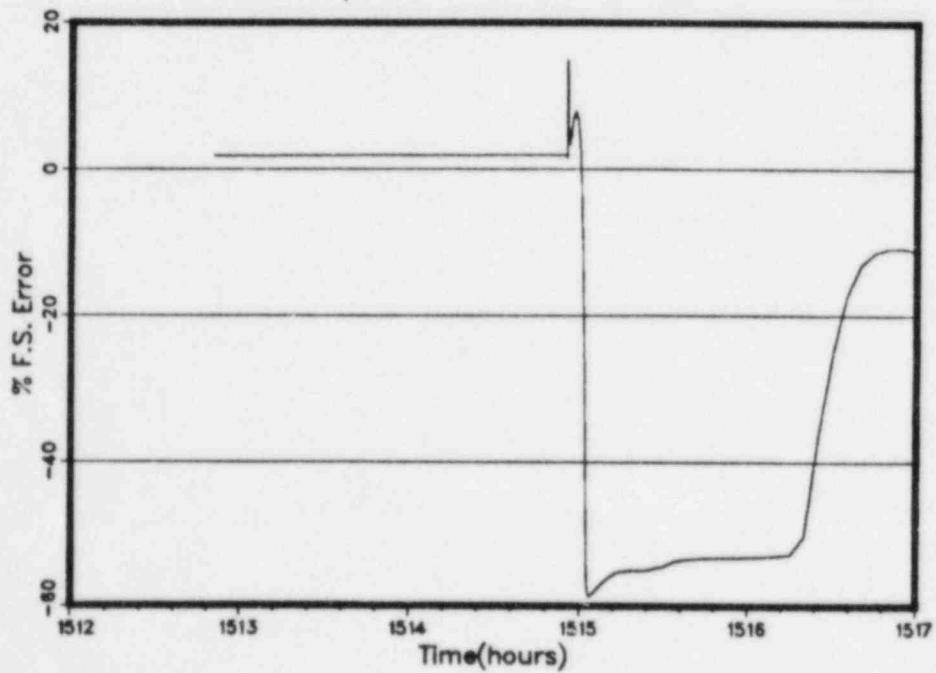


Figure T5-A-12

Trans. T5 Special Test 3 Hour Error Profile



APPENDIX B  
TRANSMITTER RESPONSE  
DURING FUNCTIONAL TESTS

This appendix contains a series of plots illustrating the response of five transmitters during each of ten functional tests. In order to conserve space, these ten functional tests are referred to by "Cal" number in the figure captions. During these tests, the stimulus pressure was varied from 0-1000 psig in 200 psi increments. The plots show the relationship of the calibration correlation and stability to exposure temperature and time. The pressure sensitivity of each transmitter is also illustrated. At the exposure temperatures noted below, the pressure sensitivity of each transmitter is also illustrated. As in Appendix A, the prefix identifier denotes the transmitter reference. A listing of the figures in this appendix is contained on the following page.

The error data presented herein is shown in percent of full-scale error. The error can be converted to error in psi by multiplying the ordinate by 10. The error can be evaluated as a percent of applied pressure by dividing the ordinate by the reference pressure x 0.1 (i.e., at 200 psi reference a 3.0% FSI error =  $3.0/0.1 \times 200 = 15\%$  error).

For convenience, the exposure temperature at each calibration interval from Table 6-3 is shown below:

#### Calibration Temperatures

<u>Calibration</u>	<u>Elapsed Time (hr)</u>	<u>Test Temperature °C (nominal)</u>		
		<u>T1, T4 &amp; T5</u>	<u>T2</u>	<u>T3</u>
0	-0.7	21	21	21
1	1.5	173	150	35
2	7	173	150	35
3	13	160	150	33
4	23	122	150	31
5	29	122	173	31
6	95	105	150	31
7	121	105	146	30
8	167	105	21	31
9	172	105	180	30

## LIST OF FIGURES

- B-1 Data Scatter Error vs Temperature
- B-2 Data Scatter Actual vs Reference Correlation-Upscale
- B-3 Cal 0 Ambient Temperature Correlation
- B-4 Cal 1 Correlation
- B-5 Cal 2 Correlation
- B-6 Cal 3 Correlation
- B-7 Cal 4 Correlation
- B-8 Cal 5 Correlation
- B-9 Cal 6 Correlation
- B-10 Cal 7 Correlation
- B-11 Cal 8 Correlation
- B-12 Cal 9 Correlation
- B-13 Cal 0 Pressure Sensitivity
- B-14 Cal 1 Pressure Sensitivity
- B-15 Cal 2 Pressure Sensitivity
- B-16 Cal 3 Pressure Sensitivity
- B-17 Cal 4 Pressure Sensitivity
- B-18 Cal 5 Pressure Sensitivity
- B-19 Cal 6 Pressure Sensitivity
- B-20 Cal 7 Pressure Sensitivity
- B-21 Cal 8 Pressure Sensitivity
- B-22 Cal 9 Pressure Sensitivity
- B-23 Calibration Interval Temperature Profile
- B-24 0 psi Calibration Stability
- B-25 200 psi Calibration Stability
- B-26 400 psi Calibration Stability
- B-27 600 psi Calibration Stability
- B-28 800 psi Calibration Stability
- B-29 1000 psi Calibration Stability

Figure T1-B-1  
 Transmitter T1 %F.S. Error Data Scatter

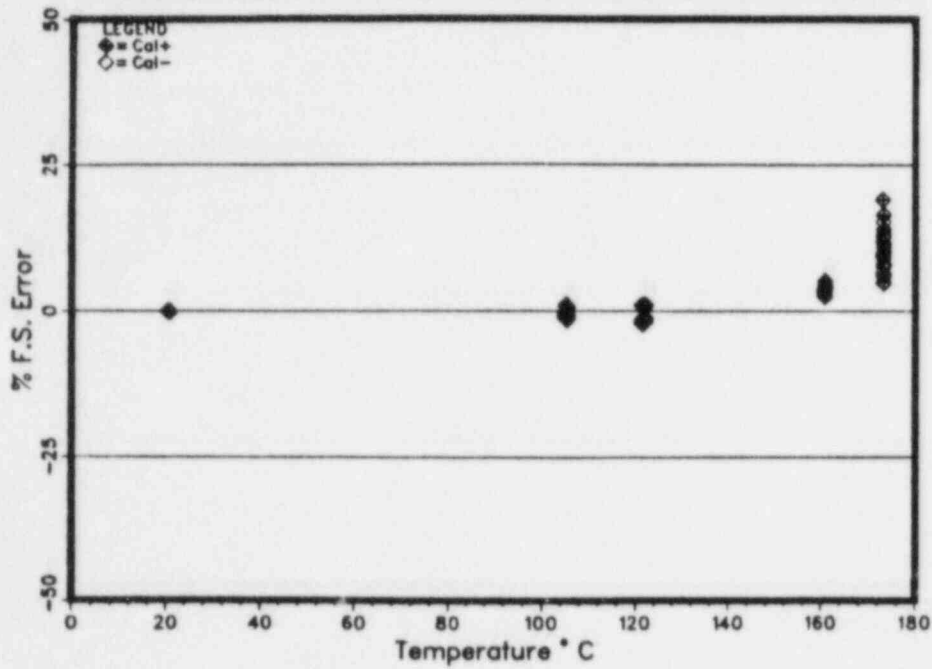


Figure T1-B-2  
 Transmitter T1 Correlation Scatter, Cal+

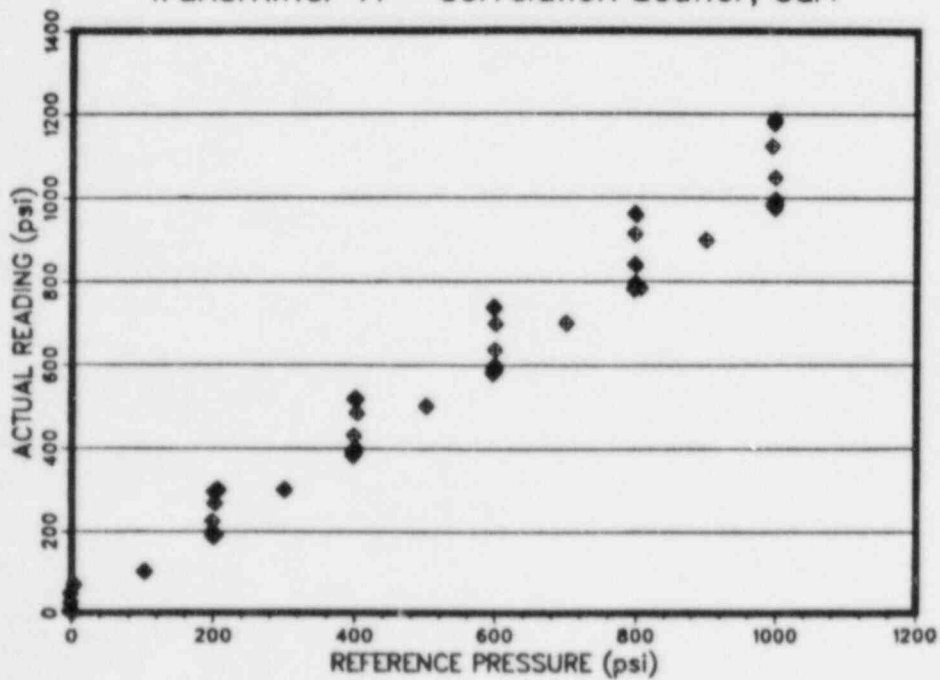


Figure T1-B-3

Transmitter T1 Cal 0 Correlation 21°C

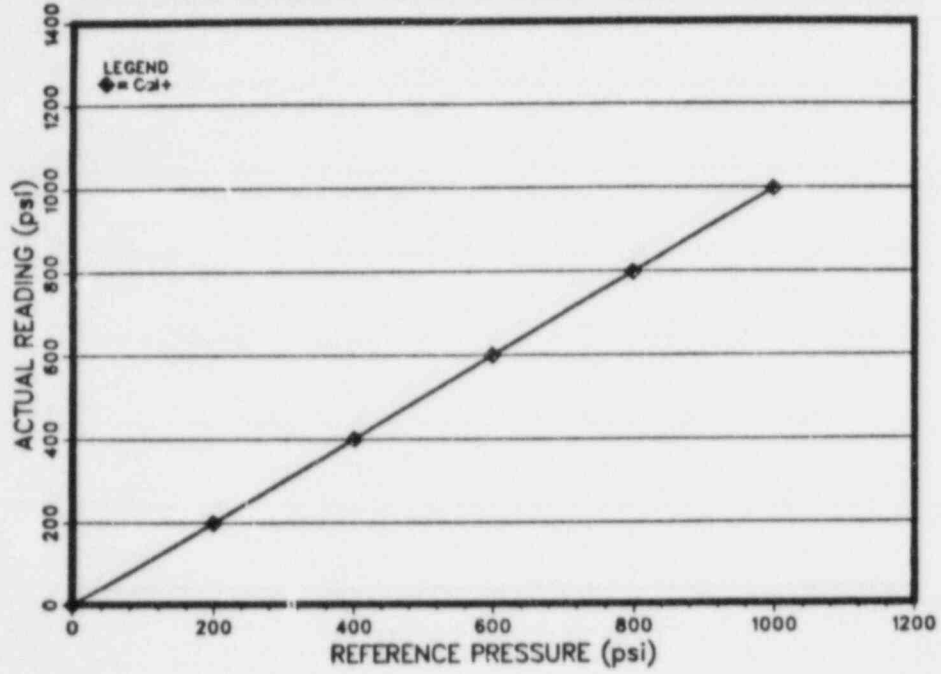


Figure T1-B-4

Transmitter T1 Cal 1 Correlation 173°C

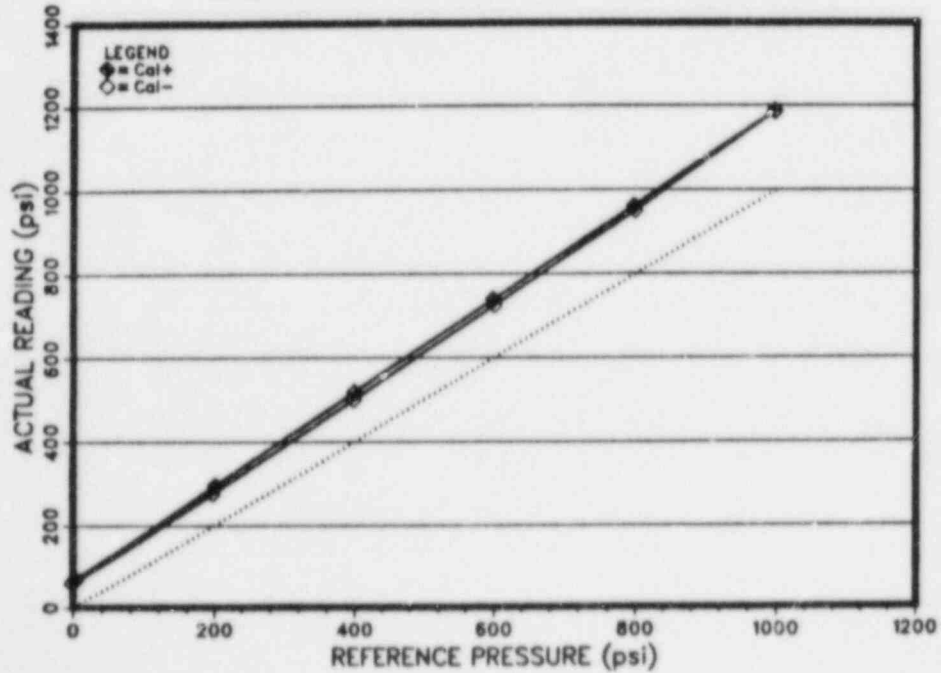


Figure T1-B-5

Transmitter T1 Cal 2 Correlation 173°C

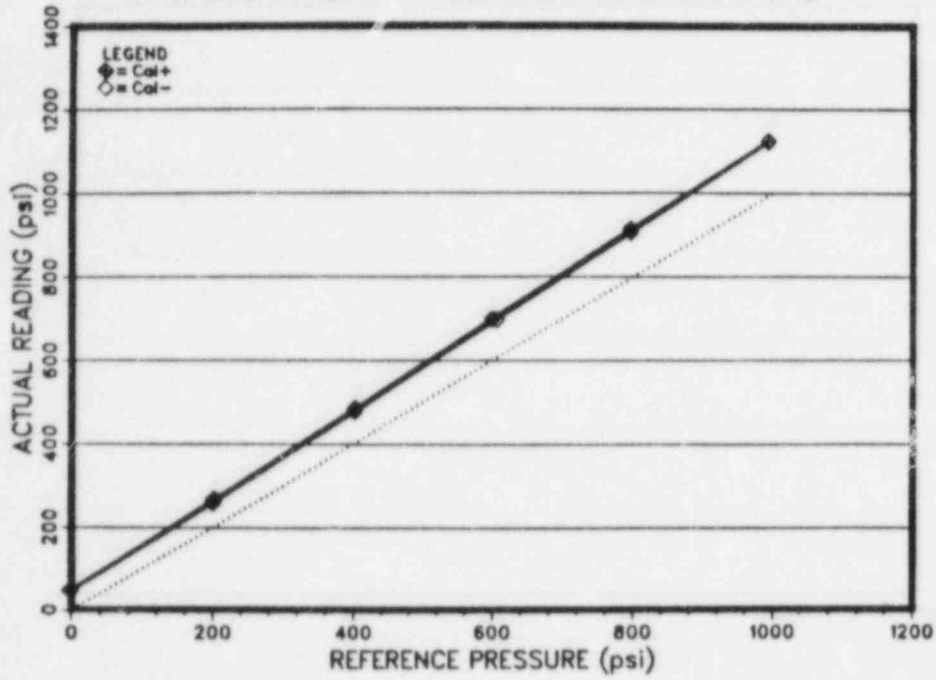


Figure T1-B-6

Transmitter T1 Cal 3 Correlation 160°C

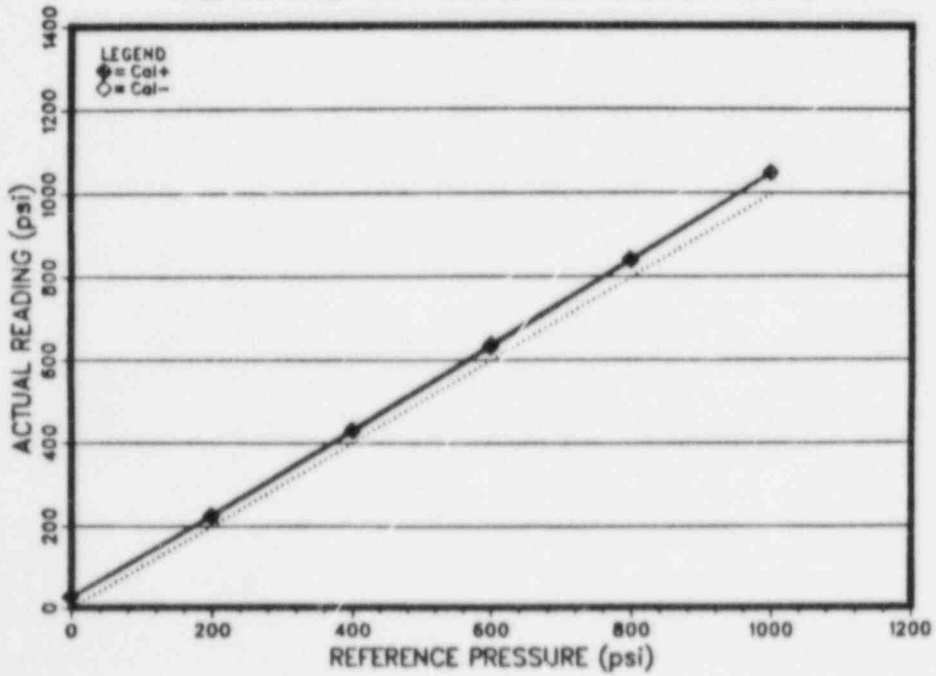


Figure T1-B-7

Transmitter T1 Cal 4 Correlation 122°C

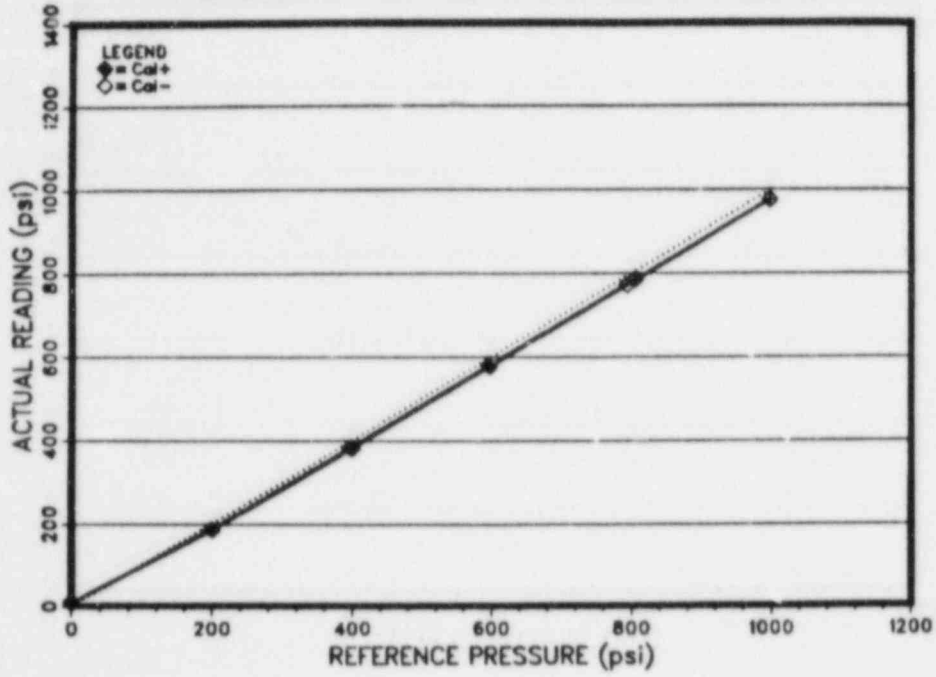


Figure T1-B-8

Transmitter T1 Cal 5 Correlation 122°C

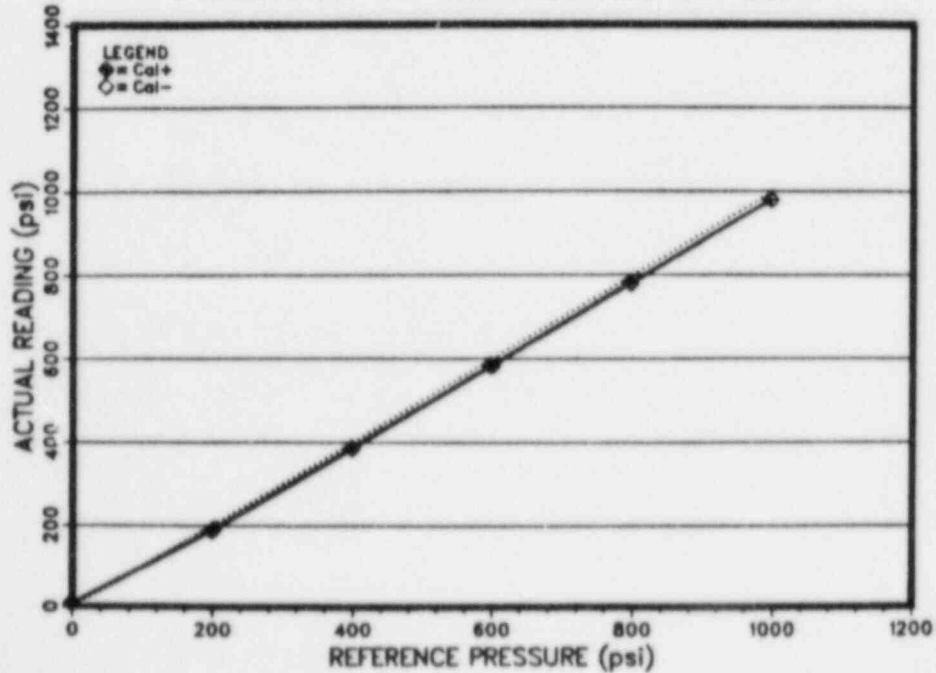


Figure T1-B-9

Transmitter T1 Cal 6 Correlation 105°C

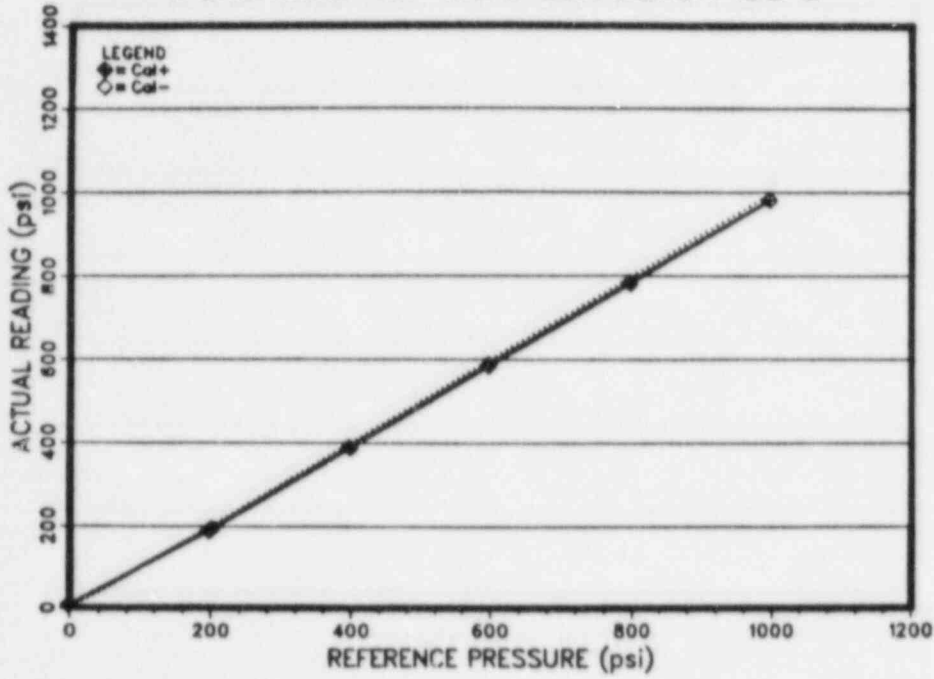


Figure T1-B-10

Transmitter T1 Cal 7 Correlation 105°C

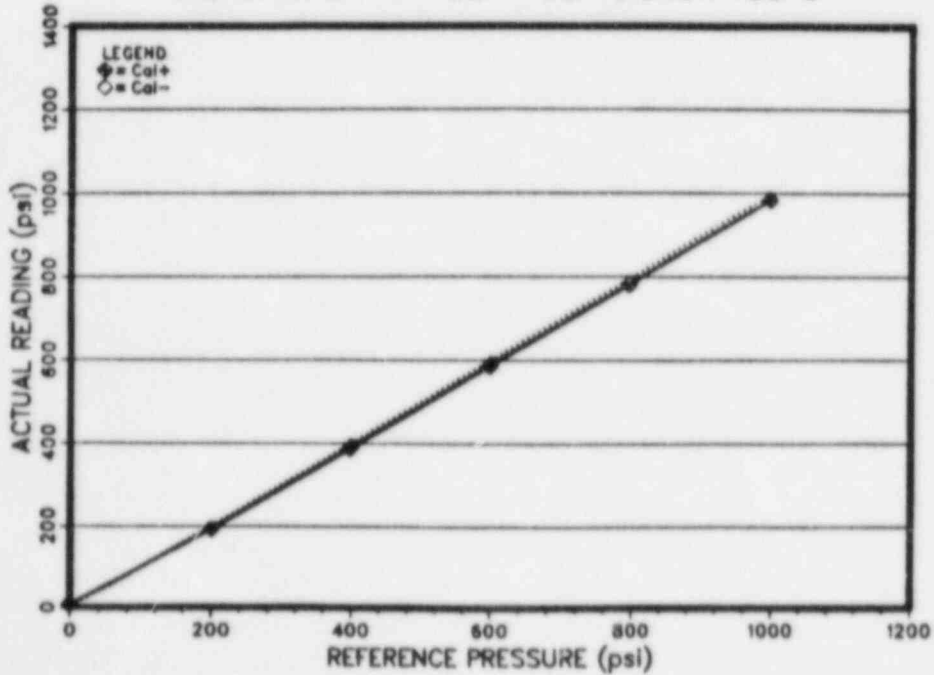


Figure T1-B-11

Transmitter T1 Cal 3 Correlation 105°C

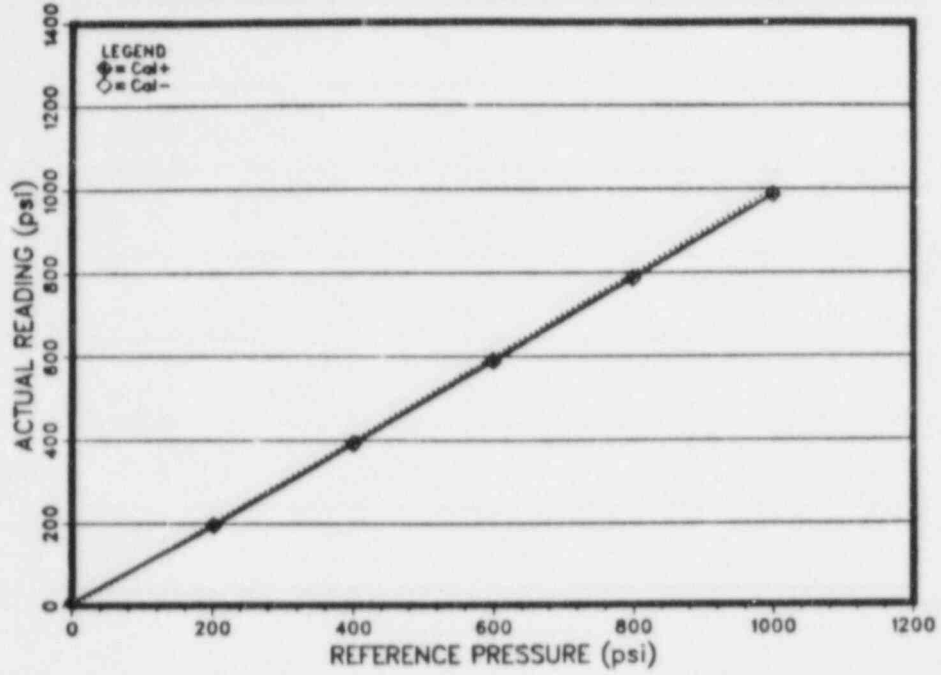


Figure T1-B-12

Transmitter T1 Cal 9 Correlation 105°C

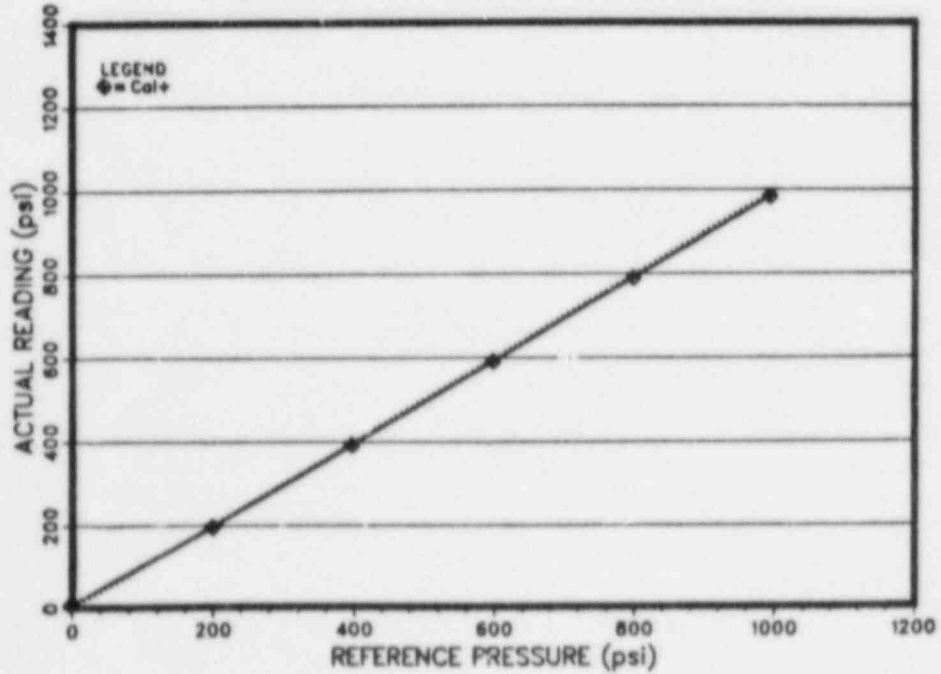


Figure T1-B-13

Trans.T1 Cal0 Pres. Sensitivity 21°C

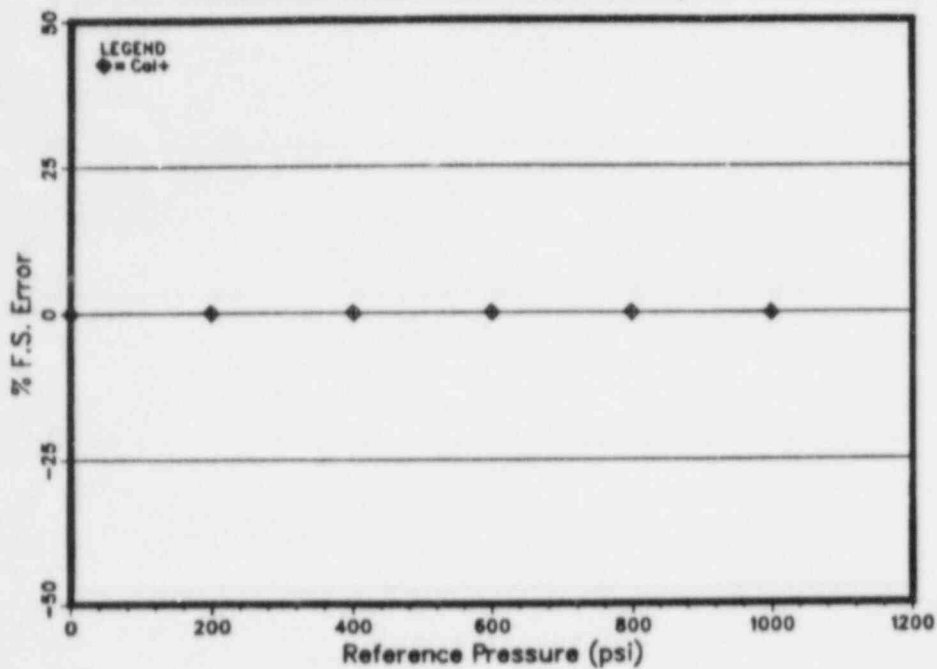


Figure T1-B-14

Trans.T1 Cal1 Pres. Sensitivity 173°C

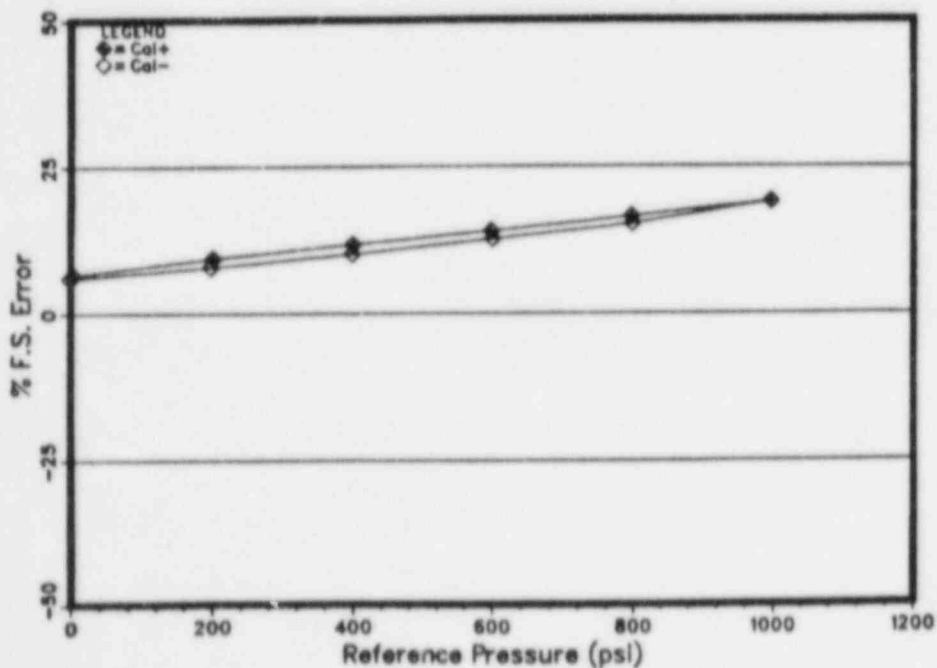


Figure T1-B-15

Trans.T1 Cal2 Pres. Sensitivity 173°C

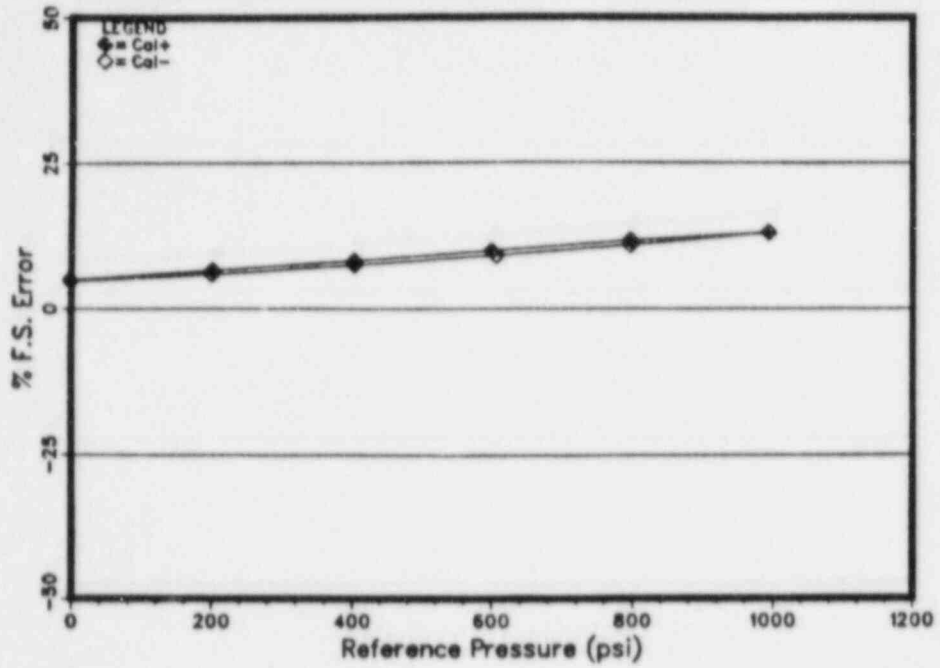


Figure T1-B-16

Trans.T1 Cal3 Pres. Sensitivity 160°C

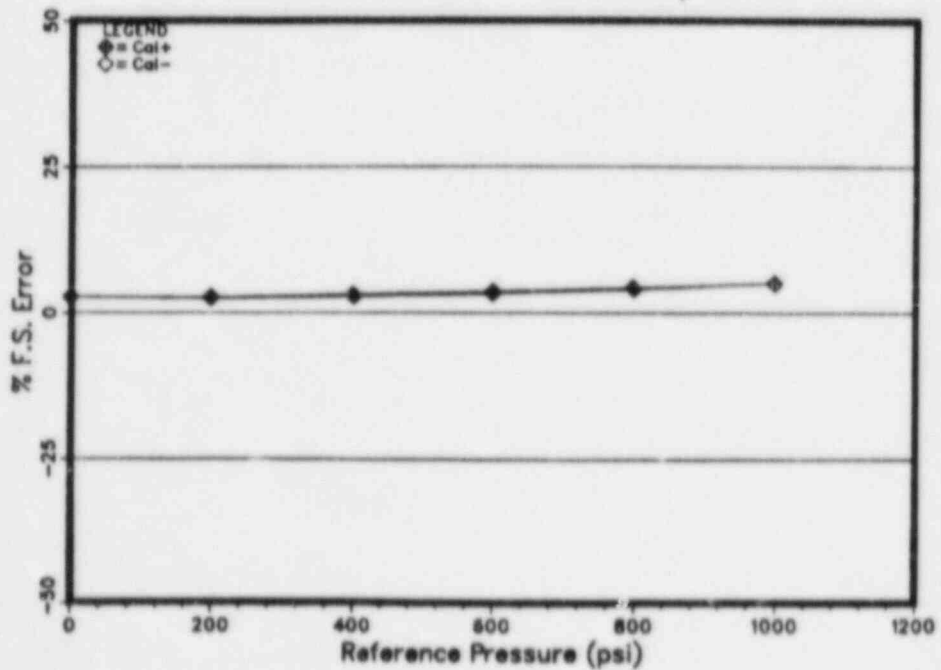


Figure T1-B-17

Trans.T1 Cal4 Pres. Sensitivity 122°C

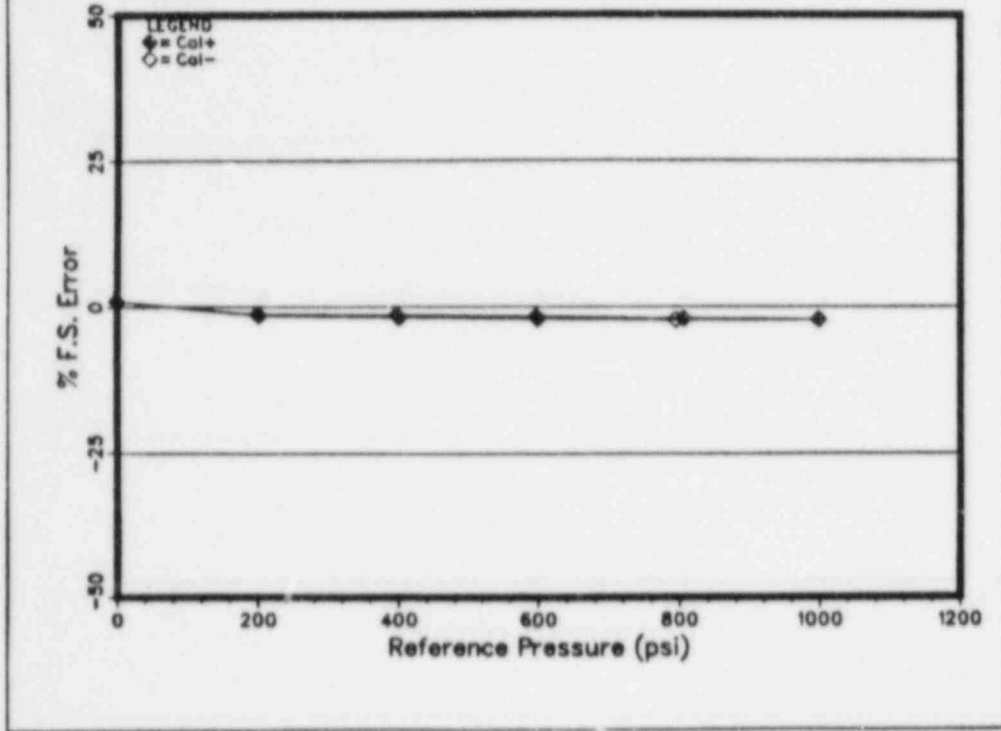


Figure T1-B-18

Trans.T1 Cal5 Pres. Sensitivity 122°C

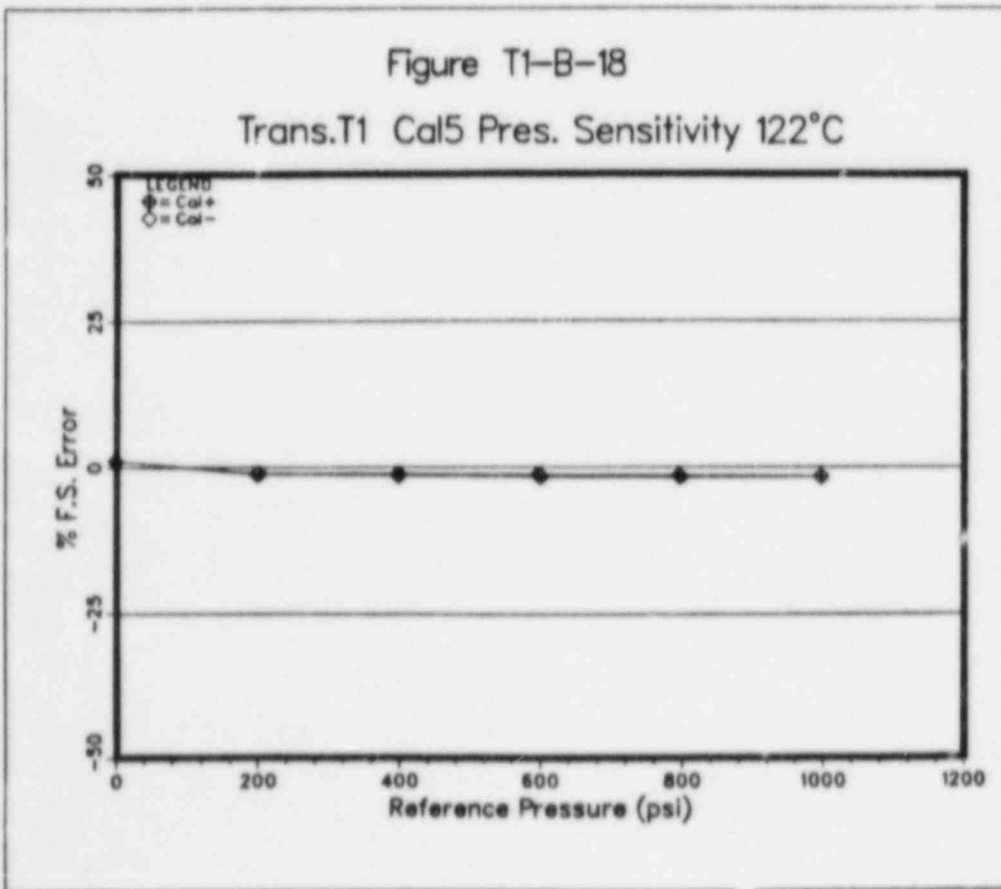


Figure T1-B-19

Trans.T1 Cal6 Pres. Sensitivity 105°C

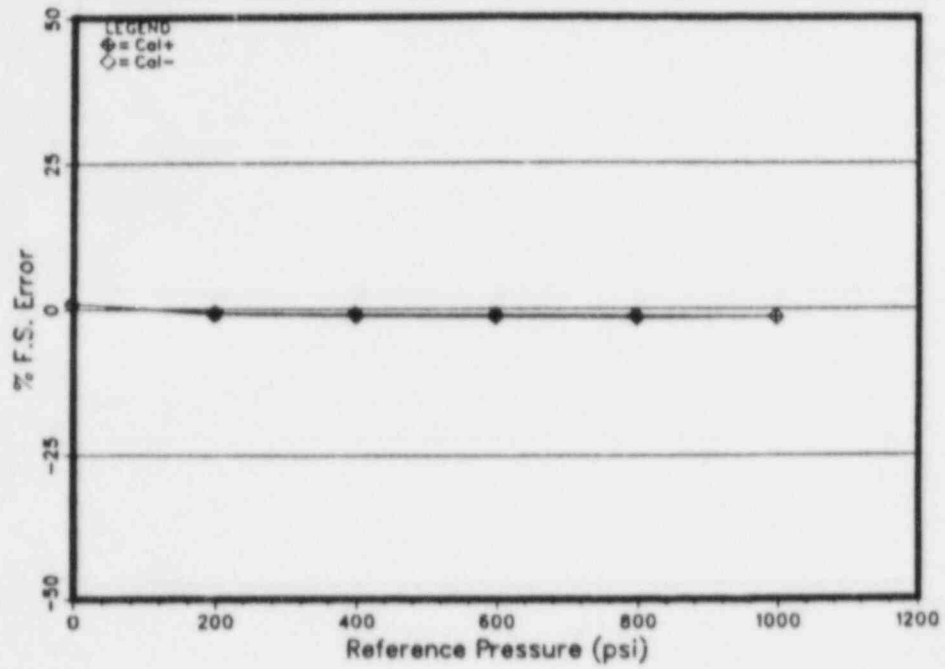


Figure T1-B-20

Trans.T1 Cal7 Pres. Sensitivity 105°C

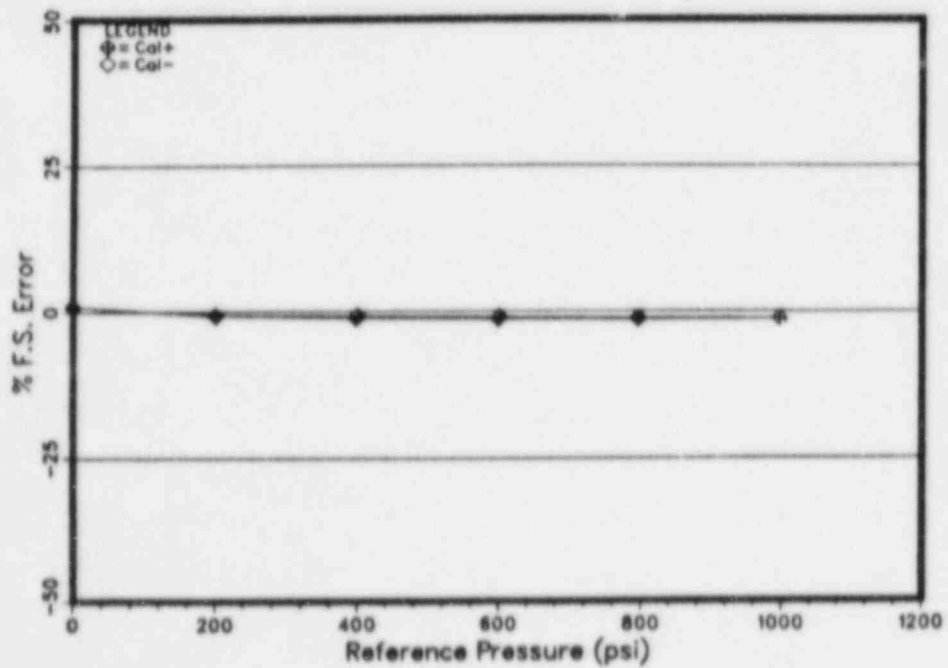


Figure T1-B-21

Trans.T1 Cal8 Pres. Sensitivity 105°C

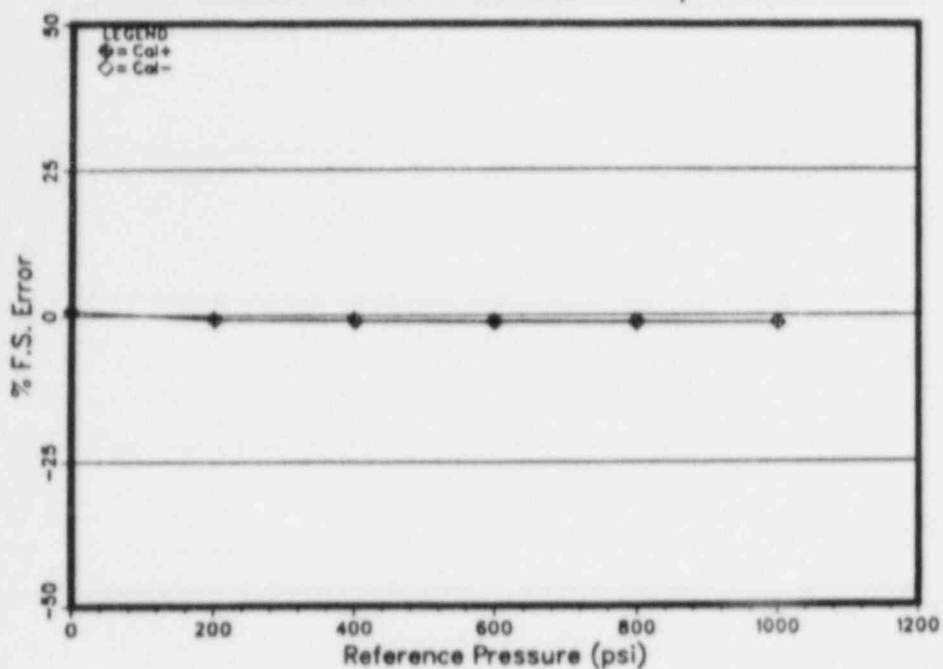


Figure T1-B-22

Trans.T1 Cal9 Pres. Sensitivity 105°C

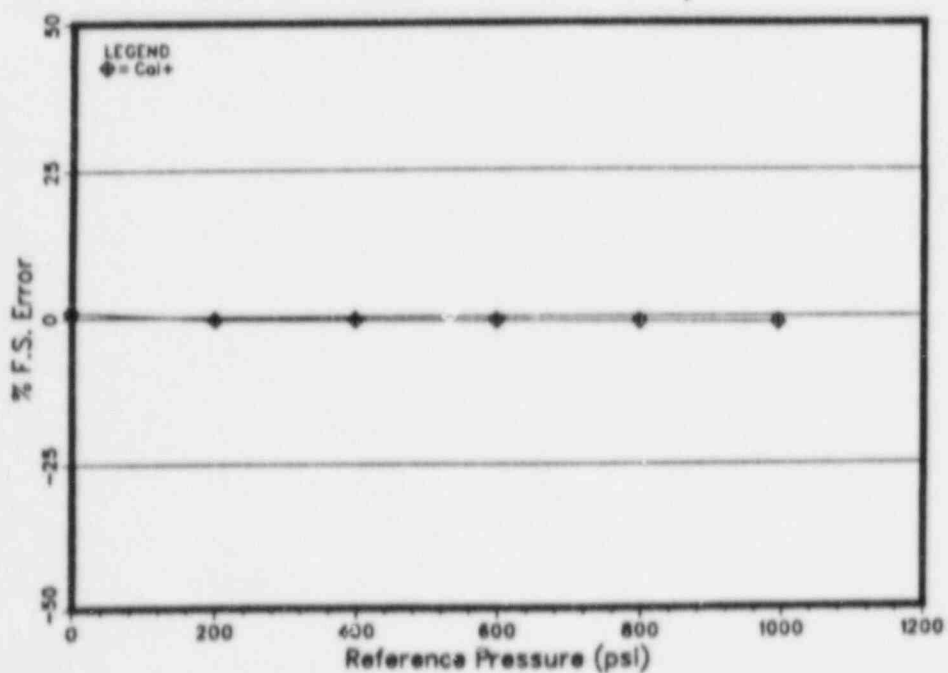


Figure T1-B-23

Trans. T1 Calibration Temperature Profile

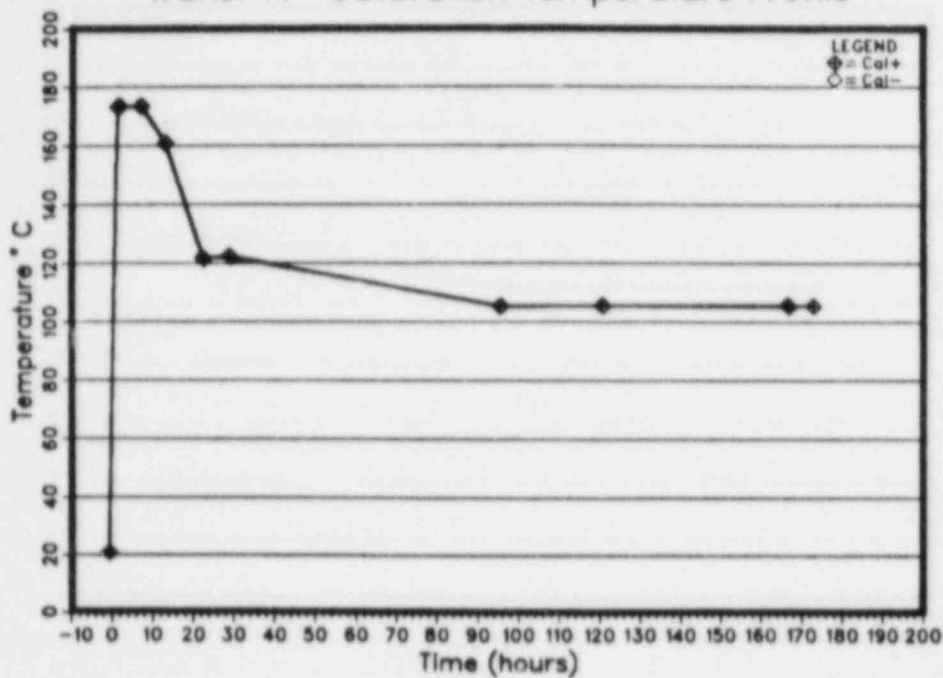


Figure T1-B-24

Transmitter T1 0 psi Calibration Stability

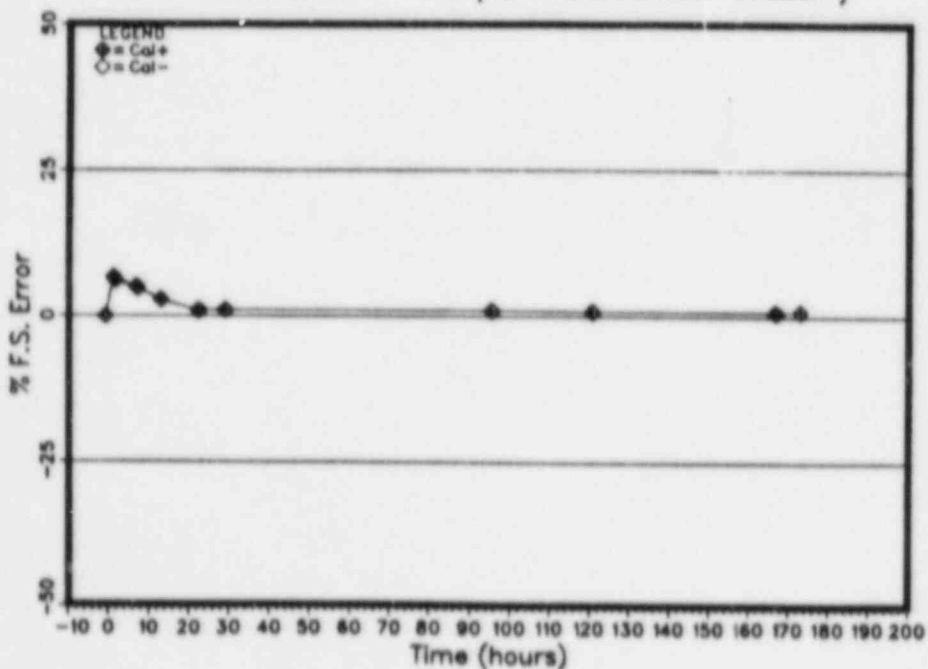


Figure T1-B-25

Transmitter T1 200 psi Calibration Stability

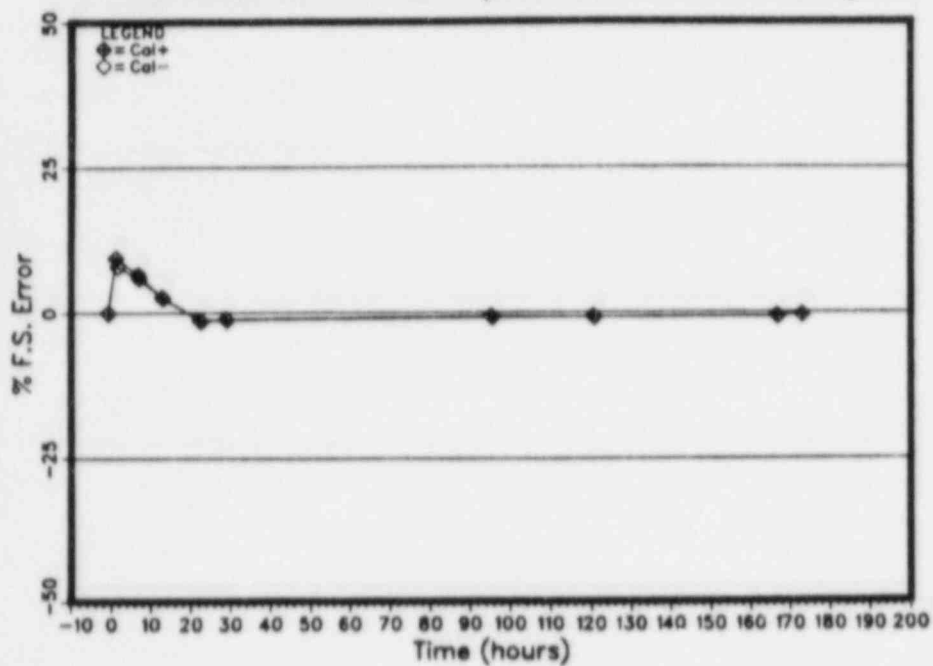


Figure T1-B-26

Transmitter T1 400 psi Calibration Stability

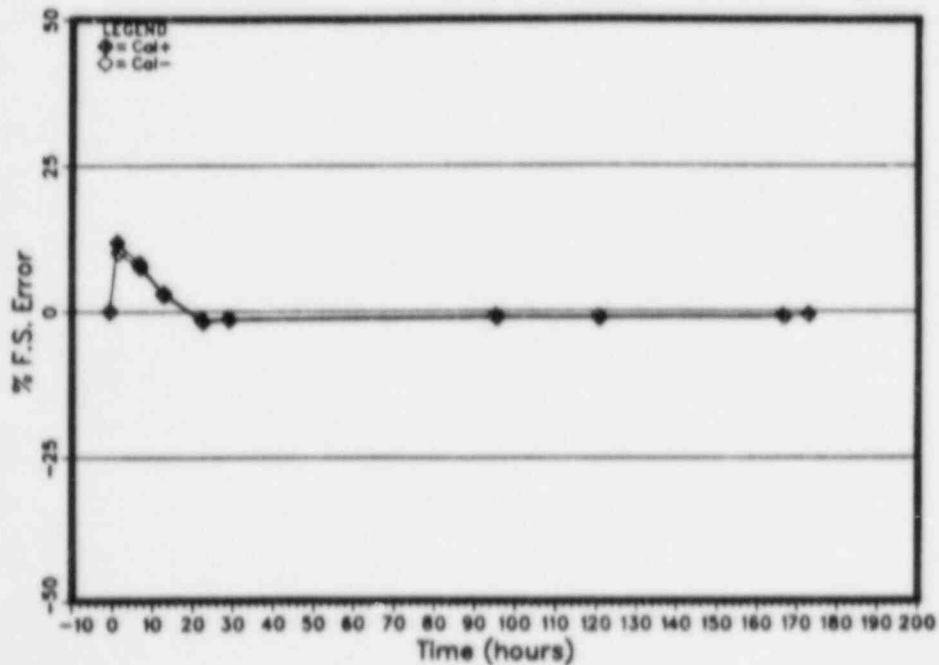


Figure T1-B-27

Transmitter T1 600 psi Calibration Stability

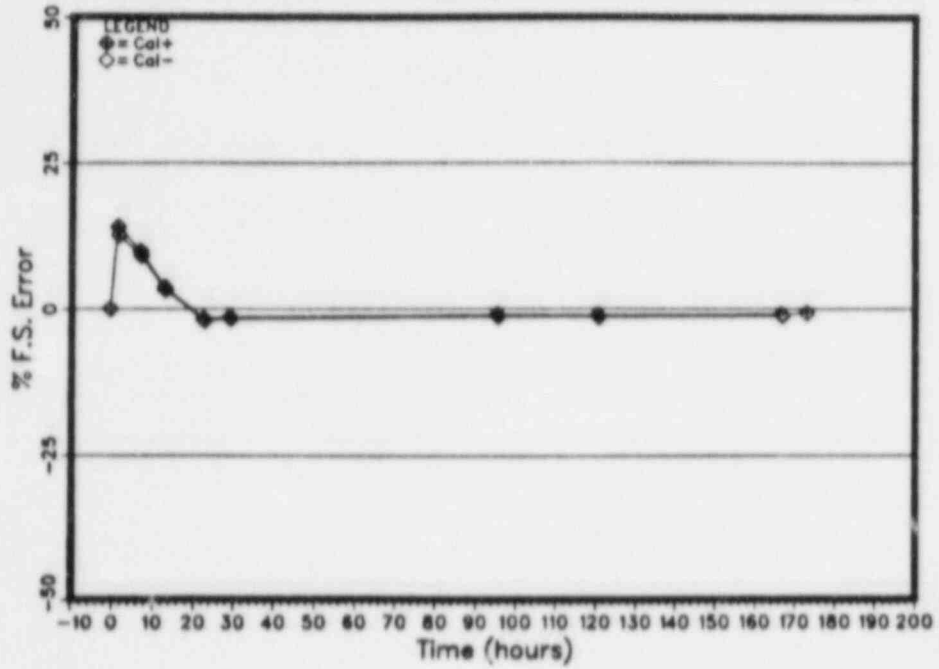


Figure T1-B-28

Transmitter T1 800 psi Calibration Stability

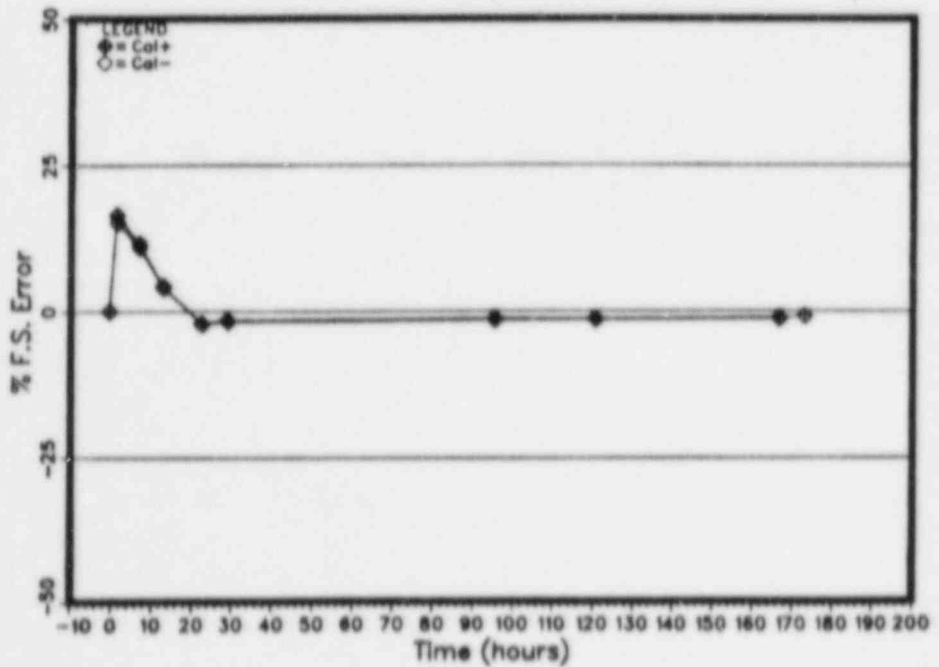


Figure T1-B-29

Transmitter T1 1000 psi Calibration Stability

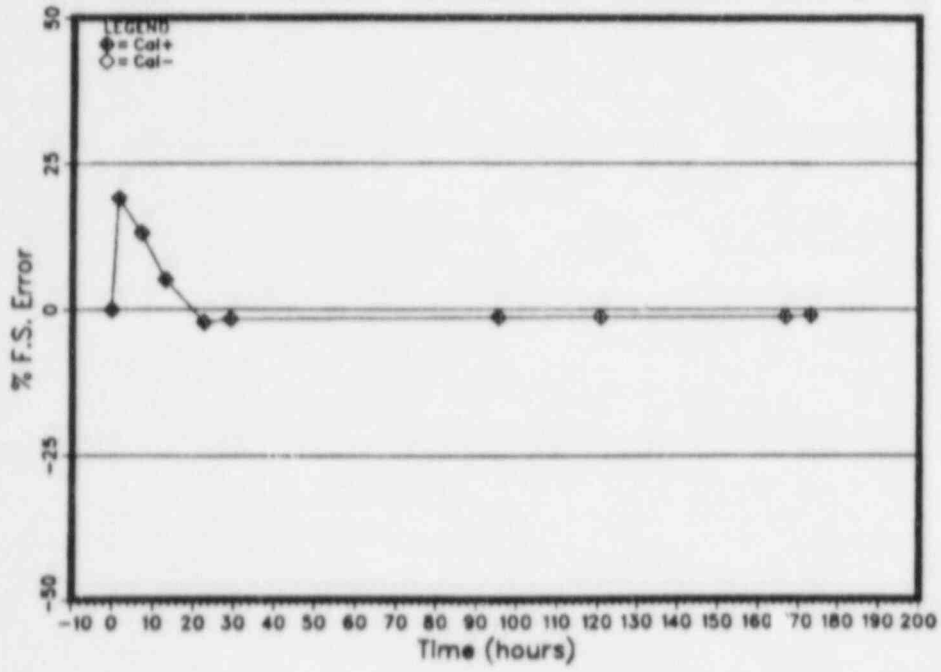


Figure T2-B-1  
 Transmitter T2 %F.S. Error Data Scatter

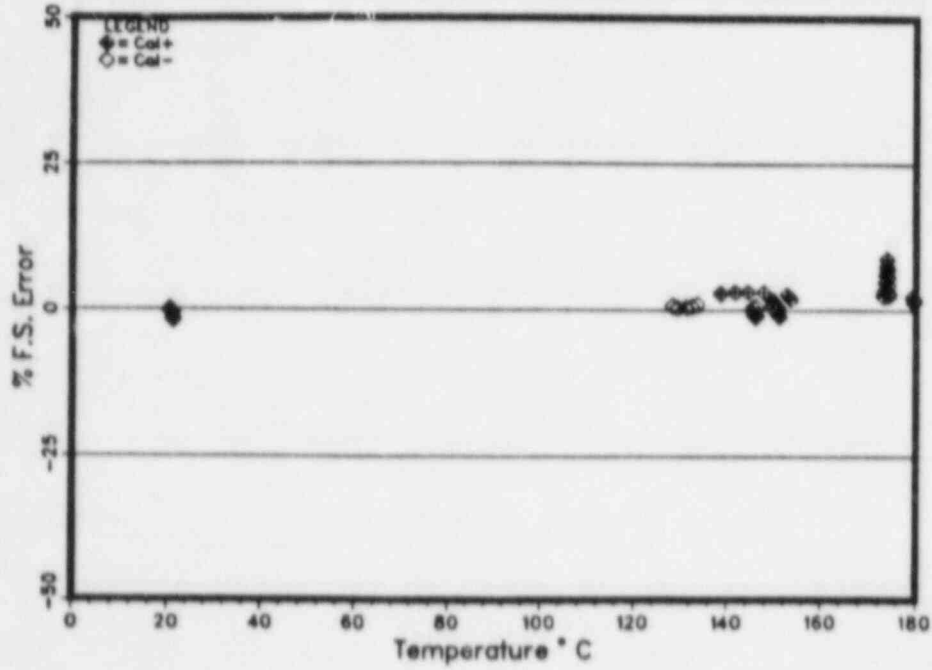


Figure T2-B-2  
 Transmitter T2 Correlation Scatter, Cal+

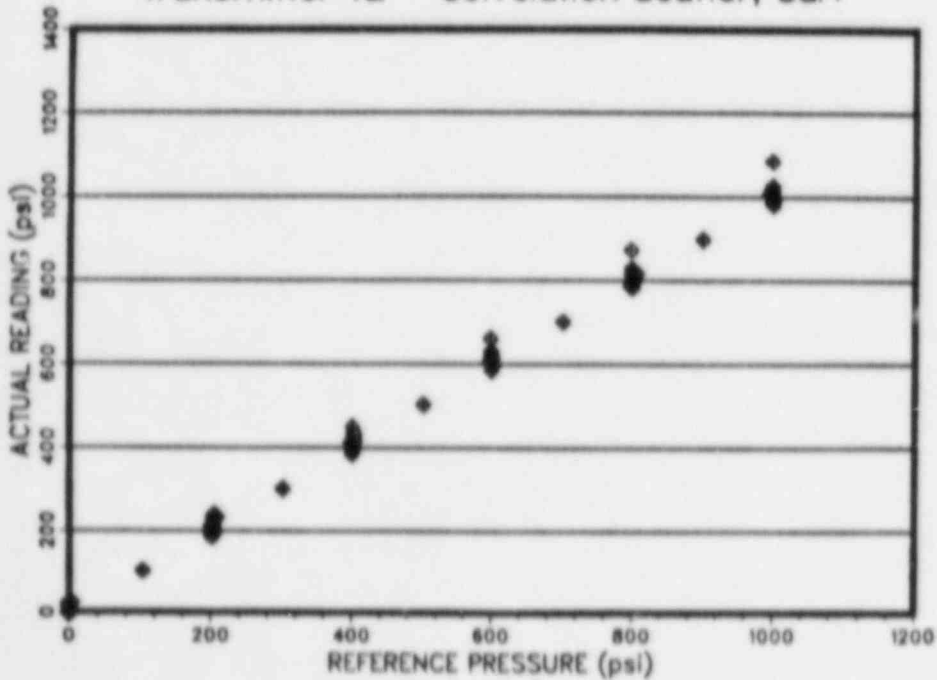


Figure T2-B-3

Transmitter T2 Cal 0 Correlation 21°C

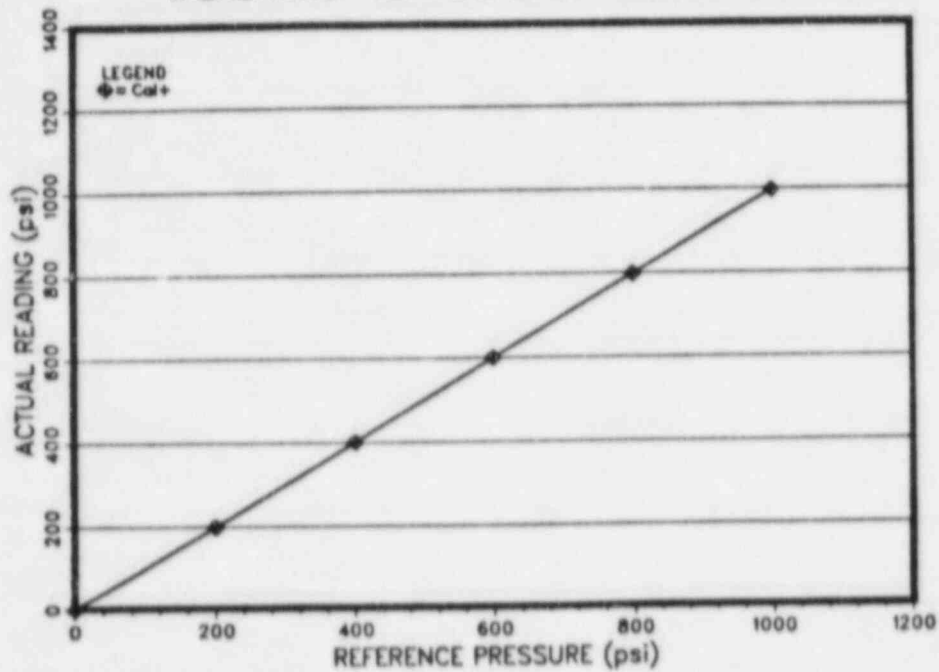


Figure T2-B-4

Transmitter T2 Cal 1 Correlation 150°C

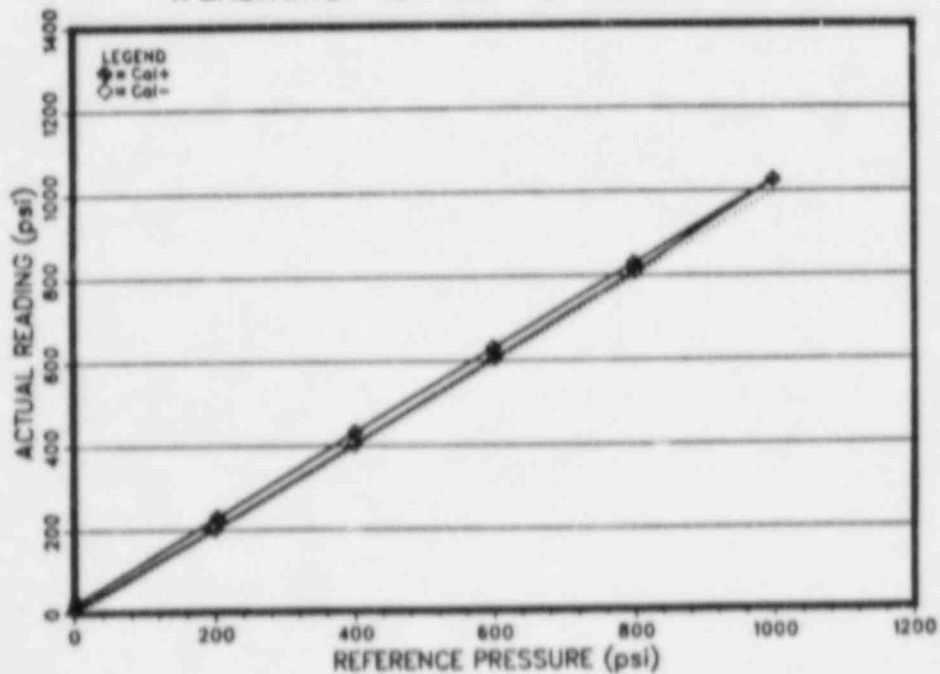


Figure T2-B-5

Transmitter T2 Cal 2 Correlation 150°C

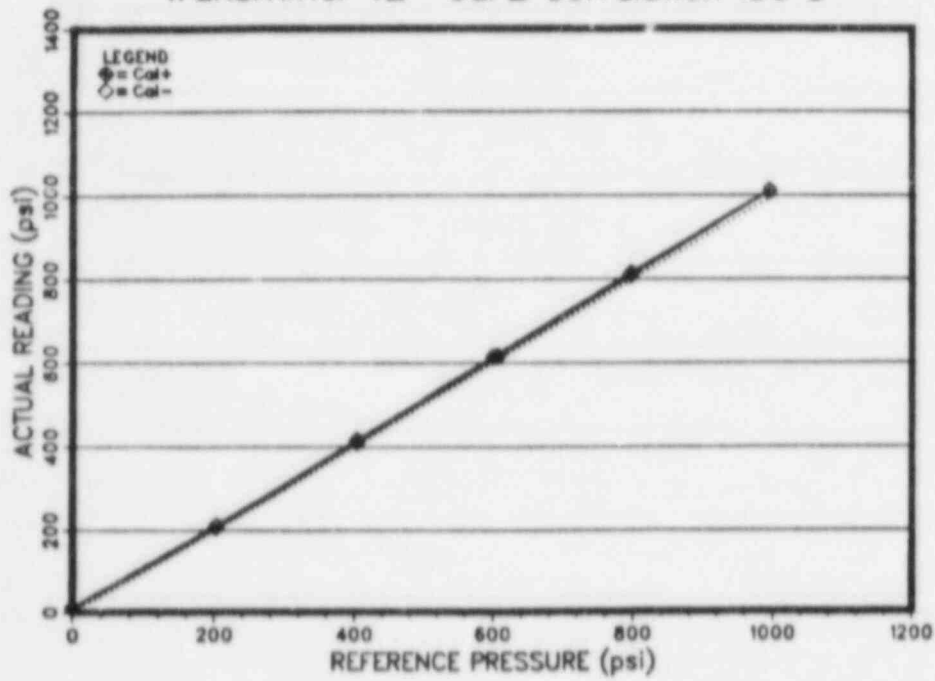


Figure T2-B-6

Transmitter T2 Cal 3 Correlation 150°C

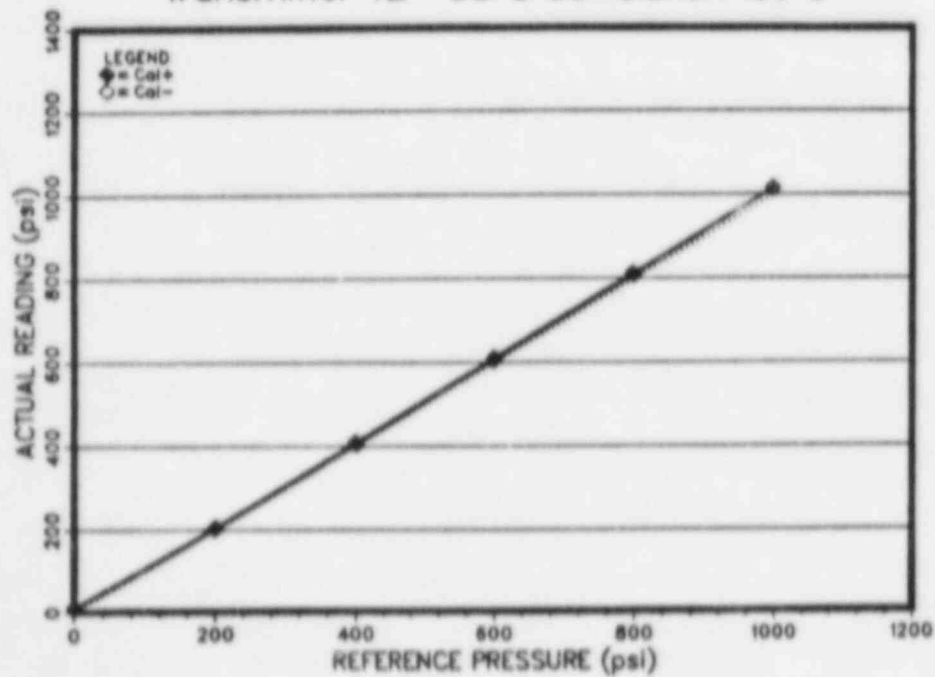


Figure T2-B-7

Transmitter T2 Cal 4 Correlation 150°C

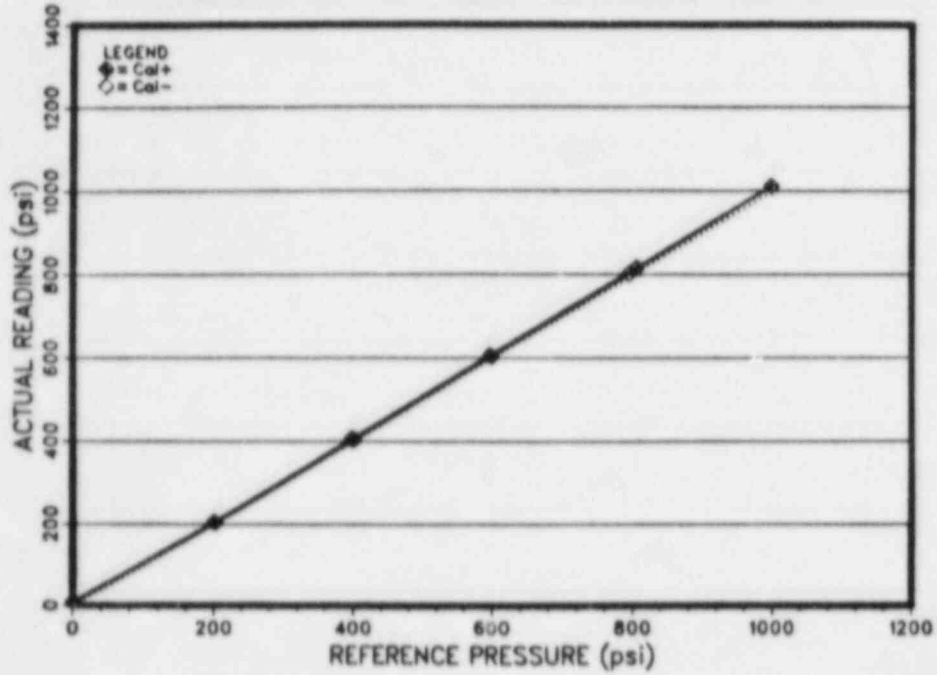


Figure T2-B-8

Transmitter T2 Cal 5 Correlation 173°C

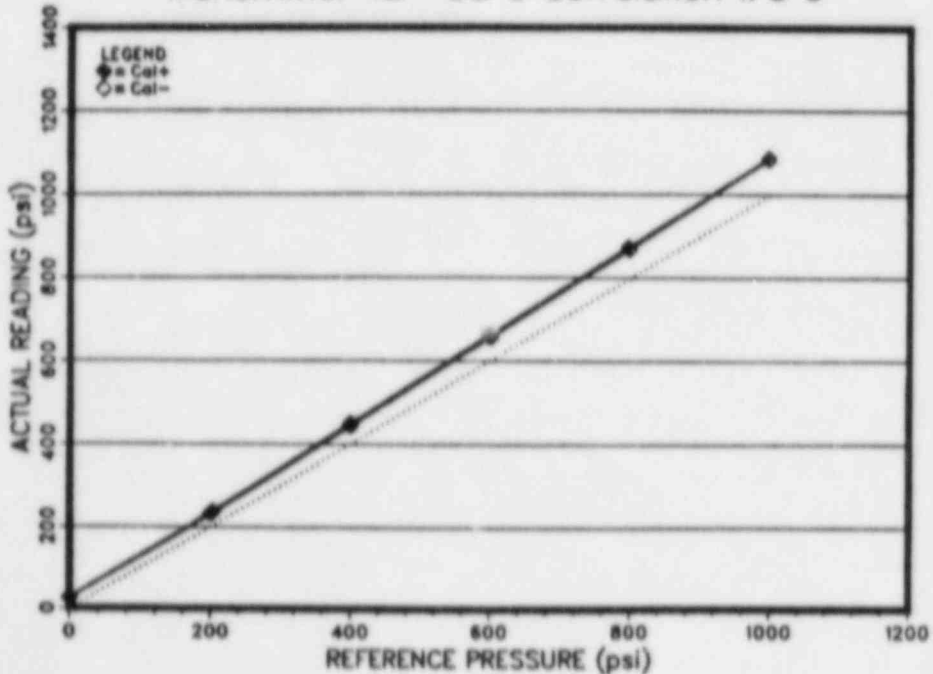


Figure T2-B-9

Transmitter T2 Cal 6 Correlation 150°C

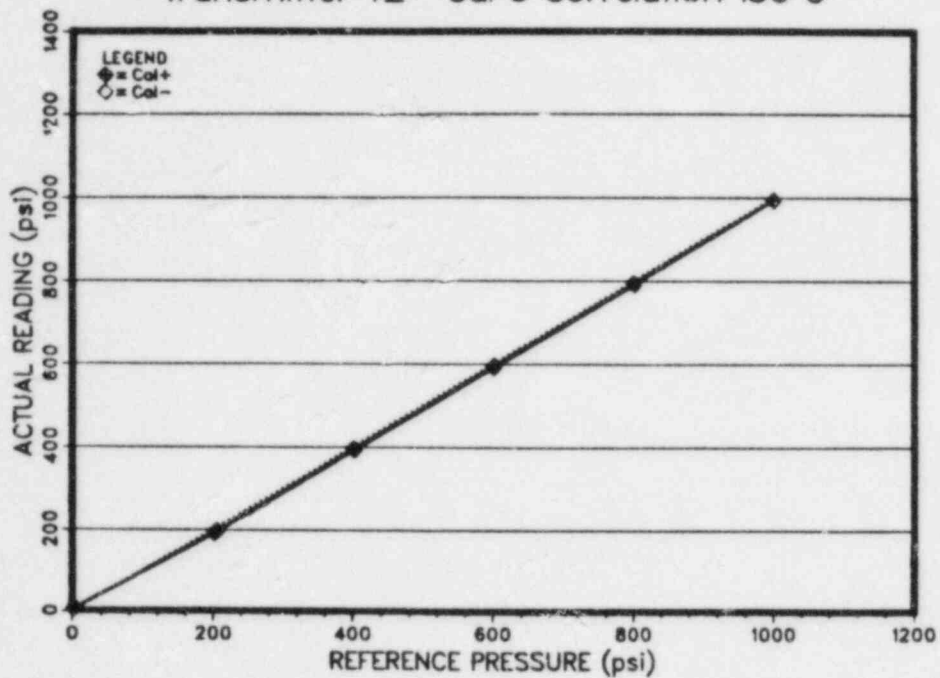


Figure T2-B-10

Transmitter T2 Cal 7 Correlation 146°C

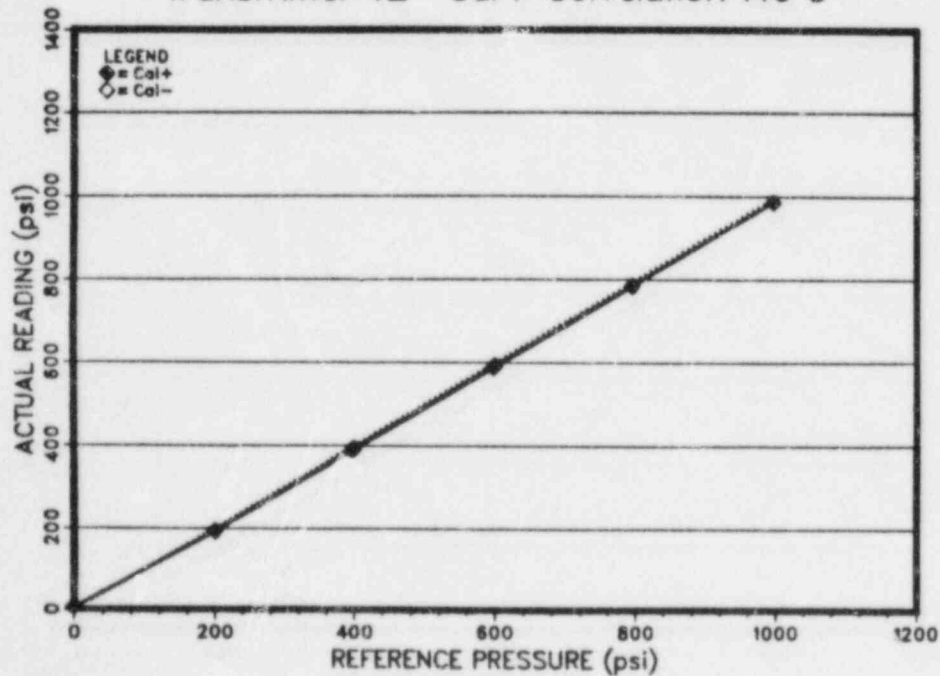


Figure T2-B-11

Transmitter T2 Cal 8 Correlation 21°C

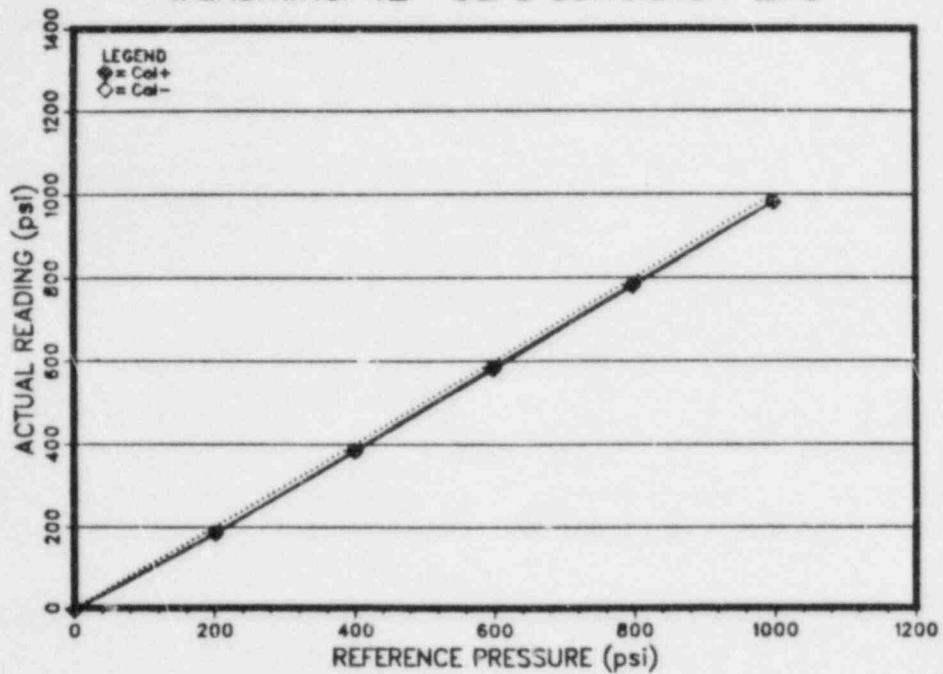


Figure T2-B-12

Transmitter T2 Cal 9 Correlation 180°C

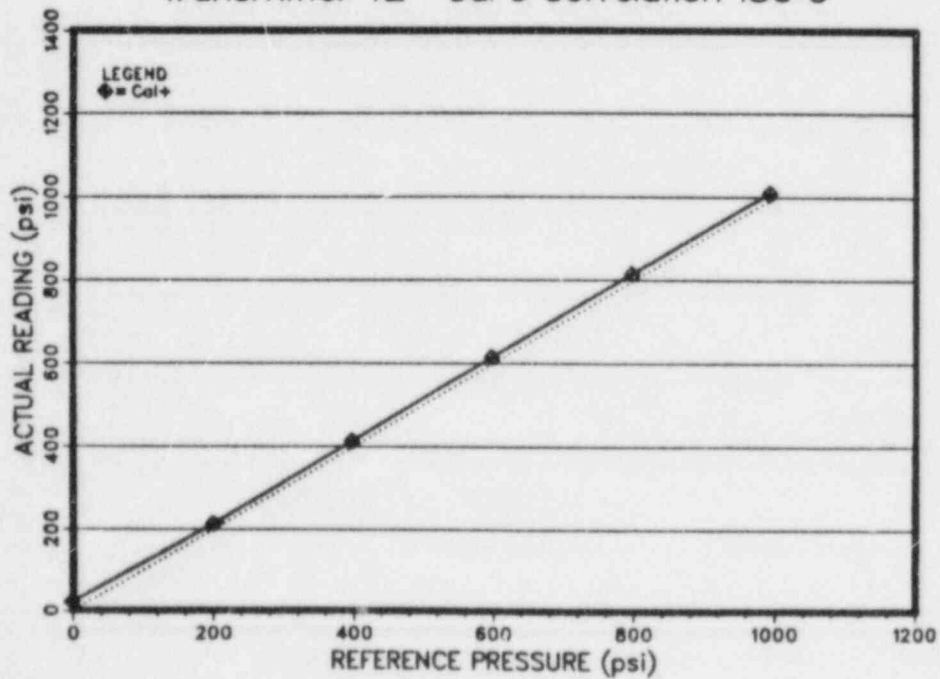


Figure T2-B-13

Trans.T2 Cal0 Pres. Sensitivity 21°C

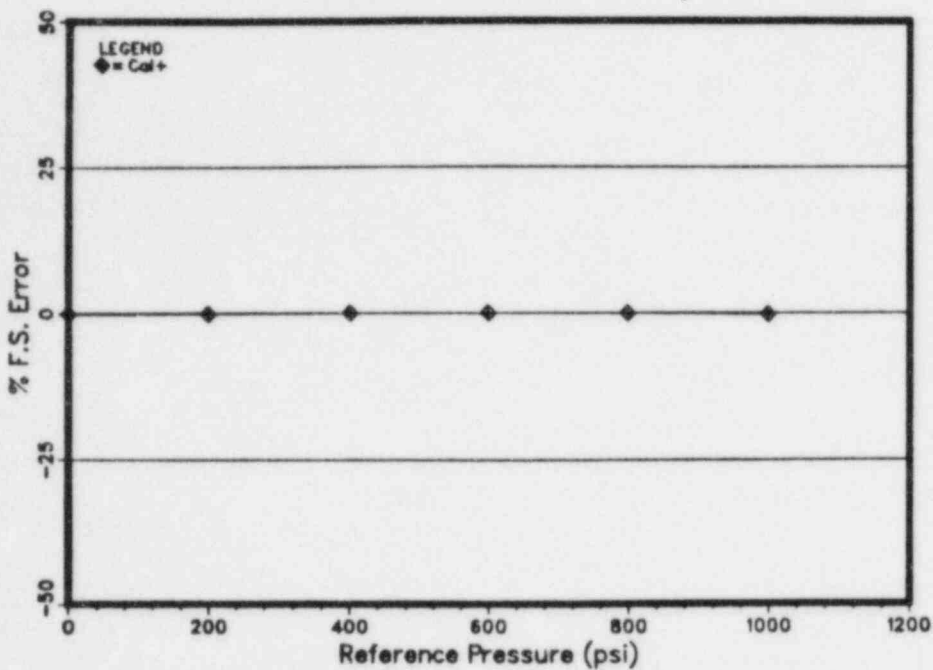


Figure T2-B-14

Trans.T2 Cal1 Pres. Sensitivity 150°C

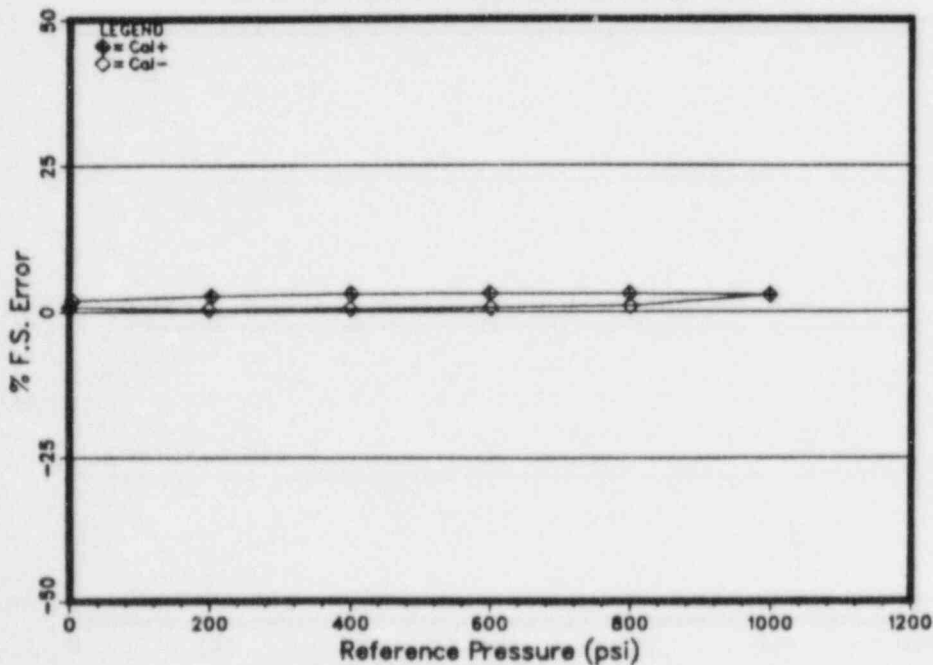


Figure T2-B-15

Trans.T2 Cal2 Pres. Sensitivity 150°C

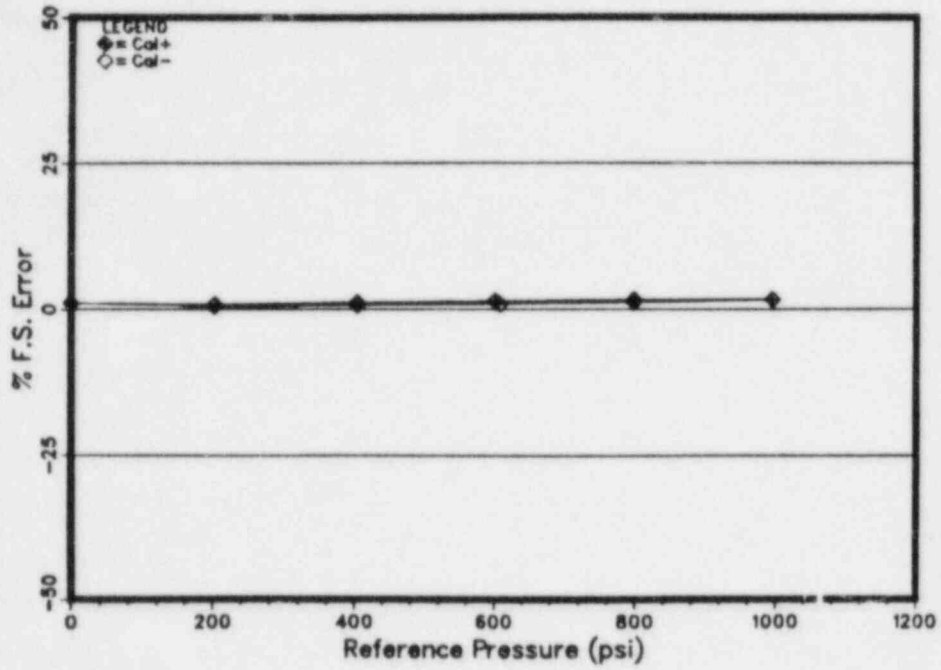


Figure T2-B-16

Trans.T2 Cal3 Pres. Sensitivity 150°C

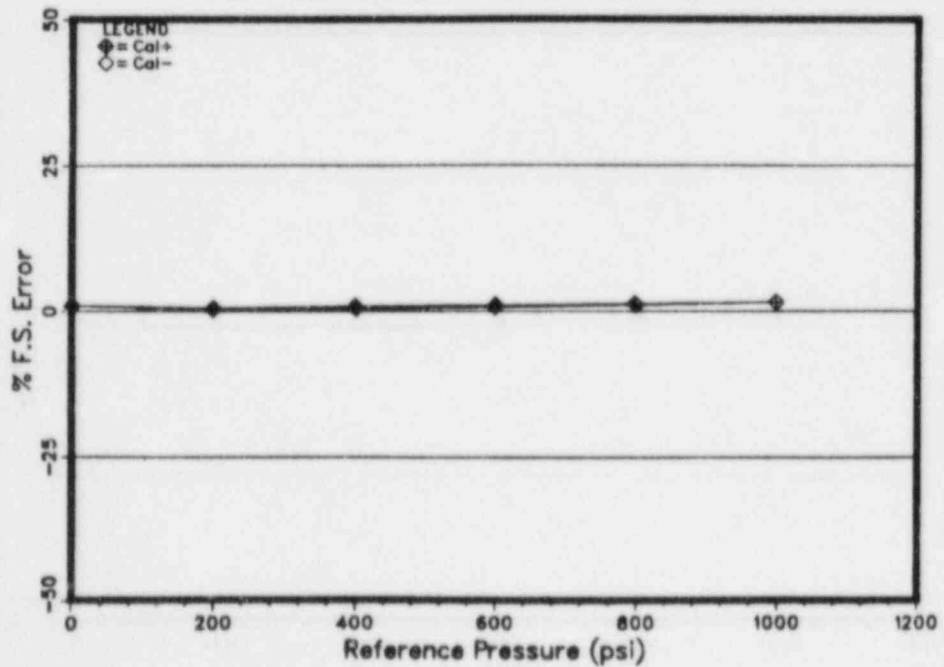


Figure T2-B-17

Trans.T2 Cal4 Pres. Sensitivity 150°C

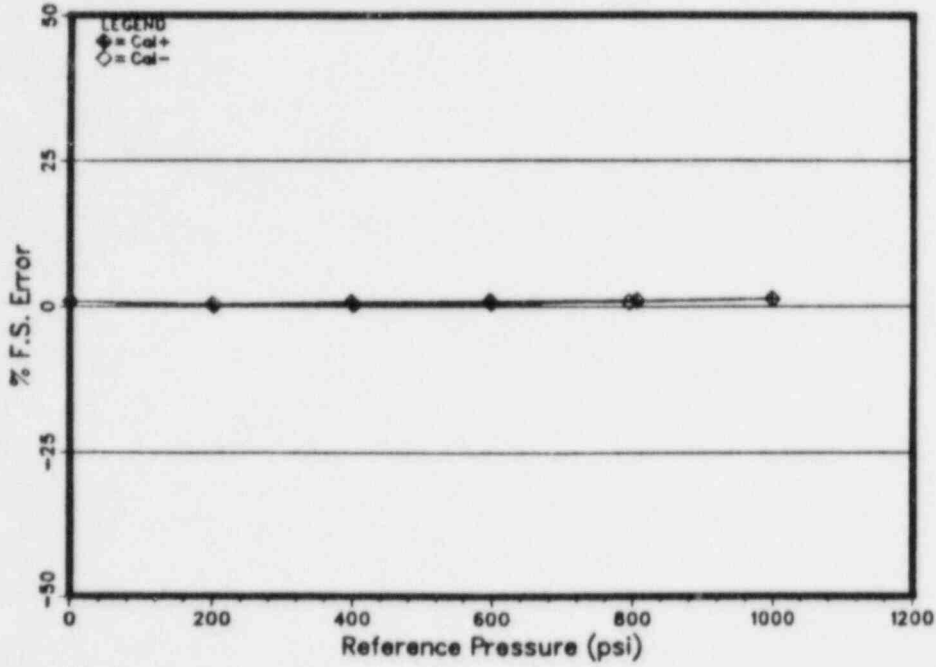


Figure T2-B-18

Trans.T2 Cal5 Pres. Sensitivity 173°C

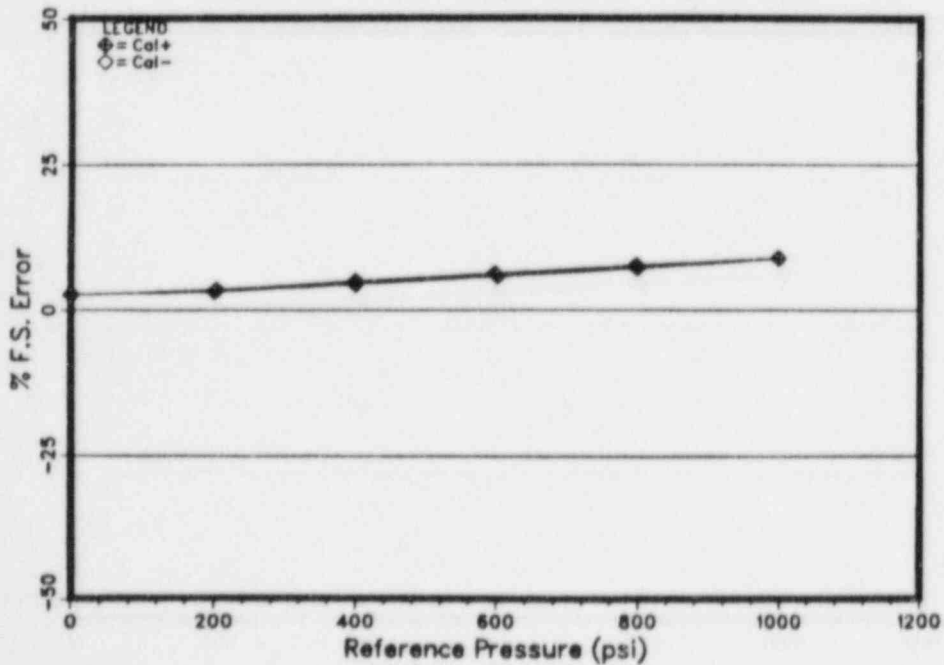


Figure T2-B-19

Trans.T2 Cal6 Pres. Sensitivity 150°C

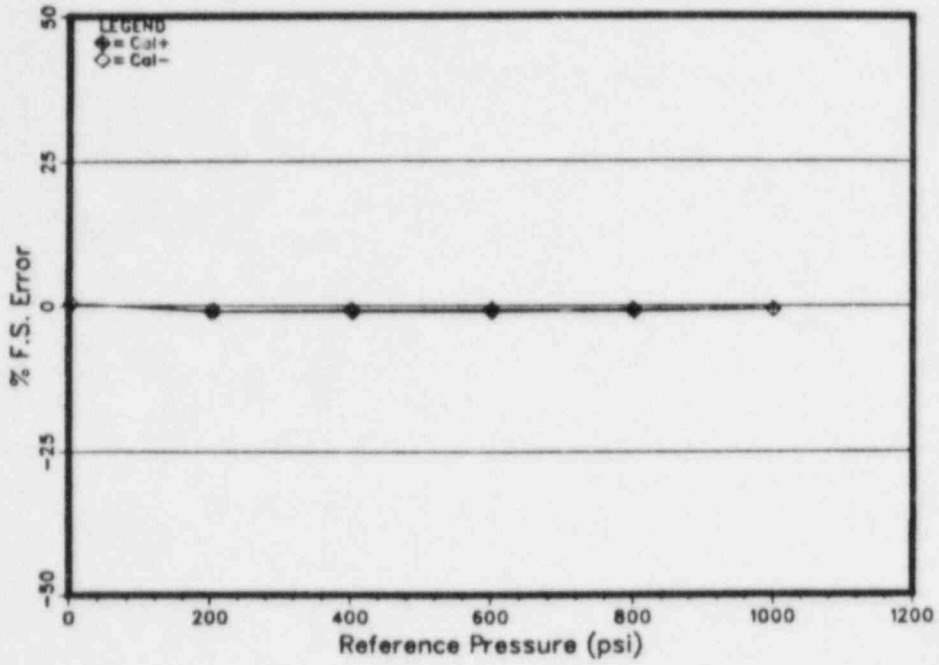


Figure T2-B-20

Trans.T2 Cal7 Pres. Sensitivity 146°C

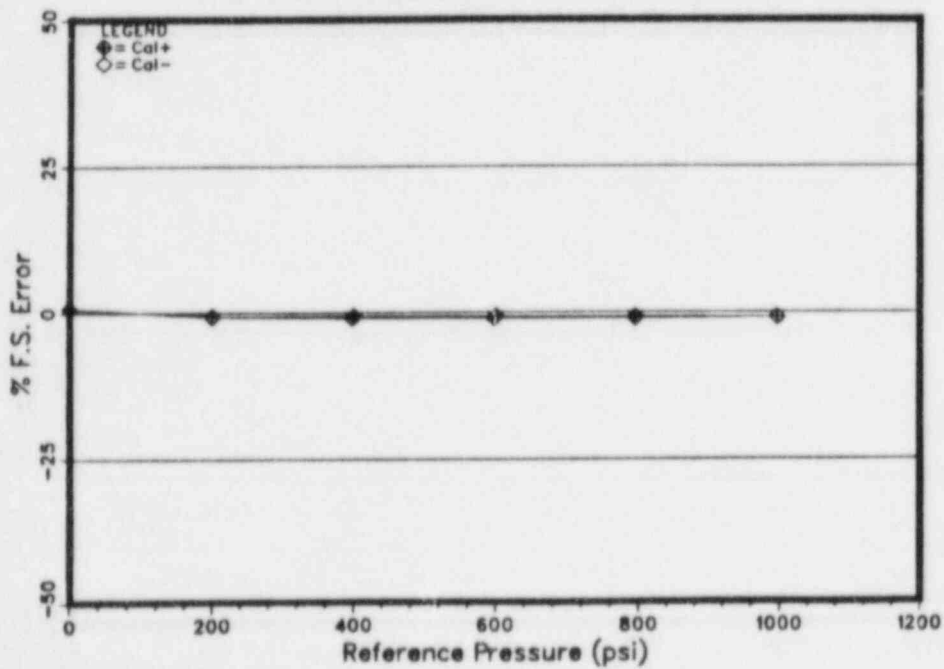


Figure T2-B-21

Trans.T2 Cal8 Pres. Sensitivity 21°C

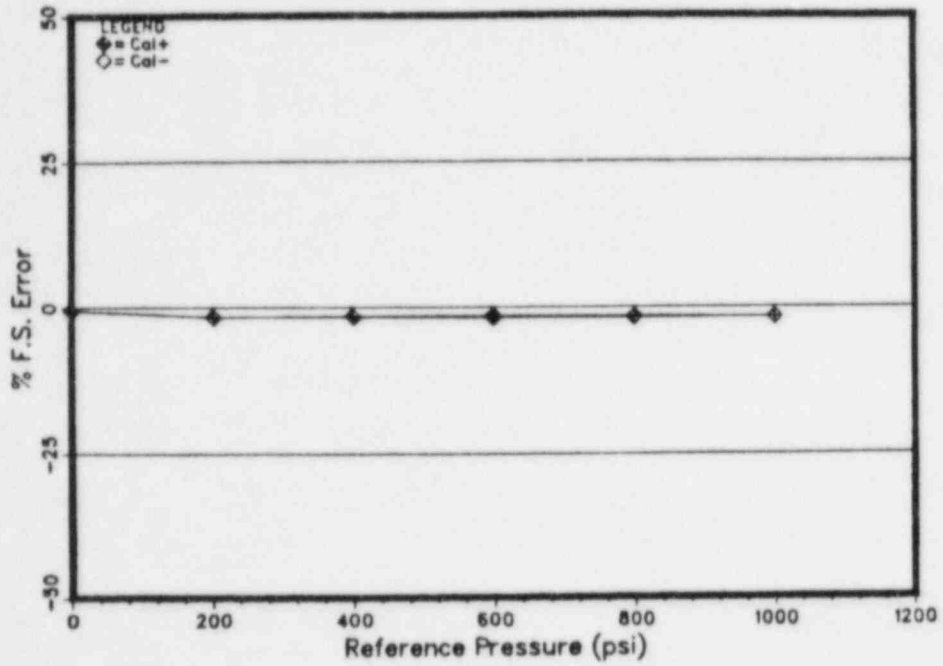


Figure T2-B-22

Trans.T2 Cal9 Pres. Sensitivity 180°C

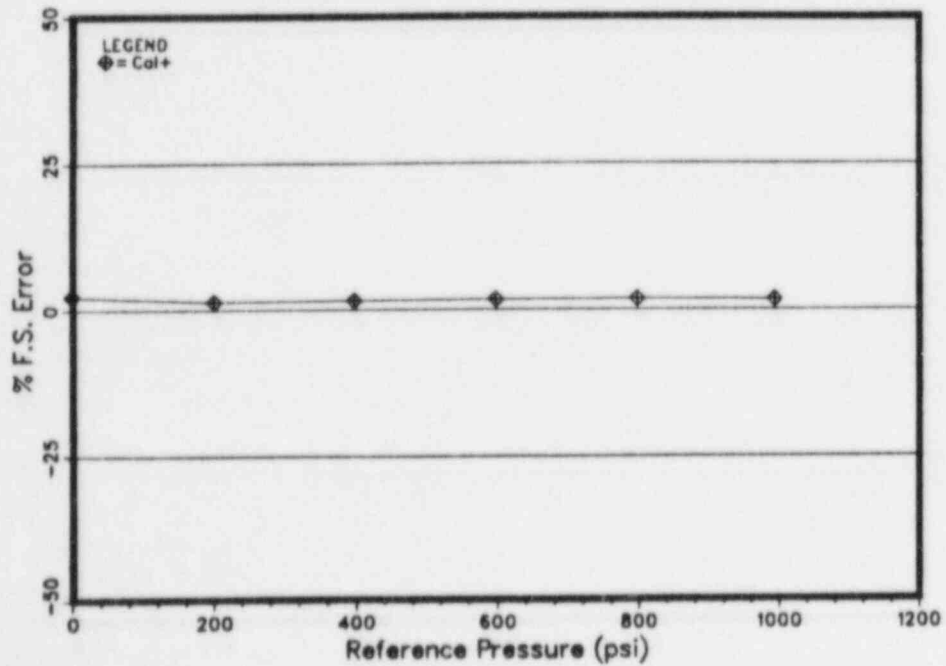


Figure T2-B-23

Trans. T2 Calibration Temperature Profile

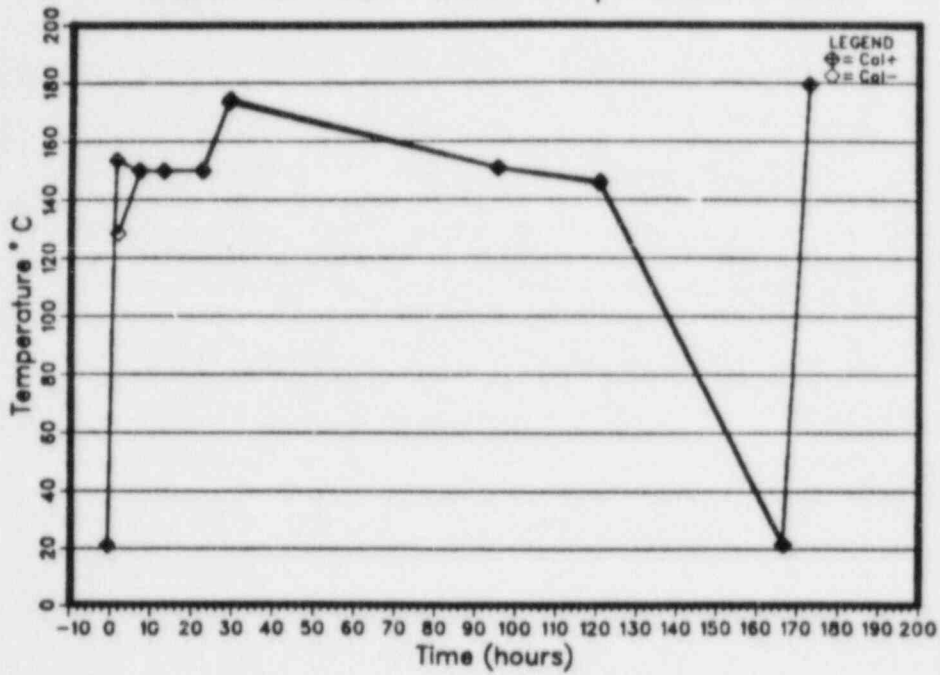


Figure T2-B-24

Transmitter T2 0 psi Calibration Stability

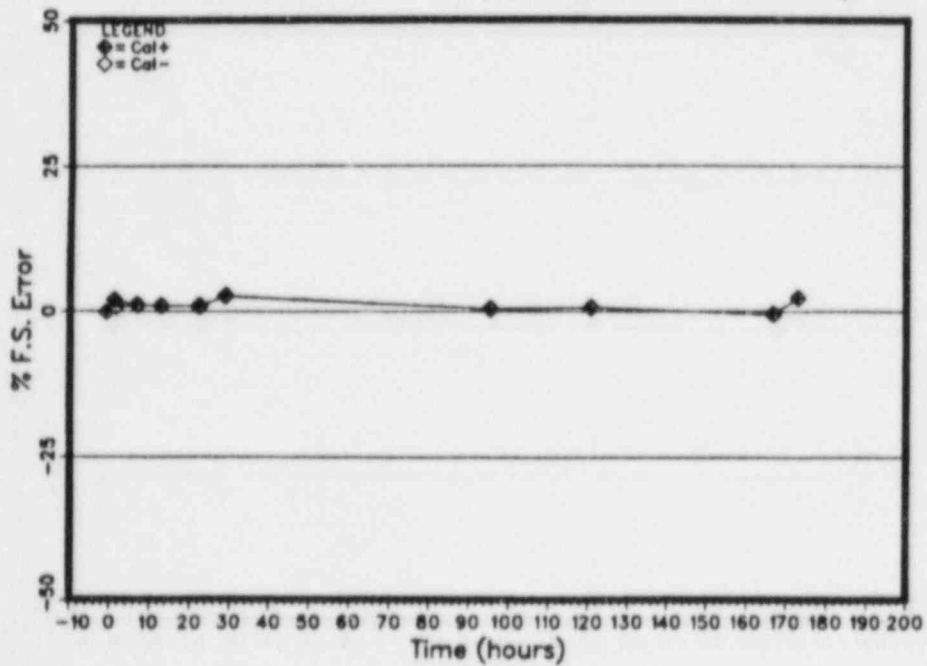


Figure T2-B-25

Transmitter T2 200 psi Calibration Stability

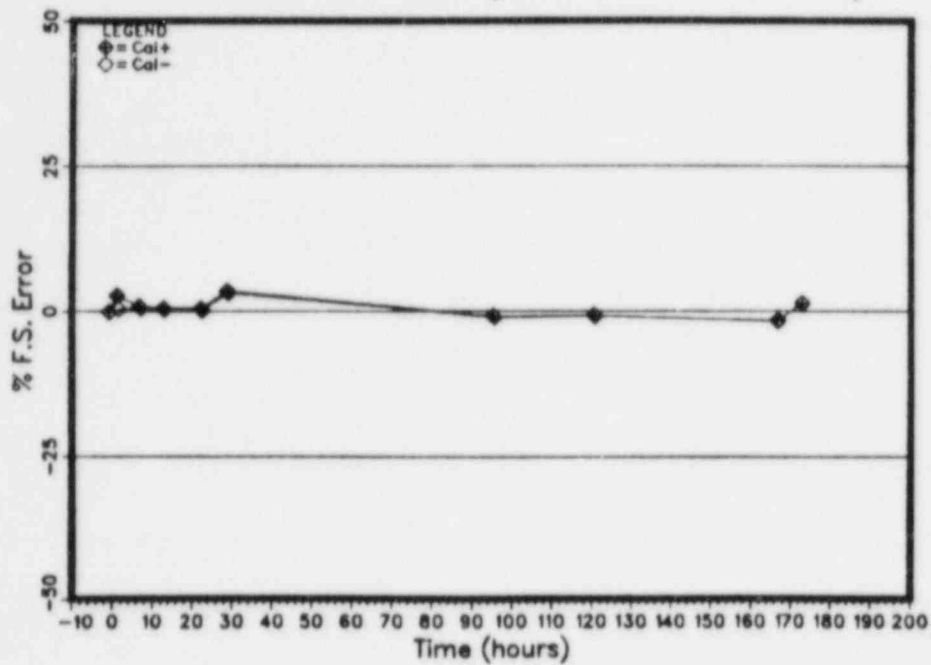


Figure T2-B-26

Transmitter T2 400 psi Calibration Stability

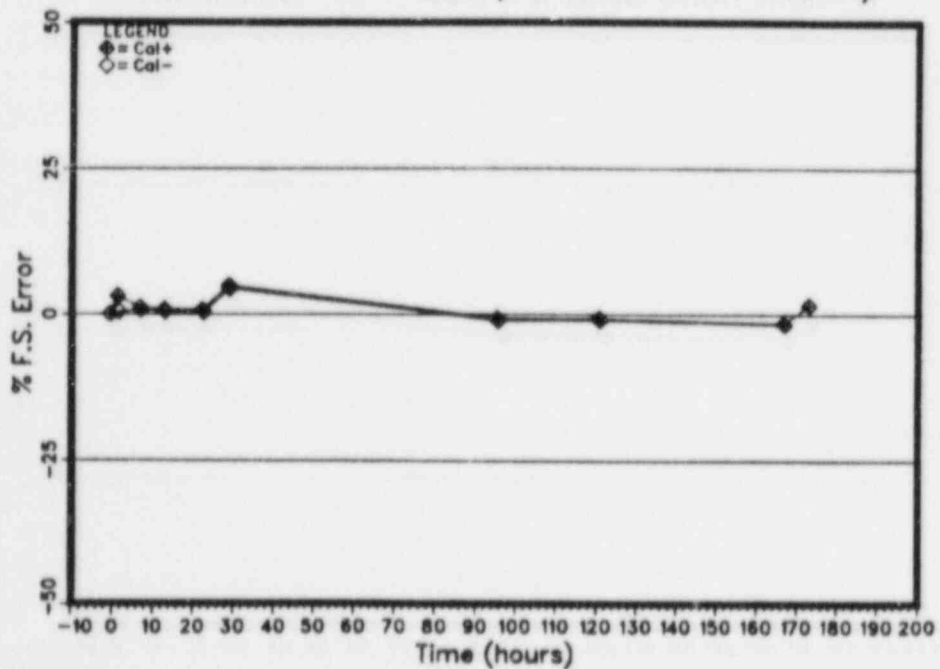


Figure T2-B-27

Transmitter T2 600 psi Calibration Stability

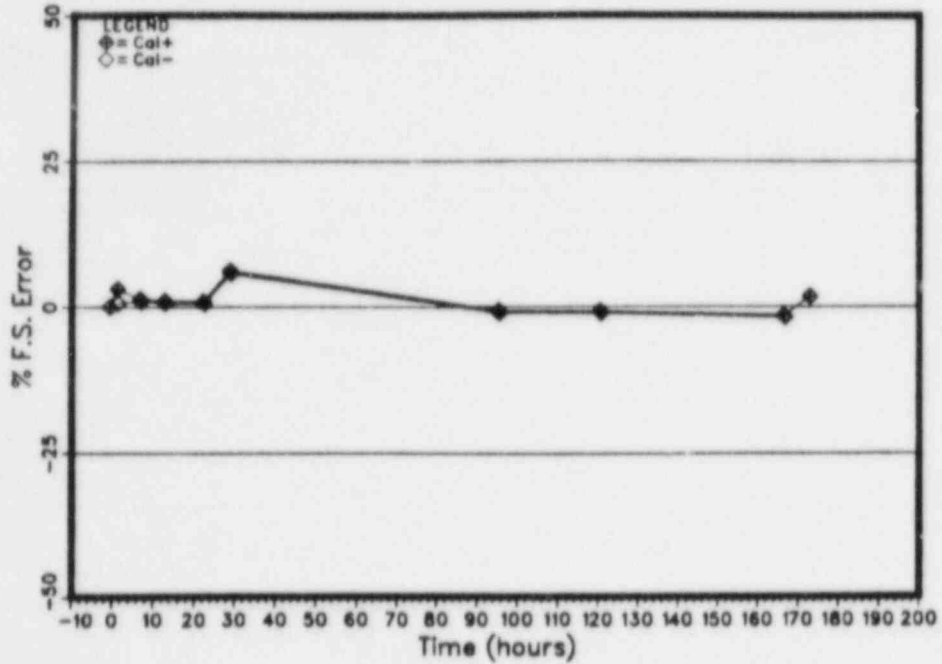


Figure T2-B-28

Transmitter T2 800 psi Calibration Stability

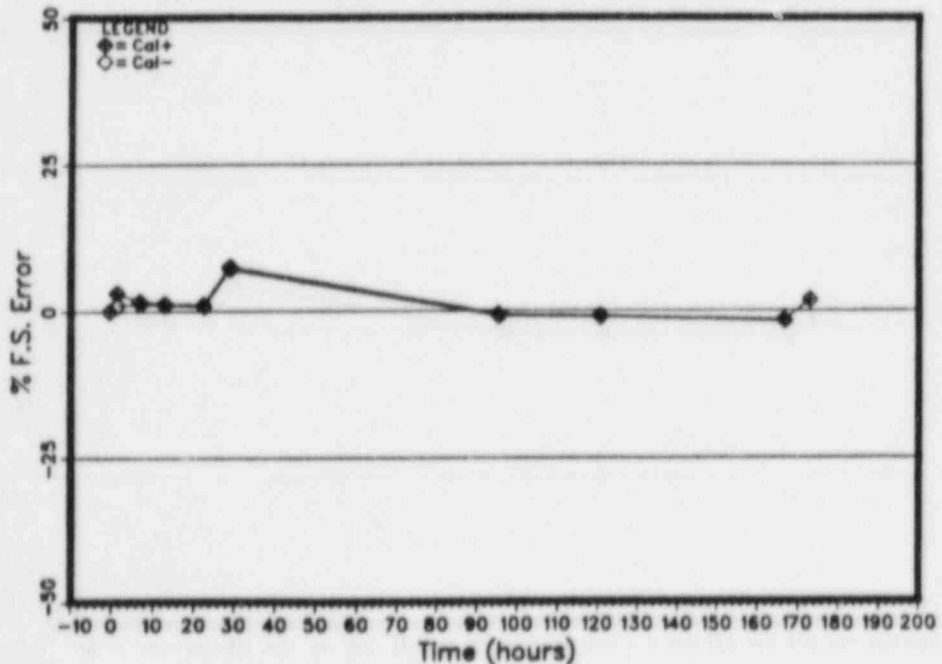


Figure T2-B-29

Transmitter T2 1000 psi Calibration Stability

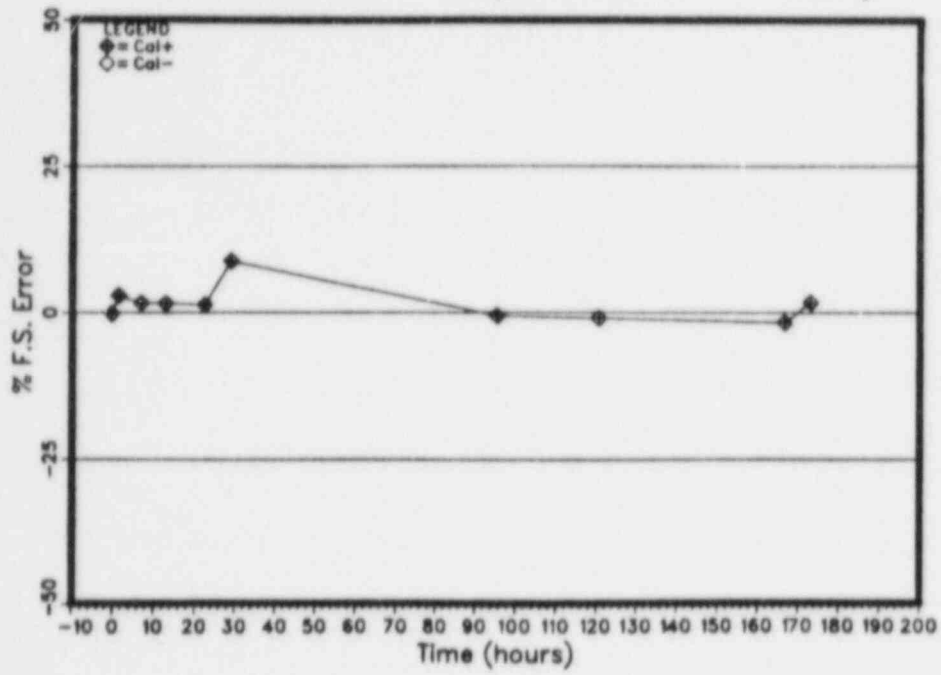


Figure T3-B-1  
 Transmitter T3 %F.S. Error Data Scatter

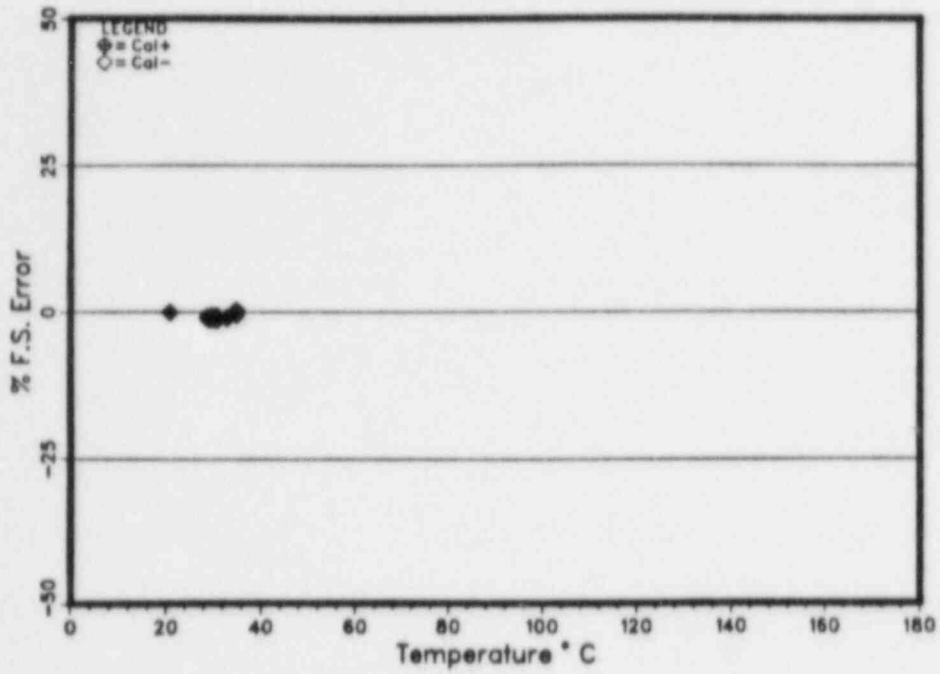


Figure T3-B-2  
 Transmitter T3 Correlation Scatter, Cal+

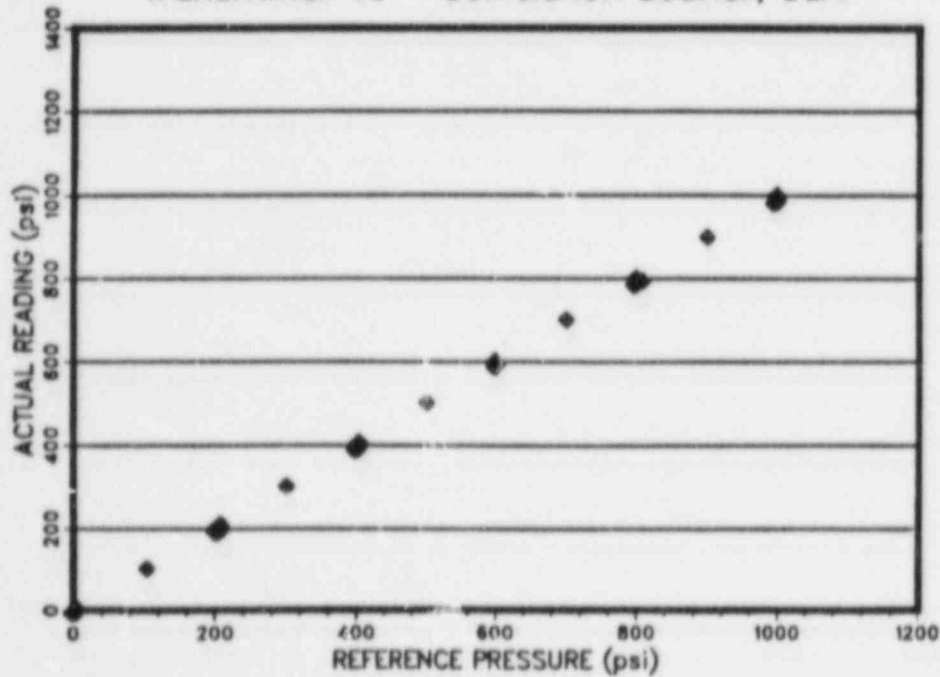


Figure T3-B-3

Transmitter T3 Cal 0 Correlation 21°C

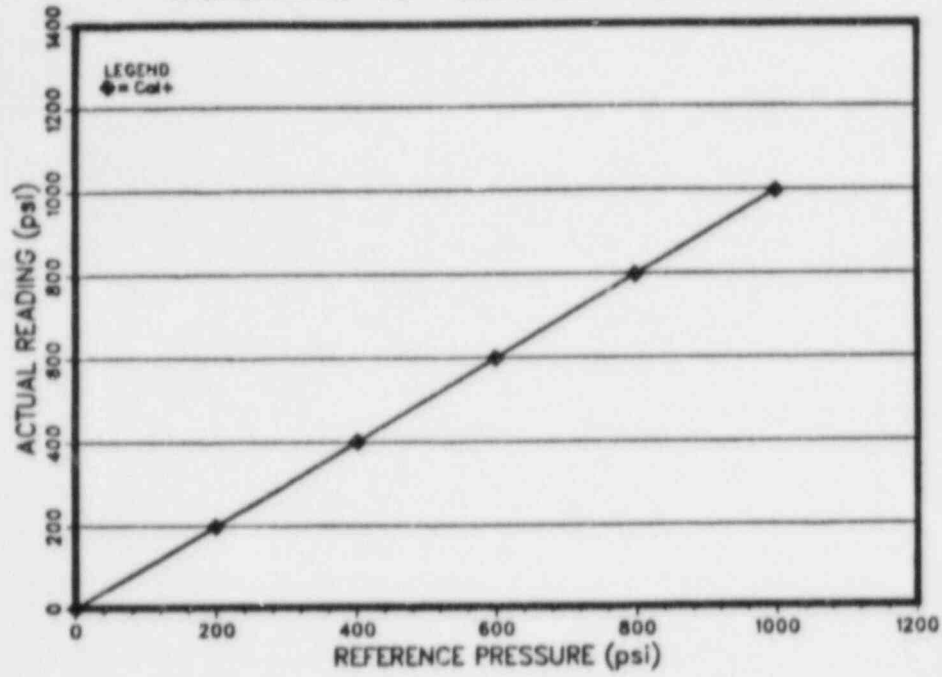


Figure T3-B-4

Transmitter T3 Cal 1 Correlation 35°C

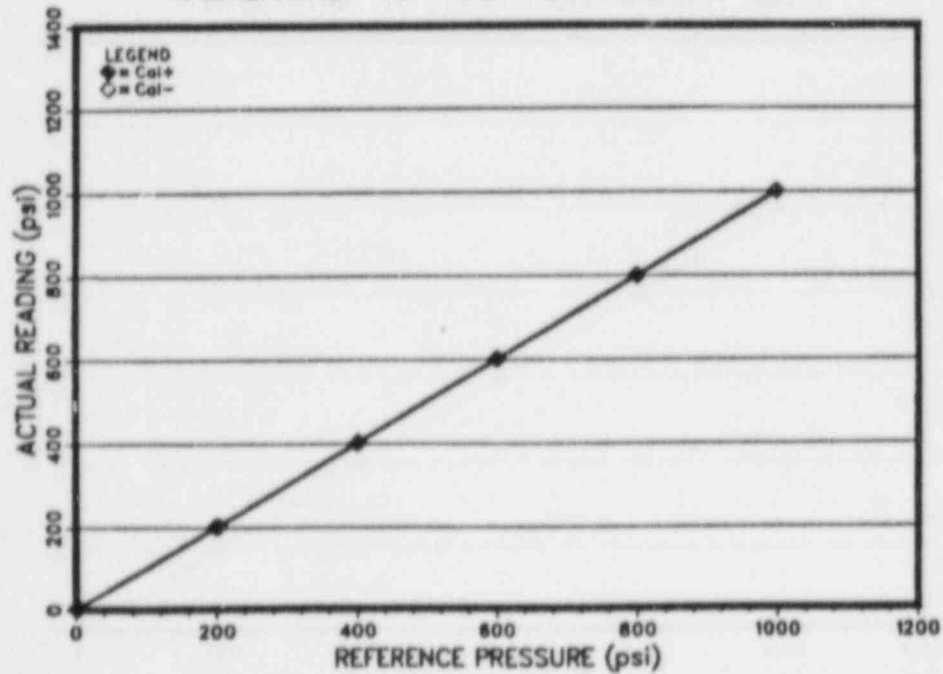


Figure T3-B-5

Transmitter T3 Cal 2 Correlation 35°C

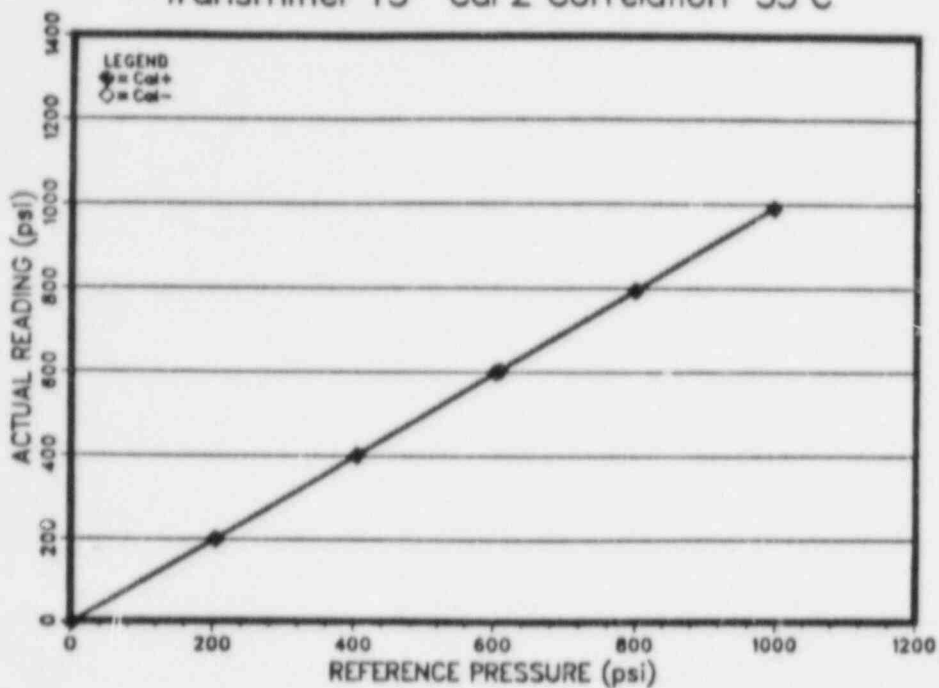


Figure T3-B-6

Transmitter T3 Cal 3 Correlation 33°C

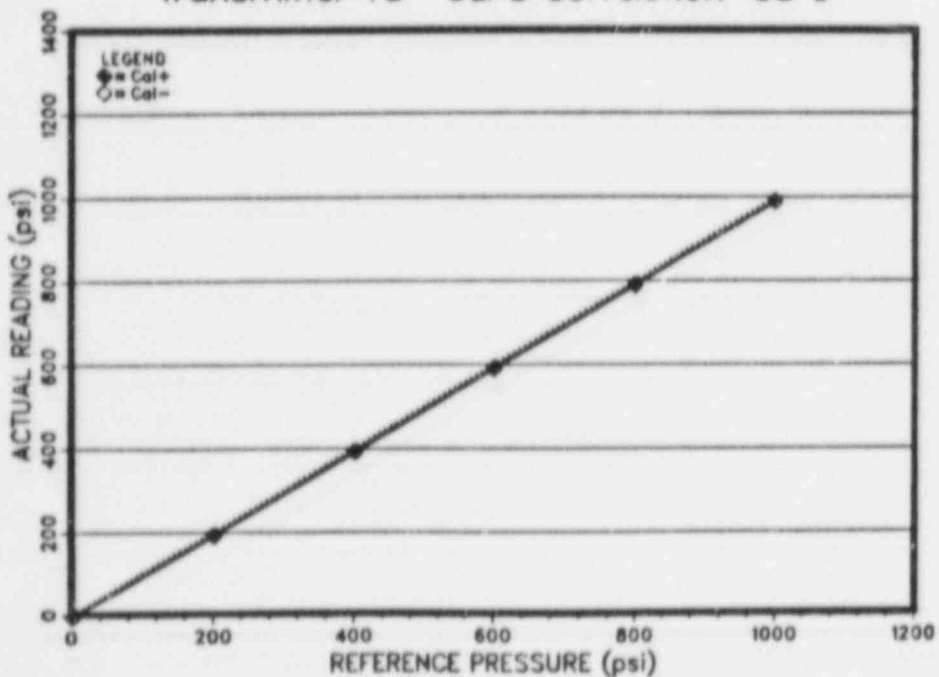


Figure T3-B-7

Transmitter T3 Cal 4 Correlation 31°C

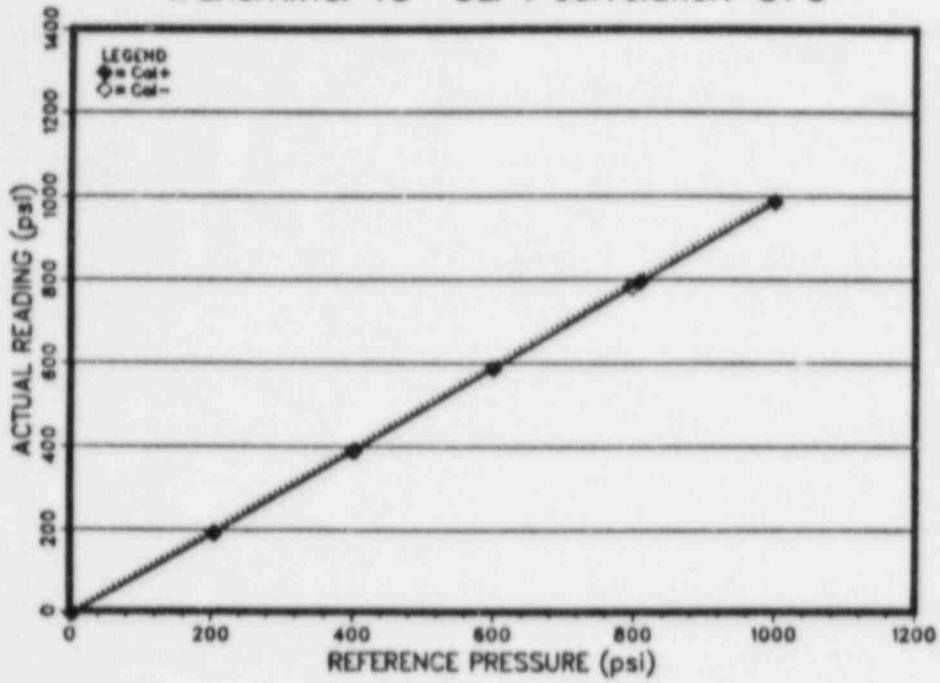


Figure T3-B-8

Transmitter T3 Cal 5 Correlation 31°C

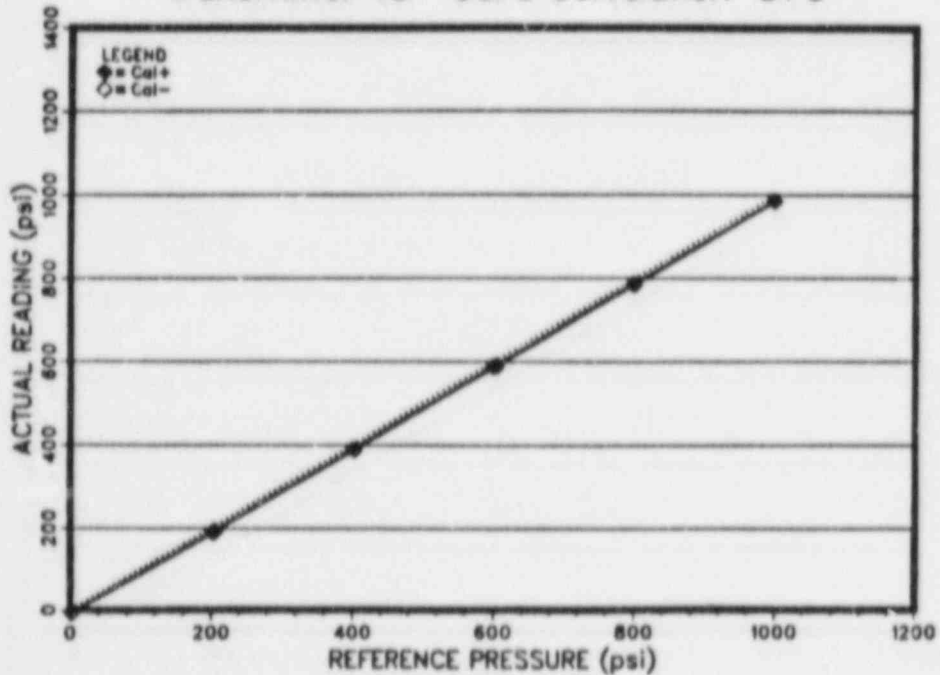


Figure T3-B-9

Transmitter T3 Cal 6 Correlation 31°C

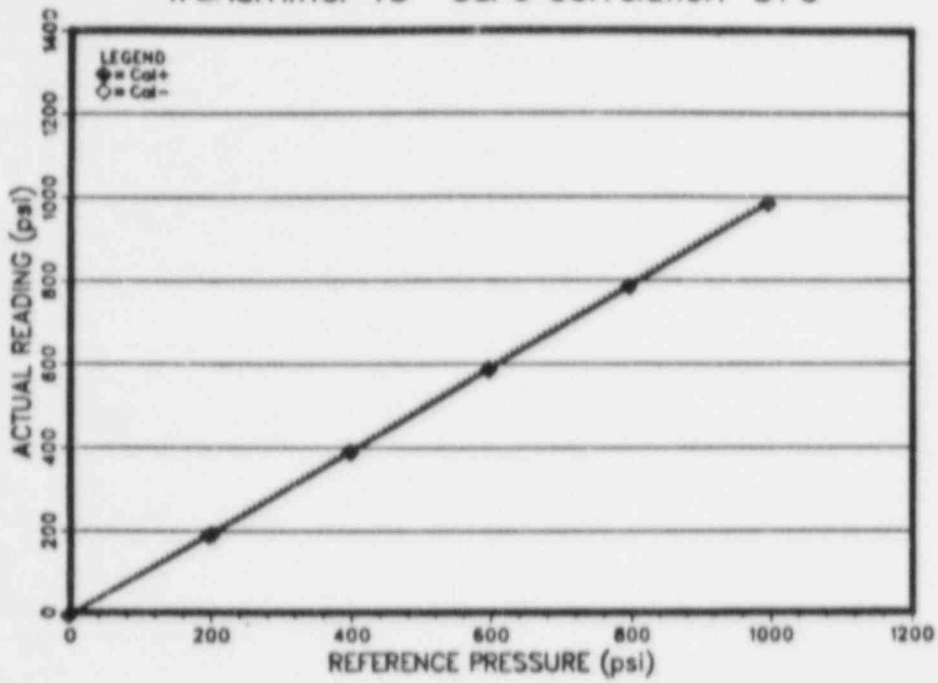


Figure T3-B-10

Transmitter T3 Cal 7 Correlation 30°C

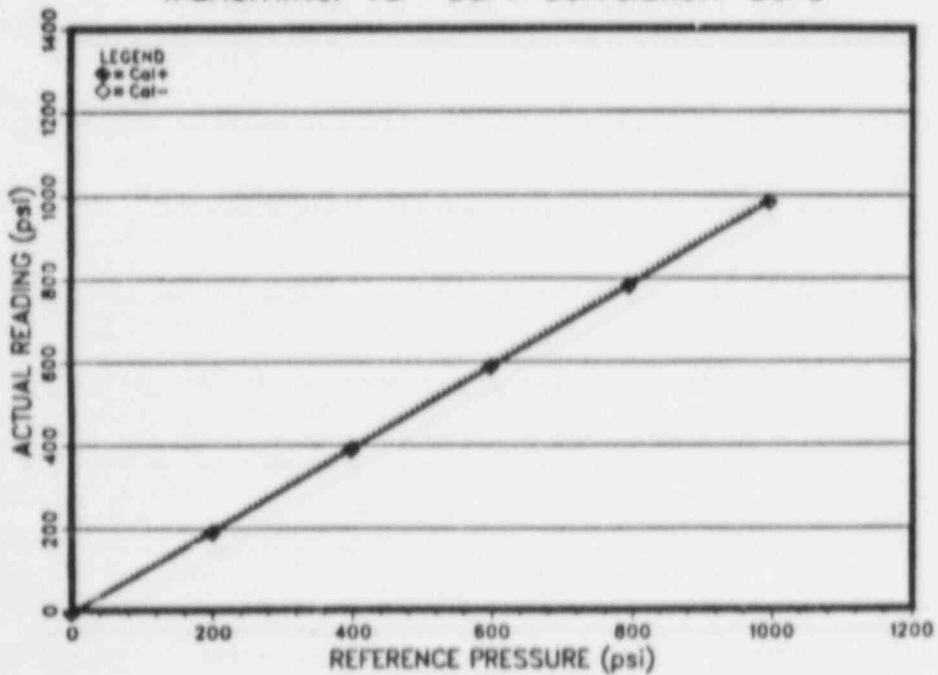


Figure T3-B-11

Transmitter T3 Cal 8 Correlation 31°C

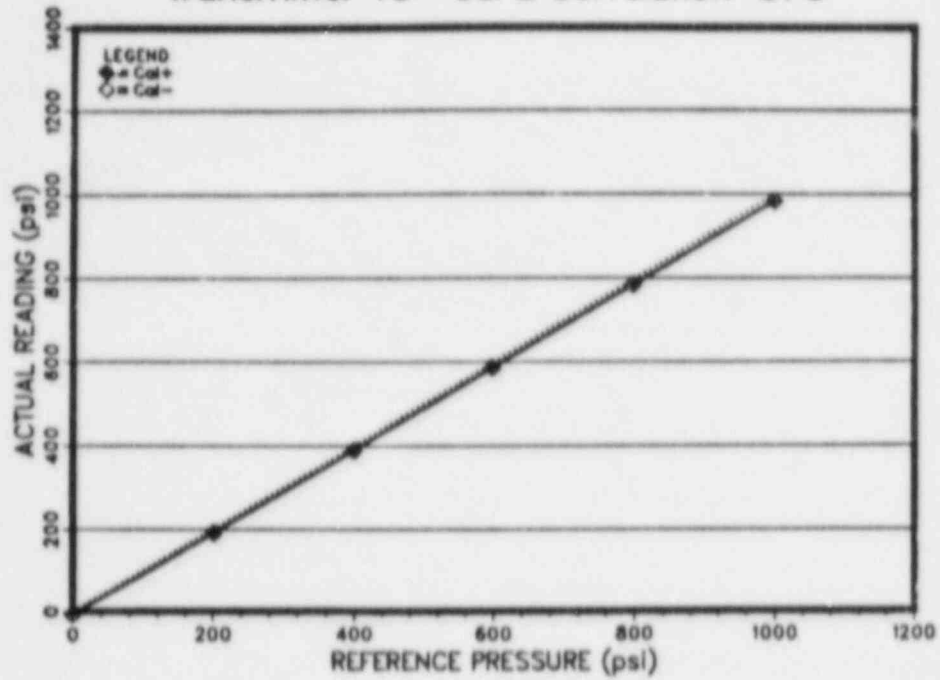


Figure T3-B-12

Transmitter T3 Cal 9 Correlation 30°C

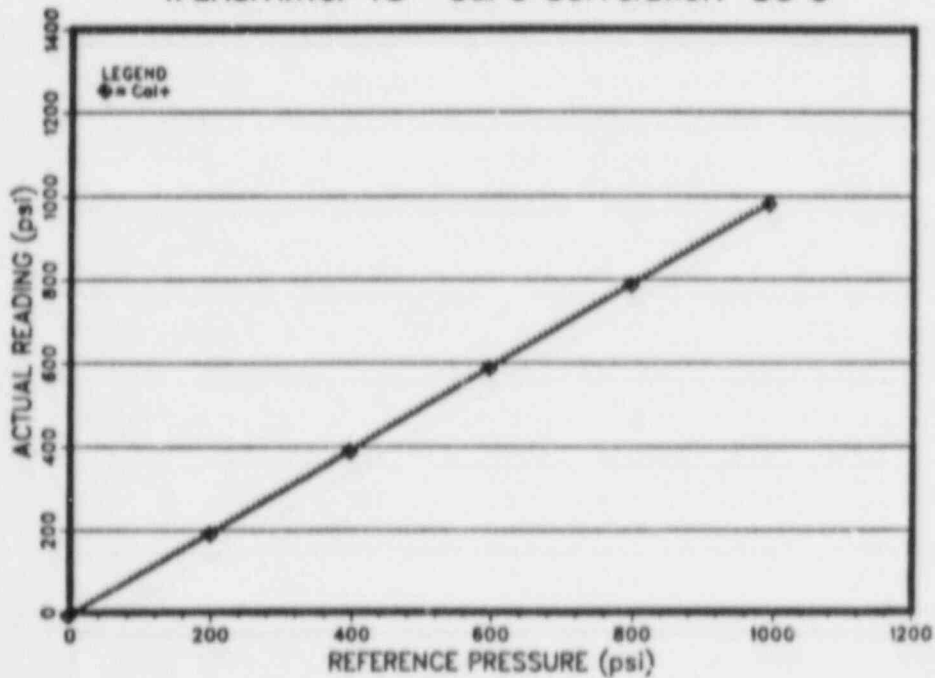


Figure T3-B-13

Trans.T3 Cal0 Pres. Sensitivity 21°C

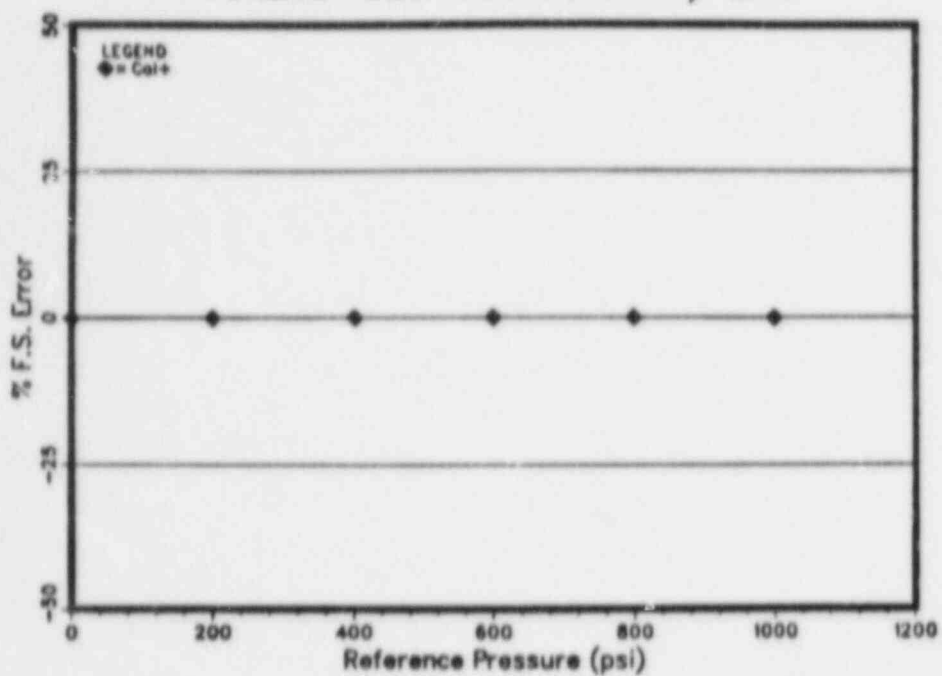


Figure T3-B-14

Trans.T3 Cal1 Pres. Sensitivity 35°C

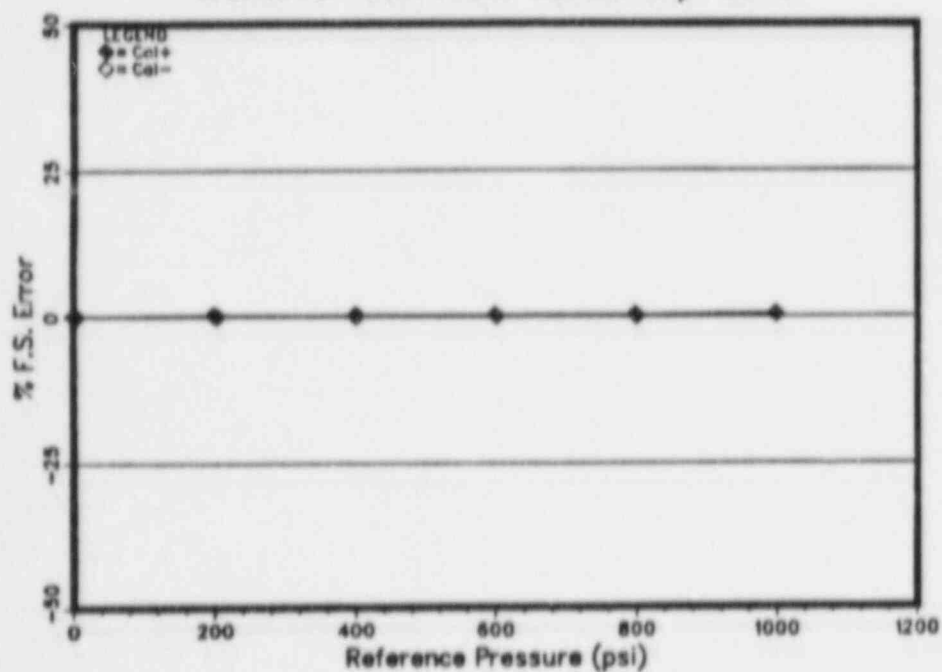


Figure T3-B-15

Trans.T3 Cal2 Pres. Sensitivity 35°C

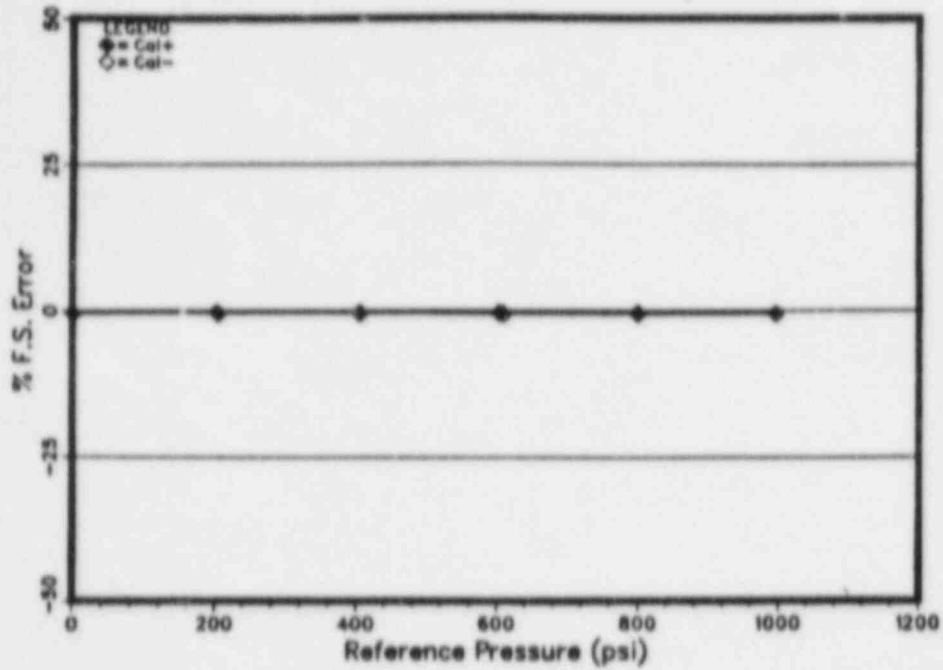


Figure T3-B-16

Trans.T3 Cal3 Pres. Sensitivity 33°C

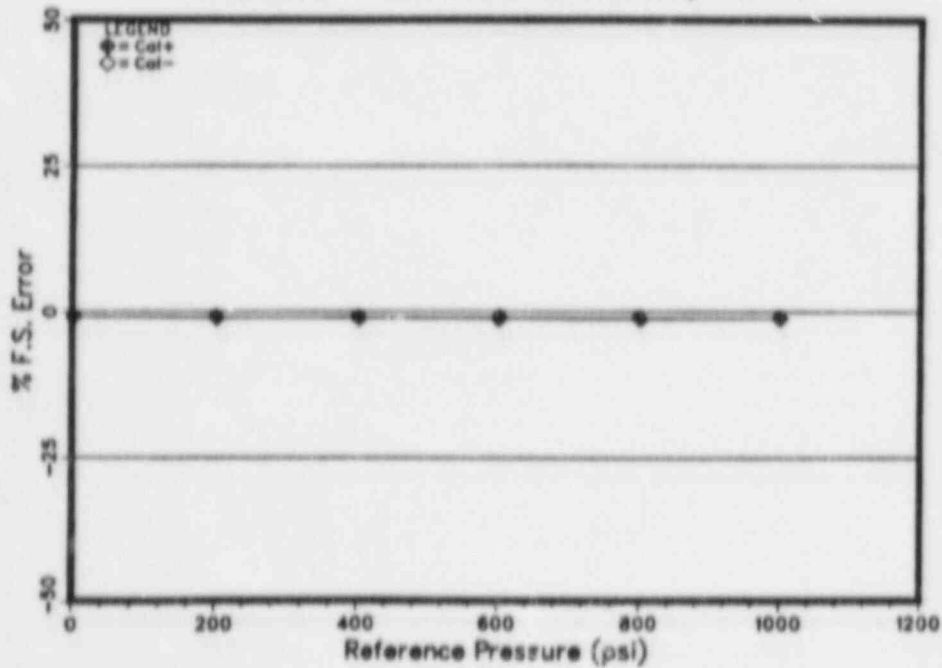


Figure T3-B-17

Trans.T3 Cal4 Pres. Sensitivity 31°C

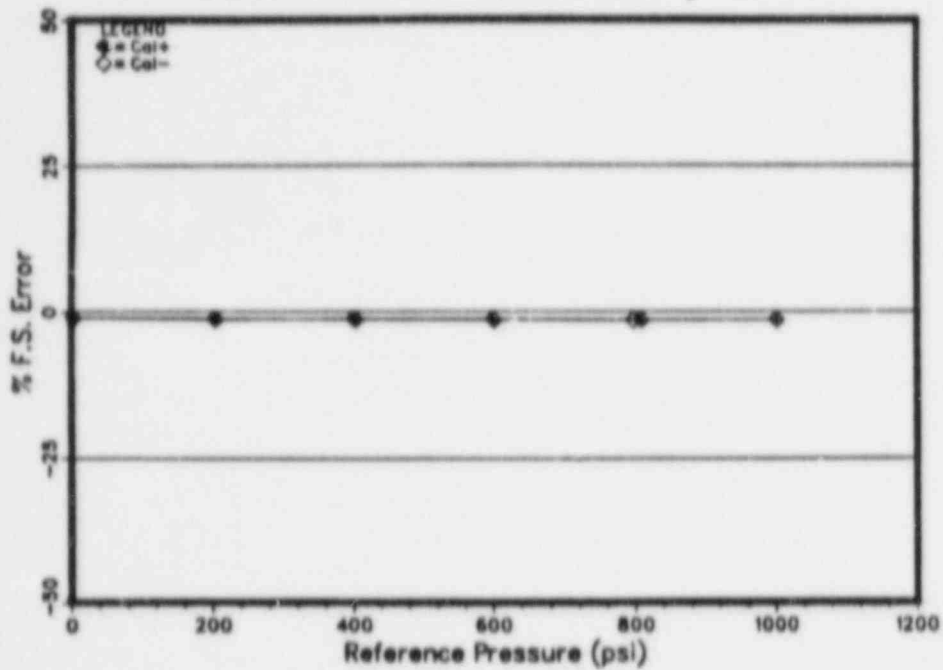


Figure T3-B-18

Trans.T3 Cal5 Pres. Sensitivity 31°C

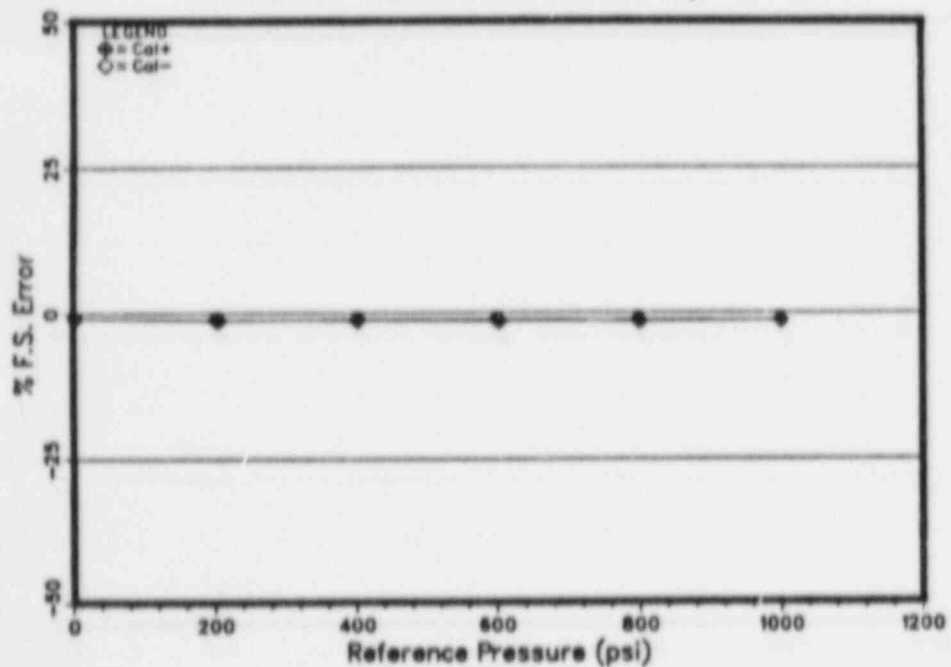


Figure T3-B-19

Trans.T3 Cal6 Pres. Sensitivity 31°C

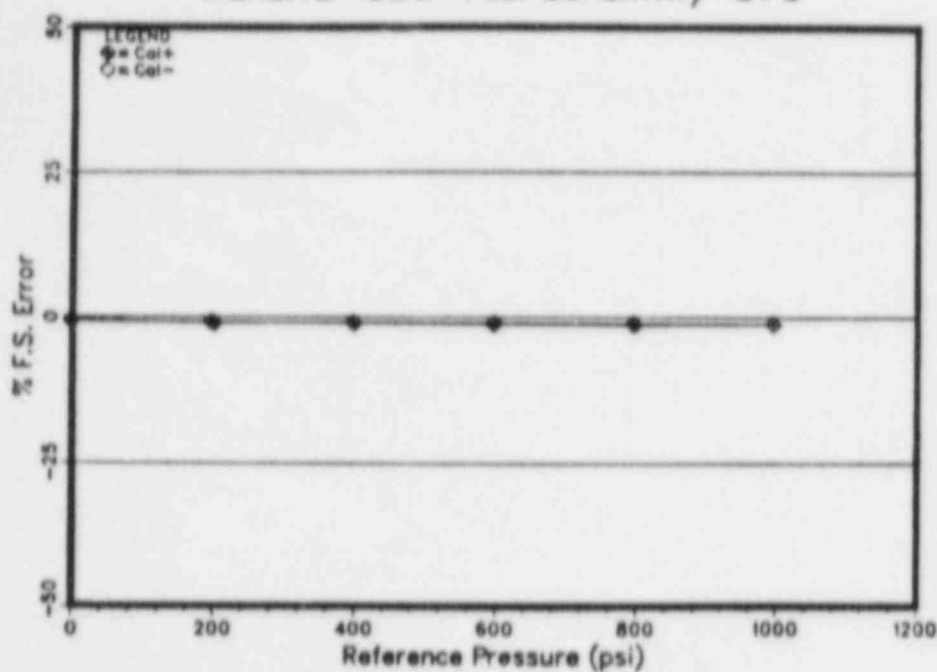


Figure T3-B-20

Trans.T3 Cal7 Pres. Sensitivity 30°C

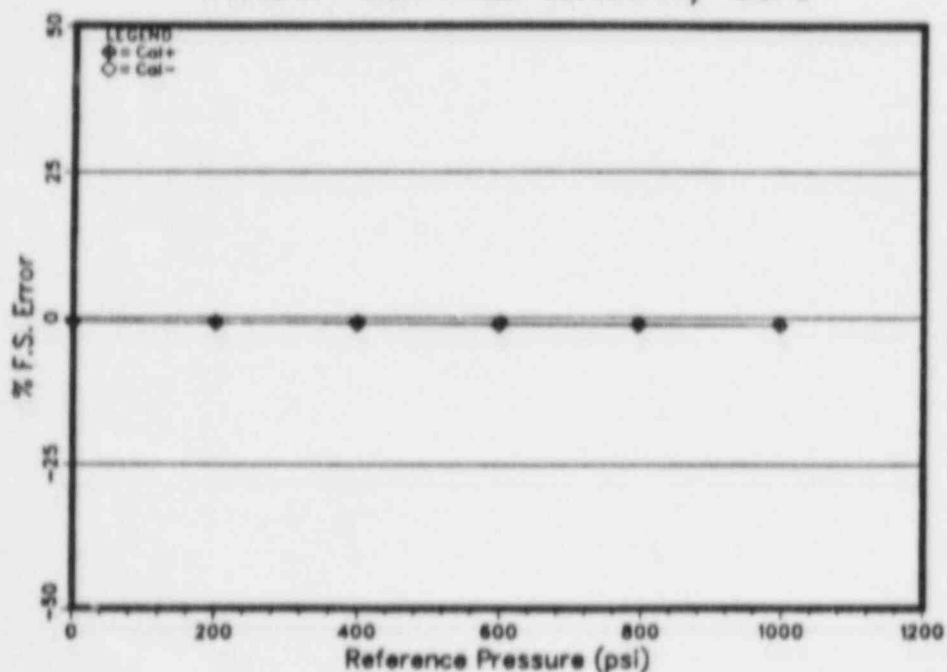


Figure T3-B-21

Trans.T3 Cal8 Pres. Sensitivity 31°C

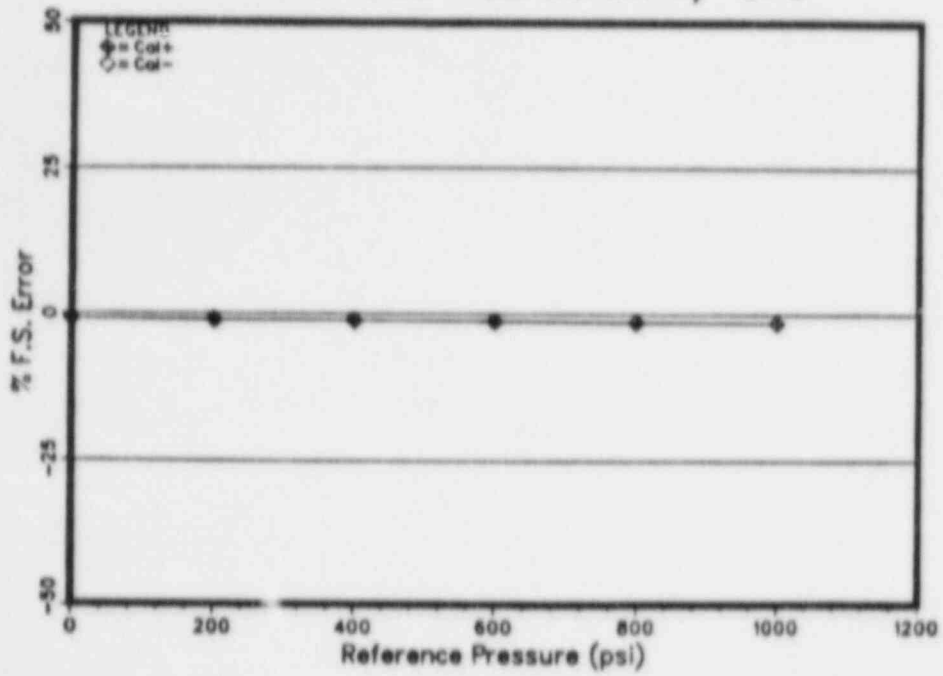


Figure T3-B-22

Trans.T3 Cal9 Pres. Sensitivity 30°C

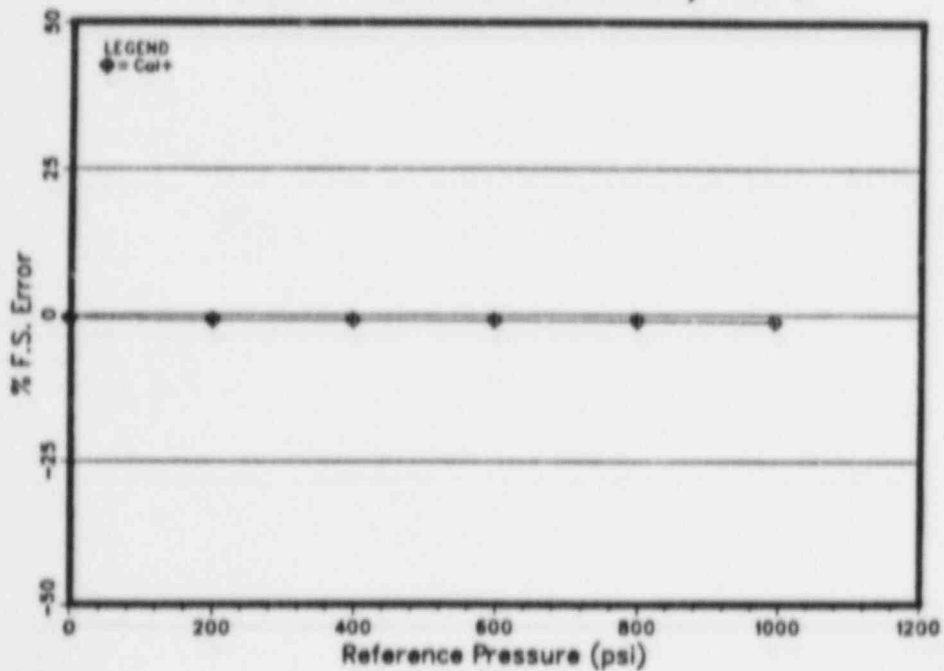


Figure T3-B-23

Trans. T3 Calibration Temperature Profile

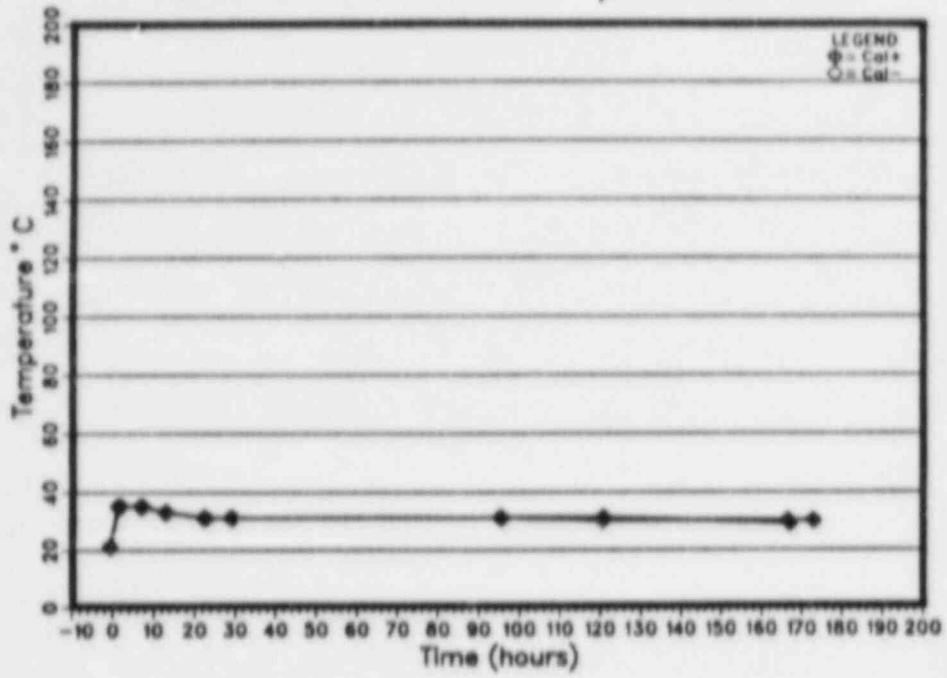


Figure T3-B-24

Transmitter T3 0 psi Calibration Stability

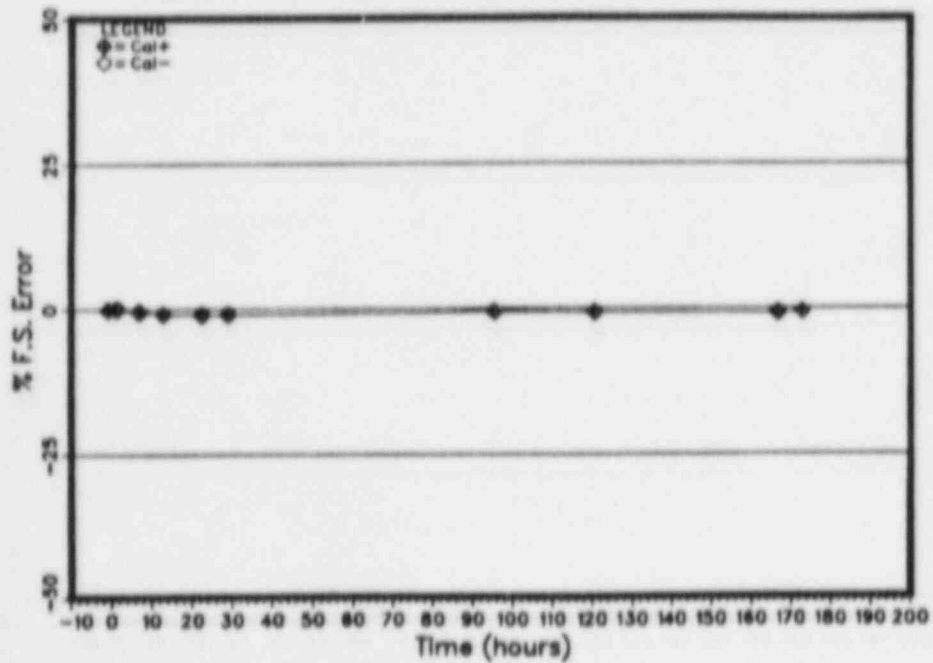


Figure T3-B-25

Transmitter T3 200 psi Calibration Stability

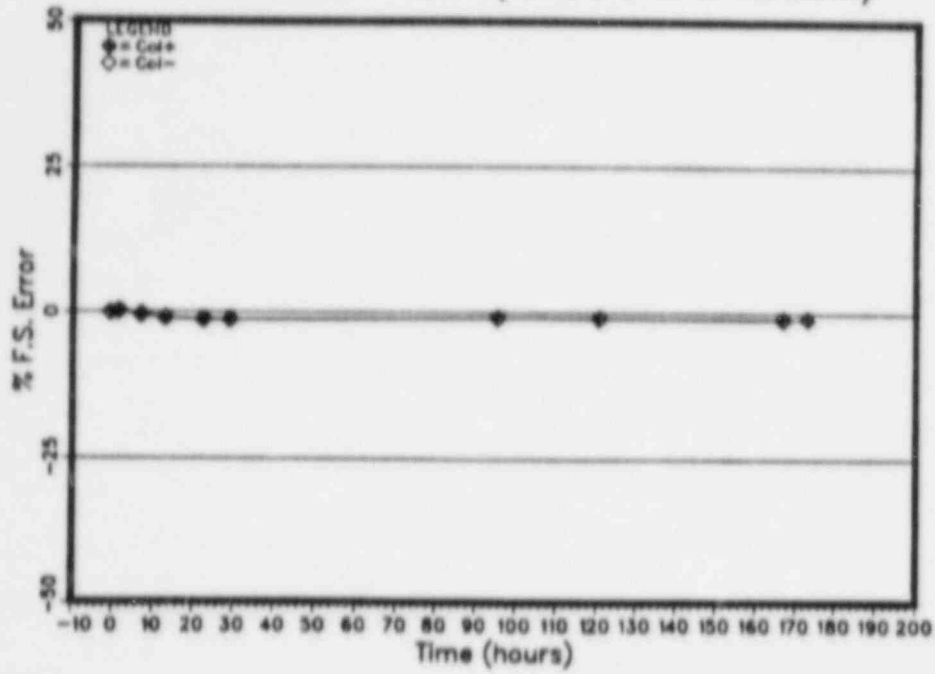


Figure T3-B-26

Transmitter T3 400 psi Calibration Stability

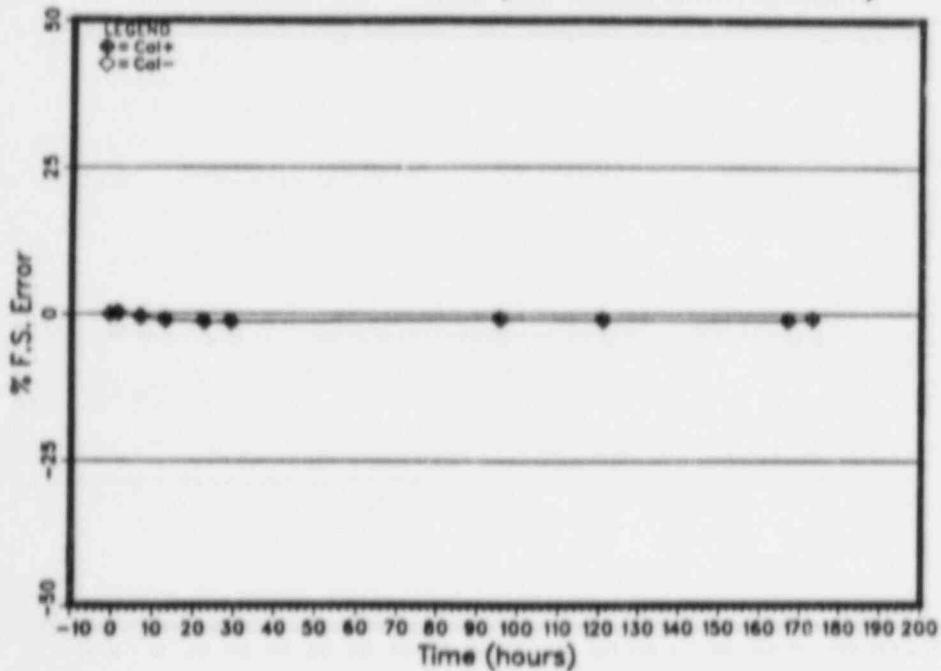


Figure T3-B-27

Transmitter T3 600 psi Calibration Stability

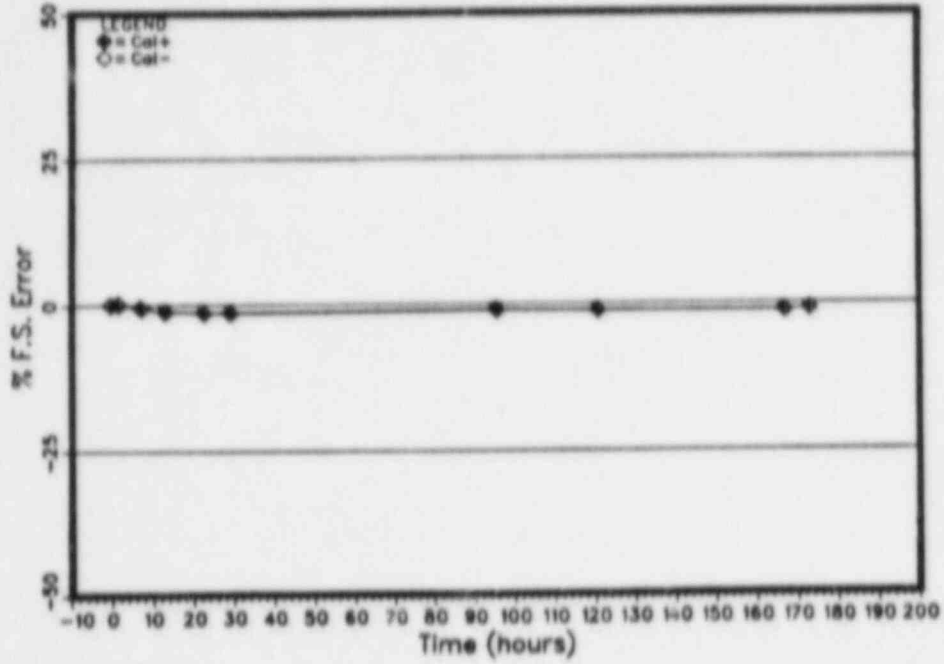


Figure T3-B-28

Transmitter T3 800 psi Calibration Stability

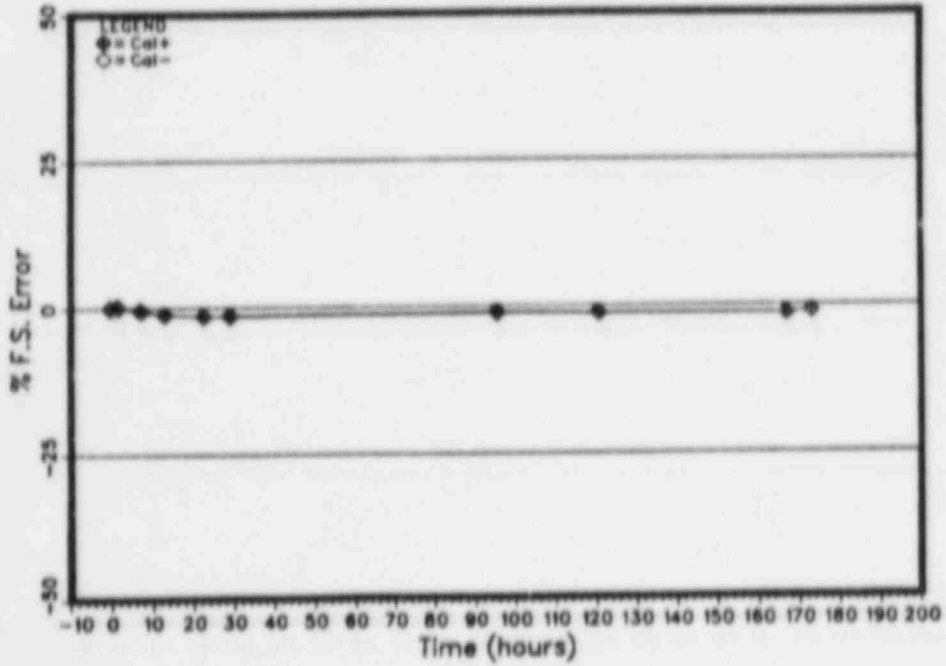


Figure T3-B-29

Transmitter T3 1000 psi Calibration Stability

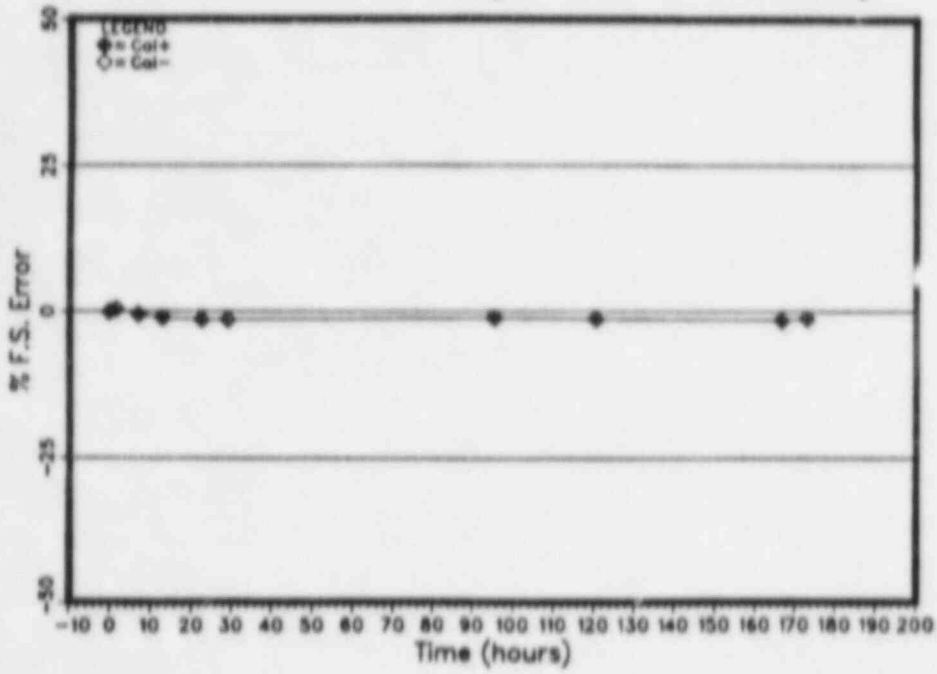


Figure T4-B-1  
 Transmitter T4 %F.S. Error Data Scatter

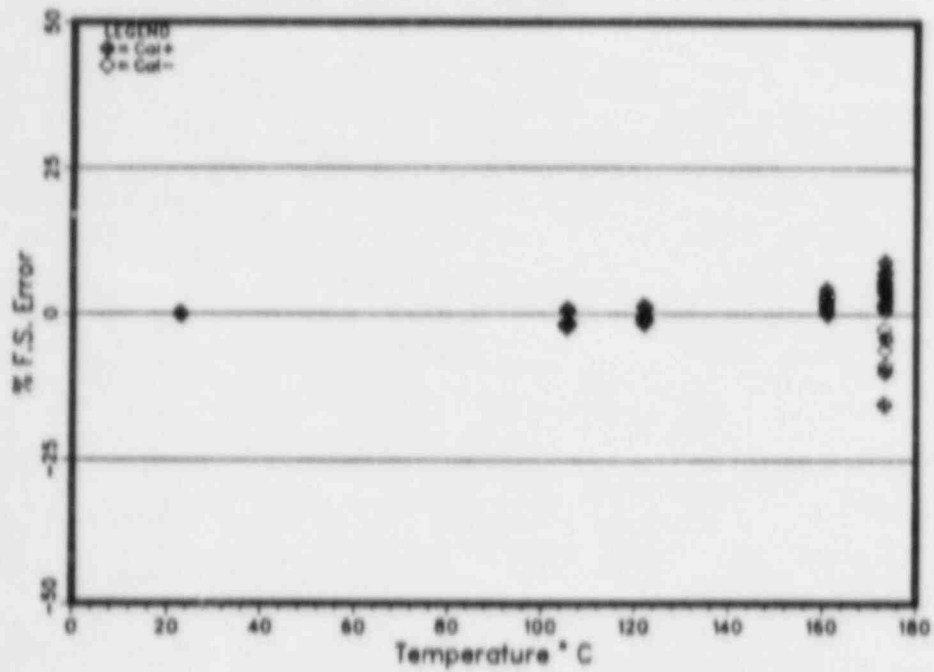


Figure T4-B-2  
 Transmitter T4 Correlation Scatter, Cal+

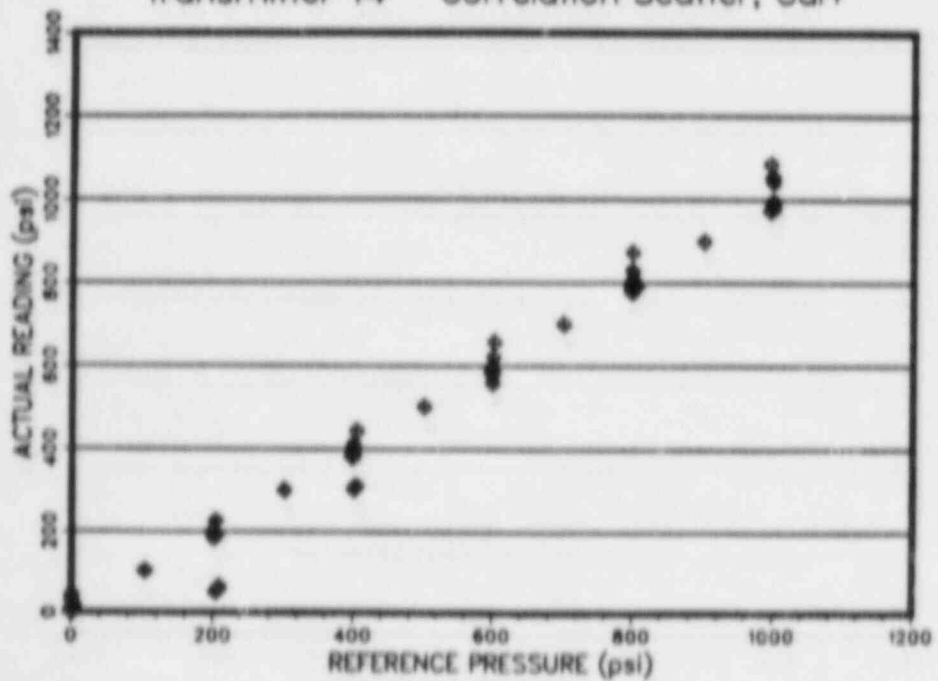


Figure T4-B-3

Transmitter T4 Cal 0 Correlation 21°C

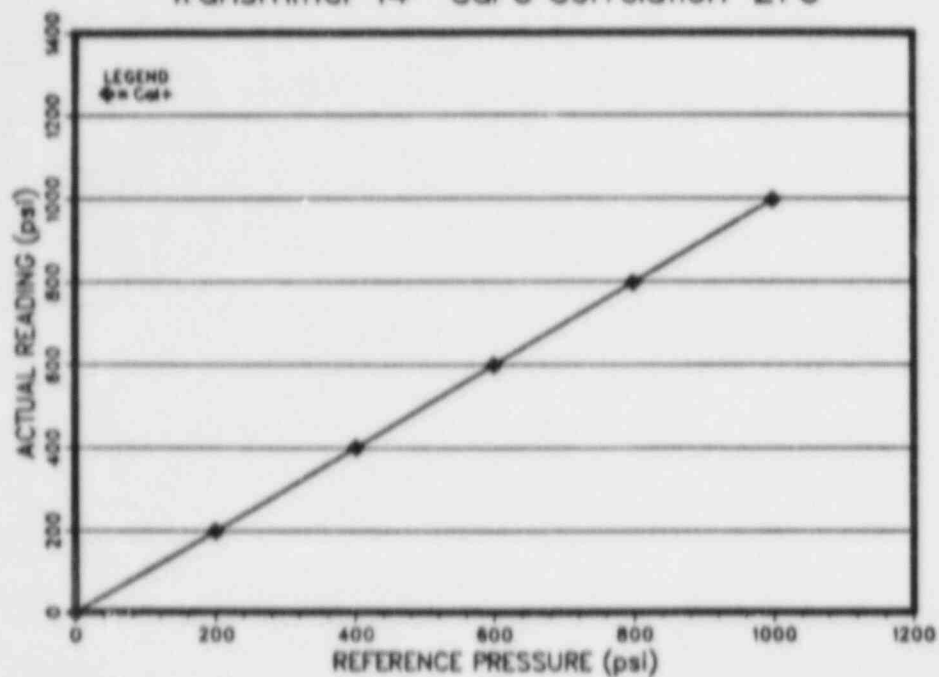


Figure T4-B-4

Transmitter T4 Cal 1 Correlation 173°C

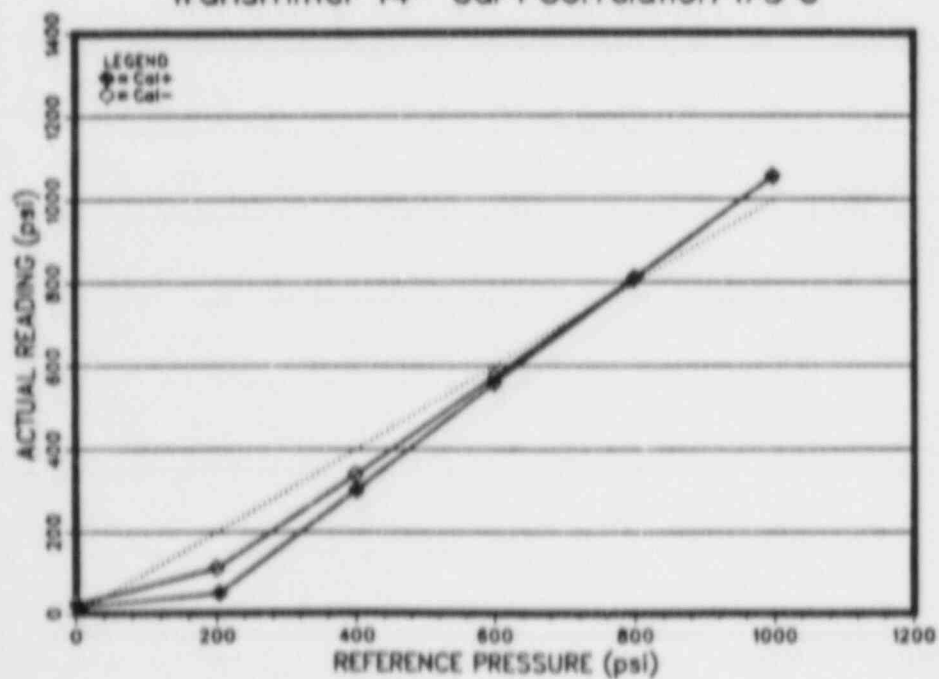


Figure T4-B-5

Transmitter T4 Cal 2 Correlation 173°C

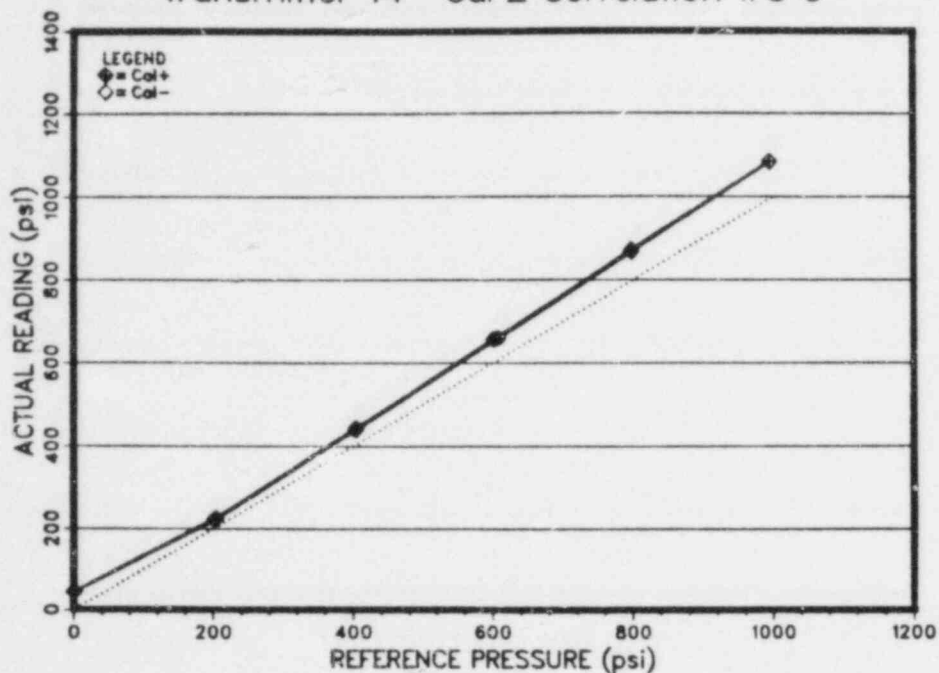


Figure T4-B-6

Transmitter T4 Cal 3 Correlation 160°C

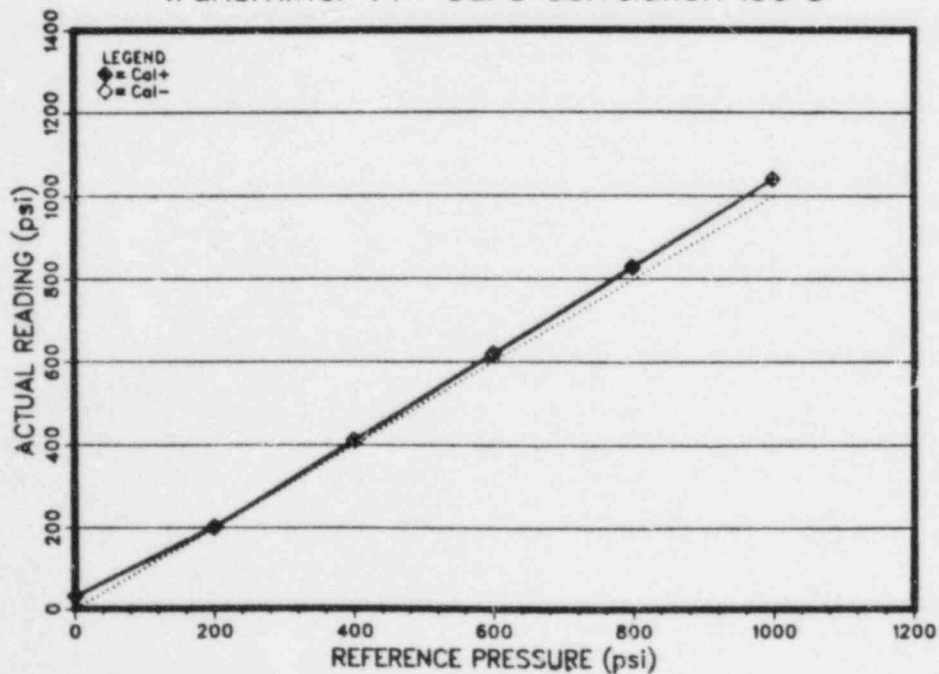


Figure T4-B-7

Transmitter T4 Cal 4 Correlation 122°C

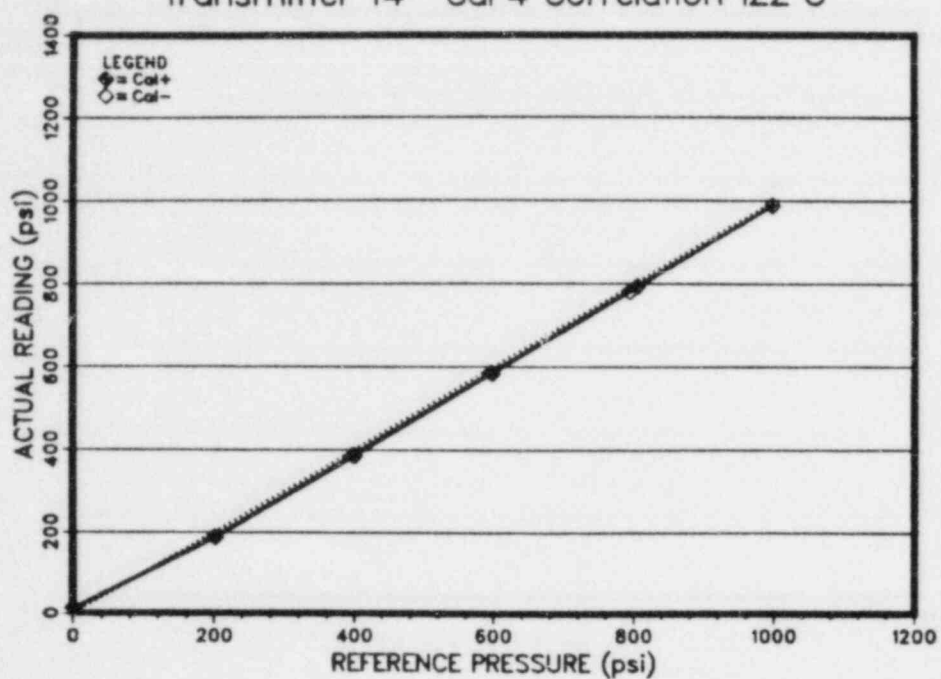


Figure T4-B-8

Transmitter T4 Cal 5 Correlation 122°C

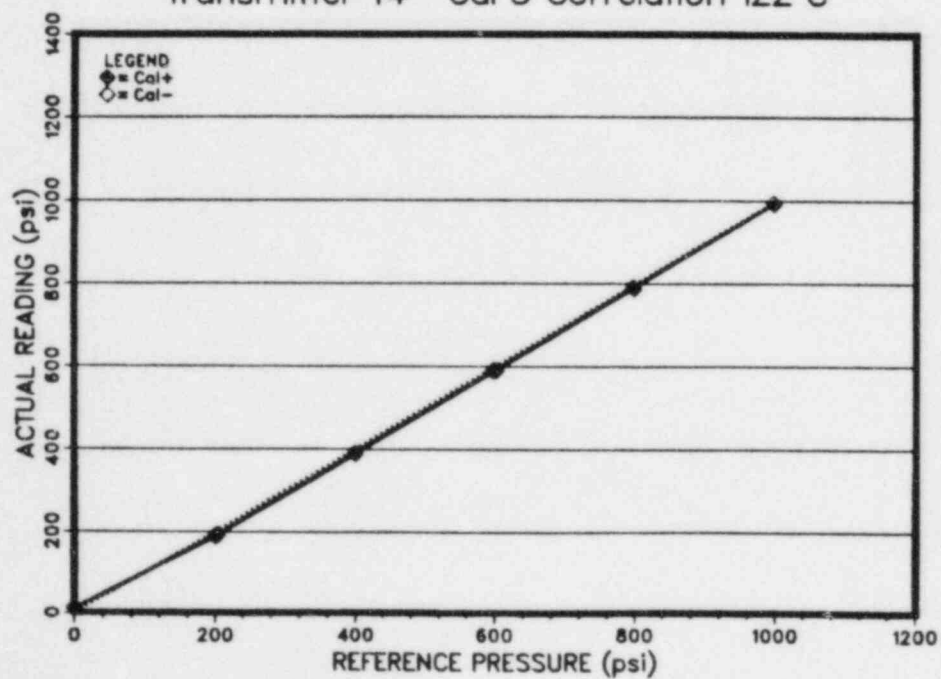


Figure T4-B-9

Transmitter T4 Cal 6 Correlation 105°C

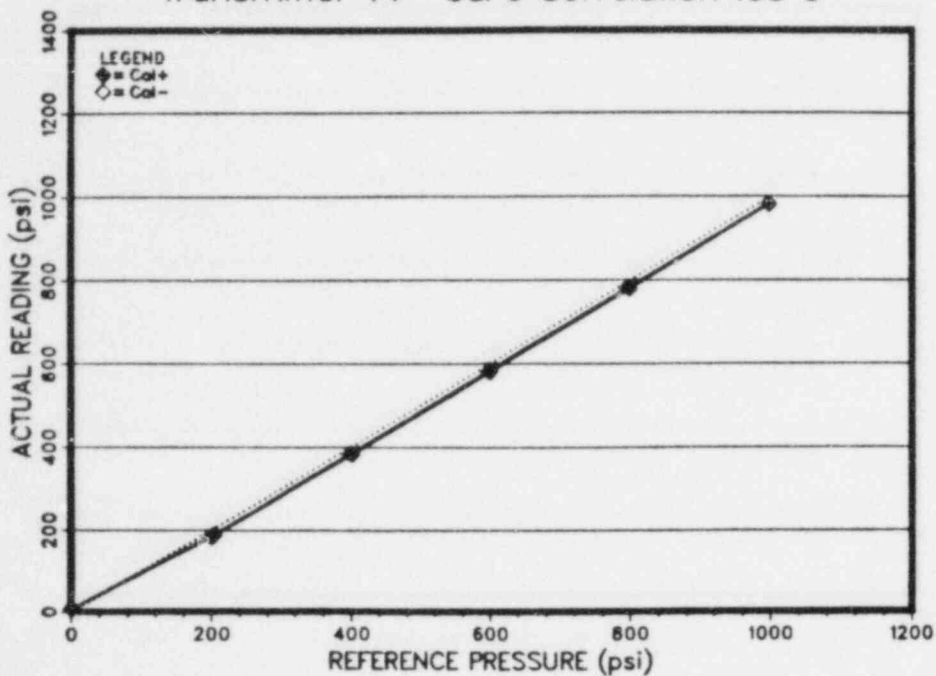


Figure T4-B-10

Transmitter T4 Cal 7 Correlation 105°C

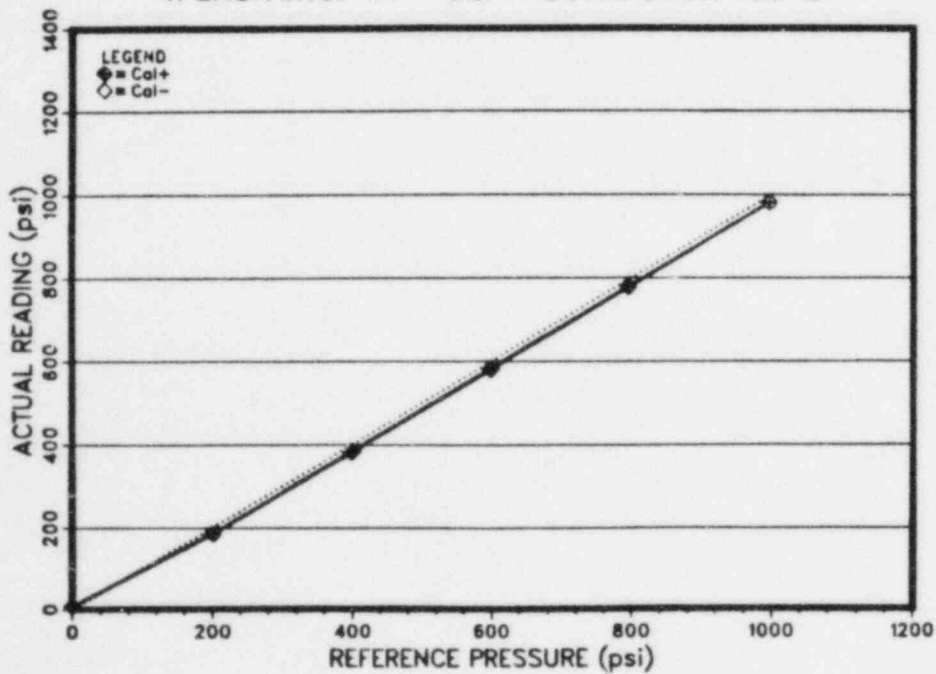


Figure T4-B-11

Transmitter T4 Cal 3 Correlation 105°C

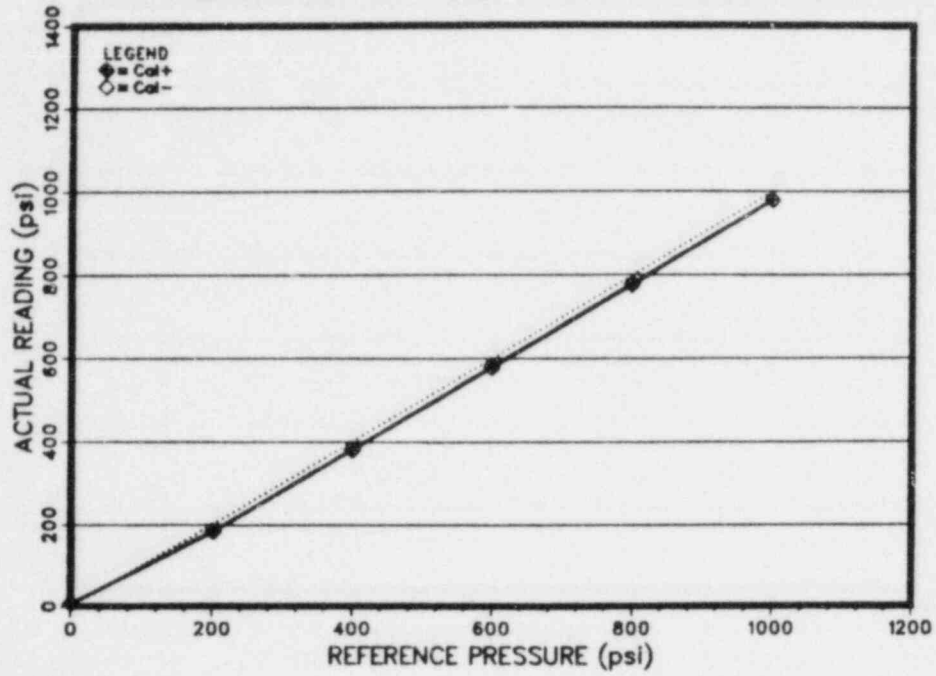


Figure T4-B-12

Transmitter T4 Cal 9 Correlation 105°C

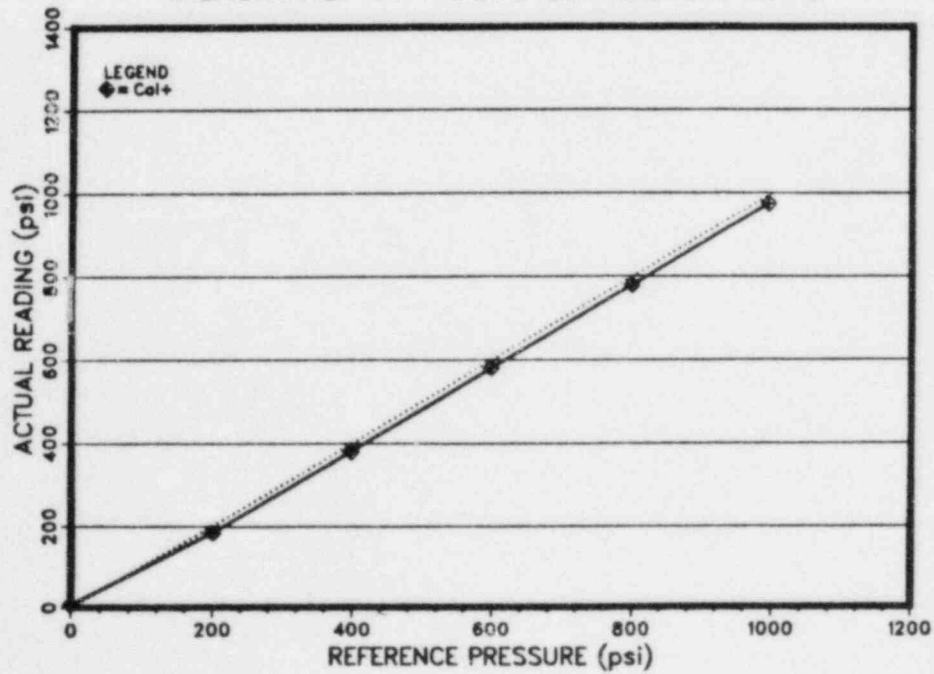


Figure T4-B-13

Trans.T4 Cal0 Pres. Sensitivity 21°C

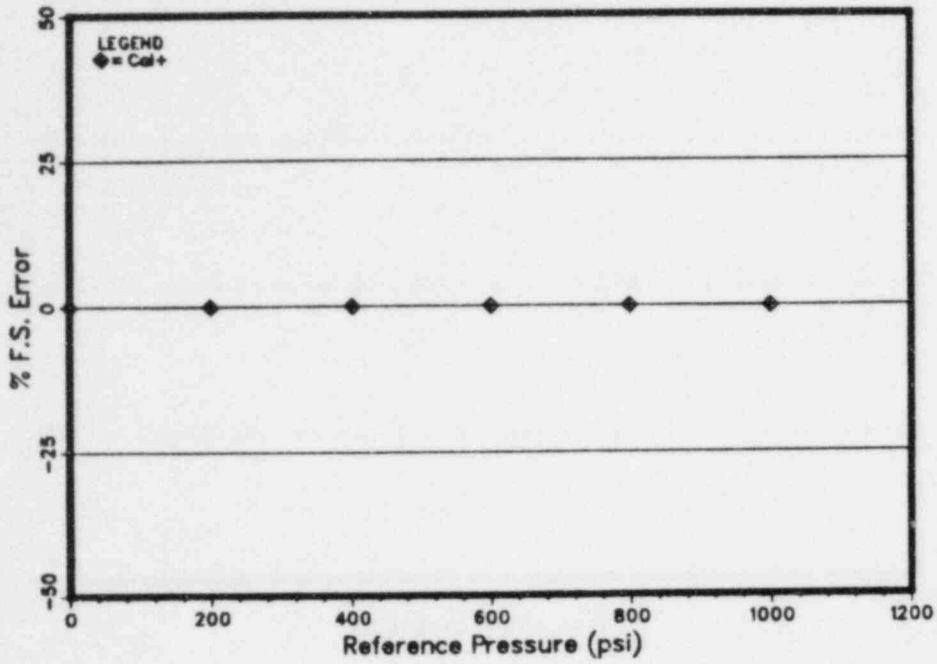


Figure T4-B-14

Trans.T4 Cal1 Pres. Sensitivity 173°C

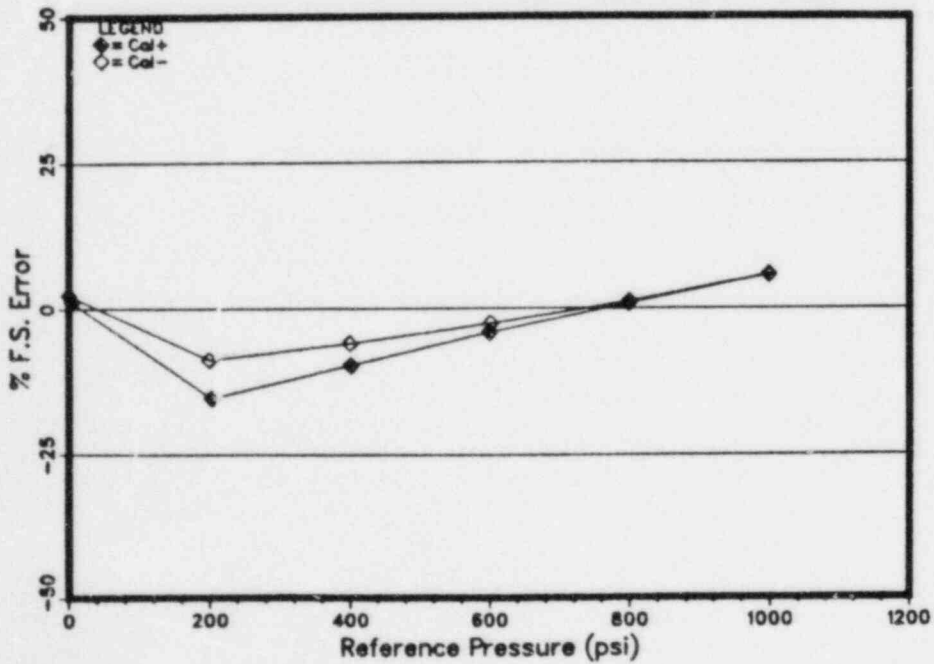


Figure T4-B-15

Trans.T4 Cal2 Pres. Sensitivity 173°C

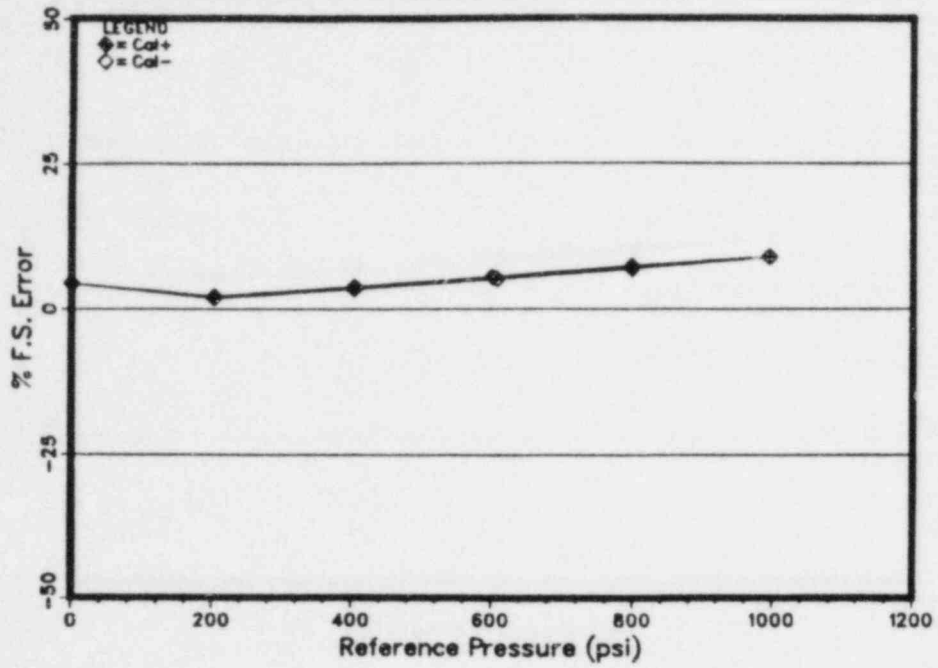


Figure T4-B-16

Trans.T4 Cal3 Pres. Sensitivity 160°C

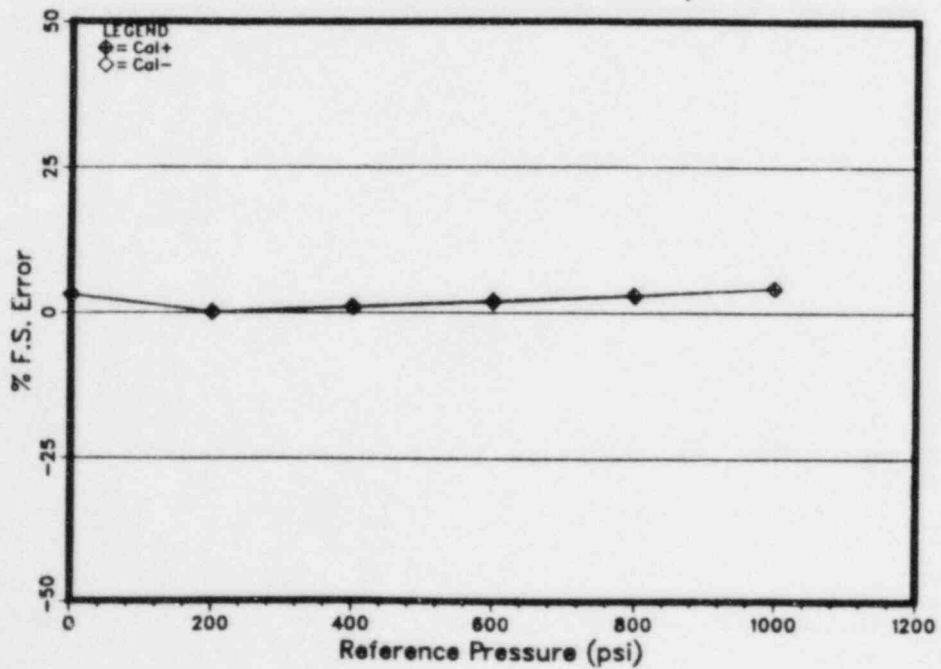


Figure T4-B-17

Trans.T4 Cal4 Pres. Sensitivity 122°C

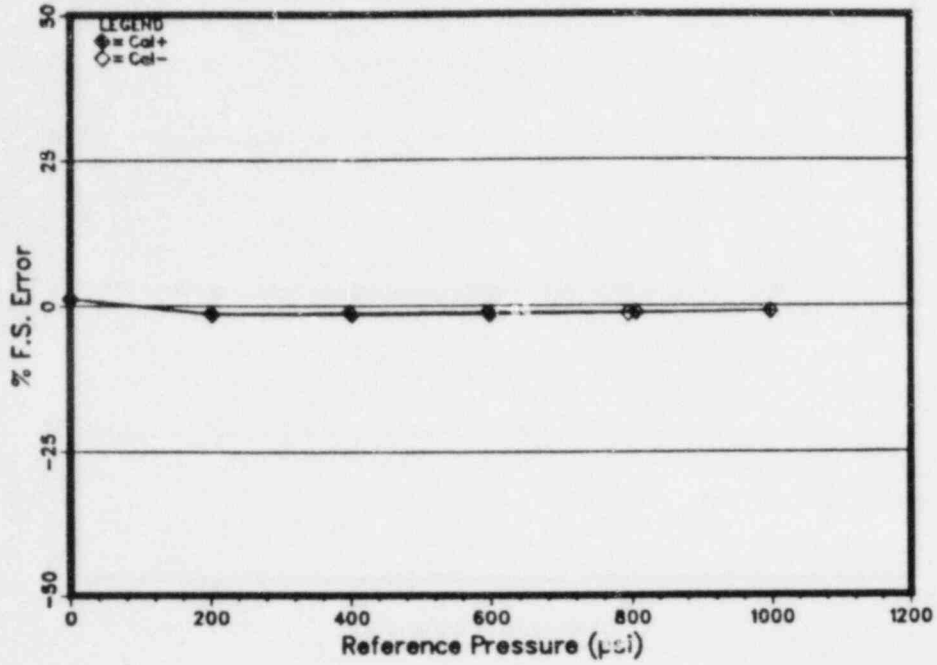


Figure T4-B-18

Trans.T4 Cal5 Pres. Sensitivity 122°C

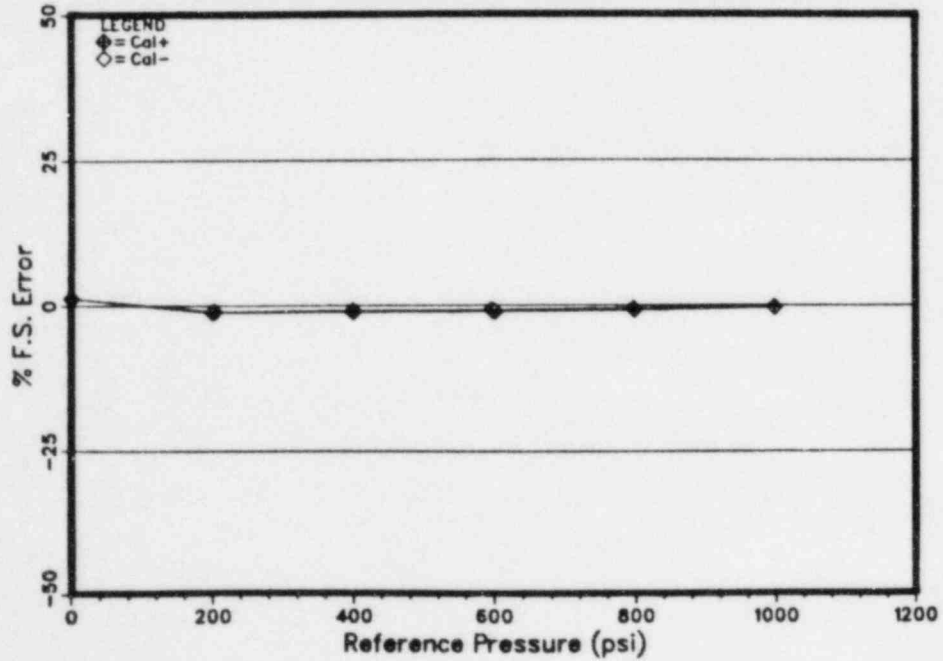


Figure T4-B-19

Trans.T4 Cal6 Pres. Sensitivity 105°C

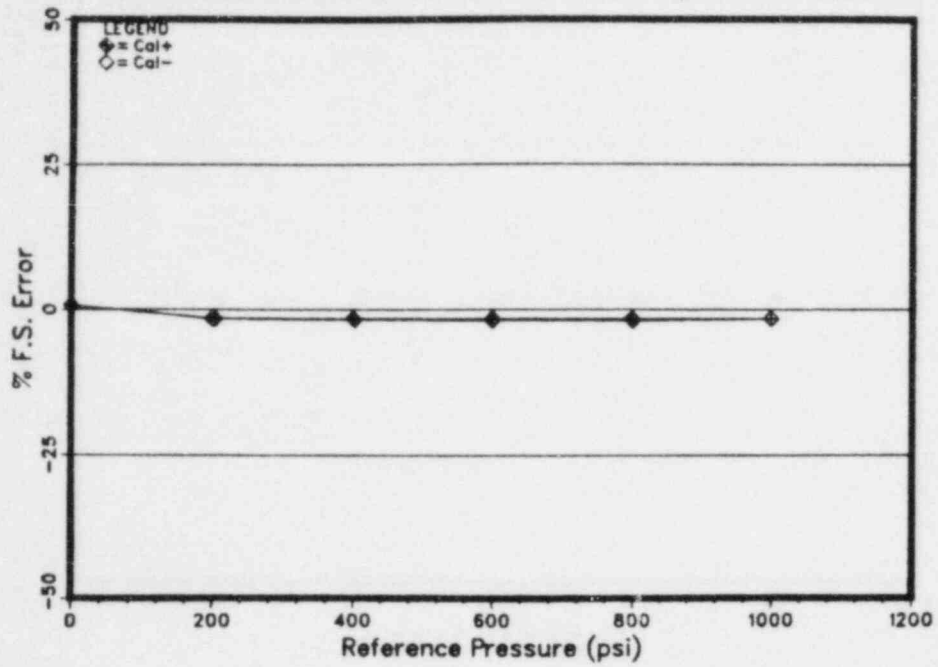


Figure T4-B-20

Trans.T4 Cal7 Pres. Sensitivity 105°C

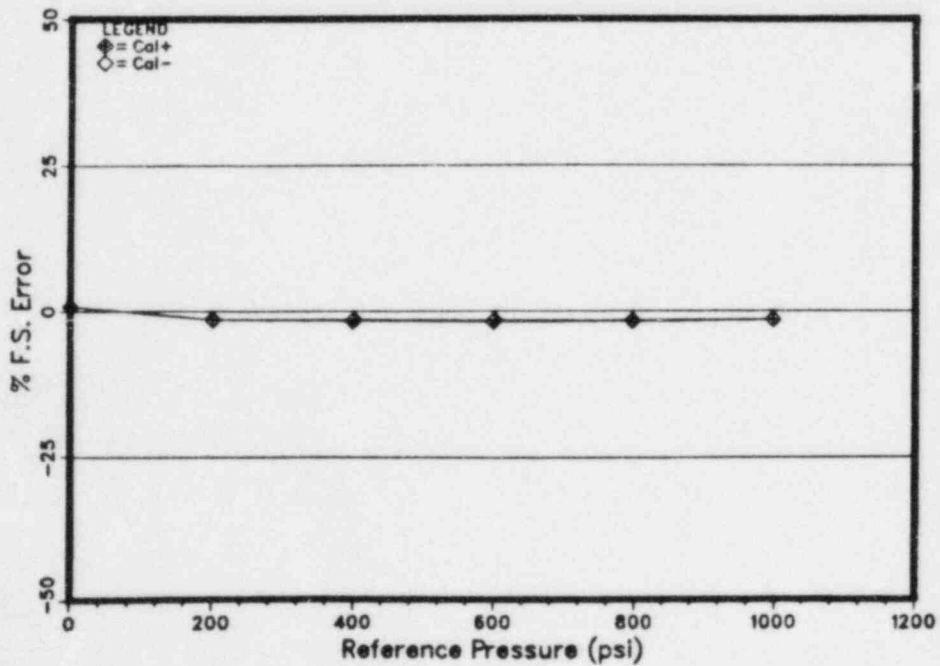


Figure T4-B-21

Trans.T4 Cal8 Pres. Sensitivity 105°C

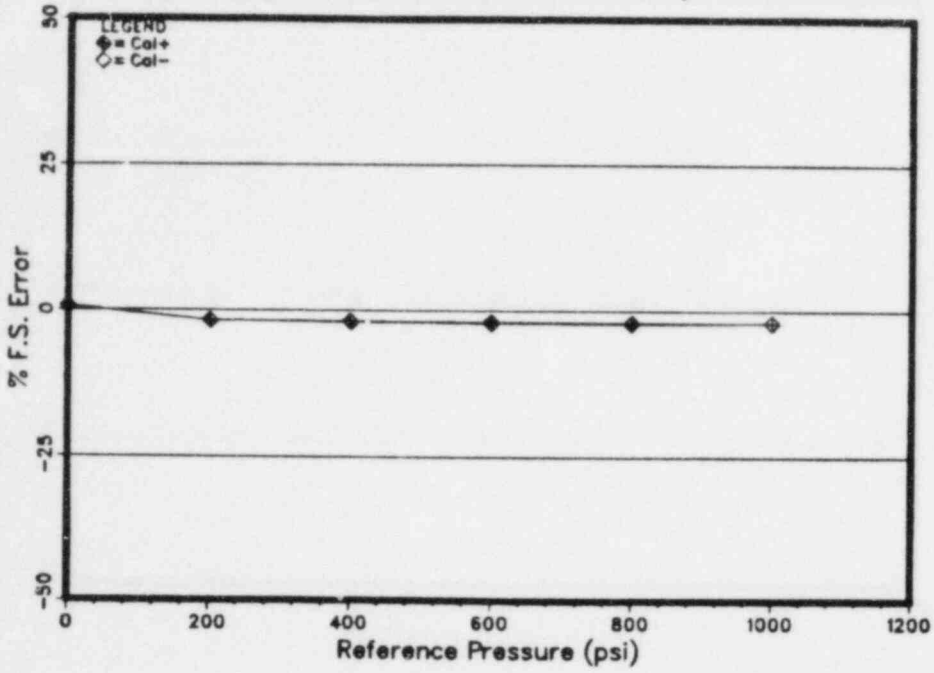


Figure T4-B-22

Trans.T4 Cal9 Pres. Sensitivity 105°C

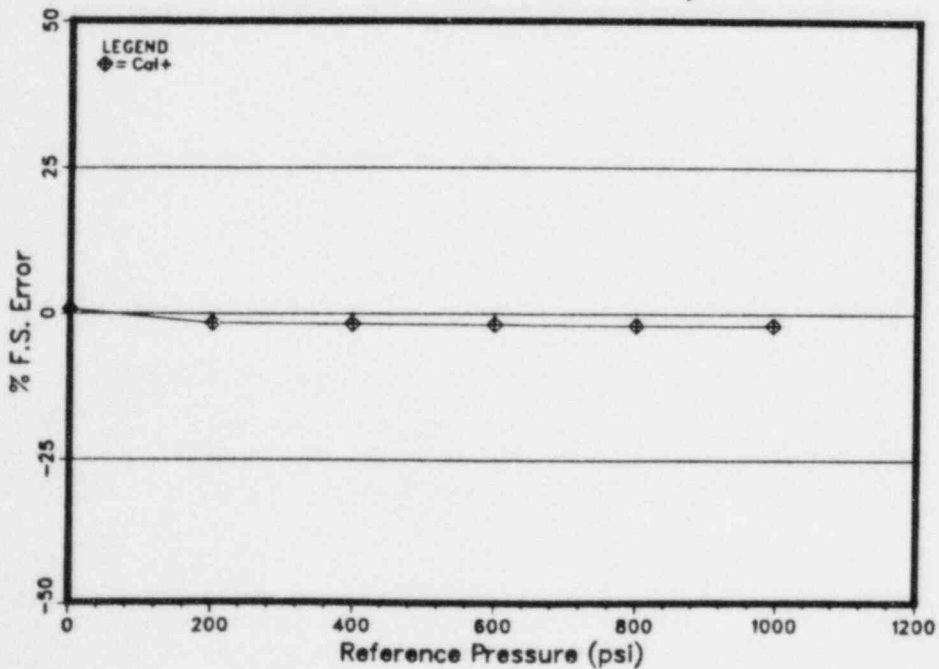


Figure T4-B-23

Trans. T4 Calibration Temperature Profile

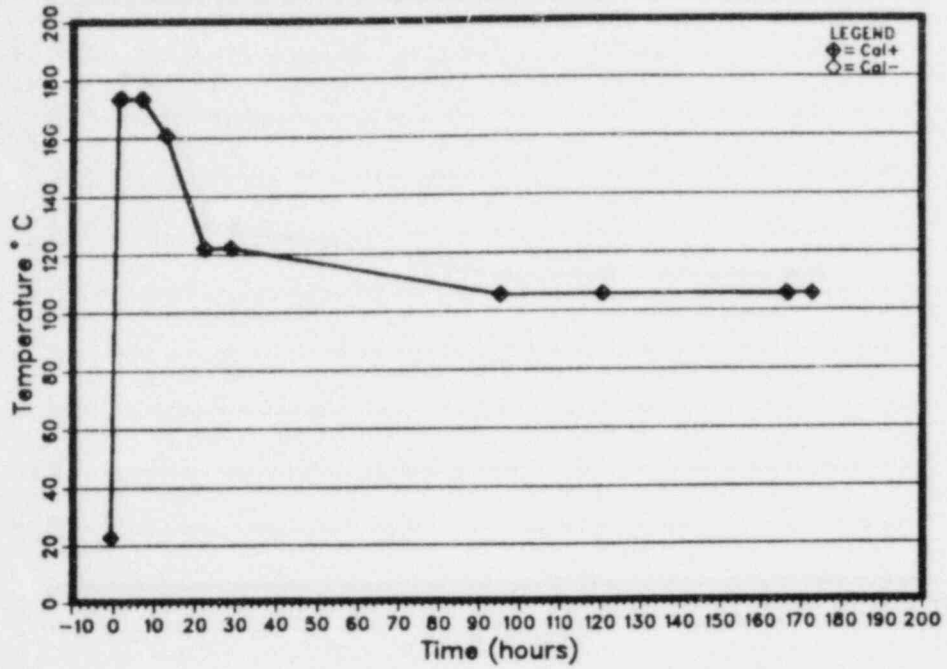


Figure T4-B-24

Transmitter T4 0 psi Calibration Stability

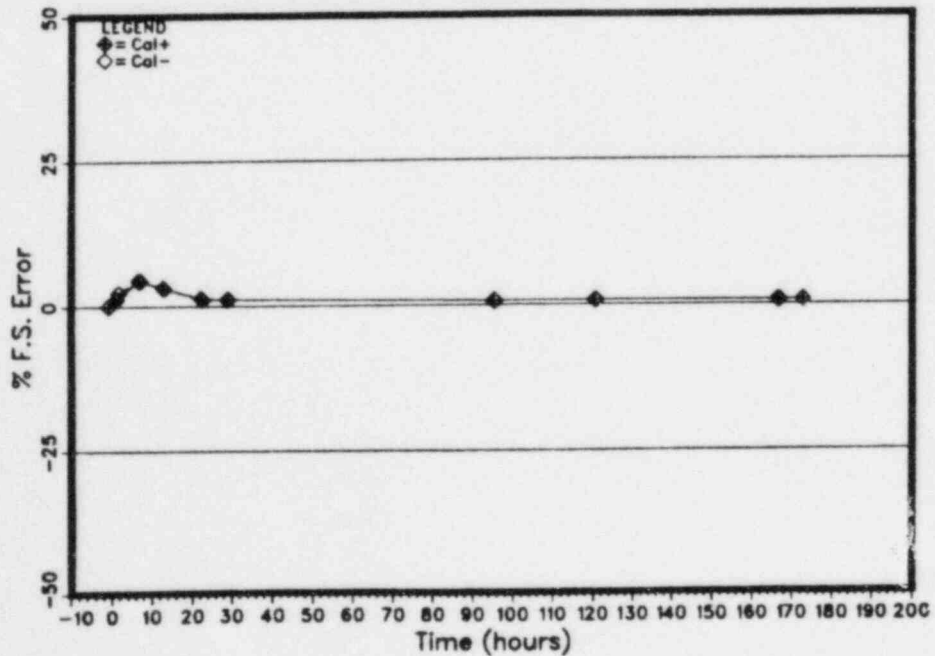


Figure T4-B-25

Transmitter T4 200 psi Calibration Stability

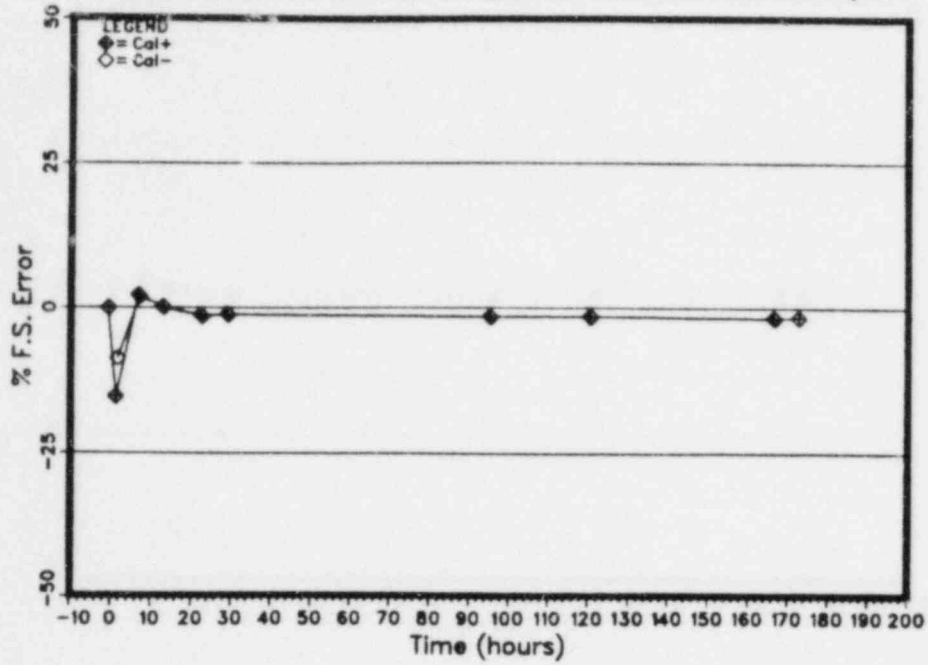


Figure T4-B-26

Transmitter T4 400 psi Calibration Stability

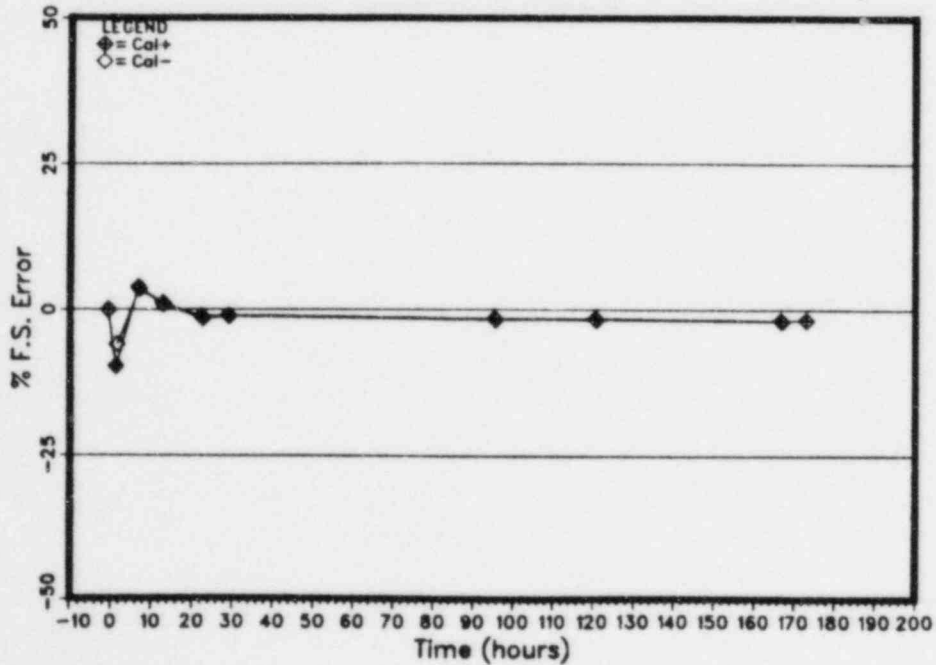


Figure T4-B-27

Transmitter T4 600 psi Calibration Stability

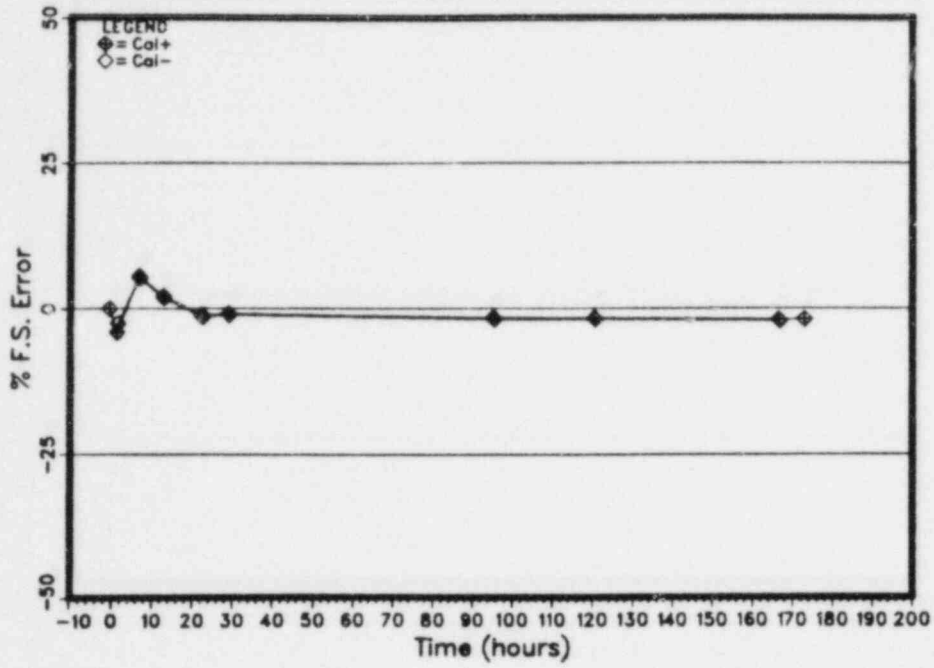


Figure T4-B-28

Transmitter T4 800 psi Calibration Stability

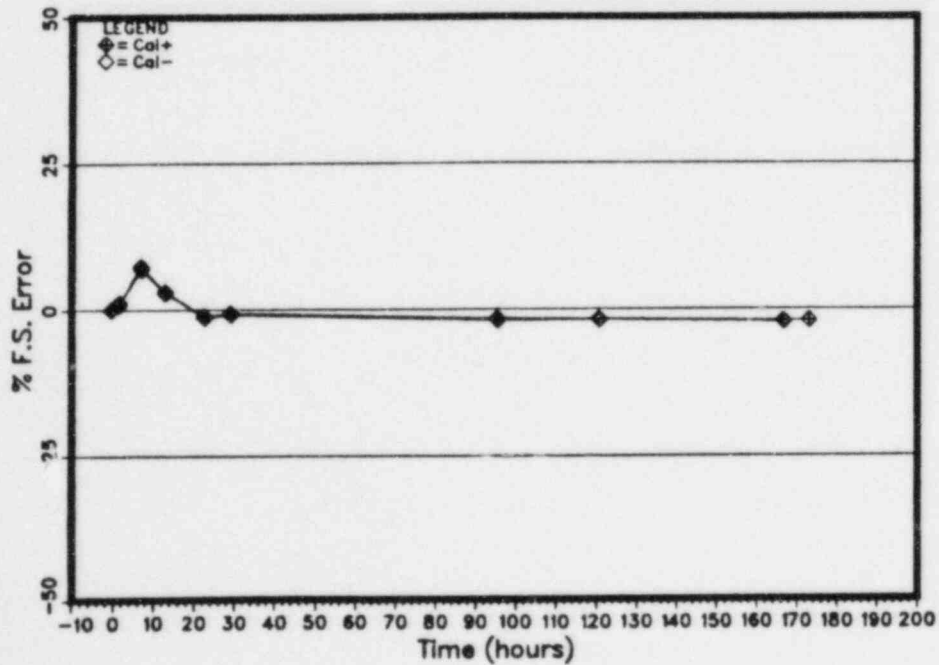


Figure T4-B-29

Transmitter T4 1000 psi Calibration Stability

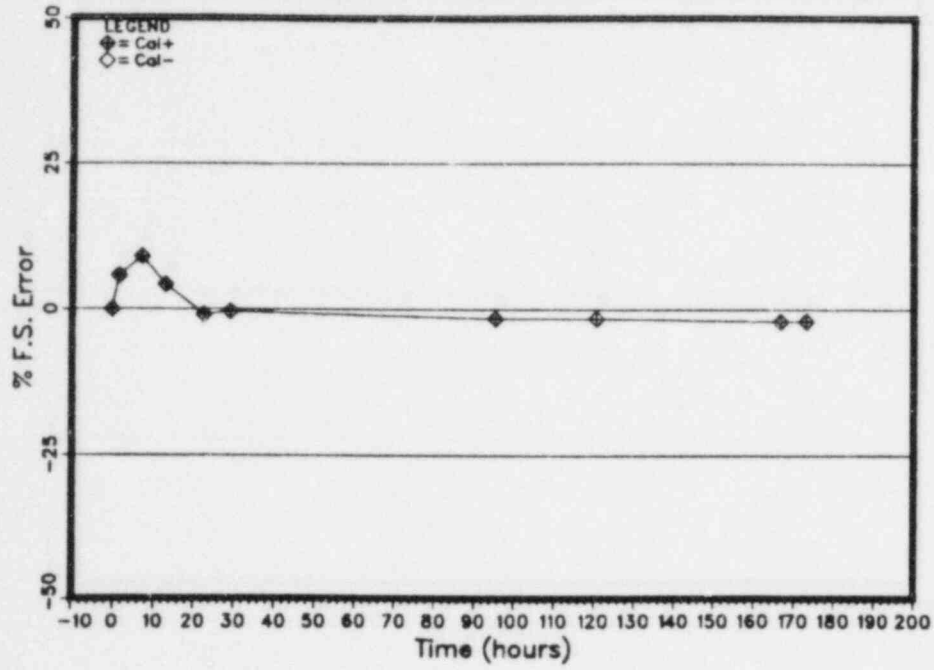


Figure T5-B-1  
 Transmitter T5 %F.S. Error Data Scatter

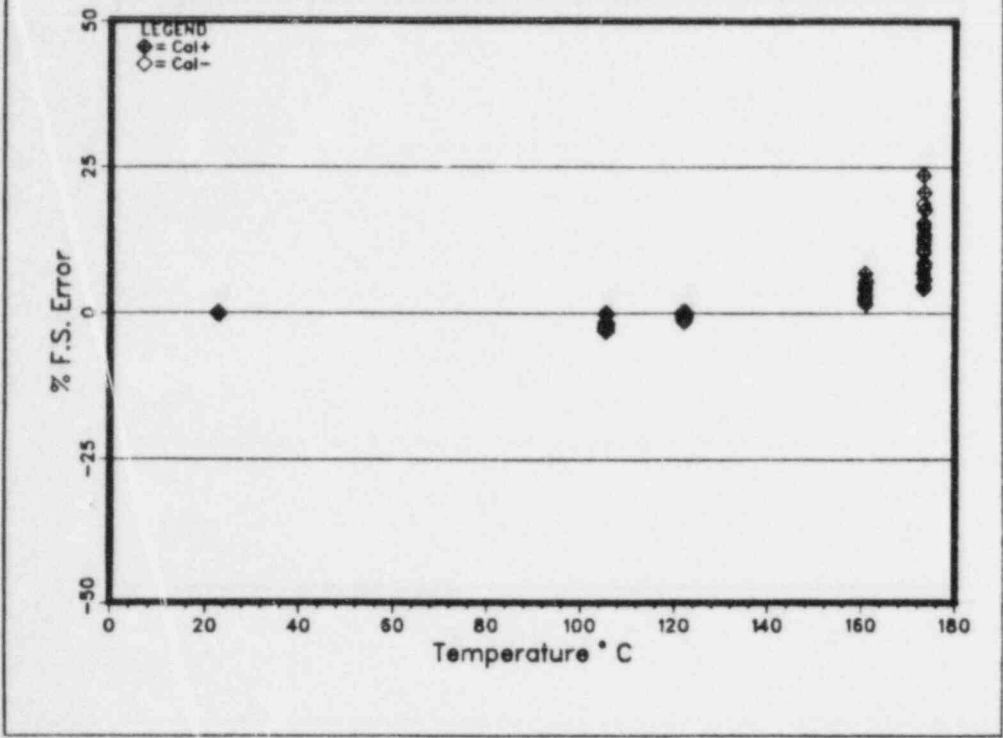


Figure T5-B-2  
 Transmitter T5 Correlation Scatter, Cal+

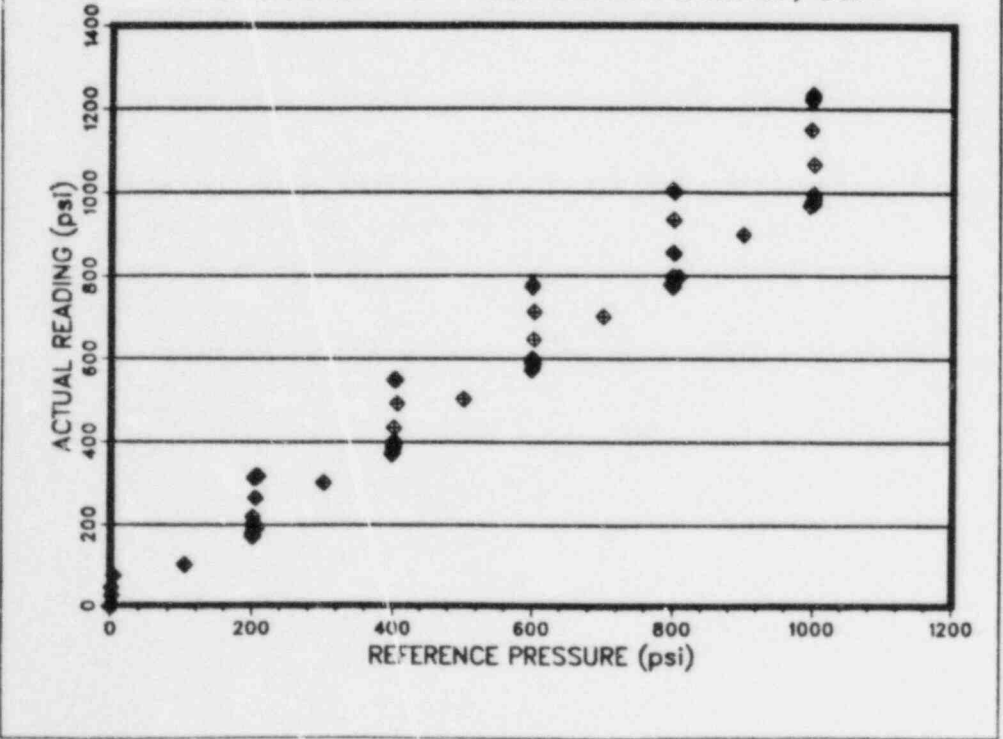


Figure T5-B-3

Transmitter T5 Cal 0 Correlation 21°C

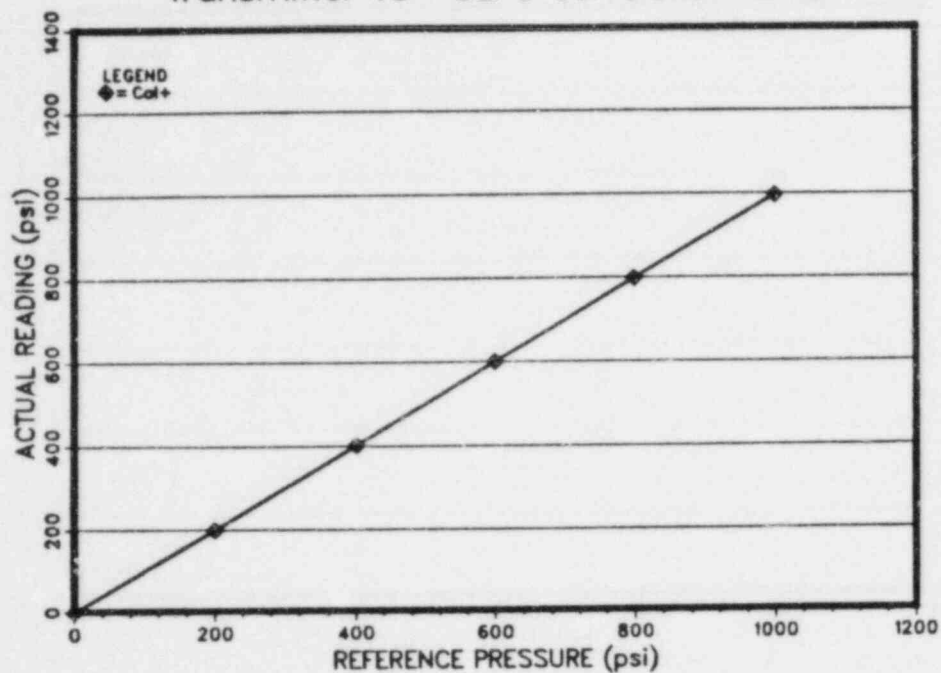


Figure T5-B-4

Transmitter T5 Cal 1 Correlation 173°C

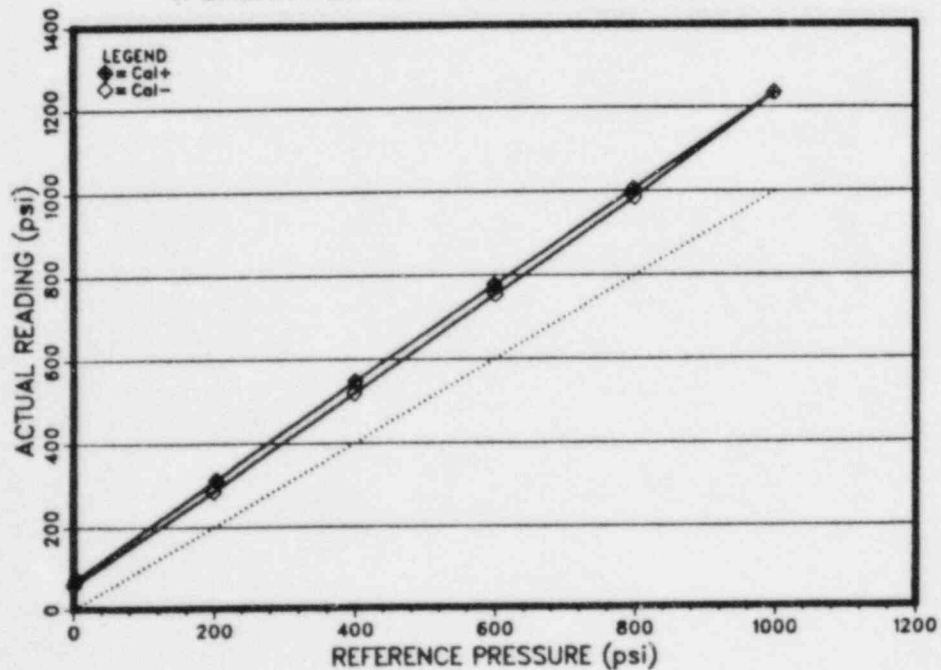


Figure T5-B-5

Transmitter T5 Cal 2 Correlation 173°C

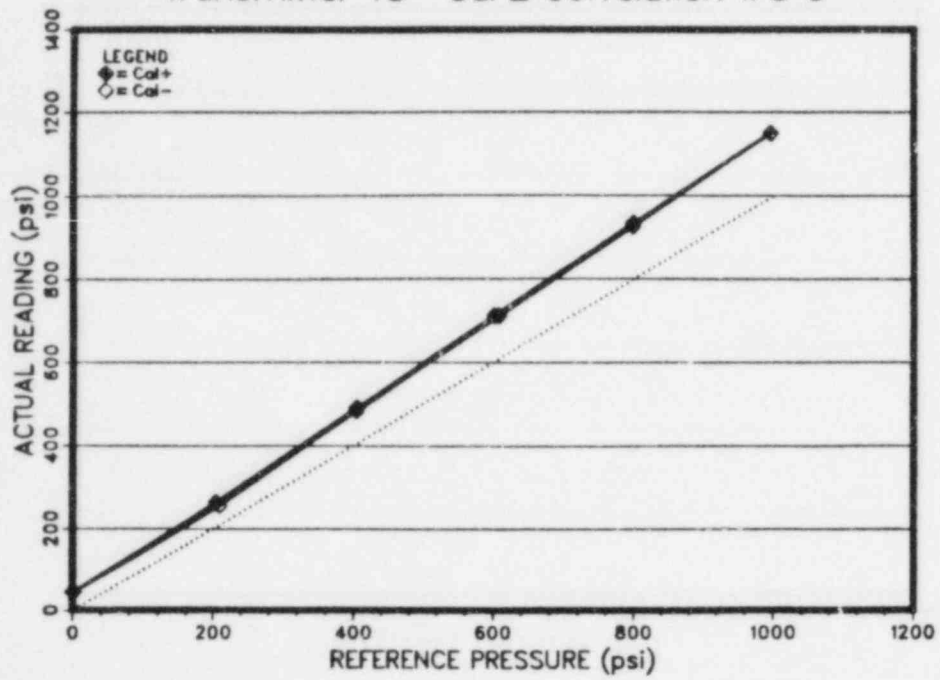


Figure T5-B-6

Transmitter T5 Cal 3 Correlation 160°C

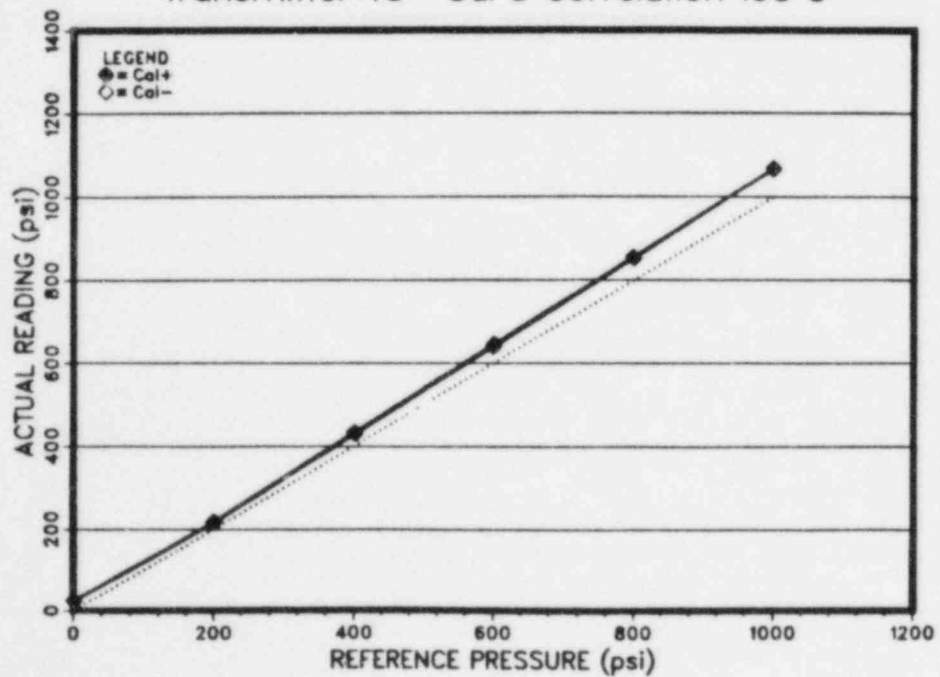


Figure T5-B-7

Transmitter T5 Cal 4 Correlation 122°C

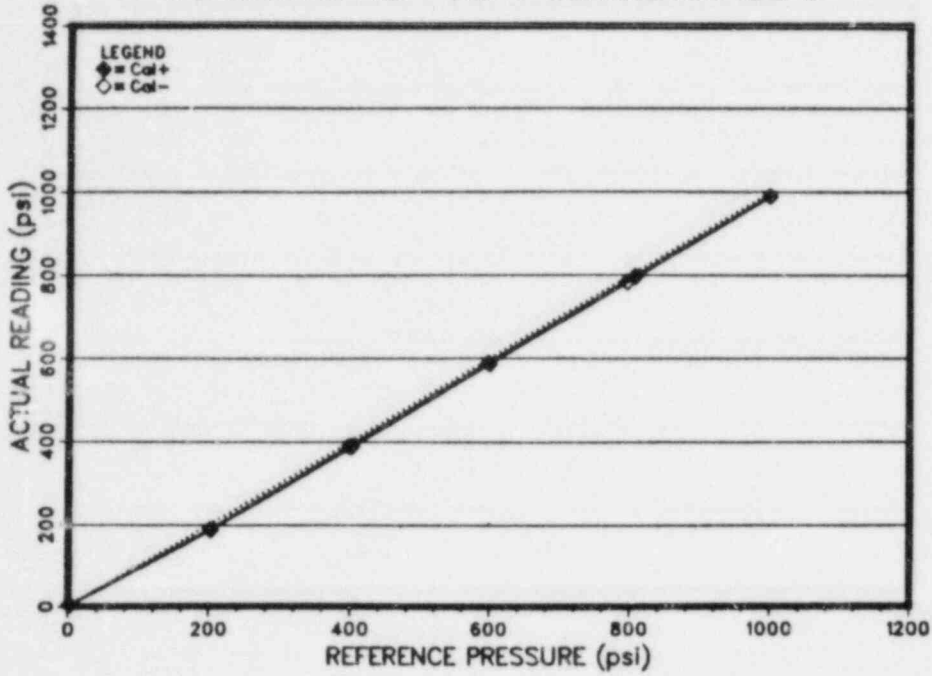


Figure T5-B-8

Transmitter T5 Cal 5 Correlation 122°C

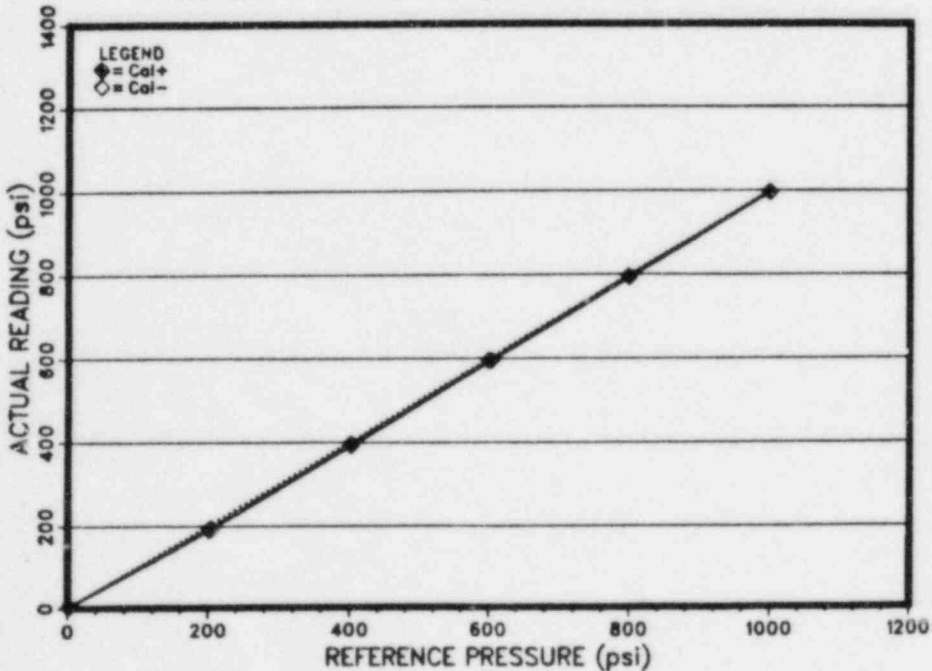


Figure T5-B-9

Transmitter T5 Cal 6 Correlation 105°C

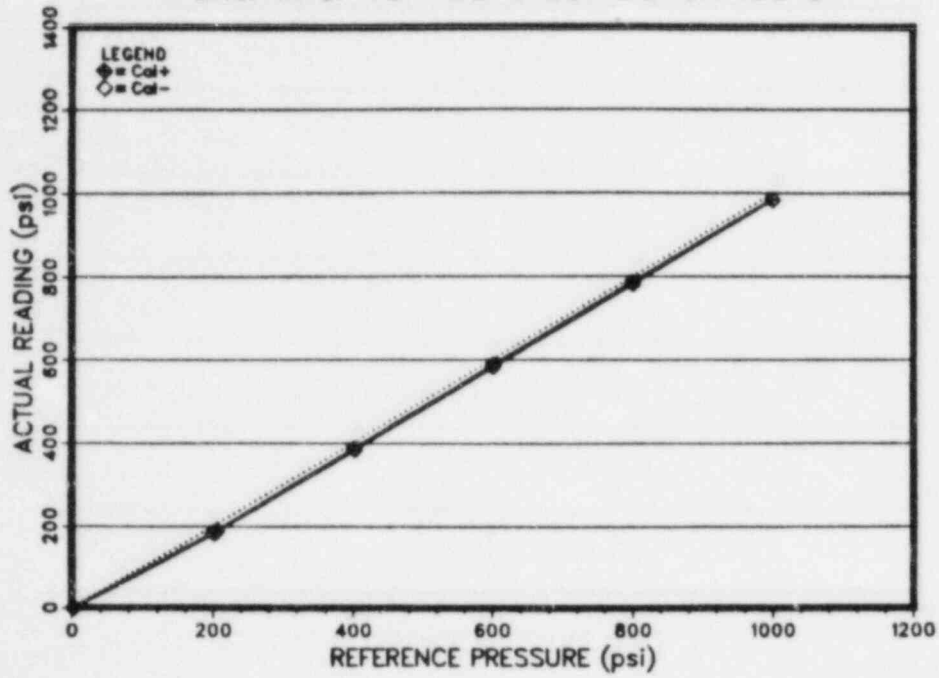


Figure T5-B-10

Transmitter T5 Cal 7 Correlation 105°C

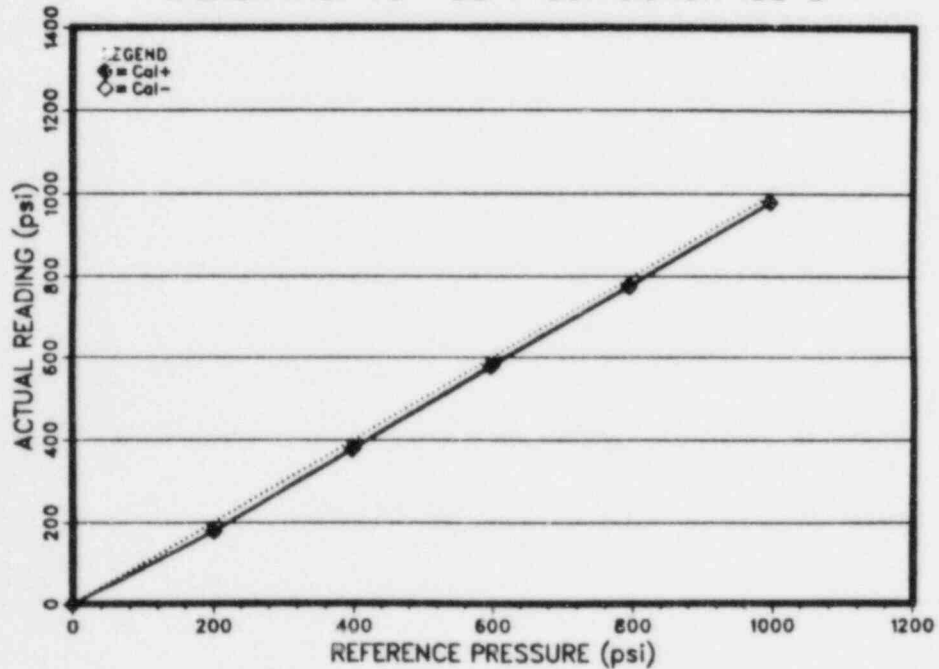


Figure T5-B-11

Transmitter T5 Cal 8 Correlation 105°C

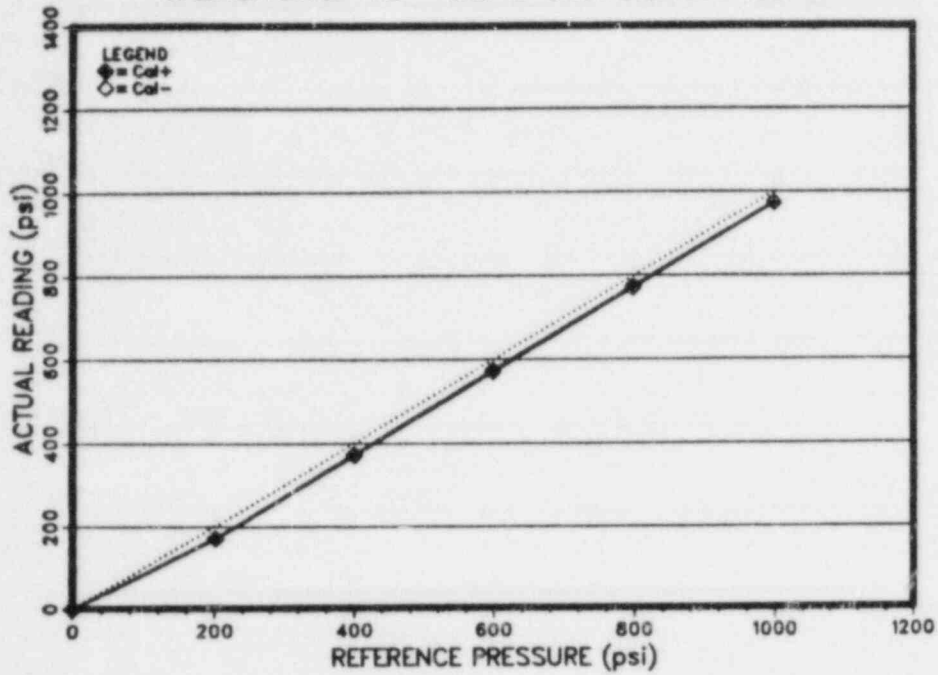


Figure T5-B-12

Transmitter T5 Cal 9 Correlation 105°C

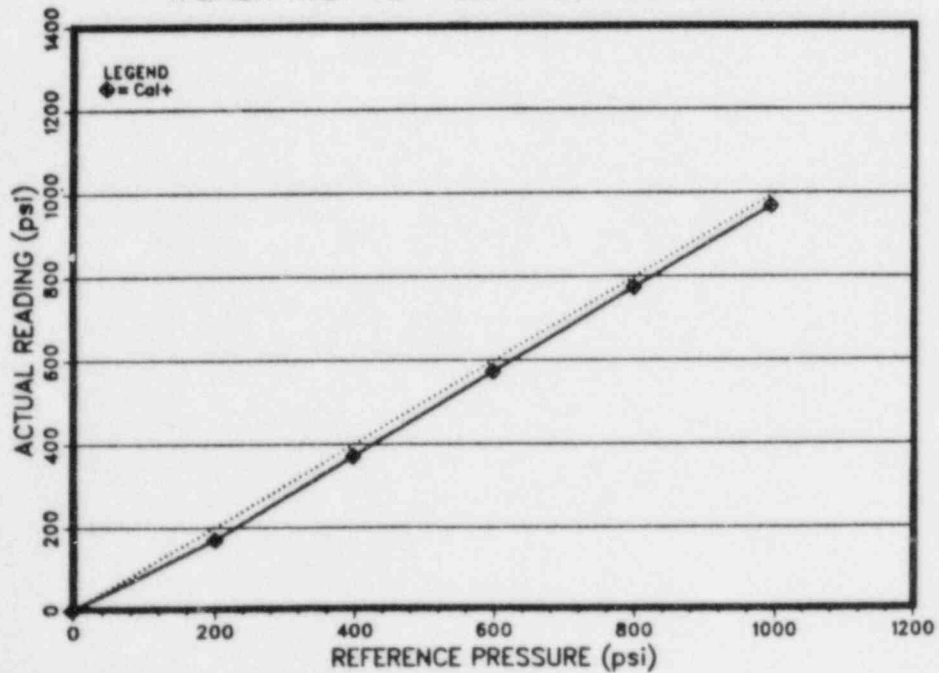


Figure T5-B-13

Trans.T5 Cal0 Pres. Sensitivity 21°C

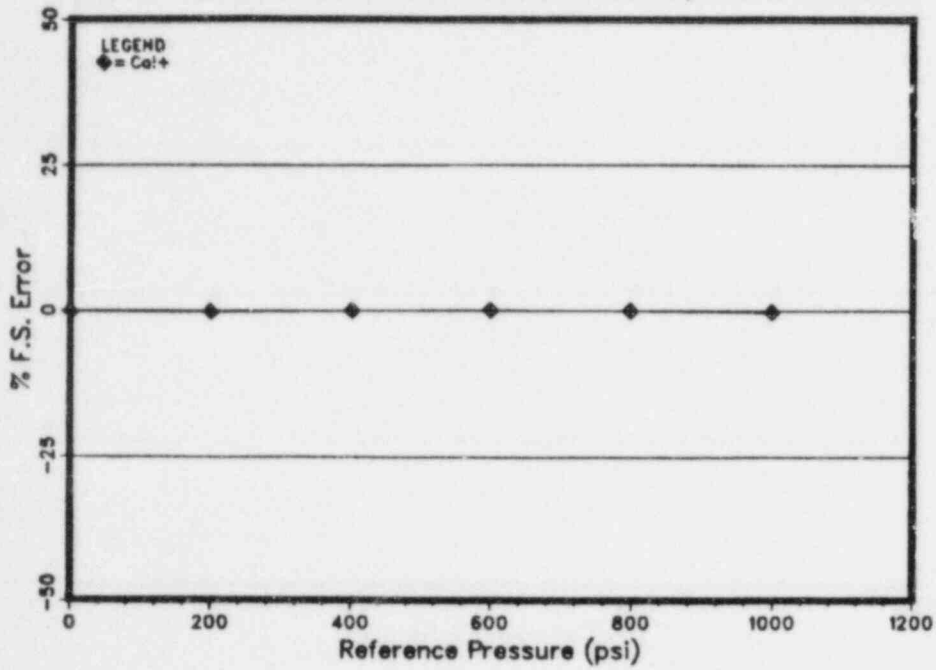


Figure T5-B-14

Trans.T5 Cal1 Pres. Sensitivity 173°C

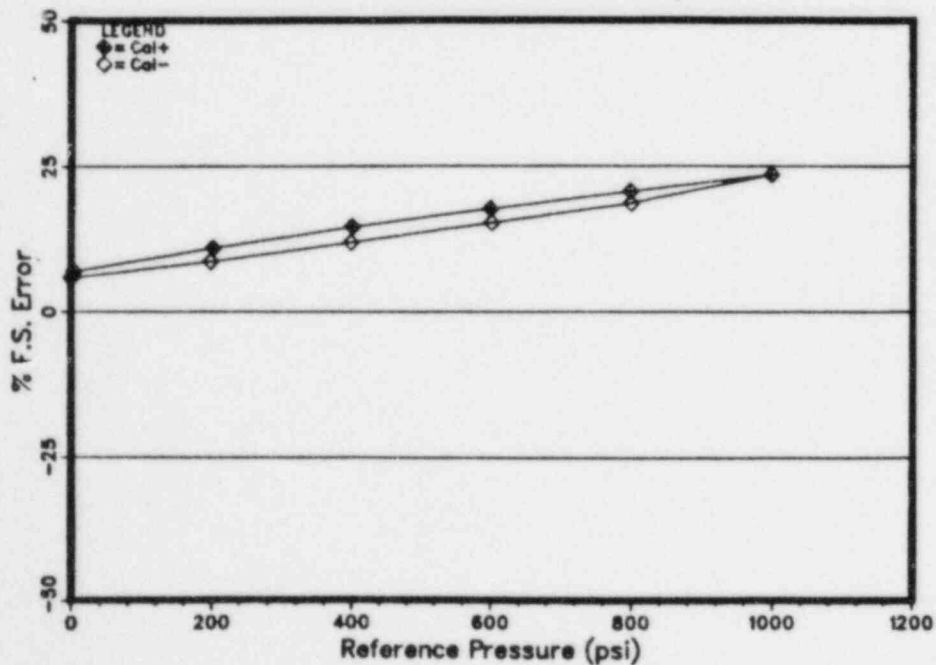


Figure T5-B-15

Trans.T5 Cal2 Pres. Sensitivity 173°C

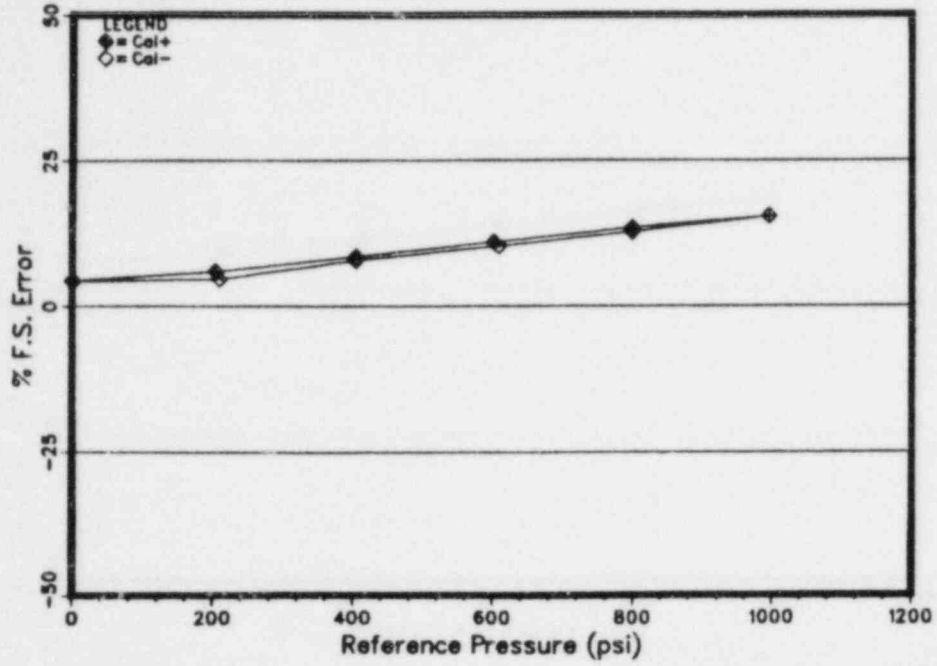


Figure T5-B-16

Trans.T5 Cal3 Pres. Sensitivity 160°C

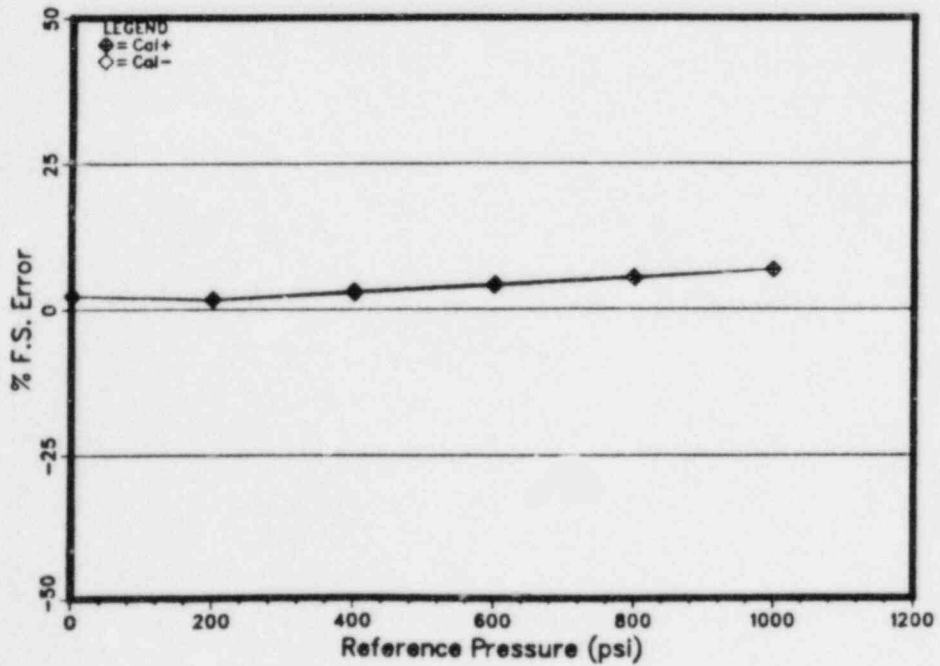


Figure T5-B-17

Trans.T5 Cal4 Pres. Sensitivity 122°C

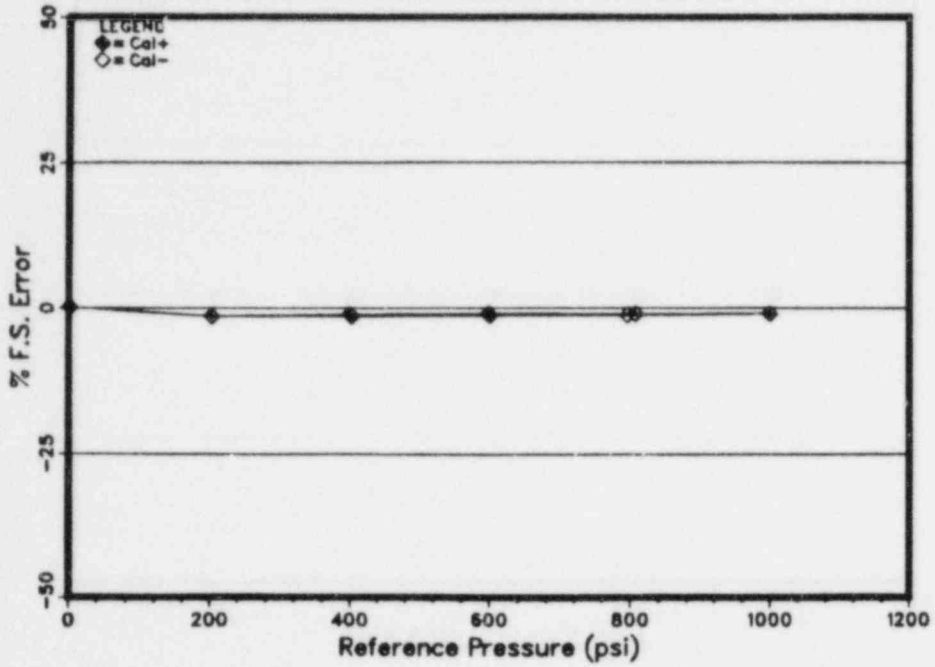


Figure T5-B-18

Trans.T5 Cal5 Pres. Sensitivity 122°C

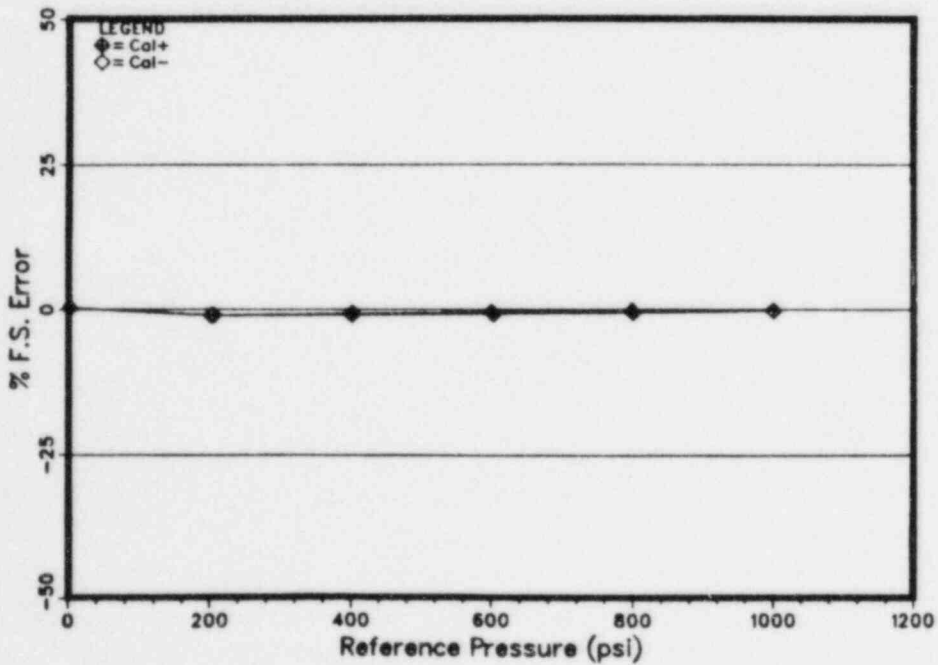


Figure T5-B-19

Trans.T5 Cal6 Pres. Sensitivity 105°C

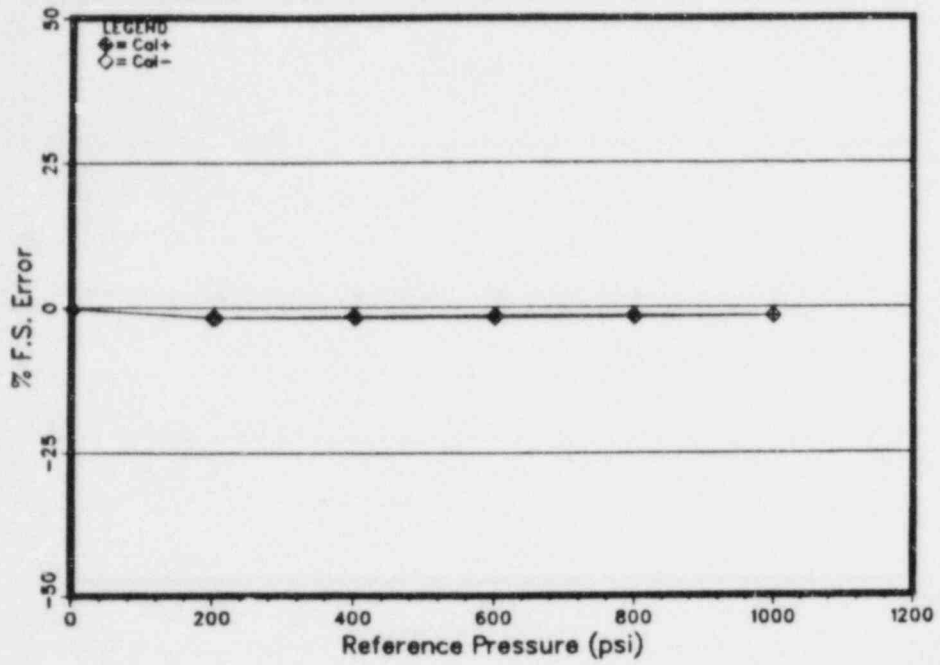


Figure T5-B-20

Trans.T5 Cal7 Pres. Sensitivity 105°C

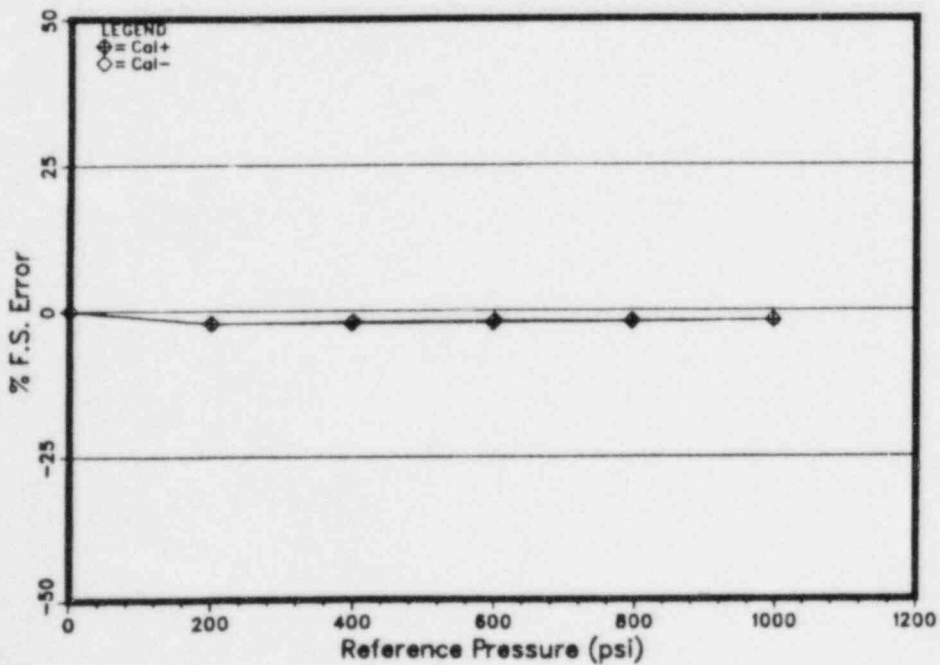


Figure T5-B-21

Trans.T5 Cal8 Pres. Sensitivity 105°C

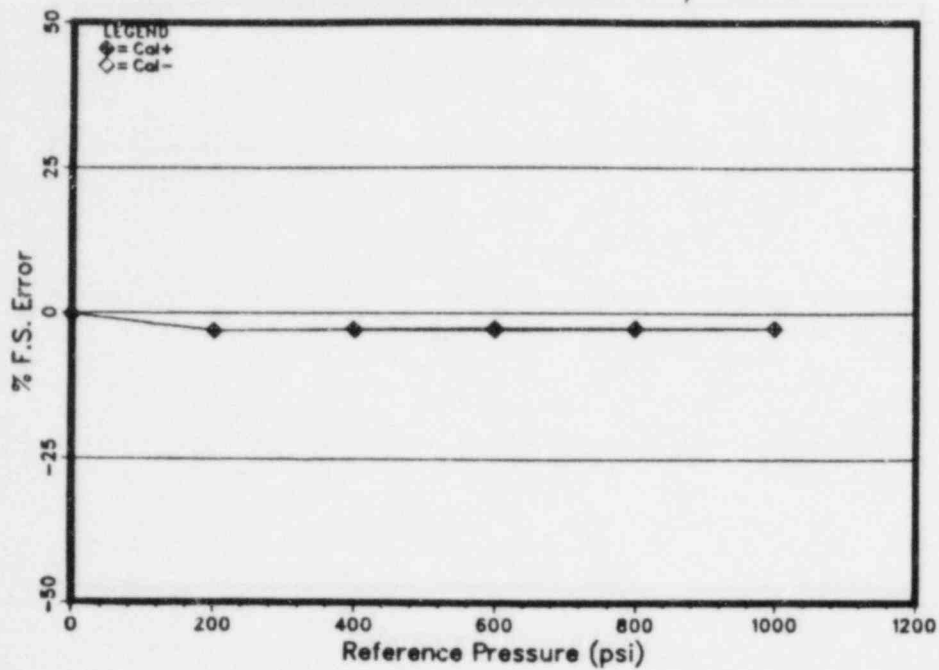


Figure T5-B-22

Trans.T5 Cal9 Pres. Sensitivity 105°C

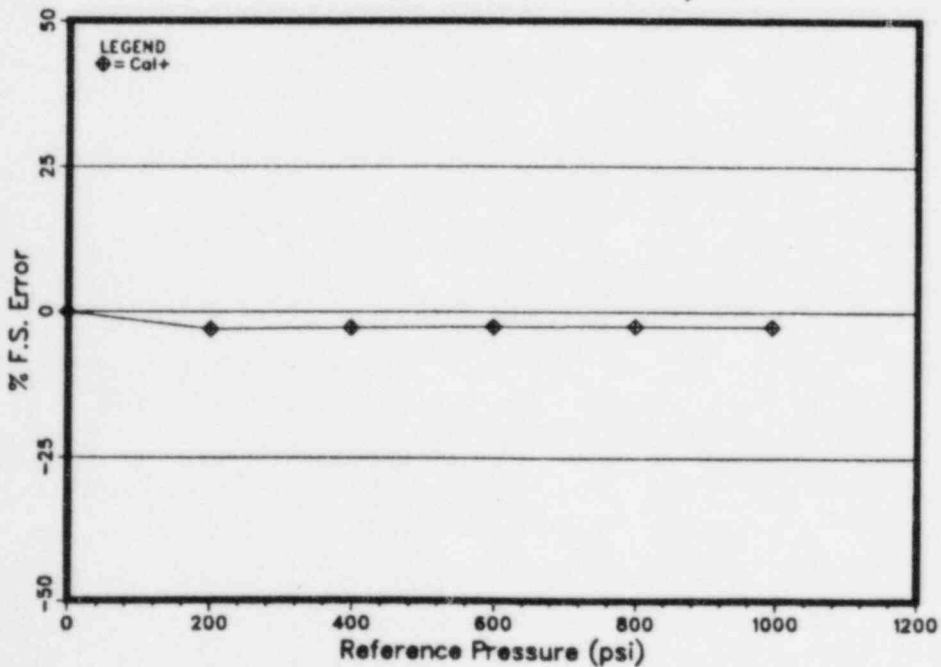


Figure T5-B-23

Trans. T5 Calibration Temperature Profile

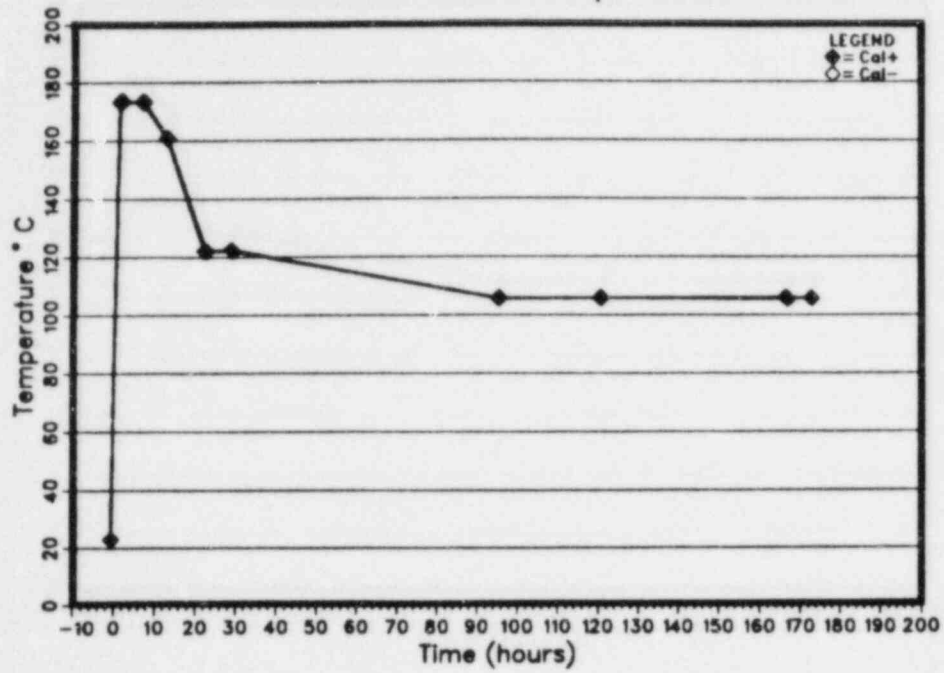


Figure T5-B-24

Transmitter T5 0 psi Calibration Stability

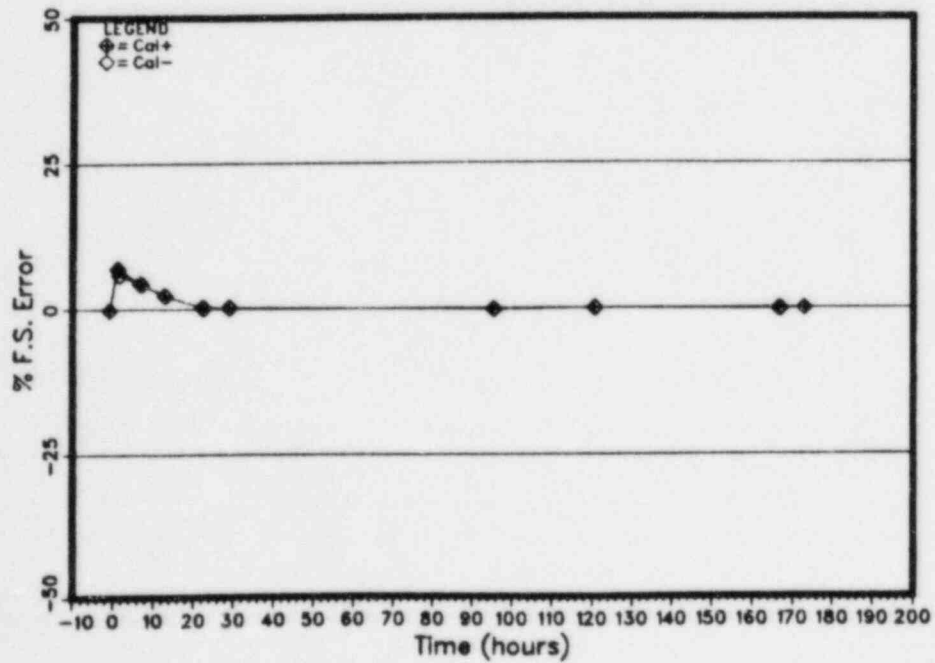


Figure T5-B-25

Transmitter T5 200 psi Calibration Stability

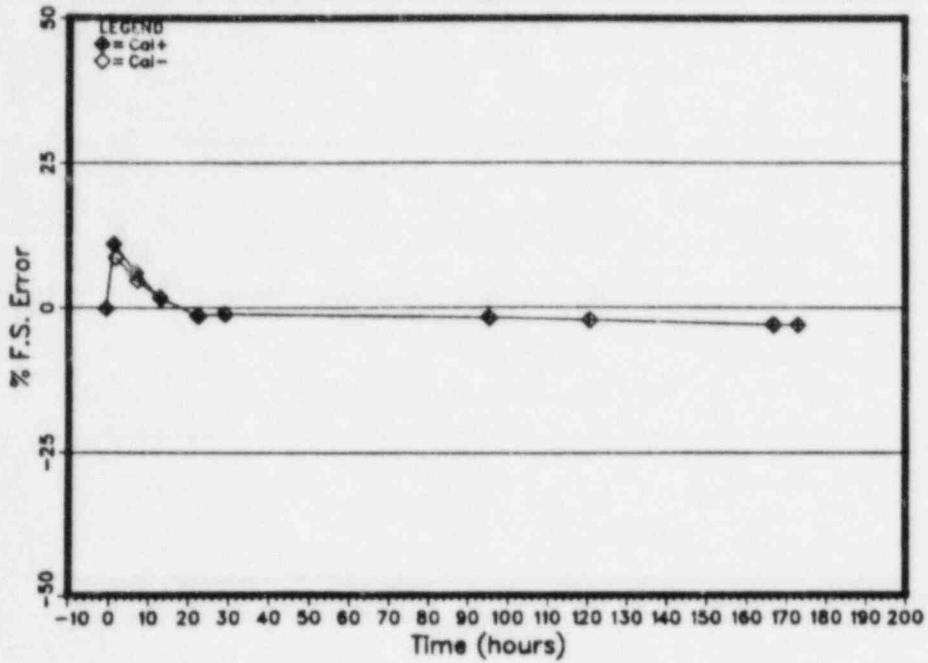


Figure T5-B-26

Transmitter T5 400 psi Calibration Stability

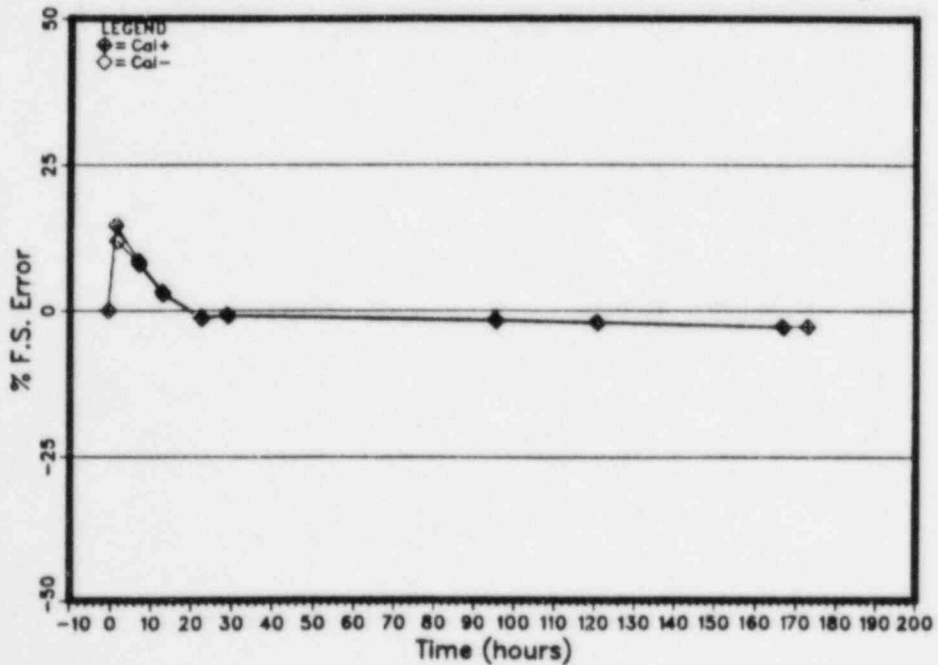


Figure T5-B-27

Transmitter T5 600 psi Calibration Stability

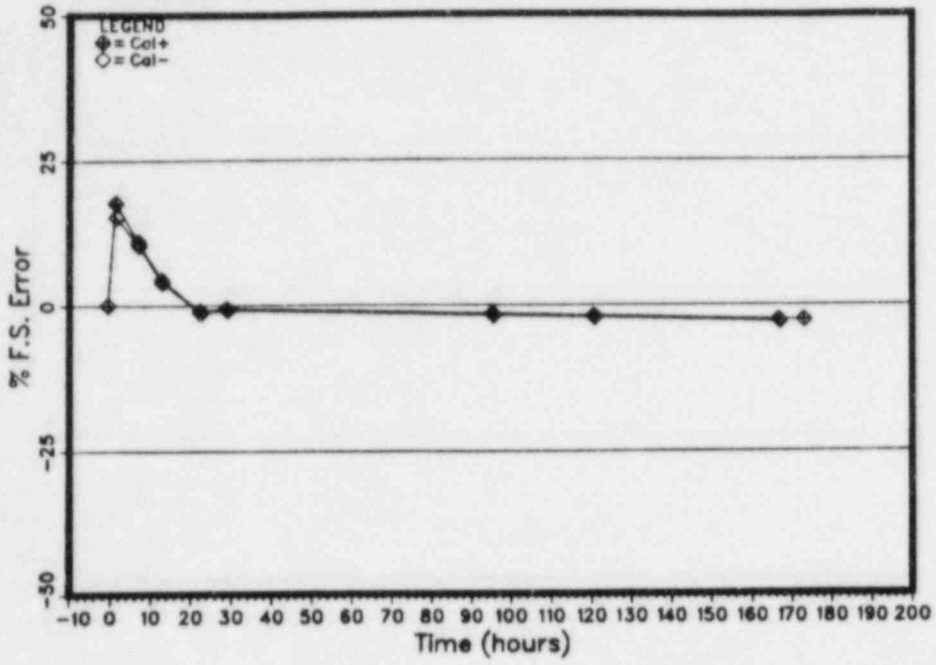


Figure T5-B-28

Transmitter T5 800 psi Calibration Stability

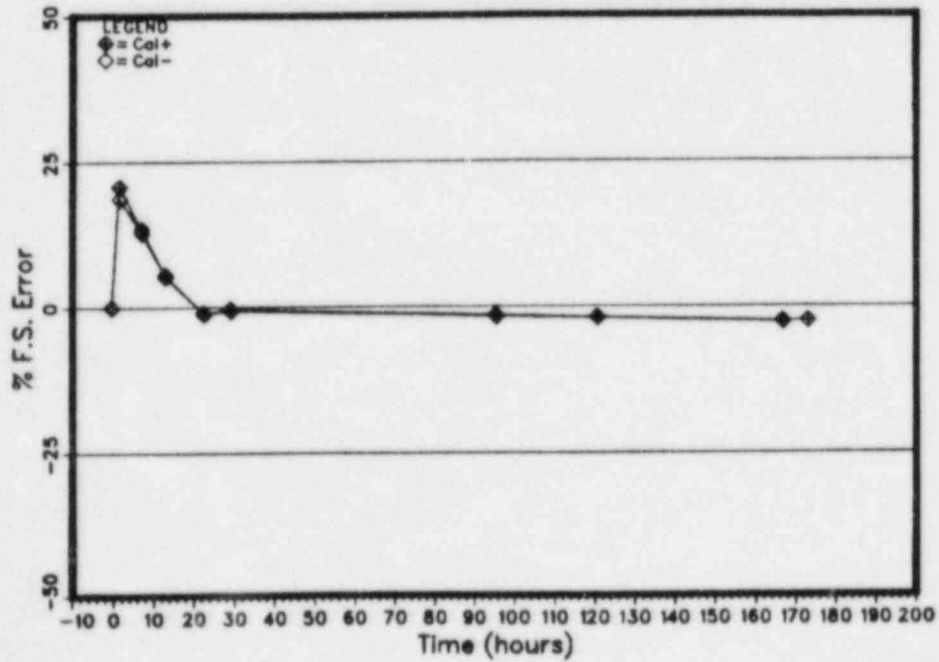
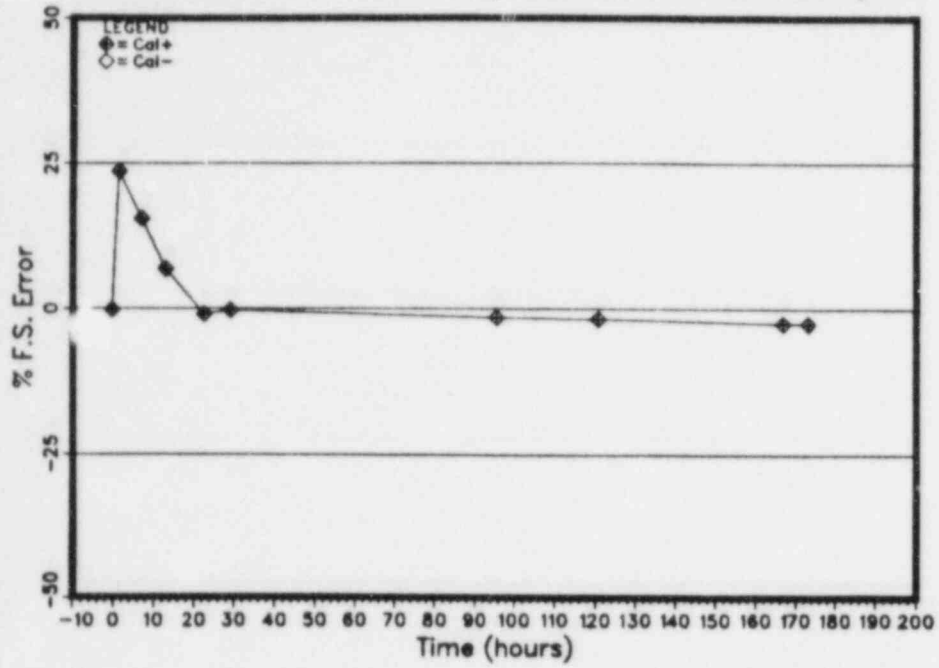


Figure T5-B-29

Transmitter T5 1000 psi Calibration Stability



DISTRIBUTION

Division of Technical Information  
and Document Control  
NRC Distribution Contractor  
U.S. Nuclear Regulatory Commission  
15700 Crabbs Branch Way  
Rockville, MD 20850  
375 copies for RV

U.S. Nuclear Regulatory Commission  
Electrical Engineering and  
Instrument Control Branch  
Room 126  
5650 Nicholson Lane  
Rockville, MD 20852  
Attn: R. Feit (10)

ITT Barton Instruments  
700 South Turnbull Canyon Road  
City of Industry, CA 91749  
Attn: L. Leyrer

0313 C. M. Craft  
1652 E. A. Salazar  
1815 R. T. Johnson, Jr.  
1822 J. A. Van den Avyl  
6400 A. W. Snyder  
6410 J. W. Hickman  
6417 D. D. Carlson  
6420 J. V. Walker  
6430 N. R. Ortiz  
6440 D. A. Dahlgren  
6442 W. A. von Rieseemann  
6445 J. H. Linebarger  
6445 L. D. Bustard  
6445 V. J. Dandini  
6445 D. T. Furgal (23)  
6445 M. J. Jacobus  
6445 E. H. Richards  
6446 L. L. Bonzon  
6446 F. V. Thome  
6447 D. L. Berry  
6450 J. A. Reuscher  
3141 C. M. Ostrander (5)  
3151 W. L. Garner  
8024 M. A. Pound

NRC FORM 336 (2-84) NRCM 1102 3201, 3202 SEE INSTRUCTIONS ON THE REVERSE	U.S. NUCLEAR REGULATORY COMMISSION <b>BIBLIOGRAPHIC DATA SHEET</b>	REPORT NUMBER (Assigned by T/DC add Vol. No. if any) NUREG/CR-3863 SAND84-1264
2 TITLE AND SUBTITLE Assessment of Class 1E Pressure Transmitter Response When Subjected to Harsh Environment Screening Tests	3 LEAVE BLANK	4 DATE REPORT COMPLETED MONTH: November      YEAR: 1984
5 AUTHOR(S) David T. Furgal, KTech Corporation Charles M. Craft Edward A. Salazar	6 DATE REPORT ISSUED MONTH: March      YEAR: 1985	8 PROJECT TASK WORK UNIT NUMBER
7 PERFORMING ORGANIZATION NAME AND MAILING ADDRESS (Include Zip Code) Sandia National Laboratories Division 6445 PO Box 5800 Albuquerque, New Mexico 87185	9 FIN OR GRANT NUMBER A-1327	11a TYPE OF REPORT b PERIOD COVERED (Inclusive Dates)
10 SPONSORING ORGANIZATION NAME AND MAILING ADDRESS (Include Zip Code) Division of Facility Operations Office of Nuclear Regulatory Research U.S. Nuclear Regulatory Commission Washington, DC 20555	12 <p>An experimental investigation into the performance of Class 1E electronic pressure transmitters exposed to environments within and beyond the design basis has been conducted. Emphasis was placed on determining the instruments' failure and degradation modes in separate and simultaneous environmental exposures. Five unaged ITT Barton Model 763 pressure transmitters were tested; each transmitter was exposed to a unique environment. The environments were (1) simulated Loss of Coolant Accident (LOCA) steam/chemical spray conditions alone, (2) temperature alone, (3) radiation alone, (4) simultaneous radiation and LOCA temperature (no steam) conditions, and (5) simultaneous radiation and simulated LOCA steam/chemical spray conditions.</p> <p>The response of the transmitters showed that temperature was the primary environmental stress affecting the tested transmitters' performance. Initial large errors that decrease with time-at-temperature were observed. We believe the source of these errors to be a common mode design weakness in the transmitter's calibration potentiometers. This weakness results from a dependency of material dielectric properties on temperature. The modification recommended by the manufacturer, although palliative in nature, did reduce this temperature-induced effect after the first few minutes of accident exposure. A potential second common failure mode which activates slowly with time-at-temperature was also identified. We believe the operation of this failure mechanism is catalyzed by the presence of a lubricant used in the production of some potentiometers. The design of this transmitter proved to be exceptionally hard to radiation effects and there appeared to be no significant synergistic effects between radiation and temperature. The observed responses of the transmitters offer support for the position of IEEE 381-1977 which recommends that electronic modules aged to varying degrees of advanced life should be tested.</p>	
14 DOCUMENT ANALYSIS - a KEYWORDS/DESCRIPTORS b IDENTIFIERS/OPEN ENDED TERMS	15 AVAILABILITY STATEMENT Unlimited 16 SECURITY CLASSIFICATION (This page) Unclassified (This report) Unclassified 17 NUMBER OF PAGES 18 PRICE	

120555078877 1 1AN1RV  
US NRC  
ADM-DIV OF TIDC  
POLICY & PUB MGT BR-PDR NUREG  
W-501  
WASHINGTON DC 20555